UNITED STATES PATENT AND TRADEMARK OFFICE

IN THE APPLICATION OF:			
McSwiggen et al.			
Serial No.	10/757,803	**Examiner:**	Amy Hudson Bowman
Filed:	January 14, 2004	**Group Art Unit:**	1635
Title	RNA Interference Mediated Inhibition of Gene Expression Using Chemically Modified Short Interfering Nucleic Acid (siNA)	**Confirmation No.:**	5421

DECLARATION UNDER 37 C.F.R. §1.132

Commissioner for Patents
P.O. Box 1450
Alexandria, VA 22313-1450

Sir:

1. I, James McSwiggen, am a named inventor of U.S. Patent Application Serial Number 10/757,803 and was formerly a Senior Research Fellow for Sirna Therapeutics, Inc., ("Sirna") located at 2950 Wilderness Place, Boulder Colorado, 80301, the sole Assignee of USSN 10/757,803. I earned a B.S. with honors in Molecular Biology from the University of Wisconsin, Madison, in 1979 and a Ph.D. in Biochemistry and Biology from the University of Oregon, Eugene, in 1985. I have performed research in the field of siRNA and other nucleic acid technologies for over 25 years. A copy of my Curriculum Vitae is attached.

2. I am a named inventor on USSN 10/757,803, entitled "RNA Interference Mediated Inhibition of Gene Expression Using Chemically Modified Short Interfering Nucleic Acid (siNA)".

3. I was employed as a research scientist at Sirna Therapeutics Inc. (formerly Ribozyme Pharmaceuticals Inc.) for 13 years. From 2000–2005, my work at Sirna involved, among other things, the analysis of gene sequences as possible siRNA targets, and the design of siRNA drugs

to attack those gene targets. From 1992–2000, my work as a Senior Scientist and Group Leader of the Enzymology/Biochemistry Department at Sirna involved the design and detailed analysis of chemically modified ribozymes. Specifically, my laboratory developed and applied novel modification strategies for ribozyme and antisense nucleic acid molecules for use in both *in vitro* and *in vivo* applications, including the use of such technologies in target validation and potential therapeutic applications. I have authored numerous publications and have been an inventor on several patents and patent applications involving the chemical modification of ribozyme and antisense nucleic acids (see attached Curriculum Vitae).

4. I was closely involved in the design strategies at Sirna to develop chemical modifications for increasing the nuclease stability of siRNAs while maintaining RNAi activity. The development of those strategies was not trivial, and there was nothing in the literature at that time to suggest a direction to take in order to achieve success, nor whether substantial internal or terminal modification of the siRNAs could even be successfully achieved. We received no guidance from the scientific literature that was published in 2000 to 2001. In fact, I believe that the literature of the day, and the general scientific community, tended to lead a person skilled in the art **away** from discovering such chemical modifications. I make this assertion, in particular, with respect to the work of Zamore et al., 2000 *Cell* 101(1):25-33, Bass, 2000 *Cell*, **101**, 235–238, Elbashir et al., 2001 *Nature* 411(6836):494-8 (Elbashir 1) and Elbashir et al., 2001, EMBO Journal, 20:6877-6888 (Elbashir 2). These papers provided early guidance on the generic design of siRNAs for gene targeting, including analyses of requirements for length, structure, chemical composition, and sequence in order to mediate RNAi. The patent examiner rejects this application, in part, based on obviousness assertions in light of patents by Cook *et al.* (US 5,587,471) and Wengel *et al.* (WO 99/14226); these will be addressed in sections below. One additional paper, Parrish et al. (Molecular Cell, 2000 Vol. 8:1077-1087), has been mentioned by the patent examiner as contributing to an obviousness rejection of this application. In fact, I believe that Parrish et al did not provide **any** guidance in the areas of siRNA design, and I will address this issue first.

5. **Parrish teaches nothing for siRNA design.** The paper by Parrish represents a broad survey of the biochemical properties of the RNAi reaction in nematodes using long dsRNAs, but it does not provide any useful information regarding the design of modified siRNA molecules. In

2000–2001 it was clear that RNAi was a conserved cellular mechanism that was present in a diverse set of organisms; it was first discovered in plants, then in nematodes, ciliates, fungi, Drosophila, and finally in mammalian cells (see for example Elbashir 1). But while the basic mechanism is conserved, it was clear to those skilled in the art that the mechanistic details could be very different from one organism to another. Specifically, the lower Eukaryotes are easily activated by long dsRNA, while publications such as Elbashir 1 noted that long dsRNA failed to stimulate RNAi in mammalian cells; this was likely due to the activation of an interferon response in mammalian cells, which is absent in the lower Eukaryotes. Likewise, Bernstein et al (2001, *RNA* **7**:1509-1521) noted that *C. elegans* and plants have a number of RNAi-related behaviors that are not found in mammalian cells, including the ability to pass the RNAi effect from one cell to the next, the ability to amplify the RNAi response such that a few dsRNA molecules can elicit a potent RNAi response, and the ability to pass the RNAi response from one cell generation to the next due to the long-lived nature of RNAi in these organisms (p1515-1516). These profound differences would teach those skilled in the art that it is unwise to generalize discoveries made in *C. elegans* to the world of mammalian RNAi.

6. A second factor that makes it difficult to draw lessons from Parrish is that all of the studies were performed using long dsRNA. The shortest dsRNA molecules used were 26 & 27 bp, but these were only used for initial base composition studies. In fact, Parrish clearly states that any molecules less than 26 bps were inactive (p1079, right column). The nucleotide modification studies were performed primarily using a 742 bp *unc*-22A sequence that apparently also contained "3–30 nt of dsRNA derived from polylinker sequences on each end, and polylinker-derived single stranded tails of 10–30 nt." (Materials & Methods, p1085). The authors checked the annealing of these sequences by agarose gel, but that would only confirm that they were stuck together, not whether they were annealed properly. These long sequences add a great deal of ambiguity to the interpretation of the results. An "inactive" modification could be such because it failed to allow the strands to anneal properly rather than being deleterious to the RNAi machinery, and an "active" modification could actually be an inactive modification that is distributed sparsely enough on the sequence that the RNAi machinery can still function. This latter possibility is of particular concern since Parrish reports that they "were able to demonstrate interference activity following incorporation of any single modified residue", but that "RNAs with two modified bases also had substantial decreases in effectiveness as RNAi triggers."

(p1081, right column). Thus, the modifications have a cumulative effect such as would be expected if the RNAi machinery was finding unmodified places on the long dsRNA to bind and activate.

7. One final argument against Parrish is that they themselves were unable to formulate a cogent conclusion to their chemical modification studies. They tested over 30 combinations of chemical modifications (their Figure 5, Figure 6, and data not shown), but in the discussion section they can only muster three short paragraphs speculating on the possible implications of these studies (p1084, left column). Their conclusions are: (1) the dsRNA might need to maintain an A-form helix to be active, (2) the antisense strand is more sensitive to modification than the sense strand, and (3) some modifications affect RNAi activity when added to either strand. These speculations are only weakly supported by the data. Coupled with the concerns mentioned above regarding long dsRNA and the difficulty of extending observations from *C. elegans* to mammalian cells, these considerations made it very difficult for us to draw any conclusions whatsoever from Parrish regarding the design of short siRNA molecules.

8. Returning, now, to the papers of Zamore, Bass, Elbashir 1 and Elbashir 2, I propose that these papers–and the general scientific community–tended to lead a person skilled in the art **away** from discovering the 5' and 3'-end sense strand and 3'-end antisense strand terminal cap chemical modifications discovered by us in the current application. I believe there are three factors that tended to lead away from such a discovery. First, there was no motivation to seek such modifications. Second, these key papers from 2001 suggested that deviations from RNA in the siRNA duplex would lead to inactivation of the siRNA. Third, nothing in the literature gave guidance as to **how** to modify siRNAs, even if the motivation to seek such modifications was present and the expectation of failure was overcome. I will address these three points in order.

9. **No motivation to seek modifications**. Even from the early papers mentioned above, it was clear that short RNA duplexes could be potent initiators of RNAi in extracts and in cell culture. Elbashir 2 used 100 nM RNA duplexes in their experiments to achieve >90% knockdown in extracts, while later studies would observe efficient knockdown at 5-10 nM siRNA. siRNAs tested at Sirna and elsewhere typically have been 10-100 fold more potent than the majority of ribozymes or antisense molecules tested. With ribozymes and antisense it was clear that RNA stability would be critical to achieving optimal activity, even in cell culture. In

contrast, the high potency of siRNAs tended to teach that no additional modification would be necessary, at least in cell culture. Also, it is common knowledge to those skilled in the art that single stranded RNA and DNA is much more susceptible to nuclease attack than double stranded nucleic acids. Thus the relatively unstructured antisense and ribozymes would be expected to require additional stabilization while the substantially double-stranded siRNA would not. An example of this thinking is seen in Elbashir 2, where an emphasis was placed on modifying the 3' single stranded ends of the siRNA, with little effort made to modify the double stranded 5' ends, let alone both the 3' and 5'-ends together.

10. The methods paper of Elbashir 3 (Elbashir et al., 2002 Methods 26:199-213) best exemplifies the mindset of the day that additional chemical modifications are unnecessary for effective RNAi activity. This paper gives specific instructions for designing and carrying out an RNAi experiment. On page 202, Protocol 1 (step 2) states that:

> Independent of the selection procedure described in Fig. 2, synthesize the sense siRNA as 5'-(N19)TT, and the sequence of the antisense siRNA as 5'-(N'19)TT, where N'19 denotes the reverse complement sequence of N19. N19 and N'19 indicate ribonucleotides; T indicates 2'-deoxythymidine.

Thus, RNA duplexes with dTdT 3' ends were considered the correct substrate for carrying out RNAi experiments. The terminal TT was there primarily to make chemical synthesis easier and less expensive, although some minor protection from **single-stranded** ribonucleases was also considered a possibility (Elbashir 2, Elbashir 3). Finally, Elbashir 3 makes specific mention of four suppliers of siRNA duplexes for RNAi research; all four companies supply the reagents in the standard form described in Protocol 1 of Elbashir 3.

11. **No expectation of success in chemical modification**. As stated above, there was no motivation to seek chemically modified siRNAs during the period in question, so it comes as no surprise that only a few papers discuss the subject. Elbashir 2 is the only paper from the period that describes a significant attempt to modify siRNAs away from their own standard of RNA with TT overhanging ends. Their efforts are incomplete, but also suggest that substantial modification will destroy RNAi activity. Under the heading "*The siRNA user guide*" (see page 6885) Elbashir 2 provides guidance to those of ordinary skill in the art on the design of siRNA duplexes. This guide states:

> Efficiently silencing siRNA duplexes are composed of 21 nt sense and 21 nt antisense siRNAs and **must** be selected to form a 19 bp double helix with 2 nt 3'-overhanging

> ends. 2'-deoxy substitutions of the 2 nt 2'-overhanging ribonucleotides do not affect RNAi, but help to reduce the costs of RNA synthesis and may enhance RNAse resistance of siRNA duplexes. **More extensive 2'-deoxy or 2'-O-methyl modifications reduce the ability of siRNAs to mediate RNAi**, probably by interfering with protein association for siRNAp assembly

(emphasis added). This reference suggests that chemical modifications are generally not tolerated by siRNAs except for substitution of the 3'-terminal nucleotides of siRNA with deoxynucleotides. Further, modifications with 2'-O-methyl or other modifications were not tolerated. Importantly, any instance where the 5'-end of the antisense strand was modified resulted in an inactive siRNA duplex.

12. Additionally, Elbashir 2 showed that modifications beyond the 3'-terminal nucleotides of the siRNA were not tolerated and provided further teachings that would have discouraged a person skilled in the art from introducing any chemical modifications to the nucleotides in the internal based-paired region of the siRNA duplex for the reasons set forth below (page 6886, right column, Elbashir 2):

> Interestingly, substitution by 2'-O-methylribose, which adopts the ribose sugar pucker, also abolished RNAi, probably because methylation of the 2'-hydroxyls blocked hydrogen bond formation or introduced steric hindrance.

Therefore, the modifications as presently claimed, all of which do not include 2'-hydroxyl groups, would not be expected to be active based on the teachings of Elbashir because they would likewise be expected to block hydrogen bond formation or introduce steric hindrance.

13. The foregoing teachings therefore discouraged us and likely steered others away from exploring chemical modification of siRNAs beyond replacing the 3'-terminal positions with deoxynucleotides. When we further surveyed the literature, there was ample evidence to suggest that people in the art were using siRNA duplexes that were either unmodified or modified only at the two overhanging nucleotide positions at the 3'-end of the siRNA. The published reports available during the 2000-2001 time period also showed that all of the synthetic siRNAs being used were 21 nt siRNA duplexes with 19 base pairs and 3'-terminal 2'-deoxy substitutions, just as described in "*The siRNA users guide*" from Elbashir 2 (see for example Bitko *et al.*, 2001, BMC Microbiology, 1, 34 page 9, left column under heading Materials and Methods section; Kumar *et al.*, 2002, Malaria Journal, 1:5, page 9, right column, under heading Transfection by

Inhibitory dsRNA; Holen *et al.,* 2002, Nucleic Acids Research, 30, 1757-1766, Figures 1, 2 and 6).

14. It was not until 2003 that scientists began to evaluate and report the use of chemical modifications other than 3'-terminal 2'-deoxy substitutions in siRNAs. See, for example, Chiu and Rana, 2003, RNA, 9:1034-1048 and Allerson *et al.,* 2005, *J. Med. Chem.* 48, 901. It is readily apparent from the publication record that those working in the RNAi field initially followed the teachings of Elbashir and others, outlined above in paragraphs 10–11, in designing siRNAs for experimental work. Only more recently has the use of more extensive chemical modifications become generally accepted.

15. We therefore carried out our initial experiments (during about 2000–2001) using the siRNAs used in the art by others, such as those set forth in Zamore, Elbashir 1, Elbashir 2 and others. We soon recognized, however, that these siRNAs had limited utility for more extensive applications in silencing of target genes in whole organisms, as such siRNAs were rapidly degraded by nucleases and possessed unfavorable pharmacokinetic and pharmacodynamic activity. The introduction of 5' and 3'-terminal cap moieties to the sense strand and 3'-terminal modifications to the antisense strand of a siRNA duplex greatly enhanced the stability of the siRNA while at the same time preserving potent RNAi activity as described in the instant application.

16. **No guidance on <u>how</u> to modify siRNAs.** It is incorrect to suggest that the teachings on the chemical modification of ribozymes and antisense would provide a roadmap for the ordinary person skilled in the art to be able to design stabilized siRNAs without loss of RNAi activity. Our own experience at Sirna argues very much to the contrary. With respect to our research, we found that chemical modification strategies for ribozymes differed greatly from those useful in antisense. For example, the modification strategy for ribozymes is dependant upon allowing the ribozymes to maintain catalytic activity, *i.e.*, by selective modification of the ribozyme binding arms and catalytic core. It required several years of research to arrive at modified ribozymes that were not only nuclease resistant but also maintained their catalytic activity (see for example Beigelman *et al.*, 1995 *The Journal of Biological Chemistry* 270:25702-25708). On the other hand, the modification strategy for antisense is dependent upon maintaining their ability to activate RNase H, and considerable research was involved in arriving

at modified antisense molecules that were both nuclease resistant and maintained the ability to activate RNase H (see for example Monia *et al.*, 1993 *J. Biol. Chem.* 268:14514-14522).

17. The following examples illustrate some of the many differences between ribozymes, antisense and siRNA. (1) Both ribozymes and antisense are substantially single-stranded prior to interacting with their target, while siRNA is almost completely in a duplex form; it is well known to those skilled in the art that single-stranded nucleic acid is more susceptible to nuclease attack than is double-stranded nucleic acid. (2) Ribozymes and antisense will tolerate substantial 5' and 3' terminal modifications, an observation that we have used to good effect to protect these molecules from exonuclease attack (c.f. Beigelman *et al.*); in contrast, the activity of siRNAs are almost completely destroyed by blocking the 5' end of the antisense strand of the siRNA with chemical modification, however, in the case of the sense strand, 5' and 3'-terminal modifications are tolerated. This modification strategy could only be determined through experimental work that we performed. (3) The activity of an antisense molecule is destroyed by modifications that alter the DNA-like structure at the core of molecule; in contrast ribozymes form a complex RNA secondary structure to be active. It was not clear in 2001 whether the siRNA duplex would need to maintain an RNA-like structure or whether other structures would be permitted. (4) Antisense molecules and ribozymes are active in the nucleus, while the RNAi activity occurs in the cytoplasm.

18. Because of our experience with modified ribozymes and antisense oligonucleotides, and understanding that the mechanism of RNA interference was different than both of these technologies, we had no faith that the results we observed with modifications of ribozymes and antisense oligonucleotides would inform us regarding the effects of chemical modifications in RNA interference. Accordingly, when we began investigating RNA interference technologies for targeted gene silencing we started from scratch, evaluating systematically the position and type of chemical modifications that siRNAs could tolerate without significantly diminishing the ability to mediate RNAi. In addition, the foregoing references (e.g., Elbashir 2) indicated to us that siRNAs are structurally and mechanistically distinct from previously characterized antisense and ribozymes nucleic acid technologies. Based on this distinction, we did not expect the chemical modification patterns of ribozyme and antisense to be useful for determining successful chemical modification strategies for siRNA.

19. The publications in the art during about 2000–2001, including, for example, the work of Zamore, Bass, Elbashir 1 and Elbashir 2, did in fact provide us general guidelines as to the design of active siRNA duplexes. These teachings can be summarized as follows: (a) double-stranded siRNAs are composed of 21 nt sense and 21 nt antisense siRNAs; (b) these siRNAs **must** be selected to form a 19 bp double helix; (c) the siRNA duplexes must contain 2 nt 3'-overhanging ends; (d) these 3'-overhanging nucleotide ends can be composed of two 2'-deoxythymidine nucleotides; (e) chemical modification of the internal positions within the siRNA duplex is not tolerated as they interfere the with RNAi activity of the siRNAs; (f) modifications other than 2'-deoxynucleotides at the 3'-end are not tolerated; (g) modification of the sense strand or the antisense strand fully with 2'-deoxynucleotides or 2'-O-methyl nucleotides abolish activity of the siRNAs to mediate RNAi, therefore demonstrating the need for the presence of ribonucleotides in the siRNAs for RNAi, and (h) chemical modification (e.g., 2'-O-methylribose) of nucleotides in the internal region of the siRNA duplex abolished activity of siRNAs to mediate RNAi.

20. In 2001–2002, well before any of the published reports referenced above, we performed detailed, systematic analyses to determine the extent and pattern of chemical modifications that would be tolerated in siRNA duplexes; testing, for example, various modifications other than 2'-deoxy substitutions at the 3'-terminal positions of the siRNAs, and the addition of various capping structures to the 5' and 3' ends of the oligos to help block exonucleases.

21. We first evaluated the serum stability of the siRNA constructs taught in Elbashir in comparison with duplexes having 5' and 3'-terminal cap moieties on the sense strand and 3'-terminal modifications on the antisense strand of the siRNA duplex, and additionally 2'-O-methyl, 2'-deoxy-2'-fluoro and other modifications at various positions. The constructs as taught by Elbashir had a stability half-life ($t_{½}$) of 15 seconds in human serum, compared to a $t_{½}$ of 32-40 days for the modified constructs we made. This work is described more fully in the instant application, which includes the experimental details and results of testing duplexes having 5' and 3'-terminal cap moieties on the sense strand and 3'-terminal modifications on the antisense strand of the siRNA duplex and 2'-O-methyl and 2'-deoxy-2'-fluoro modified duplexes based on our systematic analysis of siRNA structure and function.

22. Surprisingly, and contrary to Elbashir 2, we discovered that extensive chemical modification of siRNA duplexes could be tolerated, even to the point where all ribonucleotides of the siRNA could be substituted without abolishing RNAi activity, and where three of the four ends of the duplex oligos were capped by nuclease-resistant adducts (excluding the 5' antisense terminus). Specifically, we found that modified duplexes with 5' and 3'-terminal cap moieties on the sense strand and 3'-terminal modifications on the antisense strand of the siRNA duplex were highly potent mediators of RNA interference. We were the first ones to clearly demonstrate that contrary to the teachings in the art, active siRNAs can be designed with chemical modifications at a number of positions, including at every position within the duplex and on three of the four termini (excluding the 5' antisense terminus).

23. Applying what we learned in these experiments to the design of modified duplexes resulted in active double stranded nucleic acid constructs with potent activity as described in the present application and the preceding priority applications.

24. Based on publications such as Elbashir 1 and Elbashir 2, it is my belief that one would not have been motivated to make a chemically synthesized double stranded nucleic acid molecule, wherein the double stranded nucleic acid comprises a first strand and a second strand; the first strand comprises a sense region and the second strand comprises an antisense region; each strand is about 18 to about 27 nucleotides in length, about 18 to about 23 nucleotides of each strand are complementary to each other, and at least 19 nucleotides of the second strand are complementary to a target RNA sequence; and the first strand includes a terminal cap moiety at the 5'-end ***and*** the 3'-end of said first strand ***and*** the second strand includes a terminal cap moiety at the 3'-end of said second strand, wherein said 3'-end terminal cap moiety is independently selected from the group consisting of 4',5'-methylene nucleotide; 1-(beta-D-erythrofuranosyl) nucleotide, 4'-thio nucleotide; 1,5-anhydrohexitol nucleotide; L-nucleotides; *threo*-pentofuranosyl nucleotide; acyclic 3',4'-seco nucleotide; acyclic 3,4-dihydroxybutyl nucleotide; acyclic 3,5-dihydroxypentyl nucleotide, 3'-3'-inverted nucleotide moiety; 3'-3'-inverted abasic moiety; 3'-2'-inverted nucleotide moiety; 3'-2'-inverted abasic moiety; and said 5'-end cap moiety is selected from the group consisting of 4',5'-methylene nucleotide; 1-(beta-D-erythrofuranosyl) nucleotide; 4'-thio nucleotide, 1,5-anhydrohexitol nucleotide; L-nucleotide; LNA; *threo*-pentofuranosyl nucleotide; acyclic 3',4'-seco nucleotide; 3,4-dihydroxybutyl

nucleotide; 3,5-dihydroxypentyl nucleotide, 5'-5'-inverted nucleotide moiety; and 5'-5'-inverted abasic moiety as described in the instant application, because such publications indicated that such modifications would not be tolerated in an siRNA (see for example Elbashir 2).

25. In conclusion, a person working in the field of RNA interference at the time of filing the application for which I prepared this Declaration would not have been motivated to apply terminal cap moieties as presently claimed to both the 3' and 5'-ends of the sense strand and 3'-end of the antisense strand of siRNAs merely because such modifications were used to stabilize antisense and ribozymes. In fact, the literature clearly demonstrated that the knowledge derived from antisense and ribozyme technologies for stabilizing oligonucleotides could not be readily applied to obtain active siRNAs (see, for example, Elbashir 2). It is my belief that those working in the general field of oligo- and poly-nucleotides for therapeutic use in the 2000–2002 timeframe would have believed, as we did, that the mechanism of RNA interference differed so significantly from both ribozymes and antisense oligonucleotides that the knowledge derived from those technologies likely could not be directly applied with any appreciable expectation of success. In fact, as discussed above, people in the art (see for example Elbashir 2) had tried the approaches used for antisense oligonucleotides and ribozymes to modify siRNAs (beyond the 3'-terminal nucleotides with deoxynucleotide) but failed to generate active siRNAs!

26. I hereby certify that all statements made herein of my own knowledge are true and that all statements made on information and belief are believed to be true; and further that these statements were made with the knowledge that willful false statements and the like so made are punishable by fine or imprisonment, or both, under Section 1001 of Title 18 of the United States Code and that such willful false statements may jeopardize the validity of the application or any patents issued thereon.

Date: 3/14/2006 By: 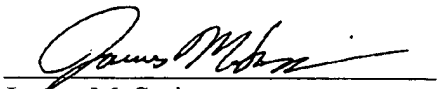
James McSwiggen

TAB 1

Cell, Vol. 101, 25–33, March 31, 2000, Copyright ©2000 by Cell Press

RNAi: Double-Stranded RNA Directs the ATP-Dependent Cleavage of mRNA at 21 to 23 Nucleotide Intervals

Phillip D. Zamore,*# Thomas Tuschl,†#
Phillip A. Sharp,‡§ and David P. Bartel§‖
*Department of Biochemistry and Molecular Biology
University of Massachusetts Medical School
Worcester, Massachusetts 01655
†Department of Cellular Biochemistry
Max-Planck-Institute for Biophysical Chemistry
Am Faßberg 11
D-37077 Göttingen
Germany
‡Center for Cancer Research and
§Department of Biology
Massachusetts Institute of Technology
Cambridge, Massachusetts 02139
‖The Whitehead Institute for Biomedical Research
9 Cambridge Center
Cambridge, Massachusetts 02142

Summary

Double-stranded RNA (dsRNA) directs the sequence-specific degradation of mRNA through a process known as RNA interference (RNAi). Using a recently developed *Drosophila* in vitro system, we examined the molecular mechanism underlying RNAi. We find that RNAi is ATP dependent yet uncoupled from mRNA translation. During the RNAi reaction, both strands of the dsRNA are processed to RNA segments 21–23 nucleotides in length. Processing of the dsRNA to the small RNA fragments does not require the targeted mRNA. The mRNA is cleaved only within the region of identity with the dsRNA. Cleavage occurs at sites 21–23 nucleotides apart, the same interval observed for the dsRNA itself, suggesting that the 21–23 nucleotide fragments from the dsRNA are guiding mRNA cleavage.

Introduction

The term RNA interference, or "RNAi," was initially coined by Fire and coworkers (Fire et al., 1998) to describe the observation that double-stranded RNA (dsRNA) can block gene expression when it is introduced into worms (for reviews see Fire, 1999; Hunter, 2000; Hunter, 1999; Montgomery and Fire, 1998; Sharp, 1999; Wagner and Sun, 1998). Their discovery built upon the previous, puzzling observation that sense and antisense RNA (asRNA) were equally effective in suppressing specific gene expression (Guo and Kemphues, 1995), a paradox resolved by the finding that small amounts of dsRNA contaminate sense and antisense preparations (Fire et al., 1998). RNAi has since been discovered in a wide variety of animals, including flies (Kennerdell and Carthew, 1998; Misquitta and Paterson, 1999), trypanosomes (Ngo et al., 1998), planaria (Sánchez-Alvarado and Newmark, 1999), hydra (Lohmann et al., 1999), zebrafish (Wargelius et al., 1999), and mice (Wianny and Zernicka-Goetz, 2000), and appears to be related to gene silencing phenomena in plants ("cosuppression"; Vaucheret et al., 1998; Waterhouse et al., 1998, 1999; Baulcombe, 1999) and the fungus *Neurospora* ("quelling"; Cogoni et al., 1996; Cogoni and Macino, 1999a, 1999b).

RNAi occurs posttranscriptionally and involves mRNA degradation (Montgomery et al., 1998; Ngo et al., 1998). In addition to providing a powerful tool for creating gene-specific phenocopies of loss-of-function mutations, RNAi may also play an important biological role in protecting the genome against instability caused by the accumulation of transposons and repetitive sequences (Ketting et al., 1999; Tabara et al., 1999). In *C. elegans*, dsRNA blocks specific gene expression even when expressed by bacteria fed to the worms (Timmons and Fire, 1998). RNAi in animals may also represent an ancient antiviral response, just as posttranscriptional gene silencing appears to protect plants from viral infection (Baulcombe, 1999; Grant, 1999; Ratcliff et al., 1999). The breadth of RNAi-like processes suggests that RNAi may encompass gene silencing phenomena, including cellular strategies for gene regulation, well beyond the initial observation that dsRNA can produce RNAi.

Genetic screens in both *C. elegans* and *Neurospora* have identified genes required for RNAi (Cogoni and Macino, 1997; Tabara et al., 1999). Mutations in a subset of these genes, including *rde-2*, *rde-3*, *mut-2*, and *mut-7*, permit the mobilization of transposons in the worm germline (Ketting et al., 1999; Tabara et al., 1999; Grishok et al., 2000). A second class of mutants, including the *rde-1* and *rde-4* loci, are defective for RNAi but show no other phenotypic abnormalities (Tabara et al., 1999). The *rde-1* and *rde-4* genes are required for the initiation of heritable RNAi, a phenomenon in which RNAi established by injection of dsRNA in a worm leads to heritable gene silencing in the F2 generation and beyond (Grishok et al., 2000). In contrast, *rde-2* and *mut-7* are not required for the initiation of heritable interference but are required downstream in the tissue where the interference occurs. Mello and colleagues have proposed that *rde-1* and *rde-4* respond to dsRNA by producing a secondary extragenic agent that is used by the downstream genes *rde-2* and *mut-7* to target specific mRNAs for posttranscriptional gene silencing (Grishok et al., 2000). In this view, *rde-1* and *rde-4* act as initiators of RNAi, whereas *rde-2* and *mut-7* are effectors. These authors propose that other stimuli that lead to gene silencing, such as the accumulation of transposons or repetitive DNA in the genome or the introduction of a transgene, are interpreted by a separate set of initiator genes that produce the same secondary extragenic agent.

In *Neurospora*, the *qde-3* gene, which is required for quelling (a form of posttranscriptional silencing in which an endogenous gene is silenced by the introduction of a transgenic copy of the gene), may be an example of an initiator gene that responds to the presence of a transgene (Cogoni and Macino, 1999b). *qde-3* is a member of the RecQ DNA helicase family, which includes

#To whom correspondence should be addressed (e-mail: phillip.zamore@umassmed.edu [P. D. Z.], ttuschl@mpibpc.gwdg.de [T. T.]).

the human genes for Bloom's syndrome and Werner's syndrome.

One candidate for the secondary extragenic agent itself is the 25 nucleotide-long RNAs associated with posttranscriptional gene silencing in plants (Hamilton and Baulcombe, 1999). These RNAs, which correspond to both the sense and antisense strands of the silenced gene, are only detected in plants undergoing silencing. The level of expression of these short RNAs also correlates with the extent of gene silencing. It remains to be shown if the 25 nt RNAs are the actual agents or merely the products of gene silencing.

Two other genes implicated in posttranscriptional gene silencing, *qde-1* in *Neurospora* (Cogoni and Macino, 1999a) and *ego-1* in *C. elegans* (Smardon et al., 2000), are homologous to a tomato protein that displays RNA-directed RNA-polymerase activity in vitro (Schiebel et al., 1993a, 1993b, 1998). RNA-directed RNA polymerases have been implicated in the initial formation of the silencing agent or in the amplification of dsRNA. Amplification of injected dsRNA by an endogenous RNA-directed RNA polymerase would help explain how a very small number of dsRNA molecules can inactivate a much larger population of mRNAs and how the dsRNA can apparently persist in the animal for many days and even into subsequent generations. *ego-1* mutants are defective for RNAi for maternally, but not zygotically, expressed mRNAs. Interestingly, *ego-1* is also required for germline development in *C. elegans* (Qiao et al., 1995).

Biochemical analysis of RNAi has become possible with the development of an in vitro *Drosophila* embryo lysate that recapitulates dsRNA-dependent silencing of gene expression (Tuschl et al., 1999). In the in vitro system, dsRNA—but not sense or asRNA—targets a corresponding mRNA for degradation yet does not affect the stability of an unrelated control mRNA. Furthermore, preincubation of the dsRNA in the lysate potentiates its activity for target mRNA degradation, suggesting that the dsRNA must be converted to an active form by binding proteins in the extract or by covalent modification (Tuschl et al., 1999).

Here, we use the in vitro system to analyze the requirements of RNAi and to determine the fate of the dsRNA and the mRNA. RNAi in vitro requires ATP but does not require either mRNA translation or recognition of the 7-methyl-guanosine cap of the targeted mRNA. The dsRNA but not single-stranded RNA is processed in vitro to a population of 21–23 nt species. Deamination of adenosines within the dsRNA does not appear to be required for formation of the 21–23 nt RNAs. Furthermore, we find that the mRNA is cleaved only in the region corresponding to the sequence of the dsRNA and that the mRNA is cleaved at 21–23 nt intervals, strongly suggesting that the 21–23 nt fragments from the dsRNA are targeting the cleavage of the mRNA.

Results and Discussion

RNAi Requires ATP

Drosophila embryo lysates faithfully recapitulate RNAi (Tuschl et al., 1999). Previously, dsRNA-mediated gene silencing was monitored by measuring the synthesis of

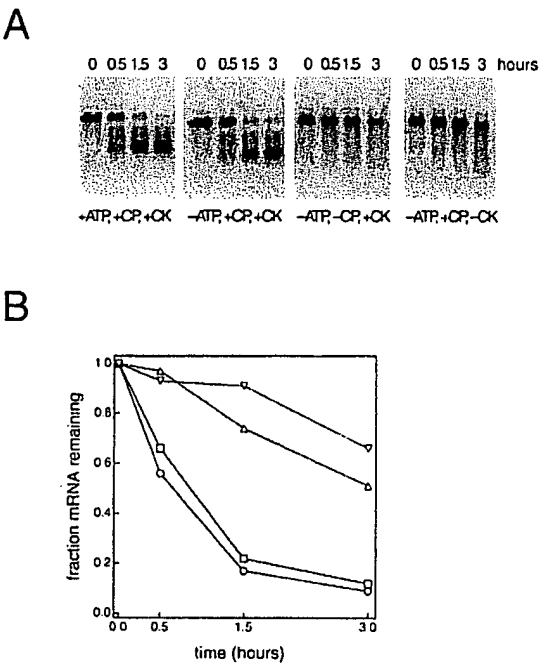

Figure 1. RNAi Requires ATP

(A) Denaturing agarose-gel analysis of 5′-^{32}P-radiolabeled *Rr*-luc mRNA incubated for the times indicated in an in vitro RNAi reaction with or without ATP, creatine phosphate (CP), or creatine kinase (CK), as indicated below each panel.

(B) Quantitation of the data in (A). Circles, +ATP, +CP, +CK; squares, -ATP, +CP, +CK; triangles, -ATP, -CP, +CK; inverted triangles, -ATP, +CP, -CK.

luciferase protein from the targeted mRNA. Thus, these RNAi reactions contained an ATP-regenerating system, needed for the efficient translation of the mRNA. To test if ATP was, in fact, required for RNAi, the lysates were depleted for ATP by treatment with hexokinase and glucose, which converts ATP to ADP, and RNAi was monitored directly by following the fate of ^{32}P-radiolabeled *Renilla reniformis* luciferase (*Rr*-luc) mRNA (Figure 1). Treatment with hexokinase and glucose reduced the endogenous ATP level in the lysate from 250 μM to below 10 μM (data not shown). ATP regeneration required both exogenous creatine phosphate and creatine kinase, which acts to transfer a high-energy phosphate from creatine phosphate to ADP. When ATP-depleted extracts were supplemented with either creatine phosphate or creatine kinase separately, no RNAi was observed. Therefore, RNAi requires ATP in vitro. When ATP, creatine phosphate, and creatine kinase were all added together to reactions containing the ATP-depleted lysate, dsRNA-dependent degradation of the *Rr*-luc mRNA was restored (Figure 1). The addition of exogenous ATP was not required for efficient RNAi in the depleted lysate, provided that both creatine phosphate and creatine kinase were present, demonstrating that the endogenous concentration (250 μM) of adenosine nucleotide is sufficient to support RNAi. RNAi with a *Photinus pyralis* luciferase (*Pp*-luc) mRNA was also ATP dependent (data not shown).

The stability of the *Rr*-luc mRNA in the absence of

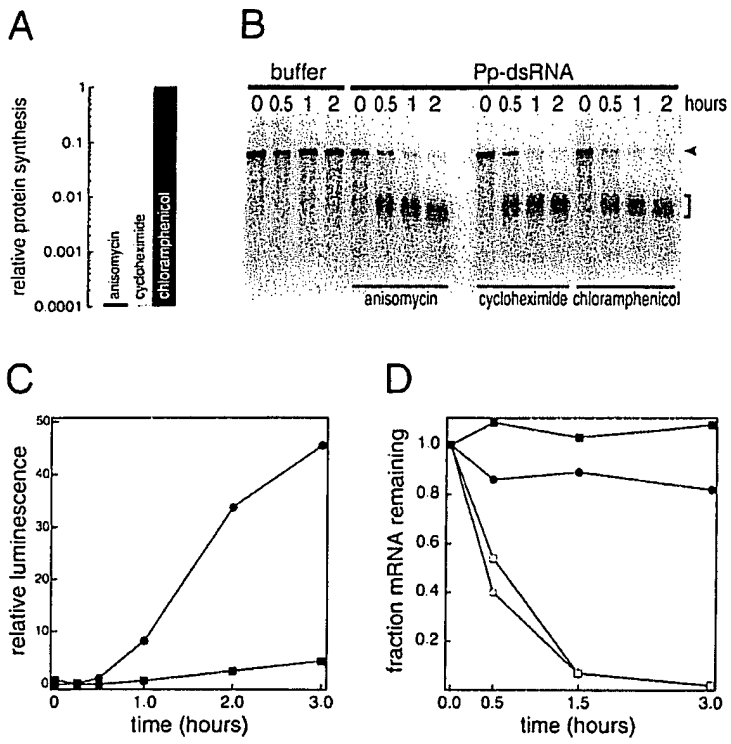

Figure 2. RNAi Does Not Require mRNA Translation

(A) Protein synthesis, as reflected by luciferase activity produced after incubation of *Rr*-luc mRNA in the in vitro RNAi reaction for 1 hr, in the presence of the protein synthesis inhibitors anisomycin, cycloheximide, or chloramphenicol, relative to a reaction without any inhibitor.

(B) Denaturing agarose-gel analysis of 5′-^{32}P-radiolabeled *Pp*-luc mRNA after incubation for the indicated times in a standard RNAi reaction with and without protein synthesis inhibitors. The arrowhead indicates the position of full-length mRNA in the gel, and the bracket marks the position of stable, 5′ cleavage products.

(C) Translation of 7-methyl-guanosine- and adenosine-capped *Pp*-luc mRNAs (circles and squares, respectively) in the RNAi reaction in the absence of dsRNA, as measured by luciferase activity produced in a 1 hr incubation.

(D) Incubation in an RNAi reaction of uniformly ^{32}P-radiolabeled 7-methyl-guanosine-capped *Pp*-luc mRNA (circles) and adenosine-capped *Pp*-luc mRNA (squares), in the presence (open symbols) and absence (filled symbols) of 505 bp *Pp*-luc dsRNA.

Rr-dsRNA was reduced in ATP-depleted lysates relative to that observed when the energy regenerating system was included, but decay of the mRNA under these conditions did not display the rapid decay kinetics characteristic of RNAi in vitro, nor did it generate the stable mRNA cleavage products characteristic of dsRNA-directed RNAi (data not shown). These experiments do not establish if the ATP requirement for RNAi is direct, implicating ATP in one or more steps in the RNAi mechanism, or indirect, reflecting a role for ATP in maintaining high concentrations of another nucleoside triphosphate in the lysate.

Translation Is Not Required for RNAi In Vitro

The requirement for ATP suggested that RNAi might be coupled to mRNA translation, a highly energy-dependent process. To test this possibility, various inhibitors of protein synthesis were added to the reaction. We tested the eukaryotic translation inhibitors anisomycin, an inhibitor of initial peptide bond formation, cycloheximide, an inhibitor of peptide chain elongation, and puromycin, a tRNA mimic that causes premature termination of translation (Cundliffe, 1981). Each of these inhibitors reduced protein synthesis in the *Drosophila* lysate by more than 1,900-fold (Figure 2A; data not shown). In contrast, chloramphenicol, an inhibitor of *Drosophila* mitochondrial protein synthesis (Page and Orr-Weaver, 1997), had no effect on translation in the lysates (Figure 2A). Despite the presence of anisomycin, cycloheximide, or chloramphenicol, RNAi proceeded at normal efficiency (Figure 2B). Puromycin also did not perturb efficient RNAi (data not shown). Thus, protein synthesis is not required for RNAi in vitro.

Translational initiation is an ATP-dependent process that involves recognition of the 7-methyl guanosine cap of the mRNA (Merrick and Hershey, 1996; Kozak, 1999). The *Drosophila* lysate used to support RNAi in vitro also recapitulates the cap dependence of translation: *Pp*-luc mRNA with a 7-methyl-guanosine cap was translated greater than 10-fold more efficiently than was the same mRNA with an A(5′)ppp(5′)G cap (Figure 2C). Both RNAs were equally stable in the *Drosophila* lysate, showing that this difference in efficiency cannot be merely explained by more rapid decay of the mRNA with an adenosine cap (also see Gebauer et al., 1999). Although the translational machinery can discriminate between *Pp*-luc mRNAs with 7-methyl-guanosine and adenosine caps, the two mRNAs were equally susceptible to RNAi in the presence of *Pp*-dsRNA (Figure 2D). These results suggest that steps in cap recognition are not involved in RNAi.

dsRNA Is Processed to 21–23 Nucleotide Species

RNAs 25 nt in length are generated from both the sense and antisense strands of genes undergoing posttranscriptional gene silencing in plants (Hamilton and Baulcombe, 1999). We find that dsRNA is also processed to small RNA fragments (Figures 3A and 3B). When incubated in lysate, approximately 15% of the input radioactivity of both the 501 bp *Rr*-dsRNA and the 505 bp *Pp*-dsRNA appeared in 21 to 23 nt RNA fragments. Because the dsRNAs are more than 500 bp in length, the 15% yield of fragments implies that multiple 21–23 nt RNAs are produced from each full-length dsRNA molecule. No other stable products were detected. The small RNA species were produced from dsRNAs in which both

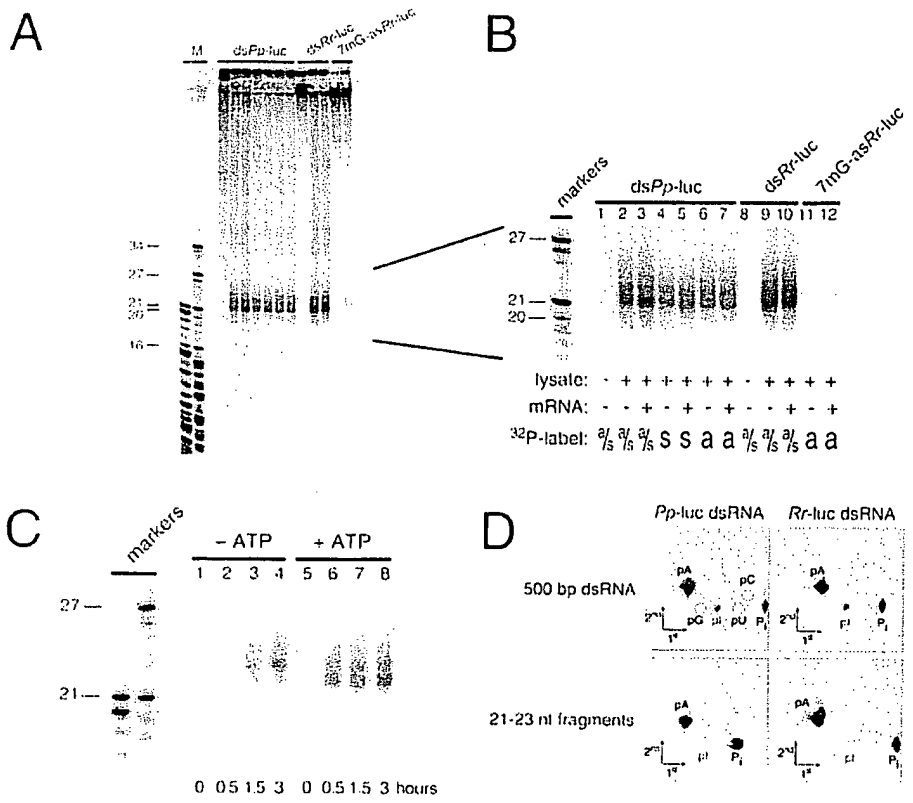

Figure 3. 21–23 nt RNA Fragments Are Produced upon Incubation of dsRNA in *Drosophila* Embryo Lysate

(A) Denaturing acrylamide-gel analysis of the products formed in a 2 hr incubation of uniformly ^{32}P-radiolabeled dsRNAs or capped asRNA in lysate under standard RNAi conditions, in the presence or absence of target mRNAs.

(B) An enlargement of the portion of the gel in (A) corresponding to 17 to 27 nt. For *Pp*-dsRNA, the sense (lanes 4 and 5) or the antisense (lanes 6 and 7) or both strands (lanes 1, 2, and 3) were labeled. For *Rr*-luc dsRNA, both strands were radioactive (lanes 8, 9, and 10).

(C) An enlargement of the 17 to 27 nt region of a gel showing the products formed upon incubation of uniformly ^{32}P-radiolabeled dsRNAs in lysate without and with ATP.

(D) Adenosine deamination in full-length dsRNA and the 21–23 nt RNA species assessed by two-dimensional thin-layer chromatography. Circles correspond to positions of unlabeled 5′-nucleotide monophosphate standards visualized under UV light. Inorganic phosphate (P_i) was produced by the degradation of mononucleotides by phosphatases that contaminate commercially available nuclease P1 (Auxilien et al., 1996).

strands were uniformly ^{32}P-radiolabeled (Figure 3B, lanes 2, 3, 9, and 10). Formation of the 21–23 nt RNAs from the dsRNA did not require the presence of the corresponding mRNA (Figure 3B, compare lane 2 with lane 3 and lane 9 with lane 10), demonstrating that the small RNA species is generated by processing of the dsRNA, rather than as a product of dsRNA-targeted mRNA degradation. We note that 22 nucleotides corresponds to two turns of an A-form RNA–RNA helix.

When dsRNAs radiolabeled within either the sense or the antisense strand were incubated with lysate in a standard RNAi reaction, 21–23 nt RNAs were generated with comparable efficiency (Figure 3B, compare lanes 4 and 6). These data support the idea that the 21–23 nt RNAs are generated by symmetric processing of the dsRNA. A variety of data support the idea that the 21–23 nt RNA is efficiently generated only from dsRNA and is not the consequence of an interaction between single-stranded RNA and the dsRNA. First, a ^{32}P-radiolabeled 505 nt *Pp*-luc sense RNA or asRNA was not efficiently converted to the 21–23 nt product when it was incubated with 5 nM nonradioactive 505 bp *Pp*-dsRNA (data not shown). Second, in the absence of mRNA, a 501 nt 7-methyl-guanosine-capped *Rr*-asRNA produced only a barely detectable amount of 21–23 nt RNA (Figure 3B, lane 11; capped single-stranded RNAs are as stable in the lysate as dsRNA [Tuschl et al., 1999]), probably due to a small amount of dsRNA contaminating the antisense preparation. However, when *Rr*-luc mRNA was included in the reaction with the ^{32}P-radiolabeled, capped *Rr*-asRNA, a small amount of 21–23 nt product was generated, corresponding to 4% of the amount of 21–23 nt RNA produced from an equimolar amount of *Rr*-dsRNA. This result is unlikely to reflect the presence of contaminating dsRNA in the *Rr*-asRNA preparation, since significantly more product was generated from the asRNA in the presence of the *Rr*-luc mRNA than in the absence (compare lanes 12 and 11). Instead, the data suggest that asRNA can interact with the complementary mRNA sequences to form dsRNA in the reaction and that the

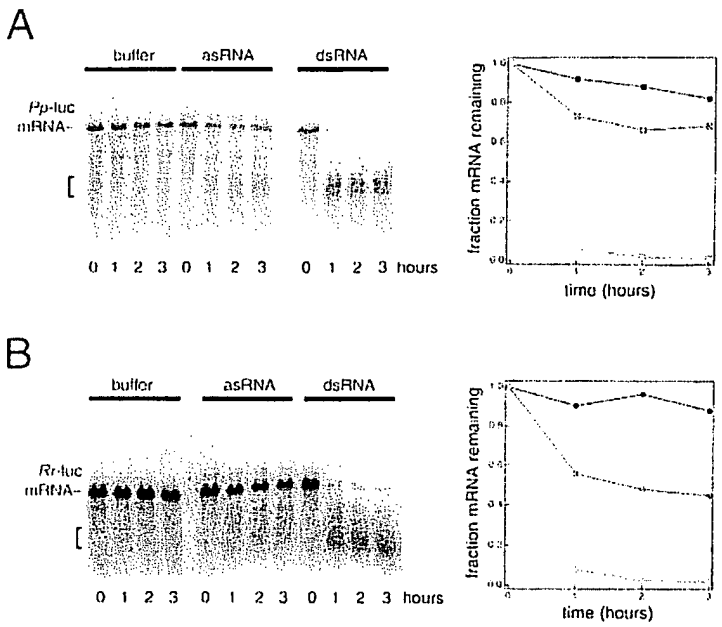

Figure 4. asRNA Causes a Small Amount of RNAi In Vitro

(A) Denaturing agarose-gel analysis of *Pp*-luc mRNA incubated in a standard RNAi reaction with buffer, 505 nt *Pp*-asRNA, or 505 bp *Pp*-dsRNA for the times indicated.

(B) The same analysis for the *Rr*-luc mRNA. Quantitation of the gel data in both (A) and (B) is given to the right of each panel. Buffer, black symbols; asRNA, blue symbols; dsRNA, red symbols.

resulting dsRNA is subsequently processed to the small RNA species. *Rr*-asRNA can support a low level of bona fide RNAi in vitro (see below), consistent with this explanation.

We next asked if production of the 21–23 nt RNAs from dsRNA required ATP (Figure 3C). When the 505 bp *Pp*-dsRNA was incubated in a lysate depleted for ATP by treatment with hexokinase and glucose, 21–23 nt RNA was produced (lanes 1–4, "−ATP"), albeit six times slower than when ATP was regenerated in the depleted lysate by the inclusion of creatine kinase and creatine phosphate (lanes 5–8, "+ ATP"). Therefore, ATP may not be required for production of the 21–23 nt RNA species but may instead simply enhance its formation. Alternatively, ATP may be required for processing of the dsRNA, but at a concentration less than that remaining after hexokinase treatment. We do not yet understand the molecular basis for the slower mobility of the small RNA fragments generated in the ATP-depleted lysate.

Wagner and Sun (1998) and Sharp (1999) have speculated that the requirement for dsRNA in gene silencing by RNAi reflects the involvement of a dsRNA-specific adenosine deaminase in the process. dsRNA adenosine deaminases unwind dsRNA by converting adenosine to inosine, which does not base pair with uracil. dsRNA adenosine deaminases function in the posttranscriptional editing of mRNA (reviewed by Bass, 1997). To test for the involvement of dsRNA adenosine deaminase in RNAi, we examined the degree of conversion of adenosine to inosine in the 501 bp *Rr*-luc and 505 bp *Pp*-luc dsRNAs after incubation with *Drosophila* embryo lysate in a standard in vitro RNAi reaction (Figure 3D). We also determined the degree of adenosine deamination in the 21–23 nt species. The full-length dsRNA radiolabeled with [^{32}P]-adenosine was incubated in the lysate, and both the full-length dsRNA and the 21–23 nt RNA products were purified from a denaturing acrylamide gel, cleaved to mononucleotides with nuclease P1, and analyzed by two-dimensional thin-layer chromatography.

A significant fraction of the adenosines in the full-length dsRNA were converted to inosine after 2 hr (3.1% and 5.6% conversion for *Pp*-luc and *Rr*-luc dsRNAs, respectively). In contrast, only 0.4% (*Pp*-dsRNA) or 0.7% (*Rr*-dsRNA) of the adenosines in the 21–23 nt species were deaminated. These data imply that fewer than 1 in 27 molecules of the 21–23 nt RNA species contain an inosine. Therefore, it is unlikely that dsRNA-dependent adenosine deamination within the 21–23 nt species is required for its production.

asRNA Generates a Small Amount of RNAi In Vitro

When mRNA was ^{32}P-radiolabeled within the 5′-7-methyl-guanosine cap, stable 5′ decay products accumulated during the RNAi reaction (see, for example, Figures 1A and 2B). Such stable 5′ decay products were observed for both the *Pp*-luc and *Rr*-luc mRNAs when they were incubated with their cognate dsRNAs (indicated by the brackets in Figures 4A and 4B). Previously, we reported that efficient RNAi does not occur when asRNA is used in place of dsRNA (Tuschl et al., 1999). Nevertheless, mRNA was measurably less stable when incubated with asRNA than with buffer (Figures 4A and 4B). This was particularly evident for the *Rr*-luc mRNA: approximately 90% of the RNA remained intact after a 3 hr incubation in lysate, but only 50% when asRNA was added. Less than 5% remained when dsRNA was added. Interestingly, the decrease in mRNA stability caused by asRNA was accompanied by the formation of a small amount of the stable 5′ decay products characteristic of the RNAi reaction with dsRNA. This finding parallels the observation that a small amount of 21–23 nt product formed from the asRNA when it was incubated with the mRNA (see above) and lends strength to the idea that asRNA can enter the RNAi pathway, albeit inefficiently.

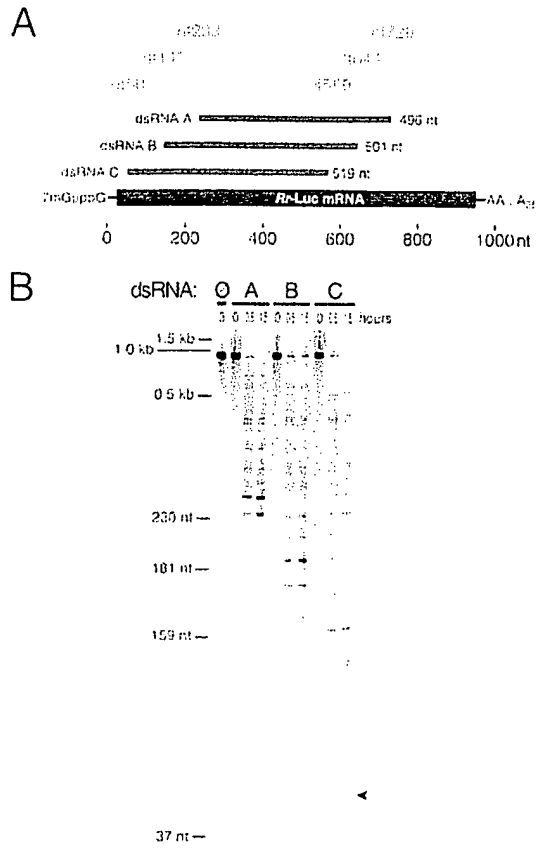

Figure 5. The dsRNA Determines the Boundaries of the Cleavage Products

(A) Schematic of the positions of the three dsRNAs, A, B, and C, relative to the *Rr*-luc mRNA.

(B) Denaturing acrylamide-gel analysis of the stable, 5′ cleavage products produced after incubation of the *Rr*-luc mRNA for the indicated times with each of the three dsRNAs, A, B, and C, or with buffer (zero with strikethrough). The positions of RNA markers radiolabeled within their 5′ cap is shown at left. The arrowhead denotes a faint cleavage site that is indicated with an open blue circle in Figure 6B.

mRNA Cleavage Sites Are Determined by the Sequence of the dsRNA

The sites of mRNA cleavage were examined using three different dsRNAs, "A," "B," and "C," displaced along the *Rr*-luc sequence by approximately 100 nt. The positions of these relative to the *Rr*-luc mRNA sequence are shown (Figure 5A). Each of the three dsRNAs was incubated in a standard RNAi reaction with *Rr*-luc mRNA ^{32}P-radiolabeled within the 5′ cap (Figure 5B). In the absence of dsRNA, no stable 5′ cleavage products were detected for the mRNA, even after 3 hr of incubation in lysate. In contrast, after a 20 min incubation, each of the three dsRNAs produced a ladder of bands corresponding to a set of mRNA cleavage products characteristic for that particular dsRNA. For each dsRNA, the stable, 5′ mRNA cleavage products were restricted to the region of the *Rr*-luc mRNA that corresponded to the dsRNA (Figures 5B and 6). For dsRNA A, the lengths of the 5′ cleavage products ranged from 236 to just under ~750 nt; dsRNA A spans nucleotides 233 to 729 of the *Rr*-luc mRNA. Incubation of the mRNA with dsRNA B produced mRNA 5′ cleavage products ranging in length from 150 to ~600 nt; dsRNA B spans nucleotides 143 to 644 of the mRNA. Finally, dsRNA C produced mRNA cleavage products from 66 to ~500 nt in length. This dsRNA spans nucleotides 50 to 569 of the *Rr*-luc mRNA. Therefore, the dsRNA not only provides specificity for the RNAi reaction, selecting which mRNA from the total cellular mRNA pool will be degraded, but also determines the boundaries of cleavage along the mRNA sequence.

The mRNA Is Cleaved at 21–23 Nucleotide Intervals

To gain further insight into the mechanism of RNAi, we mapped the positions of several mRNA cleavage sites for each of the three dsRNAs (Figure 6). Remarkably, most of the cleavages occurred at 21–23 nt intervals (Figure 6A). This spacing is especially striking in light of our observation that the dsRNA is processed to a 21–23 nt RNA species and the finding of Hamilton and Baulcombe that a 25 nt RNA correlates with posttranscriptional gene silencing in plants (Hamilton and Baulcombe, 1999). Of the 16 cleavage sites we mapped (two for dsRNA A, five for dsRNA B, and nine for dsRNA C), all but two reflect the 21–23 nt interval. One of the two exceptional cleavages was a weak cleavage site produced by dsRNA C (indicated by an arrowhead in Figure 5B and an open blue circle in Figure 6B). This cleavage occurred 32 nt 5′ to the next cleavage site. The other exception is particularly intriguing. After four cleavages spaced 21–23 nt apart, dsRNA C caused cleavage of the mRNA just 9 nt 3′ to the previous cleavage site (Figures 6A and 6B, red arrowhead). This cleavage occurred in a run of seven uracil residues and appears to "reset" the ruler for cleavage; the next cleavage site was 21–23 nt 3′ to the exceptional site. The three subsequent cleavage sites that we mapped were also spaced 21–23 nt apart. Curiously, of the sixteen cleavage sites mapped for the three different dsRNAs, fourteen occur at uracil residues. We do not yet understand the significance of this finding, but it suggests that mRNA cleavage is determined by a process that measures 21–23 nt intervals and that has a sequence preference for cleavage at uracil. In preliminary experiments, the 21–23 nt RNA species produced by incubation of ~500 bp dsRNA in the lysate caused sequence-specific interference in vitro when isolated from an acrylamide gel and added to a new RNAi reaction in place of the full-length dsRNA (our unpublished data).

A Model for dsRNA-Directed mRNA Cleavage

Our biochemical data, together with recent genetic experiments in *C. elegans* and *Neurospora* (Cogoni and Macino, 1999a; Ketting et al., 1999; Tabara et al., 1999; Grishok et al., 2000), suggest a model for how dsRNA targets mRNA for destruction (Figure 7). In this model, the dsRNA is first cleaved to 21 to 23 nt long fragments in a process likely to involve genes such as the *C. elegans* loci *rde-1* and *rde-4*. The resulting fragments, probably as short asRNAs bound by RNAi-specific proteins, would then pair with the mRNA and recruit a nuclease that cleaves the mRNA. Alternatively, strand exchange could occur in a protein-RNA complex that transiently

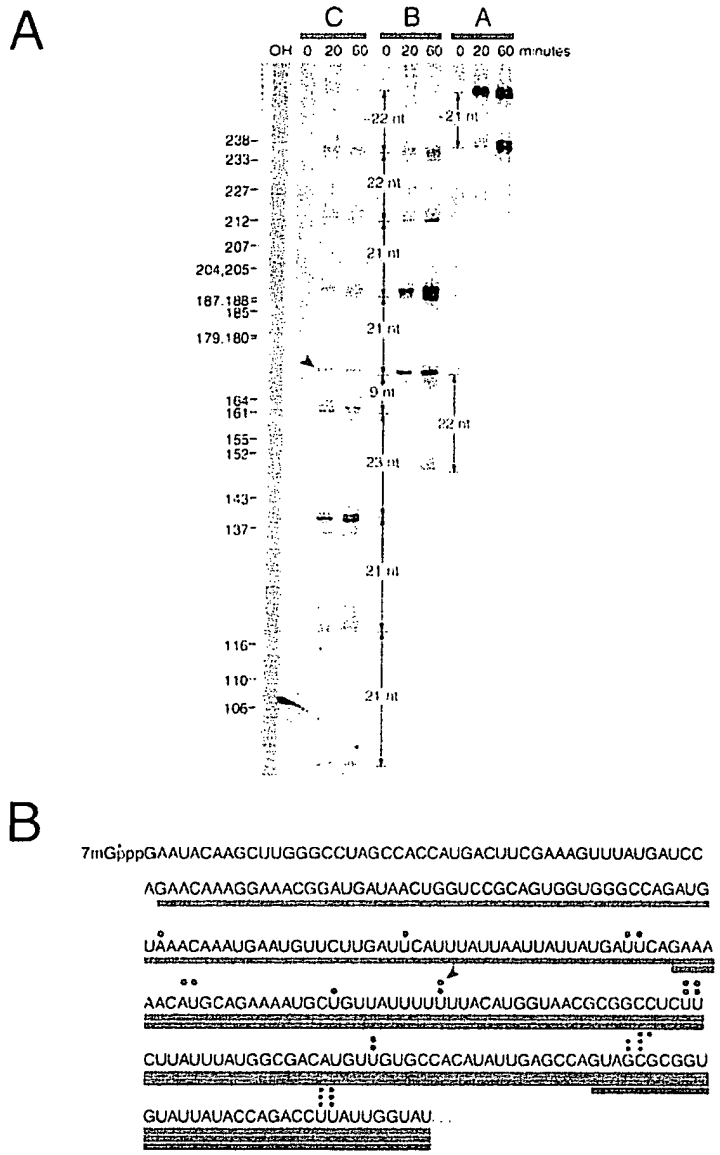

Figure 6. The mRNA Is cleaved in 21–23 nt Intervals

(A) High-resolution denaturing acrylamide-gel analysis of a subset of the 5′ cleavage products described in Figure 5B. The positions of some of the partial T1 digestion products of *Rr*-luc mRNA are indicated at left. "OH" marks the lane in which a partial base-hydrolysis ladder was loaded.

(B) The cleavage sites in (A) mapped onto the first 267 nt of the *Rr*-luc mRNA. The blue bar below the sequence indicates the position of dsRNA C, and blue circles indicate the position of cleavage sites caused by this dsRNA. The green bar denotes the position of dsRNA B, and green circles, the cleavage sites. The magenta bar indicates the position of dsRNA A, and magenta circles, the cleavages. An exceptional cleavage within a run of seven uracils is marked with a red arrowhead in both (A) and (B).

holds a 21–23 nt dsRNA fragment close to the mRNA. Separation of the two strands of the dsRNA following fragmentation might be assisted by an ATP-dependent RNA helicase, explaining the ATP enhancement of 21–23 nt RNA production we observed.

We envision that each small RNA fragment produces one, or at most two, cleavages in the mRNA, perhaps at the 5′ or 3′ ends of the 21–23 nt fragment. The small RNAs may be amplified by an RNA-directed RNA polymerase such as that encoded by the *ego-1* gene in *C. elegans* (Smardon et al., 2000) or the *qde-1* gene in *Neurospora* (Cogoni and Macino, 1999a), producing long-lasting posttranscriptional gene silencing in the absence of the dsRNA that initiated the RNAi effect. Heritable RNAi in *C. elegans* requires the *rde-1* and *rde-4* genes to initiate but not to persist in subsequent generations. The *rde-2*, *rde-3*, and *mut-7* genes in *C. elegans* are required in the tissue where RNAi occurs but are not required for initiation of heritable RNAi (Grishok et al., 2000). These "effector" genes (Grishok et al., 2000) are likely to encode proteins functioning in the actual selection of mRNA targets and in their subsequent cleavage. ATP may be required at any of a number of steps during RNAi, including complex formation on the dsRNA, strand dissociation during or after dsRNA cleavage, pairing of the 21–23 nt RNAs with the target mRNA, mRNA cleavage, and recycling of the targeting complex. Testing these ideas with the in vitro RNAi system will be an important challenge for the future.

Experimental Procedures

In Vitro RNAi

In vitro RNAi reactions and lysate preparation were as described previously (Tuschl et al., 1999) except that the reaction contained 0.03 μg/ml creatine kinase, 25 mM creatine phosphate (Fluka), and 1 mM ATP. Creatine phosphate was freshly dissolved at 500 mM in

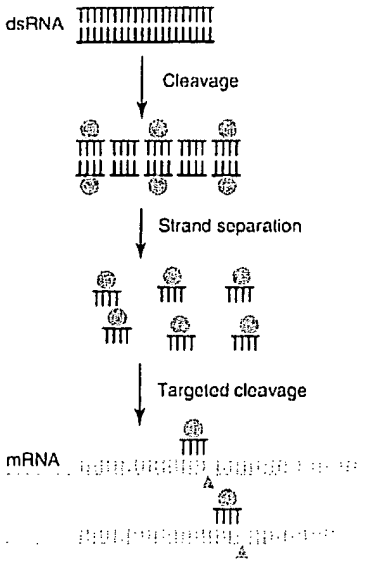

Figure 7. Proposed Model for RNAi

RNAi is envisioned to begin with cleavage of the dsRNA to 21–23 nt products by a dsRNA-specific nuclease, perhaps in a multiprotein complex. These short dsRNAs might then be dissociated by an ATP-dependent helicase, possibly a component of the initial complex, to 21–23 nt asRNAs that could then target the mRNA for cleavage. The short asRNAs are imagined to remain associated with the RNAi-specific proteins (ochre circles) that were originally bound by the full-length dsRNA, thus explaining the inefficiency of asRNA to trigger RNAi in vivo and in vitro. Finally, a nuclease (triangles) would cleave the mRNA.

water for each experiment. GTP was omitted from the reactions, except in Figures 2 and 3.

RNA Synthesis

Pp-luc and *Rr*-luc mRNAs and *Pp*- and *Rr*-dsRNAs (including dsRNA B in Figure 6) were synthesized by in vitro transcription as described previously (Tuschl et al., 1999). To generate transcription templates for dsRNA C, the 5′ sense RNA primer was gcgtaatacgactcactata GAACAAAGGAAACGGATGAT and the 3′ sense RNA primer was GAAGAAGTTATTCTCCAAAA; the 5′ asRNA primer was gcgtaatac gactcactataGAAGAAGTTATTCTCCAAAA and the 3′ asRNA primer was GAACAAAGGAAACGGATGAT. For dsRNA A, the 5′ sense RNA primer was gcgtaatacgactcactataGTAGCGCGGTGTATTATACC and the 3′ sense RNA primer was GTACAACGTCAGGTTTACCA; the 5′ asRNA primer was gcgtaatacgactcactataGTACAACGTCAGGTTT ACCA and the 3′ asRNA primer was GTAGCGCGGTGTATTATACC (lowercase, T7 promoter sequence).

mRNAs were 5′ end labeled using guanylyl transferase (Gibco/BRL), S-adenosyl methionine (Sigma), and α-^{32}P-GTP (3000 Ci/mmol; New England Nuclear) according to the manufacturer's directions. Radiolabeled RNAs were purified by poly(A) selection using the Poly(A) Tract III kit (Promega). Nonradioactive 7-methyl-guanosine- and adenosine-capped RNAs were synthesized in in vitro transcription reactions with a 5-fold excess of 7-methyl-G(5′)ppp(5′)G or A(5′)ppp(5′)G relative to GTP. Cap analogs were purchased from New England Biolabs.

ATP Depletion and Protein Synthesis Inhibition

ATP was depleted by incubating the lysate for 10 min at 25°C with 2 mM glucose and 0.1 U/μl hexokinase (Sigma). Protein synthesis inhibitors were purchased from Sigma and dissolved in absolute ethanol as 250-fold concentrated stocks. The final concentrations of inhibitors in the reaction were anisomycin, 53 μg/ml; cycloheximide, 100 μg/ml; and chloramphenicol, 100 mg/ml. Relative protein synthesis was determined by measuring the activity of *Rr* luciferase protein produced by translation of the *Rr*-luc mRNA in the RNAi reaction after 1 hr as described previously (Tuschl et al., 1999).

Analysis of dsRNA Processing

Internally α-^{32}P-ATP-labeled dsRNAs (505 bp *Pp*-luc or 501 *Rr*-luc) or 7-methyl-guanosine-capped *Rr*-luc antisense RNA (501 nt) were incubated at 5 nM final concentration in the presence or absence of unlabeled mRNAs in *Drosophila* lysate for 2 hr in standard conditions. Reactions were stopped by the addition of 2× proteinase K buffer and deproteinized as described previously (Tuschl et al., 1999). Products were analyzed by electrophoresis in 15% or 18% polyacrylamide sequencing gels. Length standards were generated by complete RNase T1 digestion of α-^{32}P-ATP-labeled 501 nt *Rr*-luc sense RNA and asRNA.

For analysis of mRNA cleavage, 5′-^{32}P-radiolabeled mRNA (described above) was incubated with dsRNA as described previously (Tuschl et al., 1999) and analyzed by electrophoresis in 5% (Figure 5B) and 6% (Figure 6C) polyacrylamide sequencing gels. Length standards included commercially available RNA size standards (FMC Bioproducts) radiolabeled with guanylyl transferase as described above and partial base hydrolysis and RNase T1 ladders generated from the 5′-radiolabeled mRNA.

Deamination Assay

Internally α-^{32}P-ATP-labeled dsRNAs (5 nM) were incubated in *Drosophila* lysate for 2 hr at standard conditions. After deproteinization, samples were run on 12% sequencing gels to separate full-length dsRNAs from the 21–23 nt products. RNAs were eluted from the gel slices in 0.3 M NaCl overnight, ethanol precipitated, collected by centrifugation, and redissolved in 20 μl water. The RNA was hydrolyzed into nucleoside 5′ phosphates with nuclease P1 (10 μl reaction containing 8 μl RNA in water, 30 mM KOAc [pH 5.3], 10 mM $ZnSO_4$, and 10 μg or 3 units nuclease P1, for 3 hr at 50°C). Samples (1 μl) were cospotted with nonradioactive 5′ mononucleotides (0.05 O. D. units [A_{260}] of pA, pC, pG, pI, and pU) on cellulose HPTLC plates (EM Merck) and separated in the first dimension in isobutyric acid/25% ammonia/water (66/1/33, v/v/v) and in the second dimension in 0.1 M sodium phosphate, pH 6.8/ammonium sulfate/1-propanol (100/60/2, v/w/v; Silberklang et al., 1979). Migration of the nonradioactive internal standards was determined by UV shadowing.

Acknowledgments

We acknowledge Heike Taubner, Sayda M. Elbashir, and Winfried Lendeckel for assistance, and Herbert Jäckle and his research group and members of the Bartel laboratory for their support and advice. The authors thank Terri Orr-Weaver for providing fly resources and Marlene Castle for maintaining population cages. This work was supported by a German BMBF Biofuture grant number 0311856 (T. T.), by the National Institutes of Health through a United States Public Health Service MERIT award, the National Science Foundation, and partially by the National Cancer Institute through a Cancer Center Support core grant (P. A. S.), and by the Searle Scholars Program/The Chicago Community Trust (D. P. B.).

Received March 2, 2000; revised March 10, 2000.

References

Auxilien, S., Crain, P.F., Trewyn, R.W., and Grosjean, H. (1996). Mechanism, specificity and general properties of the yeast enzyme catalysing the formation of inosine 34 in the anticodon of transfer RNA. J. Mol. Biol. *262*, 437–458.

Bass, B.L. (1997). RNA editing and hypermutation by adenosine deamination [published erratum appears in Trends Biochem Sci. 1997 Jul;22(7):278]. Trends Biochem. Sci. *22*, 157–162.

Baulcombe, D.C. (1999). Fast forward genetics based on virus-induced gene silencing. Curr. Opin. Plant Biol. *2*, 109–113.

Cogoni, C., and Macino, G. (1997). Isolation of quelling-defective (qde) mutants impaired in posttranscriptional transgene-induced

gene silencing in Neurospora crassa. Proc. Natl. Acad. Sci. USA *94*, 10233–10238.

Cogoni, C., and Macino, G. (1999a). Gene silencing in *Neurospora crassa* requires a protein homologous to RNA-dependent RNA polymerase. Nature *399*, 166–169.

Cogoni, C., and Macino, G. (1999b). Posttranscriptional gene silencing in Neurospora by a RecQ DNA helicase. Science *286*, 2342–2344.

Cogoni, C., Irelan, J.T., Schumacher, M., Schmidhauser, T.J., Selker, E.U., and Macino, G. (1996). Transgene silencing of the al-1 gene in vegetative cells of Neurospora is mediated by a cytoplasmic effector and does not depend on DNA-DNA interactions or DNA methylation. EMBO J. *15*, 3153–3163.

Cundliffe, E. (1981). Antibiotic inhibitors of ribosome function. In The Molecular Basis of Antibiotic Action, E. Gale et al., eds. (New York: Wiley), pp. 402–547.

Fire, A. (1999). RNA-triggered gene silencing. Trends Genet. *15*, 358–363.

Fire, A., Xu, S., Montgomery, M.K., Kostas, S.A., Driver, S.E., and Mello, C.C. (1998). Potent and specific genetic interference by double-stranded RNA in *Caenorhabditis elegans*. Nature *391*, 806–811.

Gebauer, F., Corona, D.F., Preiss, T., Becker, P.B., and Hentze, M.W. (1999). Translational control of dosage compensation in Drosophila by Sex-lethal: cooperative silencing via the 5′ and 3′ UTRs of msl-2 mRNA is independent of the poly(A) tail. EMBO J. *18*, 6146–6154.

Grant, S.R. (1999). Dissecting the mechanisms of posttranscriptional gene silencing: divide and conquer. Cell *96*, 303–306.

Grishok, A., Tabara, H., and Mello, C. (2000). Genetic requirements for inheritance of RNAi in *C. elegans*. Science, in press.

Guo, S., and Kemphues, K.J. (1995). par-1, a gene required for establishing polarity in *C. elegans* embryos, encodes a putative Ser/Thr kinase that is asymmetrically distributed. Cell *81*, 611–620.

Hamilton, A.J., and Baulcombe, D.C. (1999). A species of small antisense RNA in posttranscriptional gene silencing in plants. Science *286*, 950–952.

Hunter, C.P. (1999). A touch of elegance with RNAi. Curr. Biol. *9*, R440–R442.

Hunter, C. (2000). Gene silencing: shrinking the black box of RNAi. Curr. Biol. *10*, R137–R140.

Kennerdell, J.R., and Carthew, R.W. (1998). Use of dsRNA-mediated genetic interference to demonstrate that *frizzled* and *frizzled 2* act in the wingless pathway. Cell *95*, 1017–1026.

Ketting, R.F., Haverkamp, T.H., van Luenen, H.G., and Plasterk, R.H. (1999). Mut-7 of *C. elegans*, required for transposon silencing and RNA interference, is a homolog of Werner syndrome helicase and RNaseD. Cell *99*, 133–141.

Kozak, M. (1999). Initiation of translation in prokaryotes and eukaryotes. Gene *234*, 187–208.

Lohmann, J.U., Endl, I., and Bosch, T.C. (1999). Silencing of developmental genes in Hydra. Dev. Biol. *214*, 211–214.

Merrick, W., and Hershey, J. (1996). The pathway and mechanism of eukaryotic protein synthesis. In Translational Control, J. Hershey et al., eds. (Cold Spring Harbor, NY: Cold Spring Harbor Laboratory Press), pp. 31–69.

Misquitta, L., and Paterson, B.M. (1999). Targeted disruption of gene function in Drosophila by RNA interference (RNA-i): a role for nautilus in embryonic somatic muscle formation. Proc. Natl. Acad. Sci. USA *96*, 1451–1456.

Montgomery, M.K., and Fire, A. (1998). Double-stranded RNA as a mediator in sequence-specific genetic silencing and co-suppression. Trends Genet. *14*, 255–258.

Montgomery, M.K., Xu, S., and Fire, A. (1998). RNA as a target of double-stranded RNA-mediated genetic interference in *Caenorhabditis elegans*. Proc. Natl. Acad. Sci. USA *95*, 15502–15507.

Ngo, H., Tschudi, C., Gull, K., and Ullu, E. (1998). Double-stranded RNA induces mRNA degradation in *Trypanosoma brucei*. Proc. Natl. Acad. Sci. USA *95*, 14687–14692.

Page, A.W., and Orr-Weaver, T.L. (1997). Activation of the meiotic divisions in Drosophila oocytes. Dev. Biol. *183*, 195–207.

Qiao, L., Lissemore, J.L., Shu, P., Smardon, A., Gelber, M.B., and Maine, E.M. (1995). Enhancers of glp-1, a gene required for cell-signaling in Caenorhabditis elegans, define a set of genes required for germline development. Genetics *141*, 551–569.

Ratcliff, F.G., MacFarlane, S.A., and Baulcombe, D.C. (1999). Gene silencing without DNA. RNA-mediated cross-protection between viruses. Plant Cell *11*, 1207–1216.

Sánchez-Alvarado, A., and Newmark, P.A. (1999). Double-stranded RNA specifically disrupts gene expression during planarian regeneration. Proc. Natl. Acad. Sci. USA *96*, 5049–5054.

Schiebel, W., Haas, B., Marinkovic, S., Klanner, A., and Sanger, H.L. (1993a). RNA-directed RNA polymerase from tomato leaves. I. Purification and physical properties. J. Biol. Chem. *268*, 11851–11857.

Schiebel, W., Haas, B., Marinkovic, S., Klanner, A., and Sanger, H.L. (1993b). RNA-directed RNA polymerase from tomato leaves. II. Catalytic in vitro properties. J. Biol. Chem. *268*, 11858–11867.

Schiebel, W., Pelissier, T., Riedel, L., Thalmeir, S., Schiebel, R., Kempe, D., Lottspeich, F., Sanger, H.L., and Wassenegger, M. (1998). Isolation of an RNA-directed RNA polymerase-specific cDNA clone from tomato. Plant Cell *10*, 2087–2101.

Sharp, P.A. (1999). RNAi and double-strand RNA. Genes Dev. *13*, 139–141.

Silberklang, M., Gillum, A.M., and RajBhandary, U.L. (1979). Use of in vitro ^{32}P labeling in the sequence analysis of nonradioactive tRNAs. Methods Enzymol. *59*, 58–109.

Smardon, A., Spoerke, J., Stacey, S., Klein, M., Mackin, N., and Maine, E. (2000). EGO-1 is related to RNA-directed RNA polymerase and functions in germ-line development and RNA interference in *C. elegans*. Curr. Biol. *10*, 169–178.

Tabara, H., Sarkissian, M., Kelly, W.G., Fleenor, J., Grishok, A., Timmons, L., Fire, A., and Mello, C.C. (1999). The rde-1 gene, RNA interference, and transposon silencing in *C. elegans*. Cell *99*, 123–132.

Timmons, L., and Fire, A. (1998). Specific interference by ingested dsRNA. Nature *395*, 854.

Tuschl, T., Zamore, P.D., Lehmann, R., Bartel, D.P., and Sharp, P.A. (1999). Targeted mRNA degradation by double-stranded RNA in vitro. Genes Dev. *13*, 3191–3197.

Vaucheret, H., Beclin, C., Elmayan, T., Feuerbach, F., Godon, C., Morel, J.B., Mourrain, P., Palauqui, J.C., and Vernhettes, S. (1998). Transgene-induced gene silencing in plants. Plant J. *16*, 651–659.

Wagner, R., and Sun, L. (1998). Functional genomics: double-stranded RNA poses puzzle. Nature *391*, 744–745.

Wargelius, A., Ellingsen, S., and Fjose, A. (1999). Double-stranded RNA induces specific developmental defects in zebrafish embryos. Biochem. Biophys. Res. Commun. *263*, 156–161.

Waterhouse, P.M., Graham, M.W., and Wang, M.B. (1998). Virus resistance and gene silencing in plants can be induced by simultaneous expression of sense and antisense RNA. Proc. Natl. Acad. Sci. USA *95*, 13959–13964.

Waterhouse, P.M., Smith, N.A., and Wang, M.-B. (1999). Virus resistance and gene silencing: killing the messenger. Trends Plant Sci. *4*, 452–457.

Wianny, F., and Zernicka-Goetz, M. (2000). Specific interference with gene function by double-stranded RNA in early mouse development. Nat. Cell Biol. *2*, 70–75.

Note Added in Proof

Recently, Hammond et al. have shown that ~25 nt RNAs are generated in cultured *Drosophila* S2 cells transfected with *cyclin E* dsRNA (Hammond, S.M., Bernstein, E., Beach, D., and Hannon, G.J. [2000]. Nature *404*, 293–296.

TAB 2

Cell, Vol. 101, 235–238, April 28, 2000, Copyright ©2000 by Cell Press

Double-Stranded RNA as a Template for Gene Silencing

Minireview

Brenda L. Bass*
Department of Biochemistry and
Howard Hughes Medical Institute
University of Utah School of Medicine
Salt Lake City, Utah 84132

When double-stranded RNA (dsRNA) corresponding to a sense and antisense sequence of an endogenous mRNA is introduced into a cell, in organisms ranging from trypanosomes to mice, the cognate mRNA is degraded and the gene is silenced (reviewed in Fire, 1999; Bosher and Labouesse, 2000). This type of posttranscriptional gene silencing (PTGS) was first discovered in *C. elegans* (Fire et al., 1998) and is called RNA interference, or RNAi. RNAi shows many similarities to the PTGS that is sometimes observed when a transgene is introduced into a cell, and the processes seem to require some of the same gene products (Catalanotto et al., 2000; Ketting and Plasterk, 2000). If transgene-induced silencing of an endogenous gene, or cosuppression, also involves dsRNA, somehow the cell must make both sense and antisense copies of the transgene sequence.

PTGS has captured the interest (and imagination) of geneticists and molecular biologists alike, and now the first clues about its mechanism will certainly bring the biochemists into the fold. As is often the case for biological processes, the first hint about the mechanism comes from the identification of molecules that appear to be reaction intermediates. In particular, several recent papers report the identification of small RNA molecules, 21–25 nucleotides in length (21- to 25-mers), that correspond to sense and antisense pieces of the dsRNA or transgene introduced into the cell.

Evidence that Small RNAs Are Required for Certain Types of PTGS

Consistent with the idea that the sense and antisense 21- to 25-mers are important for transgene-induced PTGS, they are observed in plants containing transgenes that induce silencing but are notably absent from plants whose transgenes are expressed normally (Hamilton and Baulcombe, 1999). A correlation with dsRNA-induced silencing is provided by the recent report of a nuclease activity isolated from cultured *Drosophila* S2 cells that had been transfected with dsRNA to initiate RNAi (Hammond et al., 2000). The partially purified nuclease degrades RNA in a manner consistent with the degradation known to occur during RNAi—it is sequence specific and will only degrade RNAs matching one of the strands of the dsRNA used to transfect the S2 cells. The nuclease activity was partially purified from cells that had been transfected with dsRNA, but dsRNA was not added to in vitro assays of the partially purified nuclease. So, how did the nuclease know which mRNA to degrade? Sure enough, the small 21- to 25-mers copurify with the nuclease, suggesting that these pieces somehow template degradation of the mRNA. Further, if the S2 extracts are treated with micrococcal nuclease prior to adding the mRNA, RNAi is not observed. Although micrococcal nuclease will degrade both DNA and RNA, treatment of the extract with DNase did not abrogate RNAi, suggesting it was the loss of the small RNAs that led to the loss of RNAi. (Carrier tRNA did not relieve the inhibition, suggesting micrococcal nuclease was not merely competing for nucleic acid binding.)

Further pieces of the puzzle are provided by beautiful work from a collaborative effort of Phil Zamore, Tom Tuschl, Phil Sharp, and David Bartel, published in the March 31, 2000, issue of *Cell* (Zamore et al., 2000). It was these authors who first reported RNAi could work in vitro (Tuschl et al., 1999), and this more recent study continues the characterization of their system, a cell-free extract made from syncytial blastoderm *Drosophila* embryos. In contrast to the S2 extracts, these extracts are prepared from cells that have not been previously treated with dsRNA. Rather, RNAi is performed from start to finish in a cell-free system, allowing the authors to radioactively label the dsRNA and mRNA and monitor the fate of both molecules.

In the presence or absence of the targeted mRNA, the authors find that a portion of the dsRNA is cleaved to the small pieces, and here the length of the molecules is mapped to 21–23 nucleotides. Radioactive 21- to 23-mers are observed when either the sense or antisense strand of the dsRNA is radiolabeled, verifying that both strands are cleaved, and implicating a dsRNA nuclease in the process.

The most exciting observations are made when the authors monitor the fate of the mRNA in the presence or absence of cognate dsRNA. The mRNA is degraded only in the presence of the dsRNA and only within the sequences spanned by the dsRNA. Remarkably, cleavage sites within the mRNA occur at specific sites, spaced 21–23 nucleotides apart, again suggesting cleavage was somehow templated by the small pieces of the dsRNA. After electrophoresis on a sequencing gel, a 5′ end-labeled mRNA appears as a ladder of bands at 21–23 nucleotide intervals, suggesting that each mRNA in the population is cleaved only once or twice. (Since the mRNA is radiolabeled only at its 5′ end, cleavage of each mRNA at every 21–23 nucleotide interval would result in an autoradiogram showing only the most 5′ 21–23 nucleotide piece.) The cleavage of the mRNA is unaffected by several translation inhibitors but is ATP dependent.

A Model for mRNA Degradation by RNAi

Figure 1 presents a model for how mRNA is degraded during RNAi. The model is based on the recent observations discussed above and shows how small pieces of dsRNA could direct cleavage of mRNA in a sequence-specific and catalytic manner. As shown, when dsRNA is introduced into a cell it would be targeted by a dsRNA endonuclease to generate short dsRNA pieces, ~23 nucleotides long (Figure 1A: sense strand, blue; antisense, red). Since the short RNAs copurify with the nuclease of S2 cells (Hammond et al., 2000) and are proposed to

*E-mail: bbass@howard.genetics.utah.edu.

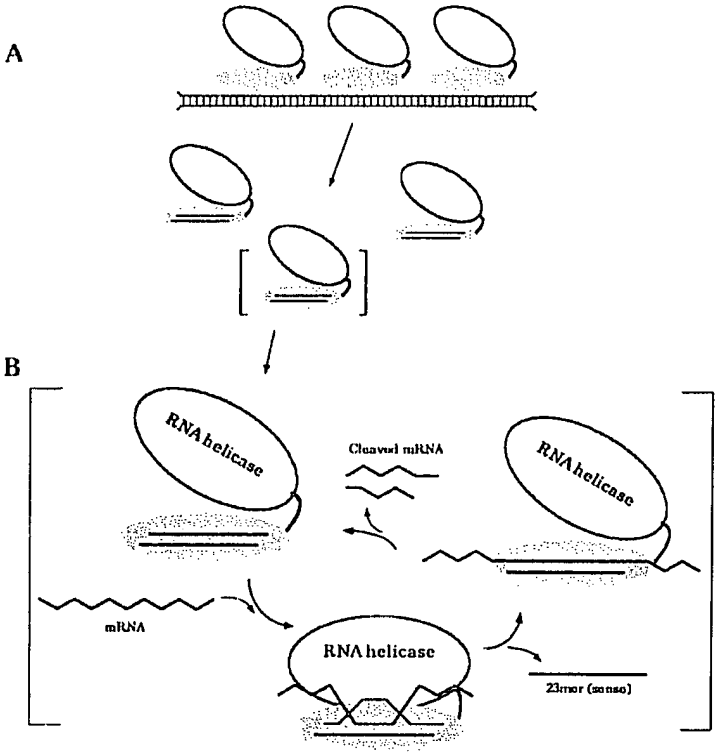

Figure 1. A Model for the Mechanism of mRNA Degradation by RNAi

The reaction is catalyzed by a hypothetical enzyme (RNAi nuclease) that contains a dsRNA binding domain (gray oval), one or more ribonuclease domains (yellow), and an RNA helicase domain (red oval). In the first step (A), the dsRNA that initiates RNAi is bound by the RNAi nuclease and degraded to small dsRNAs that remain stably bound to the RNAi nuclease (blue, sense strands and red, antisense strands). In the second step (B), these small pieces template sequence-specific cleavage of the mRNA. The helicase domain of the protein catalyzes an ATP-dependent strand exchange that replaces the sense strand of the small dsRNA template with the mRNA. The mRNA is then cleaved to regenerate the RNAi nuclease with its small dsRNA. In (A), the enzymes are proposed to coat the dsRNA in a precise register to generate specific fragments that would direct cleavage of the mRNA at specific sites.

serve a templating function, the model depicts the pieces remaining bound to a dsRNA binding domain (gray) of the enzyme. The protein–RNA complex would be in equilibrium with free RNA and protein, but according to the model the complex would be the most stable species and predominate.

In the in vitro system of Zamore and Tuschl, the targeted mRNA is cleaved at sites that are also ~23 nucleotides apart, so the model assumes the dsRNA and mRNA are cleaved by the same enzyme. As shown in Figure 1B, in the next step the mRNA (blue zigzag) must exchange with the 23 nucleotide "sense" strand (blue line) of the short dsRNA. During strand exchange, the 23 nucleotide sense strand dissociates from the enzyme and is replaced by the mRNA. The mRNA is positioned just like the original sense strand of the dsRNA and cleaved at the same sites by the ribonuclease active site(s) (yellow). Importantly, cleavage of the mRNA regenerates the nuclease just as it was when the cycle began, bound to the short sense and antisense pieces. Thus, in the model of Figure 1, the nuclease is able to carry out endless rounds of strand exchange and cleavage, perhaps explaining why RNAi appears to act catalytically (see below).

Although strand exchange between a dsRNA and one of its strands will occur slowly without a catalyst, to occur on a biological time scale the reaction probably requires catalysis. Because Zamore et al. (2000) find that cleavage of the mRNA requires ATP, the model shown in Figure 1 invokes an RNA-dependent ATPase, or RNA helicase (reviewed in de la Cruz et al., 1999). For reasons discussed below, Figure 1B shows strand exchange catalyzed by a helicase domain of the same protein that catalyzes cleavage, but the two activities could exist in separate molecules.

In theory, there are two ways that strand exchange could occur. Strand exchange could occur by a dissociative mechanism, where the dsRNA strands first dissociate completely, making the antisense strand accessible for subsequent hybridization with the mRNA (e.g., see Figure 7, Zamore et al., 2000). Alternatively, strand exchange could occur by an associative mechanism, where the mRNA somehow forms a close association with the base-paired dsRNA and invades the duplex to allow annealing. Figure 1B shows the associative type of strand exchange, since it seems most consistent with the observation that both sense and antisense strands copurify with the nuclease of *Drosophila* S2 cells, as well as the fact that this type of strand exchange appears to be operative in vitro (Homann et al., 1996).

Does PTGS by dsRNA Involve an RNase III-Like Enzyme?

Although the identity of the RNAi nuclease has not been determined, the characteristics of the short 21–25 nucleotide RNA pieces suggest they were generated by RNase III or a highly related enzyme (see Rotondo et al., 1997; Abou Elela and Ares, 1998, and references therein). RNase III is the only characterized nuclease known to cleave dsRNA at specific sites to generate dsRNA fragments of discrete sizes. For RNase III to stably bind a dsRNA, it must be at least two helical-turns in length, consistent with the observation that RNAi and transgene-induced silencing yield stable fragments of ~22 base pairs. RNase III can produce fragments

<22 base pairs from a longer dsRNA, but these shorter fragments themselves do not bind well to RNase III. In the context of the model of Figure 1, fragments less than 21–23 base pairs would not have been observed in the recent experiments because they would not remain stably bound to the enzyme and thus would be more accessible to degradation by other cellular nucleases.

Given the similarities between the cleavage products of RNase III and the RNAi nuclease, I have incorporated properties of the RNase III enzymes into the model of Figure 1. For example, RNase III makes staggered cuts that leave 3′ overhangs of two base pairs, as shown for the 23-mers of Figure 1. If RNAi involves an RNase III-like enzyme, it might explain why the small RNAs observed by Zamore and Tuschl range from 21–23 nucleotides. The initial cleavage might produce dsRNAs comprised of sense and antisense 23-mers, but the 3′ overhangs would be more accessible to single-strand-specific nucleases present in the extract, and trimmed to 21 and 22 nucleotide pieces. Zamore and Tuschl observe that cleavage of the dsRNA, unlike mRNA cleavage, does not absolutely require ATP. However, dsRNA cleavage is faster in the presence of ATP, and without ATP the pieces are predominantly the longer 23-mers. Certainly this is a clue to the role of ATP in this in vitro reaction, but at present its meaning is unclear.

The bacterial and yeast RNase III enzymes have similar open reading frame (ORF) structures, with a ribonuclease domain followed by a C-terminal motif known as a dsRNA binding motif (dsRBM). Database searches show that sequences encoding this ORF structure are also present in metazoa, and intriguingly, reveal a second group of ORFs with an RNA helicase domain, N-terminal of the ribonuclease domain and dsRBM (as noted in Rotondo et al., 1997, and references therein). Genes encoding ORFs with such a structure exist for many organisms, including *Caenorhabditis* (K12H4.8, L14331), *Drosophila* (CG4792, AE003740), humans (AB028449), and *Arabidopsis* (AF187317). Such proteins would be ideal for catalyzing the reactions shown in Figure 1 and formed the basis for the hypothetical enzyme invoked in the model.

Is RNAi Self-Propagating, and If So Why Doesn't It Last Forever?

PTGS by dsRNA has a remarkable ability to cross cell boundaries (Fire et al., 1998) and can even be passed to subsequent generations in a process that occurs via a dominant extragenic agent, possibly the small dsRNA molecules described here (Grishok et al., 2000). However, dsRNA-induced gene silencing is not maintained forever, presumably because the extragenic agent is diluted by cell division and degradation. Calculations that take into account the dilution of injected dsRNA by cell division suggest that small amounts of dsRNA can target degradation of many mRNAs (Fire et al., 1998). In the mechanism shown in Figure 1B, the enzyme bound to its small dsRNA template is regenerated with each round of annealing and cleavage, which could explain how RNAi appears to act catalytically.

RNAi may also involve amplification of the dsRNA signal by an RNA-dependent RNA polymerase (RdRP), and genes encoding proteins with sequence similarity to RdRPs are important for PTGS in both *C. elegans* (Smardon et al., 2000) and *Neurospora* (Cogoni and Macino, 1999). The model proposed in Figure 1 does not at all preclude amplification by an RdRP, and the involvement of such a polymerase could also help explain how sense and antisense transcripts might derive from a single transgene.

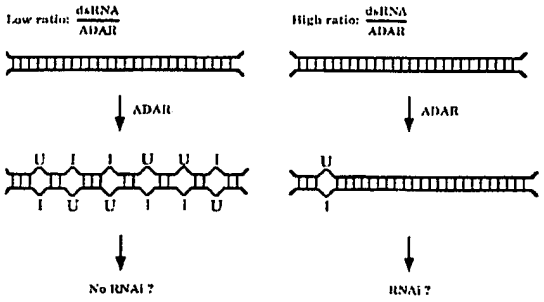

Figure 2. High Levels of ADARs Are Predicted to Antagonize RNAi

Regardless of whether there are cellular mechanisms that allow amplification of the signal, RNAi works better, in vivo and in vitro, when more dsRNA is used to initiate the process. Assuming the small 21- to 25-mer dsRNAs are the extragenic agent that propagates PTGS from one cell to the next, and to offspring, this makes sense, at least for in vivo experiments. More dsRNA would produce more 21- to 25-mer dsRNA and allow the effect to better survive dilution by cell division.

Another reason why more dsRNA might work better is that putative dsRNA binding proteins (dsRBPs) required for RNAi would have to compete with other cellular dsRBPs for the dsRNA. dsRBPs have little sequence specificity, and although they often bind very tightly to dsRNA, they will bind to any dsRNA; a substrate for one dsRBP is a substrate for all dsRBPs. In fact, Zamore and Tuschl demonstrate that their extracts contain adenosine deaminases that act on RNA (ADARs), dsRBPs that convert adenosines to inosines within dsRNA (see Morse and Bass, 1999, and references therein). Full-length dsRNA molecules that remain after incubation in the extract show 3%–6% of their adenosines deaminated, while only 0.4%–0.7% of the adenosines in the 21- to 23-mers appear as inosine. Although ADARs will deaminate 50%–60% of the adenosines in long, completely base-paired RNA of the type typically used in RNAi experiments, they are very sensitive to substrate inhibition (Hough and Bass, 1994). Given the high concentrations of RNA used by Zamore et al., as well as in most RNAi experiments, the low amounts of deamination are as expected.

Zamore and Tuschl previously showed that a large excess of dsRNA is required for optimal RNAi in their *Drosophila* cell-free system (Tuschl et al., 1999), and possibly this is due to the presence of ADARs in the extract. Since inosines, like guanosines, prefer to base pair with cytidine, ADARs change RNA sequence (A→I), as well as RNA structure (AU base pair→IU mismatch; Figure 2). At low concentrations of dsRNA, ADARs would promiscuously deaminate the dsRNA so it would no longer be homologous to the targeted mRNA; further, because of its increased single-stranded character, it would not be recognized by dsRBPs involved in RNAi.

Assuming RNAi requires the small 21- to 23-mers to bind a dsRBM as shown in Figure 1, it would make sense that few inosines would be present in this population. Although the tissue specificity of ADARs in *C. elegans* is not yet known, if like other organisms the enzyme is highest in neural tissues, this may explain why many worm neuronal genes are refractory to RNAi.

Concluding Remarks

The in vitro observations of Zamore et al. (2000) have not yet been directly connected to RNAi in vivo. In fact, given the intrinsic activities of RNase III and helicases, if the dsRNA and mRNA used in the Zamore et al. study were simply mixed with these enzymes, similar cleavage products might be observed. In this light, it could be argued that the reactions occurring in the extract are unrelated to RNAi and merely reflect that *Drosophila* embryos contain RNase III and helicases. However, since similar 21–25 nucleotide RNA pieces have now been observed in multiple systems and shown to strongly correlate with PTGS in plants, these worries seem unjustified. Regardless, future studies, perhaps using extracts made from strains containing mutations known to affect RNAi, will be important to verify the relevance of the in vitro observations.

Existing studies suggest that RNAi represents a complex set of phenomena, and the data discussed here focus on only one of these—the dsRNA-induced degradation of mRNA. As mentioned, genes encoding proteins with sequence similarity to RdRP have been implicated in PTGS; the model of Figure 1 does not preclude the involvement of these proteins. Several other genes have been identified that appear to be required for RNAi (Ketting et al., 1999; Tabara et al., 1999; reviewed in Bosher and Labouesse, 2000). The identity of only a subset of these is known, and so far, none are the RNase III enzymes discussed here. Although the idea that RNase III–type enzymes are involved in RNAi is compelling, the basic mechanism proposed in Figure 1 could be catalyzed by other proteins. In fact, among the genes identified as important for RNAi are those with homologies to other ribonucleases (*C. elegans mut-7*, Ketting et al., 1999) and helicases (*Neurospora qde-3*; see citations in Zamore et al., 2000). It even seems possible that different cells and tissue types carry out RNAi with overlapping but distinct factors, as already suggested by comparisons of PTGS in germline and soma.

The model of Figure 1 predicts that introducing 21- to 25-mer dsRNAs into a cell should trigger gene silencing, but so far all RNAi systems require dsRNAs greater than ~100 base pairs for efficient inhibition of gene expression. (Although possibly the 21- to 23-mer RNAs work in vitro [Zamore et al., 2000]). A given molar amount of a shorter dsRNA would yield fewer 21- to 25-mers, and this may explain their lower efficacy. However, it is also possible that the length requirement derives from another factor involved in RNAi, for example the putative RdRP.

There are still many mysteries about the mechanism of PTGS, but we know enough to consider the tantalizing possibility that dsRNA is an important signaling molecule in this process. While studies of PTGS usually involve introducing an exogenous sequence into a cell, either a transgene or dsRNA, it seems likely that PTGS reflects a natural biological process. Some of the genes identified as important for RNAi are also important for silencing transposon hopping in the germline (Ketting et al., 1999; Tabara et al., 1999), raising the possibility that dsRNA plays a more general role in gene silencing.

Acknowledgments

I am grateful to M. Ares, S. Knight, D. Morse, and E.G.H. Wagner for helpful discussions and apologize to those whose relevant publications could not be cited due to space limitations. Thanks to O. Uhlenbeck and M. Wickens for critically reading the manuscript and M. Beckerle and R. Benezra for their offices and patience.

Selected Reading

Abou Elela, S., and Ares, M., Jr. (1998). EMBO J. *17*, 3738–3746.

Bosher, J.M., and Labouesse, M. (2000). Nat. Cell Biol. *2*, E31–E36.

Catalanotto, C., Azzalin, G., Macino, G., and Cogoni, C. (2000). Nature *404*, 245.

Cogoni, C., and Macino, G. (1999). Nature *399*, 166–169.

de la Cruz, J., Kressler, D., and Linder, P. (1999). Trends Biochem. Sci. *24*, 192–198.

Fire, A. (1999). Trends Genet. *15*, 358–363.

Fire, A., Xu, S., Montgomery, M.K., Kostas, S.A., Driver, S.E., and Mello, C.C. (1998). Nature *391*, 806–811.

Grishok, A., Tabara, H., and Mello, C.C. (2000). Science *287*, 2494–2497.

Hamilton, A.J., and Baulcombe, D.C. (1999). Science *286*, 950–952.

Hammond, S.M., Bernstein, E., Beach, D., and Hannon, G.J. (2000). Nature *404*, 293–296.

Homann, M., Nedbal, W., and Sczakiel, G. (1996). Nucleic Acids Res. *24*, 4395–4400.

Hough, R.F., and Bass, B.L. (1994). J. Biol. Chem. *269*, 9933–9939.

Ketting, R.F., and Plasterk, R.H.A. (2000). Nature *404*, 296–298.

Ketting, R.F., Haverkamp, T.H., van Luenen, H.G., and Plasterk, R.H. (1999). Cell *99*, 133–141.

Morse, D.P., and Bass, B.L. (1999). Proc. Natl. Acad. Sci. USA *96*, 6048–6053.

Rotondo, G., Huang, J.Y., and Frendewey, D. (1997). RNA *3*, 1182–1193.

Smardon, A., Spoerke, J.M., Stacey, S.C., Klein, M.E., Mackin, N., and Maine, E.M. (2000). Curr. Biol. *10*, 169–178.

Tabara, H., Sarkissian, M., Kelly, W.G., Fleenor, J., Grishok, A., Timmons, L., Fire, A., and Mello, C.C. (1999). Cell *99*, 123–132.

Tuschl, T., Zamore, P.D., Lehmann, R., Bartel, D.P., and Sharp, P.A. (1999). Genes Dev. *13*, 3191–3197.

Zamore, P.D., Tuschl, T., Sharp, P.A., and Bartel, D.P. (2000). Cell *101*, 25–33.

TAB 3

ogy), respectively. Staining specificity was controlled by single staining, as well as by using secondary antibodies in the absence of the primary stain.

Generation of target cells

Target cells displaying a membrane-integral version of either wild-type HEL or a mutant[10] exhibiting reduced affinity for HyHEL10 ([R^{21}, D^{101}, G^{102}, N^{103}] designated HEL*) were generated by transfecting mouse J558L plasmacytoma cells with constructs analogous to those used[10] for expression of soluble HEL/HEL*, except that 14 Ser/Gly codons, the $H2K^b$ transmembrane region, and a 23-codon cytoplasmic domain were inserted immediately upstream of the termination codon by polymerase chain reaction. For mHEL–GFP, we included the EGFP coding domain in the Ser/Gly linker. Abundance of surface HEL was monitored by flow cytometry and radiolabelled-antibody binding using HyHEL5 and D1.3 HEL-specific monoclonal antibodies, for which the mutant HELs used in this work show unaltered affinities[10].

Interaction assays

For B-cell/target interaction assays, splenic B cells from 3-83 or MD4 transgenic mice[28,29] carrying (IgM + IgD) BCRs specific for HEL or $H2K^k/H2K^b$were freshly purified on Lympholyte and incubated with a twofold excess of target cells in RPMI, 50 mM HEPES pH 7.4, for the appropriate time at 37 °C before being applied to polylysine-coated slides. Cells were fixed in 4% paraformaldehyde/PBS or methanol and permeabilized with PBS/0.1% Triton X-100 before immunofluorescence. We acquired confocal images using a Nikon E800 microscope attached to BioRad Radiance Plus scanning system equipped with 488-nm and 543-nm lasers, as well as differential interference contrast for transmitted light. GFP fluorescence in living cells in real time was visualized using a Radiance 2000 and Nikon E300 inverted microscope. Images were processed using BioRad Lasersharp 1024 or 2000 software to provide single plane images, confocal projections or slicing.

Antigen presentation

Presentation of HEL epitopes to T-cell hybridomas 2G7 (specific for I-E^k[HEL^{1-18}]) and 1E5 (specific for I-E^d[$HEL^{108-116}$]) by transfectants of the LK35.2 B-cell hybridoma expressing an HEL-specific IgM BCR was monitored as described[10].

Received 12 December 2000; accepted 30 March 2001.

1. Lanzavecchia, A. Antigen-specific interaction between T and B cells. *Nature* **314**, 537–539 (1985)
2. Klaus, G. G., Humphrey, J. H., Kunkl, A. & Dongworth, D. W. The follicular dendritic cell: its role in antigen presentation in the generation of immunological memory. *Immunol. Rev.* **53**, 3–28 (1980).
3. Tew, J. G., Kosco, M. H., Burton, G. F. & Szakal, A. K. Follicular dendritic cells as accessory cells. *Immunol. Rev.* **117**, 185–211 (1990).
4. Kosco-Vilbois, M. H., Gray, D., Scheidegger, D. & Julius, M. Follicular dendritic cells help resting B cells to become effective antigen-presenting cells: induction of B7/BB1 and upregulation of major histocompatibility complex class II molecules. *J. Exp. Med.* **178**, 2055–2066 (1993)
5. Schamel, W. W. & Reth, M. Monomeric and oligomeric complexes of the B cell antigen receptor. *Immunity* **13**, 5–14 (2000).
6. Taylor, R. B., Duffus, W. P. H., Raff, M. C. & de Petris, S. Redistribution and pinocytosis of lymphocyte surface immunoglobulin molecules induced by anti-immunoglobulin antibody. *Nature* **233**, 225–227 (1971).
7. Schreiner, G. F. & Unanue, E. R. Capping and the lymphocyte: models for membrane reorganisation. *J. Immunol.* **119**, 1549–1551 (1977).
8. Cheng, P. C., Dykstra, M. L., Mitchell, R. N. & Pierce, S. K. A role for lipid rafts in B cell antigen receptor signaling and antigen targeting. *J. Exp. Med.* **190**, 1549–1560 (1999).
9. Weintraub, B. C. *et al.* Entry of B cell receptor into signaling domains is inhibited in tolerant B cells. *J. Exp. Med.* **191**, 1443–1448 (2000).
10. Batista, F. D. & Neuberger, M. S. Affinity dependence of the B cell response to antigen: a threshold, a ceiling, and the importance of off-rate. *Immunity* **8**, 751–759 (1998).
11. Nemazee, D. & Burki, K. Clonal deletion of B lymphocytes in a transgenic mouse bearing anti-MHC class I antibody genes. *Nature* **337**, 562–566 (1989).
12. Hartley, S. B. *et al.* Elimination from peripheral lymphoid tissues of self-reactive B lymphocytes recognizing membrane-bound antigens. *Nature* **353**, 765–769 (1991).
13. Dustin, M. L. *et al.* Low affinity interaction of human and rat T cell adhesion molecule CD2 with its ligands aligns adhering membranes to achieve high physiological affinity. *J. Biol. Chem.* **272**, 30889–30898 (1997).
14. Lang, J. *et al.* B cells are exquisitely sensitive to central tolerance and receptor editing by ultralow affinity, membrane-bound antigen. *J. Exp. Med.* **184**, 1685–1697 (1996).
15. Valitutti, S., Muller, S., Cella, M., Padovan, E. & Lanzavecchia, A. Serial triggering of many T-cell receptors by a few peptide–MHC complexes. *Nature* **375**, 148–151 (1995).
16. Monks, C. R., Freiberg, B. A., Kupfer, H., Sciaky, N. & Kupfer, A. Three-dimensional segregation of supramolecular activation clusters in T cells *Nature* **395**, 82–86 (1998).
17. Wulfing, C. & Davis, M. M. A receptor/cytoskeletal movement triggered by costimulation during T cell activation. *Science* **282**, 2266–2269 (1998).
18. Grakoui, A. *et al.* The immunological synapse: a molecular machine controlling T cell activation *Science* **285**, 221–227 (1999).
19. Leupin, O., Zaru, R., Laroche, T., Muller, S. & Valitutti, S. Exclusion of CD45 from the T-cell receptor signaling area in antigen-stimulated T lymphocytes. *Curr. Biol.* **10**, 277–280 (2000).
20. Cagan, R. L., Kramer, H., Hart, A. C. & Zipursky, S. L. The bride of sevenless and sevenless interaction: internalization of a transmembrane ligand. *Cell* **69**, 393–399 (1992).
21. Huang, J. F. *et al.* TCR-mediated internalization of peptide–MHC complexes acquired by T cells. *Science* **286**, 952–954 (1999).
22. Hwang, I. *et al.* T cells can use either T cell receptor or CD28 receptors to absorb and internalize cell surface molecules derived from antigen-presenting cells. *J. Exp. Med.* **191**, 1137–1148 (2000)
23. Batista, F. D. & Neuberger, M. S. B cells extract and present immobilized antigen: implications for affinity discrimination. *EMBO J.* **19**, 513–520 (2000).
24. Casten, L. A., Lakey, E. K., Jelachich, M. L., Margoliash, E. & Pierce, S. K. Anti-immunoglobulin augments the B-cell antigen-presentation function independently of internalization of receptor-antigen complex. *Proc. Natl Acad. Sci. USA* **82**, 5890–5894 (1985).
25. Siemasko, K., Eisfelder, B. J., Williamson, E., Kabak, S. & Clark, M. R. Signals from the B lymphocyte antigen receptor regulate MHC class II containing late endosomes. *J. Immunol.* **160**, 5203–5208 (1998).
26. Serre, K. *et al.* Efficient presentation of multivalent antigens targeted to various cell surface molecules of dendritic cells and surface Ig of antigen-specific B cells. *J. Immunol.* **161**, 6059–6067 (1998).
27. Green, S. M., Lowe, A. D., Parrington, J. & Karn, J. Transformation of growth factor-dependent myeloid stem cells with retroviral vectors carrying c-myc. *Oncogene* 737–751 (1989).
28. Russell, D. M. *et al.* Peripheral deletion of self-reactive B cells. *Nature* **354**, 308–311 (1991).
29. Goodnow, C. C. *et al.* Altered immunoglobulin expression and functional silencing of self-reactive B lymphocytes in transgenic mice. *Nature* **334**, 676–682 (1988).
30. Aluvihare, V. R., Khamlichi, A. A., Williams, G. T., Adorini, L. & Neuberger, M. S. Acceleration of intracellular targeting of antigen by the B-cell antigen receptor: importance depends on the nature of the antigen-antibody interaction. *EMBO J.* **16**, 3553–3562 (1997).

Supplementary information is available on *Nature*'s World-Wide Web site (http://www.nature.com) or as paper copy from the London editorial office of *Nature*.

Acknowledgements

We thank B. Amos and S. Reichelt for help and advice with confocal microscopy, and S. Munro for helpful discussions. We are indebted those who provided antibodies, transgenic mice and cell lines. F.D.B. and D.I. were supported by the Arthritis Research Campaign and Studienstiftung des deutschen Volkes, respectively.

Correspondence and requests for materials should be addressed to F.D.B. (e-mail:fdb@mrc-lmb.cam.ac.uk) or M.S.N. (e-mail:msn@mrc-lmb.cam.ac.uk)

Duplexes of 21-nucleotide RNAs mediate RNA interference in cultured mammalian cells

Sayda M. Elbashir*, Jens Harborth†, Winfried Lendeckel*, Abdullah Yalcin*, Klaus Weber† & Thomas Tuschl*

** Department of Cellular Biochemistry; and † Department of Biochemistry and Cell Biology, Max-Planck-Institute for Biophysical Chemistry, Am Fassberg 11, D-37077 Göttingen, Germany*

RNA interference (RNAi) is the process of sequence-specific, post-transcriptional gene silencing in animals and plants, initiated by double-stranded RNA (dsRNA) that is homologous in sequence to the silenced gene[1–4]. The mediators of sequence-specific messenger RNA degradation are 21- and 22-nucleotide small interfering RNAs (siRNAs) generated by ribonuclease III cleavage from longer dsRNAs[5–9]. Here we show that 21-nucleotide siRNA duplexes specifically suppress expression of endogenous and heterologous genes in different mammalian cell lines, including human embryonic kidney (293) and HeLa cells. Therefore, 21-nucleotide siRNA duplexes provide a new tool for studying gene function in mammalian cells and may eventually be used as gene-specific therapeutics.

Uptake of dsRNA by insect cell lines has previously been shown to 'knock-down' the expression of specific proteins, owing to sequence-specific, dsRNA-mediated mRNA degradation[6,10–12]. However, it has not been possible to detect potent and specific RNA interference in commonly used mammalian cell culture systems, including 293 (human embryonic kidney), NIH/3T3 (mouse fibroblast), BHK-21 (Syrian baby hamster kidney), and CHO-K1 (Chinese hamster ovary) cells, applying dsRNA that varies in size between 38 and 1,662 base pairs (bp)[10,12]. This apparent lack of RNAi in mammalian cell culture was unexpected, because RNAi exists in mouse oocytes and early embryos[13,14], and because RNAi-related, transgene-mediated co-suppression was also observed in cultured Rat-1 fibroblasts[15]. But it is known that dsRNA in the cytoplasm of mammalian cells can trigger profound physiological

reactions that lead to the induction of interferon synthesis[16]. In the interferon response, dsRNA > 30 bp binds and activates the protein kinase PKR[17] and 2′,5′-oligoadenylate synthetase (2′,5′-AS)[18]. Activated PKR stalls translation by phosphorylation of the translation initiation factors eIF2α, and activated 2′,5′-AS causes mRNA degradation by 2′,5′-oligoadenylate-activated ribonuclease L. These responses are intrinsically sequence-nonspecific to the inducing dsRNA.

Base-paired 21- and 22-nucleotide (nt) siRNAs with overhanging 3′ ends mediate efficient sequence-specific mRNA degradation in lysates prepared from *Drosophila* embryos[9]. To test whether siRNAs are also capable of mediating RNAi in cell culture, we synthesized 21-nt siRNA duplexes with symmetric 2-nt 3′ overhangs directed against reporter genes coding for sea pansy (*Renilla reniformis*, RL) and two sequence variants of firefly (*Photinus pyralis*, GL2 and GL3) luciferases (Fig. 1a, b). The siRNA duplexes were co-transfected with the reporter plasmid combinations pGL2/pRL or pGL3/pRL, into *Drosophila* S2 cells or mammalian cells using cationic liposomes. Luciferase activities were determined 20 h after transfection. In *Drosophila* S2 cells (Fig. 2a and b), the specific inhibition of luciferases was complete and similar to results previously obtained for longer dsRNAs[6,10,12,19]. In mammalian cells, where the reporter genes were 50- to 100-fold more strongly expressed, the specific suppression was less complete (Fig. 2c–j). In NIH/3T3, monkey COS-7 and Hela S3 cells (Fig. 2c–h), GL2 expression was reduced 3- to 12-fold, GL3 expression 9- to 25-fold, and RL expression 2- to 3-fold, in response to the cognate siRNAs. For 293 cells, targeting of RL luciferase by RL siRNAs was ineffective, although GL2 and GL3 targets responded specifically (Fig. 2i and j). The lack of reduction of RL expression in 293 cells may be because of its expression, 5- to 20-fold higher than any other mammalian cell line tested and/or to limited accessibility of the target sequence due to RNA secondary structure or associated proteins. Nevertheless, specific targeting of GL2 and GL3 luciferase by the cognate siRNA duplexes indicated that RNAi is also functioning in 293 cells.

The 2-nucleotide 3′ overhang in all siRNA duplexes was composed of (2′-deoxy) thymidine, except for uGL2, which contained

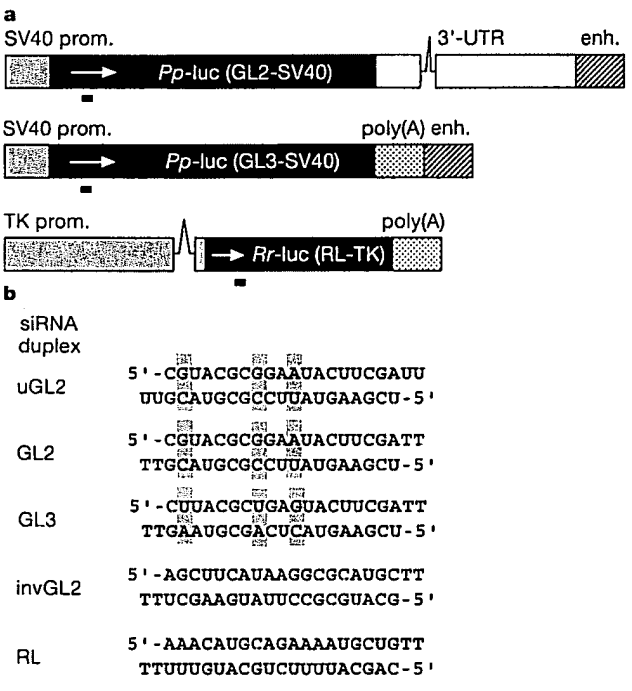

Figure 1 Reporter constructs and siRNA duplexes. **a**, The firefly (*Pp*-luc) and sea pansy (*Rr*-luc) luciferase reporter-gene regions from plasmids pGL2-Control, pGL3-Control, and pRL-TK (Promega) are illustrated; simian virus 40 (SV40) promoter (prom.); SV40 enhancer element (enh.); SV40 late polyadenylation signal (poly(A)); herpes simplex virus (HSV) thymidine kinase promoter, and two introns (lines) are indicated. The sequence of GL3 luciferase is 95% identical to GL2, but RL is completely unrelated to both. Luciferase expression from pGL2 is approximately 10-fold lower than from pGL3 in transfected mammalian cells. The region targeted by the siRNA duplexes is indicated as black bar below the coding region of the luciferase genes. **b**, The sense (top) and antisense (bottom) sequences of the siRNA duplexes targeting GL2, GL3, and RL luciferase are shown. The GL2 and GL3 siRNA duplexes differ by only three single-nucleotide substitutions (boxed in grey). As nonspecific control, a duplex with the inverted GL2 sequence, invGL2, was synthesized. The 2-nucleotide 3′ overhang of 2′-deoxythymidine is indicated as TT; uGL2 is similar to GL2 siRNA but contains ribo-uridine 3′ overhangs.

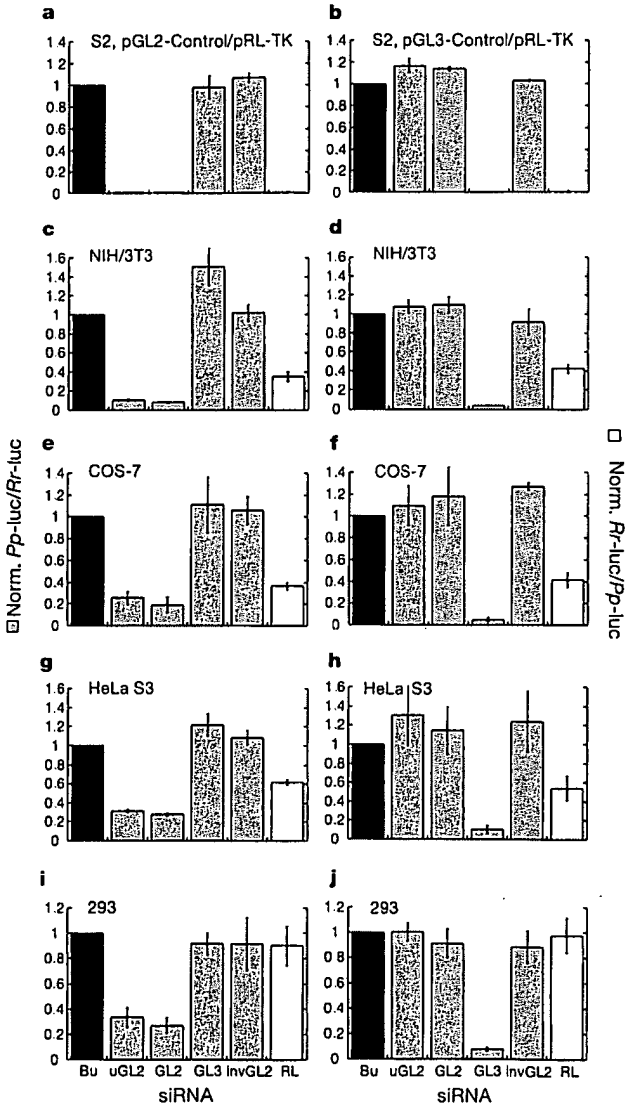

Figure 2 RNA interference by siRNA duplexes. Ratios of target to control luciferase were normalized to a buffer control (Bu, black bars); grey bars indicate ratios of *Photinus pyralis* (*Pp*-luc) GL2 or GL3 luciferase to *Renilla reniformis* (*Rr*-luc) RL luciferase (left axis), white bars indicate RL to GL2 or GL3 ratios (right axis). **a**, **c**, **e**, **g** and **i**, Experiments performed with the combination of pGL2-Control and pRL-TK reporter plasmids; **b**, **d**, **f**, **h** and **j**, experiments performed with the combination of pGL3-Control and pRL-TK reporter plasmids. The cell line used for the interference experiment is indicated at the top of each plot. The ratios of *Pp*-luc/*Rr*-luc for the buffer control (Bu) varied between 0.5 and 10 for pGL2/pRL, and between 0.03 and 1 for pGL3/pRL, respectively, before normalization and between the various cell lines tested. The plotted data were averaged from three independent experiments ± s.d.

uridine residues. The thymidine overhang was chosen because it reduces costs of RNA synthesis and may enhance nuclease resistance of siRNAs in the cell culture medium and within transfected cells. As in the *Drosophila in vitro* system (data not shown), substitution of uridine by thymidine in the 3′ overhang was well tolerated in cultured mammalian cells (Fig. 2a, c, e, g and i), and the sequence of the overhang appears not to contribute to target recognition[9].

In co-transfection experiments, 25 nM siRNA duplexes were used (Figs 2 and 3; concentration is in respect to the final volume of tissue culture medium). Increasing the siRNA concentration to 100 nM did not enhance the specific silencing effects, but started to affect transfection efficiencies, perhaps due to competition for liposome encapsulation between plasmid DNA and siRNA (data not shown). Decreasing the siRNA concentration to 1.5 nM did not reduce the specific silencing effect (data not shown), even though the siRNAs were now only 2- to 20-fold more concentrated than the DNA plasmids; the silencing effect only vanishes completely if the siRNA concentration was dropped below 0.05 nM. This indicates that siRNAs are extraordinarily powerful reagents for mediating gene silencing, and that siRNAs are effective at concentrations that are several orders of magnitude below the concentrations applied in conventional antisense or ribozyme gene-targeting experiments[20].

To monitor the effect of longer dsRNAs on mammalian cells, 50- and 500-bp dsRNAs that are cognate to the reporter genes were prepared. As a control for nonspecific inhibition, dsRNAs from humanized GFP (hG)[21] was used. In these experiments, the reporter plasmids were co-transfected with either 0.21 μg siRNA duplexes or 0.21 μg longer dsRNAs. The siRNA duplexes only reduced the expression of their cognate reporter gene, while the longer dsRNAs strongly and nonspecifically reduced reporter-gene expression. The effects are illustrated for HeLa S3 cells as a representative example (Fig. 3a and b). The absolute luciferase activities were decreased nonspecifically 10- to 20-fold by 50-bp dsRNA, and 20- to 200-fold by 500-bp dsRNA co-transfection, respectively. Similar nonspecific effects were observed for COS-7 and NIH/3T3 cells. For 293 cells, a 10- to 20-fold nonspecific reduction was observed only for 500-bp dsRNAs. Nonspecific reduction in reporter-gene expression by dsRNA > 30 bp was expected as part of the interferon response[16]. Interestingly, superimposed on the nonspecific interferon response, we detect additional sequence-specific, dsRNA-mediated silencing. The sequence-specific silencing effect of long dsRNAs, however, became apparent only when the relative reporter-gene activities were normalized to the hG dsRNA controls (Fig. 3c). Sequence-specific silencing by 50- or 500-bp dsRNAs reduced the targeted reporter-gene expression by an additional 2- to 5-fold. Similar effects were also detected in the other three mammalian cell lines tested (data not shown). Specific silencing effects with dsRNAs (356–1,662 bp) were previously reported in CHO-K1 cells, but the amounts of dsRNA required to detect a 2- to 4-fold specific reduction were about 20-fold higher than in our experiments[12]. Also, CHO-K1 cells appear to be deficient in the interferon response. In another report, 293, NIH/3T3 and BHK-21 cells were tested for RNAi using luciferase/β-galactosidase (lacZ) reporter combinations and 829-bp specific lacZ or 717-bp nonspecific green fluorescent protein (GFP) dsRNA[10]. The lack of detected RNAi in this case may be due to the less sensitive luciferase/lacZ reporter assay and the length differences of target and control dsRNA. Taken together, our results indicate that RNAi is active in mammalian cells, but that the silencing effect is difficult to detect if the interferon system is activated by dsRNA > 30 bp.

To test for silencing of endogenous genes, we chose four genes coding for cytoskeletal proteins: lamin A/C, lamin B1, nuclear mitotic apparatus protein (NuMA) and vimentin[27]. The selection was based on the availability of antibodies needed to quantitate the silencing effect. Silencing was monitored 40 to 45 h after transfection to allow for turnover of the protein of the targeted genes. As shown in Fig. 4, the expression of lamin A/C was specifically reduced by the cognate siRNA duplex (Fig. 4a), but not when nonspecific siRNA directed against firefly luciferase (Fig. 4b) or buffer (Fig. 4c) was used. The expression of a non-targeted gene, NuMA, was unaffected in all treated cells (Fig. 4d–f), demonstrating the integrity of the targeted cells. The reduction in lamin A/C proteins was more than 90% complete as quantified by western blotting (Fig. 4j, k). We note that lamin A/C 'knock-out' mice are

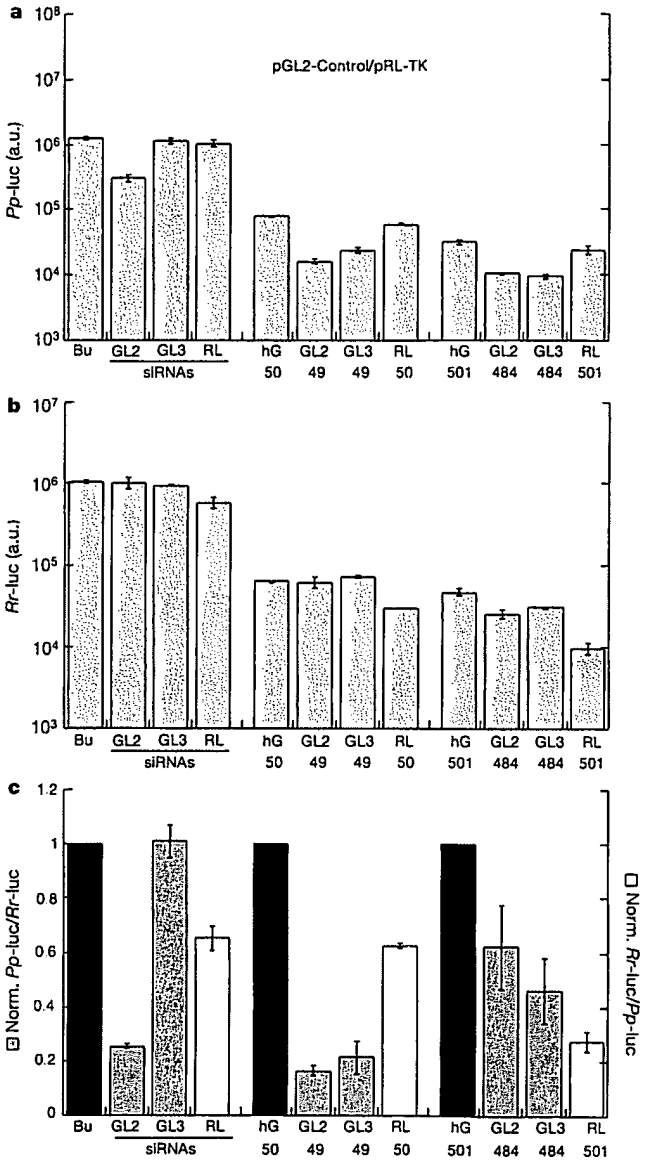

Figure 3 Effects of 21-nucleotide siRNAs, 50-bp, and 500-bp dsRNAs on luciferase expression in HeLa cells. The exact length of the long dsRNAs in base pairs is indicated below the bars. Experiments were performed with pGL2-Control and pRL-TK reporter plasmids. The data were averaged from two independent experiments ± s.d. **a**, Absolute *Pp*-luc expression, plotted in arbitrary luminescence units (a.u.). **b**, *Rr*-luc expression, plotted in arbitrary luminescence units. **c**, Ratios of normalized target to control luciferase. The ratios of luciferase activity for siRNA duplexes were normalized to a buffer control (Bu, black bars); the luminescence ratios for 50- or 500-bp dsRNAs were normalized to the respective ratios observed for 50- and 500-bp dsRNAs from humanized GFP (hG, black bars). We note that the overall differences in sequence between the 49- and 484-bp GL2 and GL3 dsRNAs are not sufficient to confer specificity for targeting GL2 and GL3 targets (43-nucleotide uninterrupted identity in 49-bp segment, 239-nucleotide longest uninterrupted identity in 484-bp segment)[30].

viable for a few weeks after birth[23] and that the lamin A/C knockdown in cultured cells was not expected to cause cell death. Lamin A and C are produced by alternative splicing in the 3′ region and are present in equal amounts in the lamina of mammalian cells (Fig. 4j, k). Transfection of siRNA duplexes targeting lamin B1 and NuMA reduced the expression of these proteins to low levels (data not shown), but we were not able to observe a reduction in vimentin expression. This could be due to the high abundance of vimentin in the cells (several per cent of total cell mass) or because the siRNA sequence chosen was not optimal for targeting of vimentin.

The mechanism of the 21-nucleotide siRNA-mediated interference process in mammalian cells remains to be uncovered, and silencing might occur post-transcriptionally and/or transcriptionally. In *Drosophila* lysate, siRNA duplexes mediate post-transcriptional gene silencing by reconstitution of siRNA-protein complexes (siRNPs), which guide mRNA recognition and targeted cleavage[6,7,9]. In plants, dsRNA-mediated post-transcriptional silencing has also been linked to DNA methylation, which may also be directed by 21-nucleotide siRNAs[24]. Methylation of promoter regions can lead to transcriptional silencing[25], but methylation in coding sequences does not[26]. DNA methylation and transcriptional silencing in mammals are well documented processes[27], yet their mechanisms have not been linked to that of post-transcriptional silencing. Methylation in mammals is predominantly directed towards CpG dinucleotide sequences. There is no CpG sequence in the RL or lamin A/C siRNA, although both siRNAs mediate specific silencing in mammalian cell culture, so it is unlikely that DNA methylation is essential for the silencing process.

Thus we have shown, for the first time, siRNA-mediated gene silencing in mammalian cells. The use of exogenous 21-nucleotide siRNAs holds great promise for analysis of gene function in human cell culture and the development of gene-specific therapeutics. It will also be of interest in understanding the potential role of endogenous siRNAs in the regulation of mammalian gene function. □

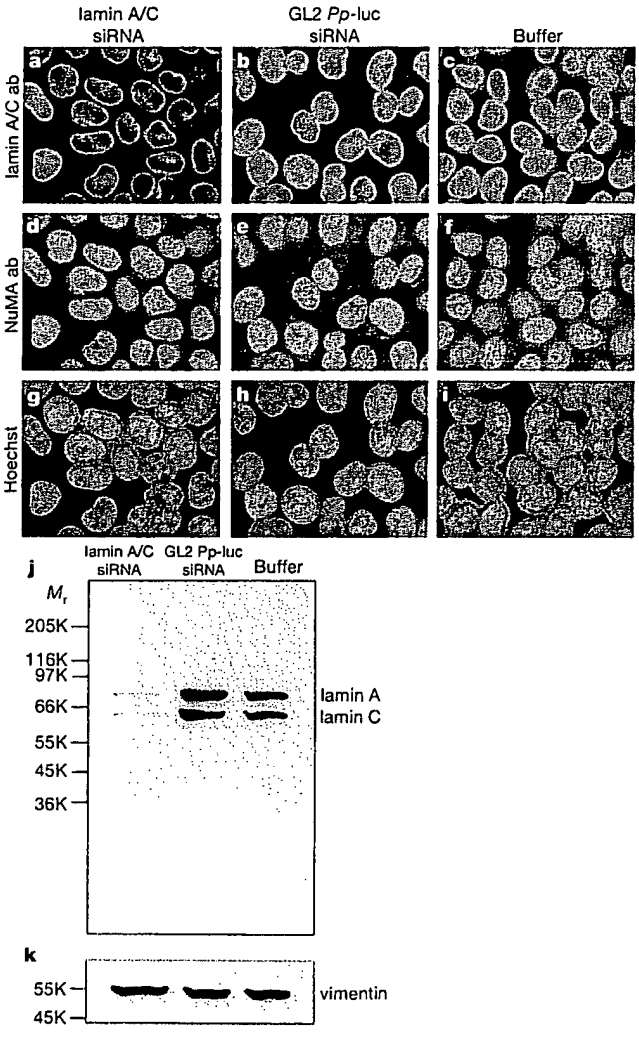

Figure 4 Silencing of nuclear envelope proteins lamin A/C in HeLa cells. Triple fluorescence staining of cells transfected with lamin A/C siRNA duplex (**a**, **d**, **g**), with GL2 luciferase siRNA duplex (nonspecific siRNA control) (**b**, **e**, **h**), and with buffer only (**c**, **f**, **i**). **a**–**c**, Staining with lamin A/C specific antibody; **d**–**f**, staining with NuMA-specific antibody; **g**–**i**, Hoechst staining of nuclear chromatin. Bright fluorescent nuclei in **a** represent untransfected cells. **j**, **k**, Western blots of transfected cells using lamin A/C- (**j**) or vimentin-specific (**k**) antibodies. The Western blot was stripped and re-probed with vimentin antibody to check for equal loading of total protein.

Methods

RNA preparation

21-nucleotide RNAs were chemically synthesized using Expedite RNA phosphoramidites and thymidine phosphoramidite (Proligo, Germany). Synthetic oligonucleotides were deprotected and gel-purified[9]. The accession numbers given below are from GenBank. The siRNA sequences targeting GL2 (Acc. No. X65324) and GL3 luciferase (Acc. No. U47296) corresponded to the coding regions 153–173 relative to the first nucleotide of the start codon; siRNAs targeting RL (Acc. No. AF025846) corresponded to region 119–139 after the start codon. The siRNA sequence targeting lamin A/C (Acc. No. X03444) was from position 608–630 relative to the start codon; lamin B1 (Acc. No. NM_005573) siRNA was from position 672–694; NuMA (Acc. No. Z11583) siRNA from position 3,988–4,010, and vimentin (Acc. No. NM_003380) from position 346–368 relative to the start codon. Longer RNAs were transcribed with T7 RNA polymerase from polymerase chain reaction (PCR) products, followed by gel purification. The 49- and 484-bp GL2 or GL3 dsRNAs corresponded to positions 113–161 and 113–596, respectively, relative to the start of translation; the 50- and 501-bp RL dsRNAs corresponded to position 118–167 and 118–618, respectively. PCR templates for dsRNA synthesis targeting humanized GFP (hG) were amplified from pAD3 (ref. 21), whereby 50- and 501-bp hG dsRNA corresponded to positions 121–170 and 121–621, respectively, to the start codon.

For annealing of siRNAs, 20 μM single strands were incubated in annealing buffer (100 mM potassium acetate, 30 mM HEPES-KOH at pH 7.4, 2 mM magnesium acetate) for 1 min at 90 °C followed by 1 h at 37 °C. The 37 °C incubation step was extended overnight for the 50- and 500-bp dsRNAs, and these annealing reactions were performed at 8.4 μM and 0.84 μM strand concentrations, respectively.

Cell culture

S2 cells were propagated in Schneider's *Drosophila* medium (Life Technologies) supplemented with 10% fetal bovine serum (FBS) 100 units ml^{-1} penicillin, and 100 μg ml^{-1} streptomycin at 25 °C. 293, NIH/3T3, HeLa S3, HeLa SS6, COS-7 cells were grown at 37 °C in Dulbecco's modified Eagle's medium supplemented with 10% FBS, 100 units ml^{-1} penicillin, and 100 μg ml^{-1} streptomycin. Cells were regularly passaged to maintain exponential growth. Twenty-four h before transfection at 50–80% confluency, mammalian cells were trypsinized and diluted 1:5 with fresh medium without antibiotics (1–3 × 10^5 cells ml^{-1}) and transferred to 24-well plates (500 μl per well). S2 cells were not trypsinized before splitting. Co-transfection of reporter plasmids and siRNAs was carried out with Lipofectamine 2000 (Life Technologies) as described by the manufacturer for adherent cell lines. Per well, 1.0 μg pGL2-Control (Promega) or pGL3-Control (Promega), 0.1 μg pRL-TK (Promega), and 0.21 μg siRNA duplex or dsRNA, formulated into liposomes, were applied; the final volume was 600 μl per well. Cells were incubated 20 h after transfection and appeared healthy thereafter. Luciferase expression was subsequently monitored with the Dual luciferase assay (Promega). Transfection efficiencies were determined by fluorescence microscopy for mammalian cells lines after co-transfection of 1.1 μg hGFP-encoding pAD3 (ref. 21) and 0.21 μg inverted GL2 siRNA, and were 70–90%. Reporter plasmids were amplified in XL-1 Blue (Stratagene) and purified using the Qiagen EndoFree Maxi Plasmid Kit.

Transfection of siRNAs for targeting endogenous genes was carried out using Oligofectamine (Life Technologies) and 0.84 μg siRNA duplex per well, but it was recently found that as little as 0.01 μg siRNAs per well are sufficient to mediate silencing. HeLa SS6 cells were transfected one to three times in approximately 15 h intervals and were assayed 40 to 45 h after the first transfection. It appears, however, that a single transfection is as efficient as multiple transfections. Transfection efficiencies as determined by immunofluorescence of targeted cells were in the range of 90%. Specific silencing of targeted genes was confirmed by at least three independent experiments.

Western blotting and immunofluorescence microscopy

Monoclonal 636 lamin A/C specific antibody[28] was used as undiluted hybridoma supernatant for immunofluorescence and 1/100 dilution for western blotting. Affinity-purified polyclonal NuMA protein 705 antibody[29] was used at a concentration of 10 μg ml^{-1} for

immunofluorescence. Monoclonal V9 vimentin-specific antibody was used at 1/2,000 dilution. For western blotting, transfected cells grown in 24-well plates were trypsinized and harvested in SDS sample buffer. Equal amounts of total protein were separated on 12.5% polyacrylamide gels and transferred to nitrocellulose. Standard immunostaining was carried out using ECL enhanced chemiluminescence technique (Amersham Pharmacia).

For immunofluorescence, transfected cells grown on glass coverslips in 24-well plates were fixed in methanol for 6 min at −10 °C. Target gene specific and control primary antibody were added and incubated for 80 min at 37 °C. After washing in phosphate buffered saline (PBS), Alexa 488-conjugated anti-rabbit (Molecular Probes) and Cy3-conjugated anti-mouse (Dianova) antibodies were added and incubated for 60 min at 37 °C. Finally, cells were stained for 4 min at room temperature with Hoechst 33342 (1 μM in PBS) and embedded in Mowiol 488 (Hoechst). Pictures were taken using a Zeiss Axiophot camera with a Fluar 40/1.30 oil objective and MetaMorph Imaging Software (Universal Imaging Corporation) with equal exposure times for the specific antibodies.

Received 20 February; accepted 26 April 2001.

1. Fire, A. RNA-triggered gene silencing *Trends Genet.* **15**, 358–363 (1999).
2. Sharp, P. A. RNA interference 2001. *Genes Dev.* **15**, 485–490 (2001).
3. Hammond, S. M., Caudy, A. A. & Hannon, G. J. Post-transcriptional gene silencing by double-stranded RNA. *Nature Rev. Genet.* **2**, 110–1119 (2001).
4. Tuschl, T. RNA interference and small interfering RNAs. *Chem. Biochem* **2**, 239–245 (2001).
5. Hamilton, A. J. & Baulcombe, D. C A species of small antisense RNA in posttranscriptional gene silencing in plants. *Science* **286**, 950–952 (1999)
6. Hammond, S. M., Bernstein, E., Beach, D. & Hannon, G. J. An RNA-directed nuclease mediates post-transcriptional gene silencing in *Drosophila* cells. *Nature* **404**, 293–296 (2000).
7. Zamore, P. D., Tuschl, T., Sharp, P. A. & Bartel, D. P. RNAi: Double-stranded RNA directs the ATP-dependent cleavage of mRNA at 21 to 23 nucleotide intervals. *Cell* **101**, 25–33 (2000).
8. Bernstein, E., Caudy, A. A., Hammond, S. M. & Hannon, G. J. Role for a bidentate ribonuclease in the initiation step of RNA interference. *Nature* **409**, 363–366 (2001).
9. Elbashir, S. M., Lendeckel, W. & Tuschl, T. RNA interference is mediated by 21 and 22 nt RNAs. *Genes Dev.* **15**, 188–200 (2001).
10. Caplen, N. J., Fleenor, J., Fire, A. & Morgan, R. A. dsRNA-mediated gene silencing in cultured *Drosophila* cells: a tissue culture model for the analysis of RNA interference *Gene* **252**, 95–105 (2000).
11. Clemens, J. C. *et al.* Use of double-stranded RNA interference in *Drosophila* cell lines to dissect signal transduction pathways. *Proc. Natl Acad. Sci USA* **97**, 6499–6503 (2000).
12. Ui-Tei, K., Zenno, S., Miyata, Y. & Saigo, K. Sensitive assay of RNA interference in *Drosophila* and Chinese hamster cultured cells using firefly luciferase gene as target. *FEBS Lett.* **479**, 79–82 (2000).
13. Wianny, F. & Zernicka-Goetz, M. Specific interference with gene function by double-stranded RNA in early mouse development. *Nature Cell Biol.* **2**, 70–75 (2000).
14. Svoboda, P., Stein, P., Hayashi, H. & Schultz, R. M. Selective reduction of dormant maternal mRNAs in mouse oocytes by RNA interference. *Development* **127**, 4147–4156 (2000).
15. Bahramian, M. B. & Zarbl, H. Transcriptional and posttranscriptional silencing of rodent alpha(1) collagen by a homologous transcriptionally self-silenced transgene. *Mol. Cell. Biol.* **19**, 274–283 (1999).
16. Stark, G. R., Kerr, I. M., Williams, B. R., Silverman, R. H. & Schreiber, R. D. How cells respond to interferons. *Annu. Rev. Biochem.* **67**, 227–264 (1998).
17. Manche, L., Green, S. R., Schmedt, C. & Mathews, M. B. Interactions between double-stranded RNA regulators and the protein kinase DAI. *Mol. Cell. Biol.* **12**, 5238–5248 (1992)
18. Minks, M. A., West, D. K., Benvin, S. & Baglioni, C. Structural requirements of double-stranded RNA for the activation of 2′,5′-oligo(A) polymerase and protein kinase of interferon-treated HeLa cells *J. Biol. Chem.* **254**, 10180–10183 (1979).
19. Clemens, M. & Williams, B. Inhibition of cell-free protein synthesis by $pppA^{2'}p^{5'}A^{2'}p^{5'}A$: a novel oligonucleotide synthesized by interferon-treated L cell extracts. *Cell* **13**, 565–572 (1978).
20. Macejak, D. G. *et al.* Inhibition of hepatitis C virus (HCV)-RNA-dependent translation and replication of a chimeric HCV poliovirus using synthetic stabilized ribozymes. *Hepatology* **31**, 769–776 (2000).
21. Kehlenbach, R. H., Dickmanns, A. & Gerace, L. Nucleocytoplasmic shuttling factors including Ran and CRM1 mediate nuclear export of NFAT *In vitro*. *J. Cell Biol.* **141**, 863–874 (1998).
22. Kreis, T. & Vale, R. *Guidebook to the Cytoskeletal and Motor Proteins*, Parts 2b and 3a (Oxford Univ. Press, Oxford, 1999).
23. Sullivan, T. *et al.* Loss of A-type lamin expression compromises nuclear envelope integrity leading to muscular dystrophy. *J. Cell Biol* **147**, 913–920 (1999).
24. Wassenegger, M. RNA-directed DNA methylation. *Plant Mol. Biol* **43**, 203–220 (2000).
25. Mette, M. F., Aufsatz, W., van der Winden, J., Matzke, M. A. & Matzke, A. J. M. Transcriptional silencing and promoter methylation triggered by double-stranded RNA. *EMBO J.* **19**, 5194–5201 (2000).
26. Wang, M.-B., Wesley, S. V., Finnegan, E. J., Smith, N. A. & Waterhouse, P. M. Replicating satellite RNA induces sequence-specific DNA methylation and truncated transcripts in plants *RNA* **7**, 16–28 (2001).
27. Razin, A. CpG methylation, chromatin structure and gene silencing—a three-way connection. *EMBO J.* **17**, 4905–4908 (1998).
28. Röber, R. A., Gieseler, R. K., Peters, J. H., Weber, K. & Osborn, M. Induction of nuclear lamins A/C in macrophages in *in vitro* cultures of rat bone marrow precursor cells and human blood monocytes, and in macrophages elicited *in vivo* by thioglycollate stimulation. *Exp. Cell Res.* **190**, 185–194 (1990).
29. Harborth, J., Wang, J., Gueth-Hallonet, C., Weber, K. & Osborn, M. Self assembly of NuMA: multiarm oligomers as structural units of a nuclear lattice. *EMBO J.* **18**, 1689–1700 (1999)
30. Parrish, S., Fleenor, J., Xu, S., Mello, C. & Fire, A. Functional anatomy of a dsRNA trigger: Differential requirement for the two trigger strands in RNA Interference. *Mol. Cell* **6**, 1077–1087 (2000).

Acknowledgements

We thank J. Martinez, J. Ludwig and D. Bartel for comments on the manuscript; L. Fredel for help with image processing; H.-J. Dehne for technical assistance; F. Döring, R. Nehring, D. Ingelfinger and C. Schneider for supplying cell lines; A. Dickmanns for the gift of the plasmid pAD3; and R. Lührmann for support. This work was funded by a Biofuture grant of the Bundesministerium für Bildung und Forschung.

Correspondence and requests for materials should be addressed to T.T. (e-mail: ttuschl@mpibpc.gwdg.de).

Ribosomal peptidyl transferase can withstand mutations at the putative catalytic nucleotide

Norbert Polacek, Marne Gaynor, Aymen Yassin & Alexander S. Mankin

Center for Pharmaceutical Biotechnology (MC 870), University of Illinois, 900 South Ashland Avenue, Chicago, Illinois 60607, USA

Peptide bond formation is the principal reaction of protein synthesis. It takes place in the peptidyl transferase centre of the large (50S) ribosomal subunit. In the course of the reaction, the polypeptide is transferred from peptidyl transfer RNA to the α-amino group of amino acyl-tRNA. The crystallographic structure of the 50S subunit showed no proteins within 18 Å from the active site, revealing peptidyl transferase as an RNA enzyme[1]. Reported unique structural and biochemical features of the universally conserved adenine residue A2451 in 23S ribosomal RNA (*Escherichia coli* numbering) led to the proposal of a mechanism of rRNA catalysis that implicates this nucleotide as the principal catalytic residue[2,3]. *In vitro* genetics allowed us to test the importance of A2451 for the overall rate of peptide bond formation. Here we report that large ribosomal subunits with mutated A2451 showed significant peptidyl transferase activity in several independent assays. Mutations at another nucleotide, G2447, which is essential to render catalytic properties to A2451 (refs 2, 3), also did not dramatically change the transpeptidation activity. As alterations of the putative catalytic residues do not severely affect the rate of peptidyl transfer the ribosome apparently promotes transpeptidation not through chemical catalysis, but by properly positioning the substrates of protein synthesis.

The proposed role of A2451 in the peptidyl transfer reaction is

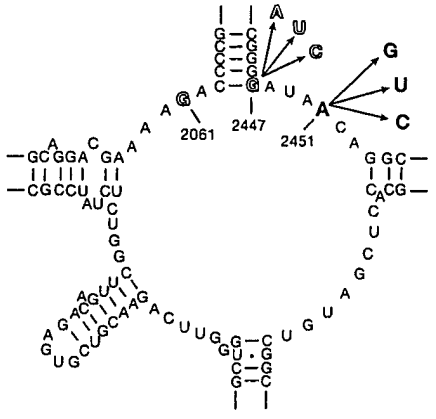

Figure 1 The secondary structure of the central loop of domain V of *T. aquaticus* 23S rRNA. Position A2451 (*E. coli* 23S rRNA numeration), the principal catalytic nucleotide in the proposed general acid–base catalytic mechanism of peptide bond formation[2,3], is shown in bold. Its tertiary interaction partners, guanine residues 2061 and 2447, suggested to be essential for rendering catalytic properties to A2451, are outlined. Arrows indicate the mutations engineered in 23S rRNA.

TAB 4

The EMBO Journal Vol. 20 No. 23 pp. 6877–6888, 2001

Functional anatomy of siRNAs for mediating efficient RNAi in *Drosophila melanogaster* embryo lysate

Sayda M.Elbashir, Javier Martinez, Agnieszka Patkaniowska, Winfried Lendeckel and Thomas Tuschl[1]

Department of Cellular Biochemistry, Max-Planck-Institute for Biophysical Chemistry, Am Fassberg 11, D-37077 Göttingen, Germany

[1]Corresponding author
e-mail: ttuschl@mpibpc.gwdg.de

S.M.Elbashir and J.Martinez contributed equally to this work

Duplexes of 21–23 nucleotide (nt) RNAs are the sequence-specific mediators of RNA interference (RNAi) and post-transcriptional gene silencing (PTGS). Synthetic, short interfering RNAs (siRNAs) were examined in *Drosophila melanogaster* embryo lysate for their requirements regarding length, structure, chemical composition and sequence in order to mediate efficient RNAi. Duplexes of 21 nt siRNAs with 2 nt 3′ overhangs were the most efficient triggers of sequence-specific mRNA degradation. Substitution of one or both siRNA strands by 2′-deoxy or 2′-*O*-methyl oligonucleotides abolished RNAi, although multiple 2′-deoxynucleotide substitutions at the 3′ end of siRNAs were tolerated. The target recognition process is highly sequence specific, but not all positions of a siRNA contribute equally to target recognition; mismatches in the centre of the siRNA duplex prevent target RNA cleavage. The position of the cleavage site in the target RNA is defined by the 5′ end of the guide siRNA rather than its 3′ end. These results provide a rational basis for the design of siRNAs in future gene targeting experiments.

Keywords: PTGS/RNA interference/small interfering RNA

Introduction

Post-transcriptional gene silencing (PTGS) mediated by double-stranded (ds) RNA represents an evolutionarily conserved cellular defence mechanism for controlling the expression of alien genes in protists, filamentous fungi, plants and animals (Fire, 1999; Bass, 2000; Cogoni and Macino, 2000; Carthew, 2001; Hammond *et al.*, 2001b; Sharp, 2001; Tuschl, 2001; Voinnet, 2001; Waterhouse *et al.*, 2001). It is believed that random integration of alien genes (such as transposons) or viral infection causes production of dsRNA, which activates sequence-specific degradation of homologous single-stranded mRNA or viral genomic RNA, thereby preventing expression or replication of the foreign genetic material. The dsRNA is used as the guide RNA in this sequence-specific RNA degradation process. In some cases, dsRNA may also be involved in amplification of the silencing signal important for systemic spread (Palauqui *et al.*, 1997; Voinnet *et al.*, 1998) or long-term maintenance of silencing (Dalmay *et al.*, 2000; Mourrain *et al.*, 2000; Smardon *et al.*, 2000). In animals, the dsRNA-triggered silencing effect is referred to as RNA interference (RNAi; Fire *et al.*, 1998).

One important feature of the mechanism of RNAi is the processing of long dsRNAs into duplexes of 21–25 nucleotide (nt) RNAs. These short RNA products were first detected in plant tissues that exhibited transgene- or virus-induced PTGS (Hamilton and Baulcombe, 1999), but were also found later in fly embryos and worms injected with long dsRNAs (Parrish *et al.*, 2000; Yang *et al.*, 2000) or in extracts from *Drosophila melanogaster* Schneider-2 (S2) cells that were transfected with dsRNA (Hammond *et al.*, 2000). The processing reaction of long dsRNAs to 21–23 nt RNAs was first recapitulated *in vitro*, in extracts prepared from *D.melanogaster* embryos (Zamore *et al.*, 2000) and later in extracts from S2 cells (Bernstein *et al.*, 2001). In the embryo lysate, it was observed that the target mRNA was cleaved in ~21 nt intervals (Zamore *et al.*, 2000) and that synthetic 21 and 22 nt RNA duplexes added to the lysate were able to guide efficient sequence-specific mRNA degradation, while duplexes of 30 bp dsRNA were inactive (Elbashir *et al.*, 2001b). The 21 nt RNA products were therefore named small interfering RNAs or silencing RNAs (siRNAs).

A ribonuclease III enzyme, dicer, is required for processing of long dsRNA into siRNA duplexes (Bernstein *et al.*, 2001). It was recently shown that dicer has an additional cellular function and is also required for excision of 21 and 22 nt small temporal RNAs (stRNAs) from ~70 nt stable stem–loop precursors (Grishok *et al.*, 2001; Hutvágner *et al.*, 2001). These tiny expressed RNA molecules are important regulators of developmental timing and control the translation of downstream regulatory genes (Ambros, 2000; Moss, 2000; Pasquinelli *et al.*, 2000). stRNAs are different from siRNAs in that the target mRNA is not degraded during silencing (Wightman *et al.*, 1993; Olsen and Ambros, 1999) and they are single stranded (Reinhart *et al.*, 2000), while siRNAs are believed to be double stranded (Elbashir *et al.*, 2001b; Hutvágner *et al.*, 2001).

In RNAi, a siRNA-containing endonuclease complex cleaves a single-stranded target RNA in the middle of the region complementary to the 21 nt guide siRNA of the siRNA duplex (Elbashir *et al.*, 2001b). This cleavage site is one helical turn displaced from the cleavage site that produced the siRNA from long dsRNA, suggesting dramatic conformational and/or compositional changes after processing of long dsRNA to 21 nt siRNA duplexes. The target RNA cleavage products are rapidly degraded because they either lack the stabilizing cap or poly(A) tail. A protein component of the ~500 kDa endonuclease or

RNA-induced silencing complex (RISC) was recently identified and is a member of the argonaute family of proteins (Hammond *et al.*, 2001a); however, it is currently unclear whether dicer is required for RISC activity.

It is also unknown whether RISC contains single- or double-stranded siRNAs. By analogy to stRNA excision, it may be envisaged that only one of the strands of a siRNA duplex is incorporated into a catalytic siRNP, but because of the symmetry of the siRNA duplex, two approximately equal populations of sense and antisense strand-containing catalytic siRNPs are produced. Synthetic siRNA duplexes cleaved sense as well as antisense target RNAs in the middle of the region covered by the siRNA duplex in *D.melanogaster* lysate (Elbashir *et al.*, 2001b). However, longer dsRNAs did not produce symmetric sense and antisense target RNA cleavage sites in embryo lysate (Elbashir *et al.*, 2001b), suggesting that the direction of processing of long dsRNA defined which of the strands of the resulting siRNA duplex could be used for guiding target degradation. Some protein, involved in the production of the 21 nt siRNA duplexes, may be deposited on the siRNA duplex to mark the strand that is going to be used for guiding target RNA cleavage.

Despite the lack of profound mechanistic understanding, RNAi has rapidly developed into an important tool for reverse genetics and has been widely applied in *Caenorhabditis elegans* (Fraser *et al.*, 2000; Gönczy *et al.*, 2000; Piano *et al.*, 2000; Maeda *et al.*, 2001), as well as in insects (see references in Lam and Thummel, 2000) and insect cell lines (Clemens *et al.*, 2000; Hammond *et al.*, 2000; Ui-Tei *et al.*, 2000). RNAi has also been shown to occur in a variety of vertebrates by targeting of mRNAs important for embryonic development. In differentiated mammalian cells, dsRNAs with >30 bp generally activate the interferon response, which leads to a global shut-off in protein synthesis as well as non-specific mRNA degradation (Stark *et al.*, 1998). This unspecific response to long dsRNAs can be bypassed using 21 nt siRNA duplexes, resulting in specific knock-down of the expression of the targeted gene (Elbashir *et al.*, 2001a; Hutvágner *et al.*, 2001), providing a new method for analysis of mammalian gene function in cultured cells.

Here we describe the results of a systematic analysis of the length, secondary structure, sugar backbone and sequence specificity of siRNA duplexes for RNAi, using the established *D.melanogaster* embryo *in vitro* system. The most potent siRNA duplexes are 21 nt long, comprising a 19 nt base-paired sequence with 2 nt 3′-overhanging ends. The 5′ end of the target-complementary siRNA strand (guide siRNA) sets the ruler to define the position of target RNA cleavage. Furthermore, we find that target recognition is extremely specific, as even single nucleotide mismatches between the siRNA duplex and the target mRNA abolish interference. These results provide a rational basis for the design of siRNAs for future gene targeting experiments.

Results

Variation of the 3′ overhang in duplexes of 21 nt siRNAs

We reported previously that two or three unpaired nucleotides at the 3′ end of siRNA duplexes were more efficient in target RNA degradation than blunt-ended duplexes (Elbashir *et al.*, 2001b). To perform a more comprehensive analysis of the function of the terminal nucleotides, we synthesized five 21 nt sense siRNAs, each displaced by one nucleotide relative to the target RNA, and eight 21 nt antisense siRNAs, each displaced by one nucleotide relative to the target (Figure 1A). By combining these sense and antisense siRNAs, a series of eight siRNA duplexes with symmetric overhanging ends were generated spanning a range from 7 nt 3′ overhang to 4 nt 5′ overhang. The interference was measured using the dual luciferase assay system (Tuschl *et al.*, 1999; Zamore *et al.*, 2000). siRNA duplexes were directed against firefly luciferase mRNA and sea pansy luciferase mRNA was used as internal control. The luminescence ratio of target to control luciferase activity was determined in the presence of siRNA duplex and was normalized to that observed in its absence. For comparison, the interference ratios of long dsRNAs (39–504 bp) are shown in Figure 1B (Elbashir *et al.*, 2001b). The interference ratios were determined at concentrations of 5 nM for long dsRNAs (Figure 1A) and at 100 nM for siRNA duplexes (Figure 1C–J). The 100 nM concentration of siRNAs was chosen because complete processing of 5 nM 504 bp dsRNA would result in 120 nM total siRNA duplexes.

The ability of 21 nt siRNA duplexes to mediate RNAi is dependent on the number of overhanging nucleotides or base pairs formed. Duplexes with 4–6 3′-overhanging nucleotides were unable to mediate RNAi (Figure 1C–F), as were duplexes with two or more 5′-overhanging nucleotides (Figure 1G–J). The duplexes with 2 nt 3′ overhangs were most efficient in mediating RNA interference, although the efficiency of silencing was also sequence dependent and up to 12-fold differences were observed for different siRNA duplexes with 2 nt 3′ overhangs (compare Figure 1D–H). Duplexes with blunted ends, 1 nt 5′ overhang or 1–3 nt 3′ overhangs were sometimes functional and sometimes completely inactive. The small silencing effect observed for the siRNA duplex with 7 nt 3′ overhang (Figure 1C) may be due to an antisense effect of the long 3′ overhang rather than to

Fig. 1. Variation of the 3′ overhang of duplexes of 21 nt siRNAs. (**A**) Outline of the experimental strategy. The capped and polyadenylated sense target mRNA is depicted and the relative positions of sense and antisense siRNAs are shown. Eight series of duplexes according to the eight different antisense strands were prepared. The siRNA sequences and the number of overhanging nucleotides were changed in 1 nt steps. (**B**) Normalized relative luminescence of target luciferase (*Photinus pyralis*, Pp-luc) to control luciferase (*Renilla reniformis*, Rr-luc) in *D.melanogaster* embryo lysate in the presence of 5 nM blunt-ended dsRNAs (Elbashir *et al.*, 2001b). The luminescence ratios determined in the presence of dsRNA were normalized to the ratio obtained for a buffer control (bu; black bar). Normalized ratios less than 1 indicate specific interference. (**C–J**) Normalized interference ratios for eight series of 21 nt siRNA duplexes. The sequences of siRNA duplexes are depicted above the bar graphs. Each part shows the interference ratio for a set of duplexes formed with a given antisense guide siRNA and five different sense siRNAs. The number of overhanging nucleotides (3′ overhang, positive numbers; 5′ overhang, negative numbers) is indicated on the *x*-axis. Data points were averaged from at least three independent experiments. Error bars represent standard deviations.

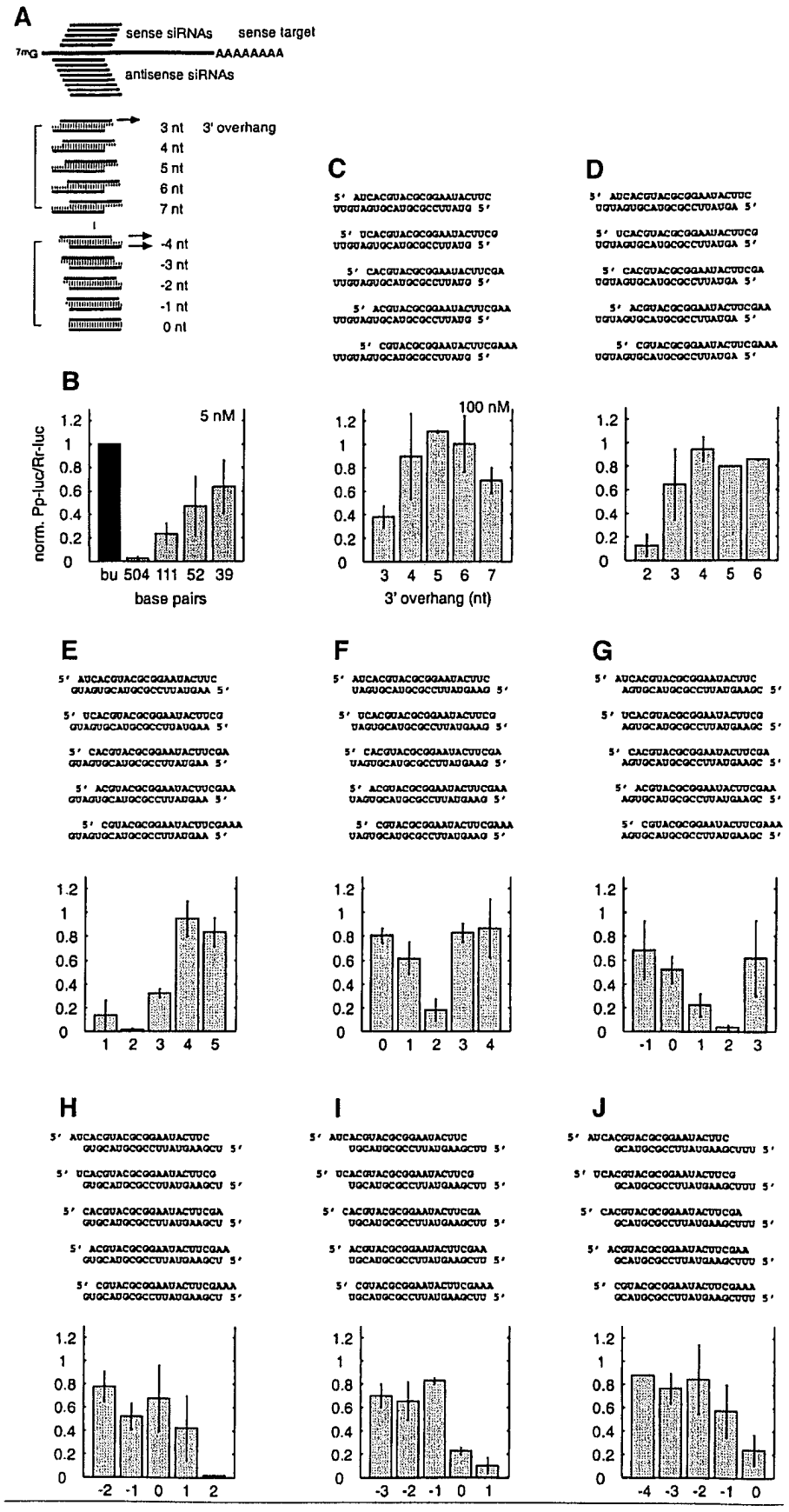
A
sense siRNAs
sense target
7mG
AAAAAAAA
antisense siRNAs
3 nt 3' overhang
4 nt
5 nt
6 nt
7 nt
-4 nt
-3 nt
-2 nt
-1 nt
0 nt
B
5 nM
norm. Pp-luc/Rr-luc
bu 504 111 52 39
base pairs
C
100 nM
3 4 5 6 7
3' overhang (nt)
D
2 3 4 5 6
E
1 2 3 4 5
F
0 1 2 3 4
G
-1 0 1 2 3
H
-2 -1 0 1 2
I
-3 -2 -1 0 1
J
-4 -3 -2 -1 0

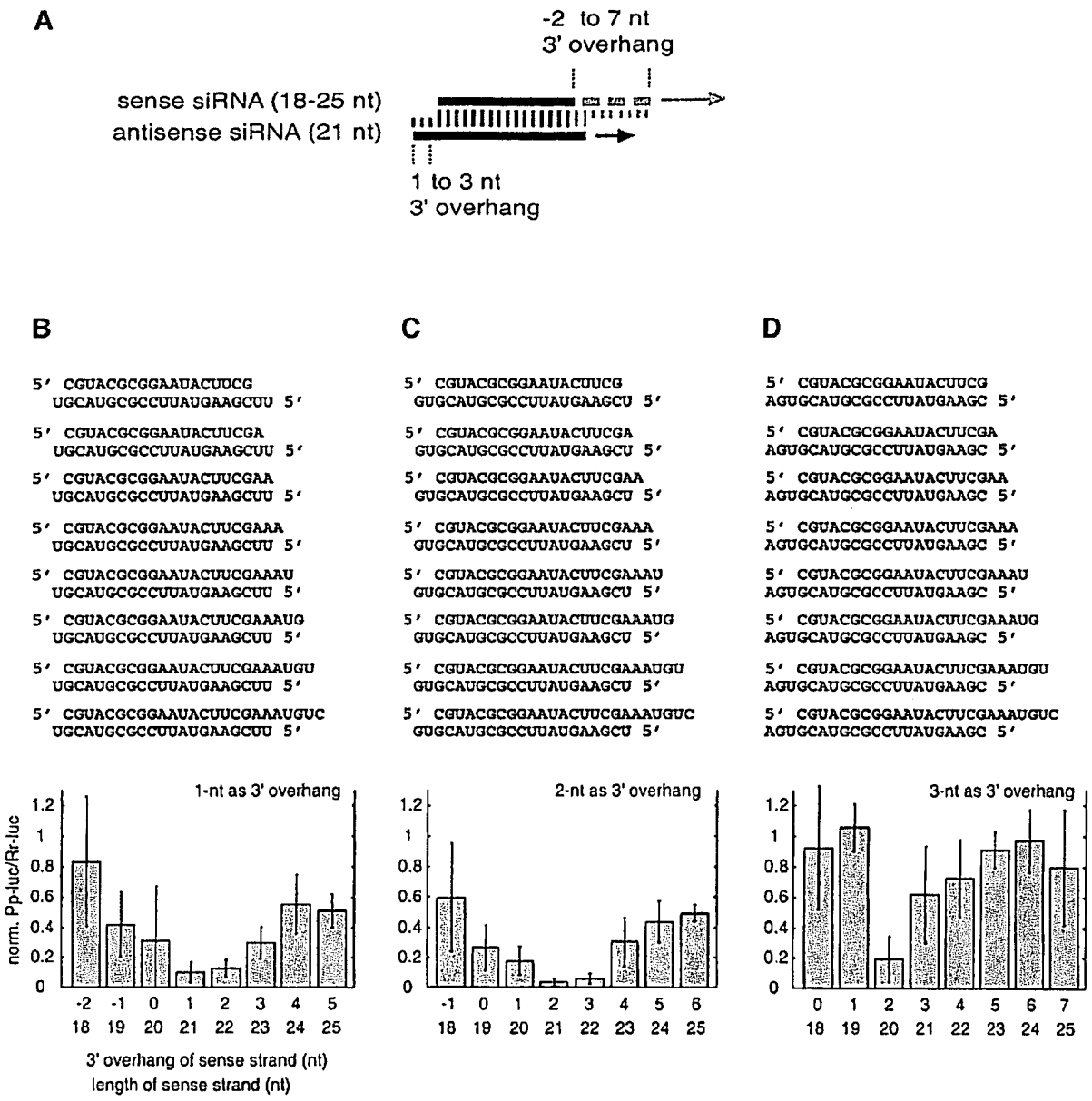

Fig. 2. Variation of the length of the sense strand of siRNA duplexes. (**A**) Representation of the experiment. Three 21 nt antisense strands were paired with eight sense siRNAs. The siRNAs were changed in length at their 3′ end. The 3′ overhang of the antisense siRNA was 1 nt (**B**), 2 nt (**C**) or 3 nt (**D**), while the sense siRNA overhang was varied for each series. The sequences of the siRNA duplexes and the corresponding interference ratios are indicated.

RNAi. Comparison of the efficiency of RNAi between long dsRNAs (Figure 1B) and the most effective 21 nt siRNA duplexes (Figure 1E, G and H) indicates that a single siRNA duplex at 100 nM concentration can be as effective as 5 nM 504 bp dsRNA.

Length variation of the sense siRNA paired to an invariant 21 nt antisense siRNA

In order to investigate the effect of the length of siRNAs on RNAi, we prepared three series of siRNA duplexes, combining three 21 nt antisense strands with eight 18–25 nt sense strands. The 3′ overhang of the antisense siRNA was fixed to 1, 2 or 3 nt in each siRNA duplex series, while the sense siRNA was varied at its 3′ end (Figure 2A). Independently of the length of the sense siRNA, we found that duplexes with 2 nt 3′ overhang of antisense siRNA (Figure 2C) were more active than those with 1 or 3 nt 3′ overhang (Figure 2B and D). In the first series, with 1 nt 3′ overhang of antisense siRNA, duplexes with 21 and 22 nt sense siRNAs, carrying a 1 and 2 nt 3′ overhang of sense siRNA, respectively, were most active. Duplexes with 19–25 nt sense siRNAs were also able to mediate RNA, but to a lesser extent. Similarly, in the second series, with 2 nt overhang of antisense siRNA, the 21 nt siRNA duplex with 2 nt 3′ overhang was most active and any other combination with the 18–25 nt sense siRNAs was active to

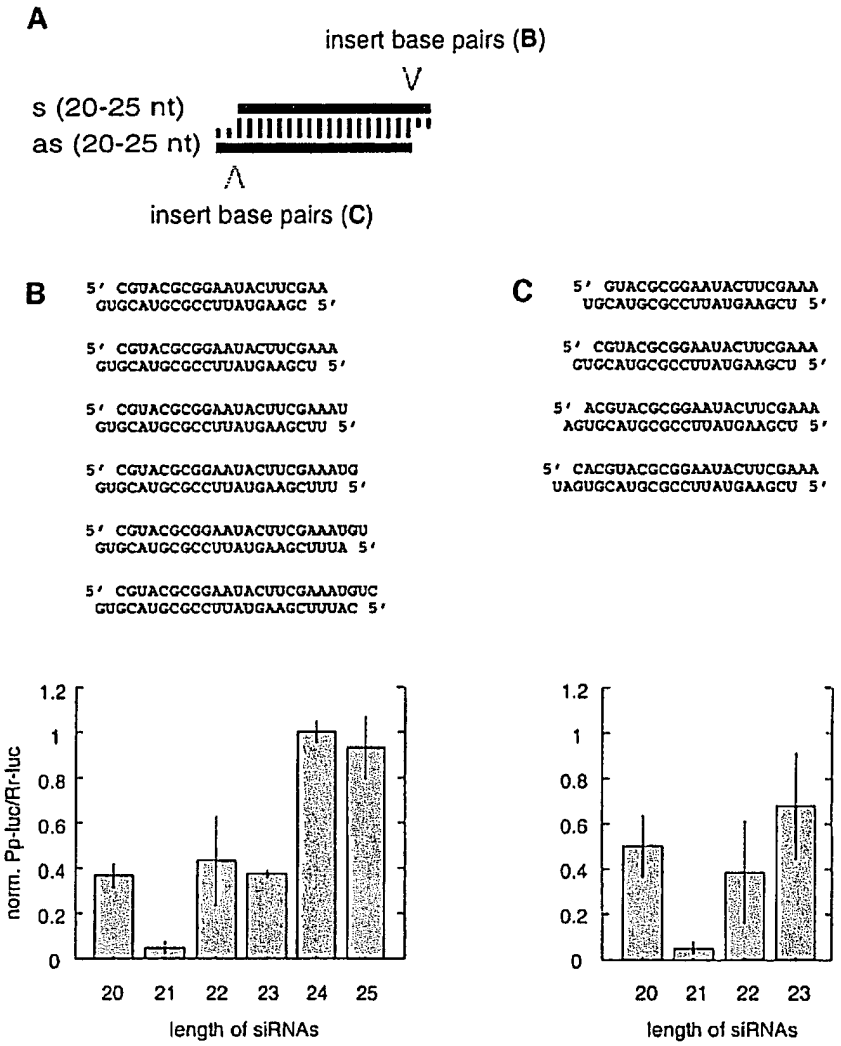

Fig. 3. Variation of the length of siRNA duplexes with preserved 2 nt 3′ overhangs. (**A**) Graphic representation of the experiment. The 21 nt siRNA duplex is identical in sequence to the one shown in Figures 1H and 2C. The siRNA duplexes were extended to the 3′ side of the sense siRNA (**B**) or the 5′ side of the sense siRNA (**C**). The siRNA duplex sequences and the respective interference ratios are indicated.

a significant degree. In the last series, with 3 nt antisense siRNA 3′ overhang, only the duplex with a 20 nt sense siRNA and 2 nt sense 3′ overhang was able to reduce target RNA expression. Together, these results indicate that the length of the siRNA as well as the length of the 3′ overhang are important, and that duplexes of 21 nt siRNAs with 2 nt 3′ overhang are optimal for RNAi.

Length variation of siRNA duplexes with a constant 2 nt 3′ overhang

We then examined the effect of simultaneously changing the length of both siRNA strands by maintaining symmetrical 2 nt 3′ overhangs (Figure 3A). Two series of siRNA duplexes were prepared, including the 21 nt siRNA duplex of Figure 1H as reference. The length of the duplexes was varied between 20 and 25 bp by extending the base-paired segment at the 3′ end of the sense siRNA (Figure 3B) or at the 3′ end of the antisense siRNA (Figure 3C).

Duplexes of 20–23 bp caused specific repression of target luciferase activity, but the 21 nt siRNA duplex was at least 8-fold more efficient than any of the other duplexes. siRNA duplexes of 24 and 25 nt did not result in any detectable interference. Sequence-specific effects were minor as variations on both ends of the duplex produced similar effects.

2′-deoxy- and 2′-O-methyl-modified siRNA duplexes

To assess the importance of the siRNA ribose residues for RNAi, duplexes with 21 nt siRNAs and 2 nt 3′ overhangs with 2′-deoxy- or 2′-*O*-methyl-modified strands were examined (Figure 4). Substitution of the 2 nt 3′ overhangs by 2′-deoxynucleotides had no effect and even the replacement of two additional ribonucleotides by 2′-deoxyribonucleotides adjacent to the overhangs in the paired region produced significantly active siRNAs. Thus, 8 out of 42 nt of a siRNA duplex were replaced by DNA

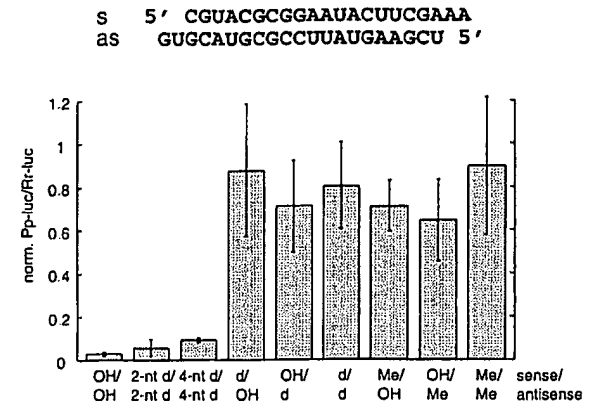

Fig. 4. Substitution of the 2′-hydroxyl groups of the siRNA ribose residues. The 2′-hydroxyl groups (OH) in the strands of siRNA duplexes were replaced by 2′-deoxy (d) or 2′-*O*-methyl (Me). 2 and 4 nt 2′-deoxy substitutions at the 3′ ends are indicated as 2- and 4-nt d, respectively. Uridine residues were replaced by 2′-deoxythymidine.

residues without loss of activity. Complete substitution of one or both siRNA strands by 2′-deoxy residues, however, abolished RNAi, as did complete substitution by 2′-*O*-methyl residues.

Definition of target RNA cleavage sites

Target RNA cleavage positions were previously determined for 22 nt siRNA duplexes and for a 21 and 22 nt duplex (Elbashir *et al.*, 2001b). The position of target RNA cleavage was located in the centre of the region covered by the siRNA duplex, 11 or 12 nt downstream of the first nucleotide that was complementary to the 21 or 22 nt siRNA guide sequence. Five distinct 21 nt siRNA duplexes with 2 nt 3′ overhang (Figure 5A) were incubated with 5′ cap-labelled sense or antisense target RNA in *D.melanogaster* lysate (Tuschl *et al.*, 1999; Zamore *et al.*, 2000). The 5′ cleavage products were resolved on sequencing gels (Figure 5B). The amount of sense target RNA cleaved correlated with the efficiency of siRNA duplexes determined in the translation-based assay, and siRNA duplexes 1, 2 and 4 (Figures 5B, 1E, G and H) cleaved target RNA faster than duplexes 3 and 5 (Figures 5B, 1D and F). Notably, the sum of radioactivity of the 5′ cleavage product and the input target RNA were not constant over time and the 5′ cleavage products did not accumulate. Presumably, the cleavage products, once released from the siRNA–endonuclease complex, were rapidly degraded due to the lack of either the poly(A) tail or the 5′ cap.

The cleavage sites for both sense and antisense target RNAs were located in the middle of the region spanned by the siRNA duplexes. The cleavage sites for each target produced by the five different duplexes varied by 1 nt according to the 1 nt displacement of the duplexes along the target sequences. The targets were cleaved precisely 11 nt downstream of the target position complementary to the 3′-most nucleotide of the sequence-complementary guide siRNA (Figure 5).

In order to determine whether the 5′ or the 3′ end of the guide siRNA sets the ruler for target RNA cleavage, we devised the experimental strategy outlined in Figure 6A

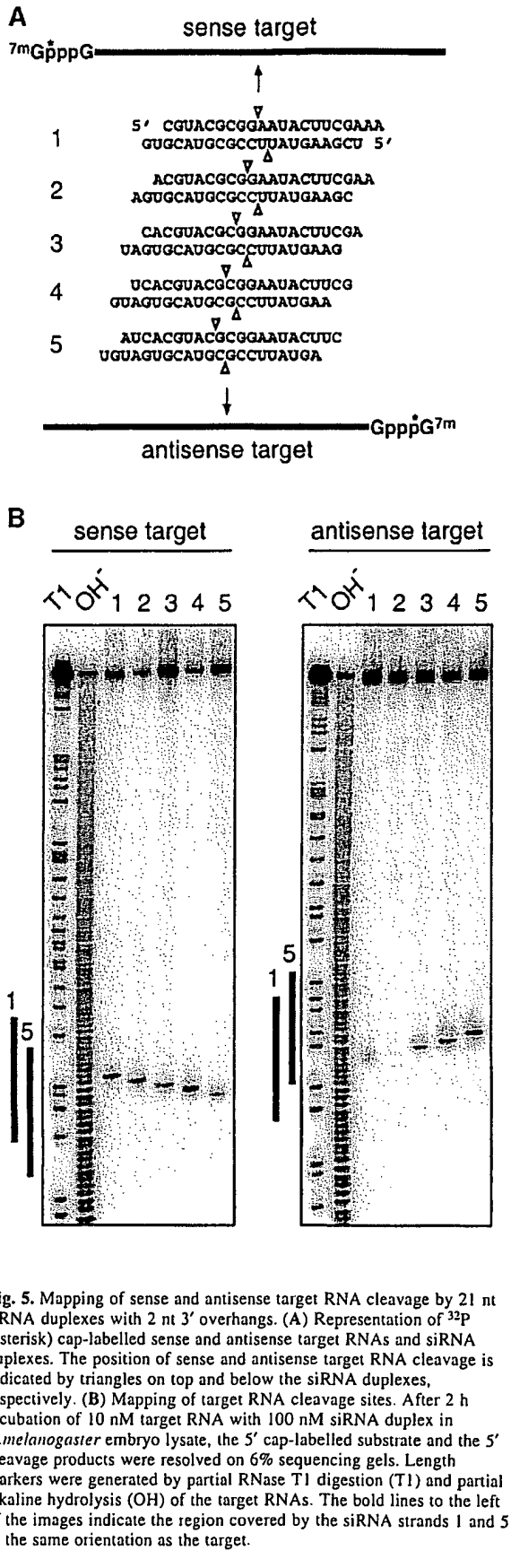

Fig. 5. Mapping of sense and antisense target RNA cleavage by 21 nt siRNA duplexes with 2 nt 3′ overhangs. (**A**) Representation of ^{32}P (asterisk) cap-labelled sense and antisense target RNAs and siRNA duplexes. The position of sense and antisense target RNA cleavage is indicated by triangles on top and below the siRNA duplexes, respectively. (**B**) Mapping of target RNA cleavage sites. After 2 h incubation of 10 nM target RNA with 100 nM siRNA duplex in *D.melanogaster* embryo lysate, the 5′ cap-labelled substrate and the 5′ cleavage products were resolved on 6% sequencing gels. Length markers were generated by partial RNase T1 digestion (T1) and partial alkaline hydrolysis (OH) of the target RNAs. The bold lines to the left of the images indicate the region covered by the siRNA strands 1 and 5 of the same orientation as the target.

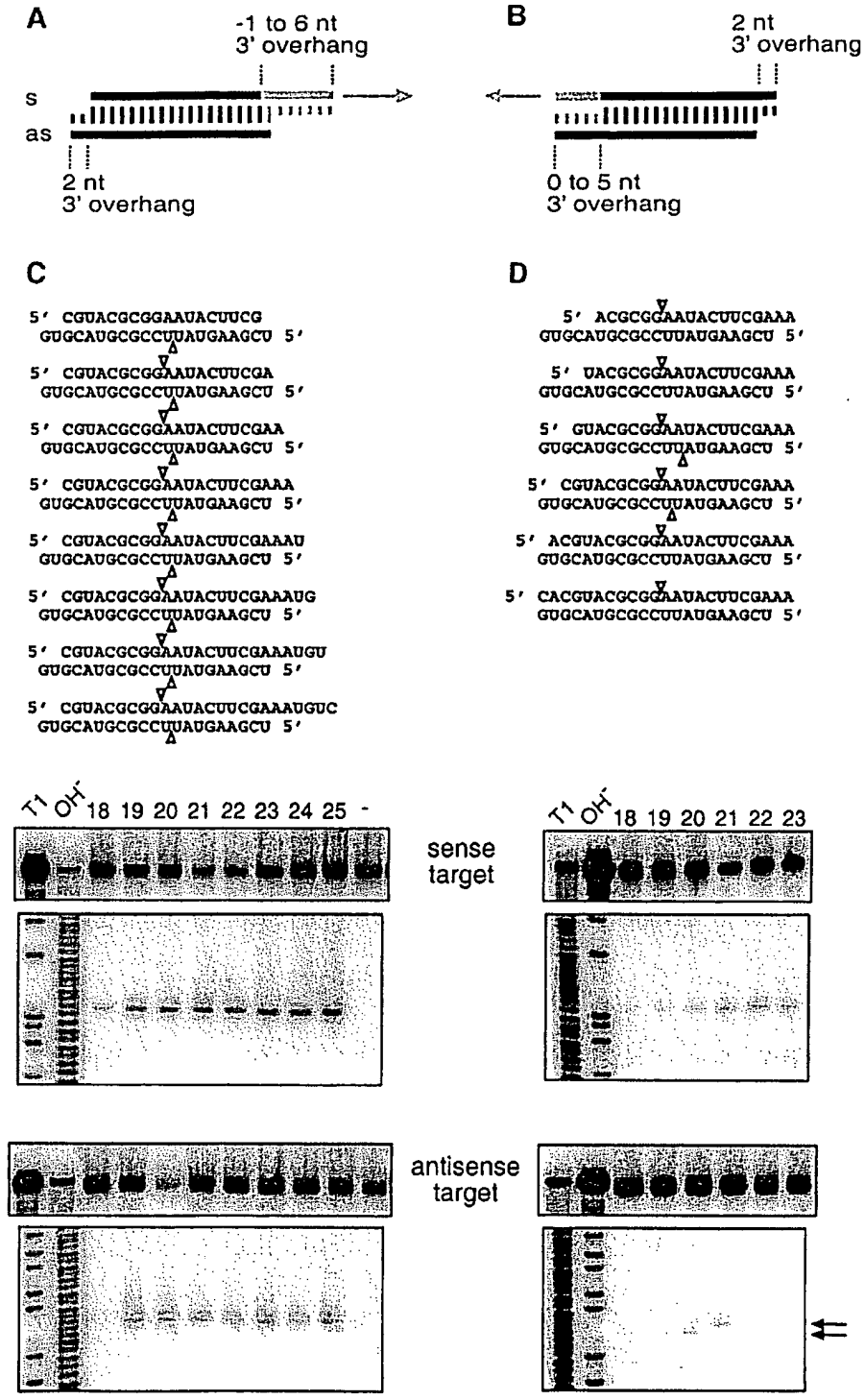

Fig. 6. The 5′ end of a guide siRNA defines the position of target RNA cleavage. (**A** and **B**) Representation of the experimental strategy. The antisense siRNA was the same in all siRNA duplexes, but the sense strand was varied between 18 and 25 nt by changing the 3′ end (A) or 18 and 23 nt by changing the 5′ end (B). The position of sense and antisense target RNA cleavage is indicated by triangles on top and below the siRNA duplexes, respectively. (**C** and **D**) Analysis of target RNA cleavage using cap-labelled sense (top) or antisense (bottom) target RNAs. The residual amount of targeted substrate and the cap-labelled 5′ cleavage products are shown. The sequences of the siRNA duplexes are indicated and the length of the sense siRNA strands is marked on top. The control lane, marked with a dash in (C), shows target RNA incubated in absence of siRNAs. Markers were as described in Figure 5. The arrows in (D), bottom, indicate the target RNA cleavage sites that differ by 1 nt.

and B. A 21 nt antisense siRNA, which was kept invariant for this study, was paired with sense siRNAs that were modified in length at either of their 5′ or 3′ ends. The position of sense and antisense target RNA cleavage was

determined as described above. Changes in the 3′ end of the sense siRNA, monitored for 1 nt 5′ overhang to 6 nt 3′ overhang, did not affect either the position of sense nor antisense target RNA cleavage (Figure 6C). Changes in the 5′ end of the sense siRNA did not affect the sense target RNA cleavage (Figure 6D, top), as expected, because the antisense siRNA was unchanged. The residual amount of uncleaved sense target RNA (Figure 6C and D top) correlated with the efficiency of siRNA duplexes determined in translation-based assays (Figure 2C and data not shown), but did not correlate with the amount of detected cleavage product. Accumulation of cleavage products was more pronounced for the longer and less efficient siRNA duplexes, suggesting that product release may have become rate limiting. Because the antisense siRNA was kept unchanged while the sense siRNA was varied, an alteration in product release implies a role of the sense siRNA strand in the target RNA degradation process.

Changes in the 5′ end of the sense siRNA, in contrast to its 3′ end, strongly affected antisense target RNA cleavage (Figure 6D, bottom). The antisense target was only cleaved when the sense siRNA was 20 or 21 nt in size. The position of cleavage differed by 1 nt, suggesting that the 5′ end of the target-recognizing siRNA sets the ruler for target RNA cleavage. This position is located between nucleotide 10 and 11 when counting in an upstream direction from the target nucleotide paired to the 5′-most nucleotide of the guide siRNA (see also Figure 5A).

Sequence effects and 2′-deoxy substitutions in the 3′ overhang

The 2 nt 3′ overhang is critical for siRNA function. We wanted to know whether the sequence of the overhanging nucleotides contributes to target recognition or is only a feature required for reconstitution of the endonuclease complex (RISC or siRNP). We synthesized sense and antisense siRNAs with AA, CC, GG, UU and UG 3′ overhangs and included the 2′-deoxy modifications TdG and TT (T, 2′-deoxythymidine; dG, 2′-deoxyguanosine). The wild-type siRNAs contained AA in the sense 3′ overhang and UG in the antisense 3′ overhang (AA/UG). All siRNA duplexes were functional in the interference assay and reduced target expression at least 5-fold (Figure 7). The most efficient siRNA duplexes, which reduced target expression >10-fold, were of the sequence type NN/UG, NN/UU, NN/TdG and NN/TT (N, any nucleotide). siRNA duplexes with an antisense siRNA 3′ overhang of AA, CC or GG were less active by a factor of 2–4 when compared with the wild-type sequence UG or the mutant UU. This reduction in RNAi efficiency is likely to be due to the contribution of the penultimate 3′ nucleotide to sequence-specific target recognition, as the 3′-terminal nucleotide was changed from G to U without effect.

Changes in the sequence of the 3′ overhang of the sense siRNA did not reveal any sequence-dependent effects, which was not surprising because the sense siRNA is not expected to contribute to the sequence-specific recognition of the sense target mRNA.

Sequence specificity of target recognition

In order to examine the sequence specificity of target recognition, we introduced sequence changes into the

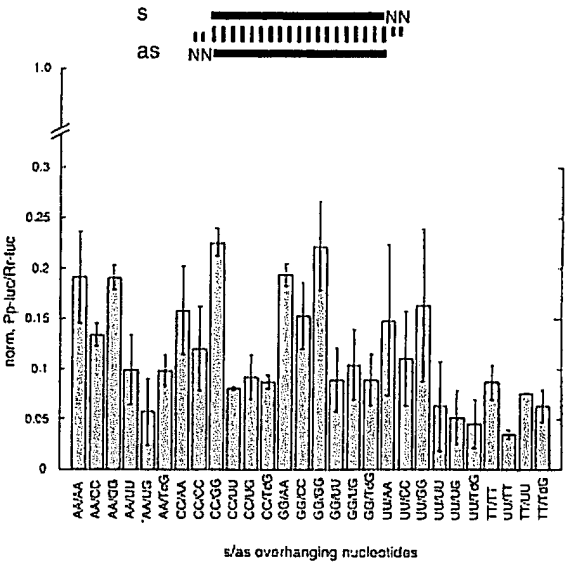

Fig. 7. Sequence variation of the 3′ overhang of siRNA duplexes. The 2 nt 3′ overhang (NN, in grey) was changed in sequence and composition as indicated (T, 2′-deoxythymidine; dG, 2′-deoxyguanosine; asterisk, wild-type siRNA duplex). Normalized interference ratios were determined as described in Figure 1. The wild-type sequence is the same as depicted in Figure 4.

paired segments of siRNA duplexes and determined the efficiency of silencing. Sequence changes were introduced by inverting short segments of 3 or 4 nt or inducing point mutations (Figure 8). The sequence changes in one siRNA strand were compensated for in the complementary siRNA strand to avoid perturbing the base-paired siRNA duplex structure. The sequence of all 2 nt 3′ overhangs was TT to reduce costs of synthesis. The TT/TT reference siRNA duplex was comparable in RNAi to the wild-type siRNA duplex AA/UG (Figure 7). The ability to mediate reporter mRNA destruction was quantified using the translation-based luminescence assay. Duplexes of siRNAs with inverted sequence segments showed dramatically reduced ability for targeting the firefly luciferase reporter (Figure 8). The sequence changes located between the 3′ end and the middle of the antisense siRNA completely abolished target RNA recognition, but mutations near the 5′ end of the antisense siRNA exhibited a small degree of silencing. Transversion of the AU base pair located directly opposite the predicted target RNA cleavage site or 1 nt further away from the predicted site prevented target RNA cleavage, therefore indicating that a single mutation within the centre of a siRNA duplex discriminates between mismatched targets.

Discussion

siRNAs are valuable reagents for inactivation of gene expression, not only in insect cells but also in mammalian cells, with a great potential for therapeutic application (Elbashir *et al.*, 2001a). We have systematically analysed the structural determinants of siRNA duplexes required to promote efficient target RNA degradation in *D.melanogaster* embryo lysate, thus providing rules for the design of most potent siRNA duplexes. A perfect siRNA duplex is able to silence gene expression with an

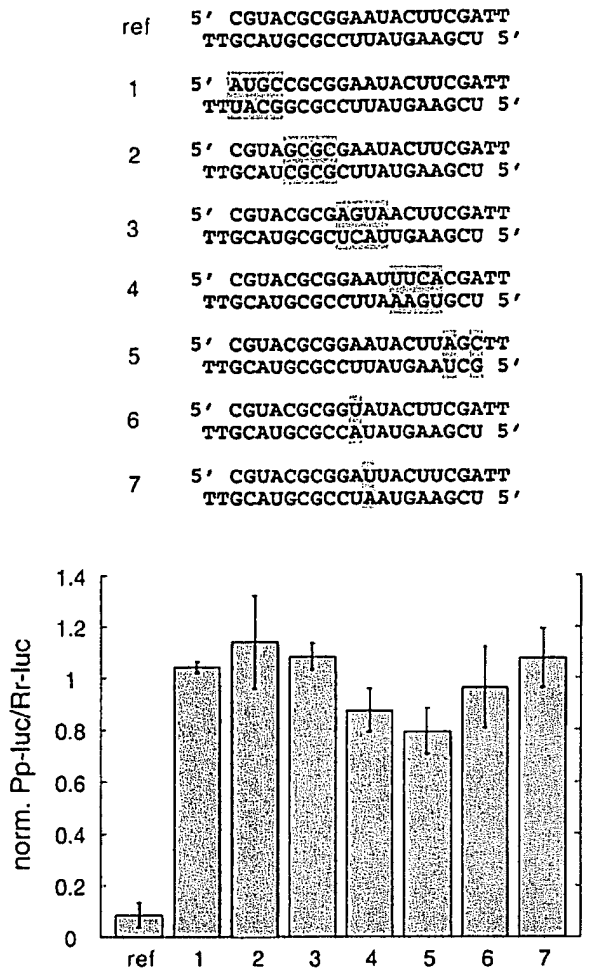

Fig. 8. Sequence specificity of target recognition. The sequences of the mismatched siRNA duplexes are shown, modified sequence segments or single nucleotides are shaded in grey. The reference duplex (ref) and the siRNA duplexes 1–7 contain 2′-deoxythymidine 2 nt overhangs. The silencing efficiency of the thymidine-modified reference duplex was comparable to the wild-type sequence (Figure 7). Normalized interference ratios were determined as described in Figure 1.

efficiency comparable to a 500 bp dsRNA, given that comparable quantities of total RNA are used.

The siRNA user guide

Efficiently silencing siRNA duplexes are composed of 21 nt sense and 21 nt antisense siRNAs and must be selected to form a 19 bp double helix with 2 nt 3′-overhanging ends. 2′-deoxy substitutions of the 2 nt 3′-overhanging ribonucleotides do not affect RNAi, but help to reduce the costs of RNA synthesis and may enhance RNase resistance of siRNA duplexes. More extensive 2′-deoxy or 2′-*O*-methyl modifications reduce the ability of siRNAs to mediate RNAi, probably by interfering with protein association for siRNP assembly.

Target recognition is a highly sequence-specific process, mediated by the siRNA complementary to the target. The 3′-most nucleotide of the guide siRNA does not contribute to the specificity of target recognition, while the penultimate nucleotide of the 3′ overhang affects target RNA cleavage and a mismatch reduces RNAi 2- to 4-fold. The 5′ end of the guide siRNA also appears more permissive for mismatched target RNA recognition when compared with the 3′ end. Nucleotides in the centre of the siRNA, located opposite to the target RNA cleavage site, are important specificity determinants and even single nucleotide changes reduce RNAi to undetectable levels. This suggests that siRNA duplexes may be able to discriminate mutant or polymorphic alleles in gene targeting experiments, which may become an important feature for future therapeutic developments.

Sense and antisense siRNAs, when associated with the protein components of the endonuclease complex or its commitment complex, were suggested to play distinct roles; the relative orientation of the siRNA duplex in this complex defines which strand can be used for target recognition (Elbashir *et al.*, 2001b). Synthetic siRNA duplexes with an equal number of overhanging nucleotides have dyad symmetry with respect to the double-helical structure, but not with respect to sequence. The association of siRNA duplexes with the RNAi proteins in the *D.melanogaster* lysate leads to the formation of two asymmetric complexes. In such hypothetical complexes, the chiral environment is distinct for sense and antisense siRNA, hence their function. The prediction obviously does not apply to palindromic siRNA sequences or to RNAi proteins that could associate as homodimers. To minimize sequence effects that may affect the ratio of sense- and antisense-targeting siRNPs, we suggest using siRNA sequences with identical 3′-overhanging sequences. We recommend adjusting the sequence of the overhang of the sense siRNA to that of the antisense 3′ overhang because the sense siRNA does not have a target in typical knock-down experiments. Asymmetry in the reconstitution of sense- and antisense-cleaving siRNPs could be, partially, responsible for the variation in RNAi efficiency observed for various 21 nt siRNA duplexes with 2 nt 3′ overhangs used in this study (Figure 1). Alternatively, the nucleotide sequence at the target site and/or the accessibility of the target RNA structure may be responsible for the variation in efficiency observed for these siRNA duplexes. It should be noted that all siRNAs used in this study are derived from a short region of one gene. Thus, it is more likely that differences in siRNA efficiency are a consequence of the primary sequences of the siRNAs and the respective target sites, rather than the secondary or tertiary structure of the targeted RNA.

Natural siRNAs versus synthetic siRNAs

In *D.melanogaster*, siRNA duplexes are produced *in vitro* and *in vivo* from long dsRNAs (Hammond *et al.*, 2000; Yang *et al.*, 2000; Zamore *et al.*, 2000). About 45% of these short RNAs are precisely 21 nt long, 28% are 22 nt long and a few percent are shorter or longer RNAs (Elbashir *et al.*, 2001b). This length distribution correlates with our finding that 21 nt siRNA duplexes are the most efficient mediators of mRNA degradation. Beside the length, the paired structure and overhang are also important. This structural feature may explain why siRNA duplexes isolated from the dsRNA processing reaction under denaturing conditions were less potent for RNAi than longer dsRNAs that were processed to siRNAs during the targeting reaction (Zamore *et al.*, 2000). Presumably,

denaturation followed by renaturation favoured the formation of the thermodynamically more stable, blunt-ended, but less active, siRNA duplexes. Isolation of siRNAs under native conditions does not reduce siRNA activity (Nykänen *et al.*, 2001).

Production of siRNAs from long dsRNA requires the RNase III enzyme dicer (Bernstein *et al.*, 2001). Dicer is a bidentate RNase III, which also contains an ATP-dependent RNA helicase domain and a PAZ domain, presumably important for dsRNA unwinding and mediation of protein–protein interactions, respectively (Cerutti *et al.*, 2000; Bernstein *et al.*, 2001). Dicer is evolutionarily conserved in worms, flies, plants, fungi and mammals (Matsuda *et al.*, 2000), and has a second cellular function important for the development of these organisms (Ray *et al.*, 1996; Jacobsen *et al.*, 1999; Grishok *et al.*, 2001; Hutvágner *et al.*, 2001; Knight and Bass, 2001). At present, it is uncertain whether dicer activity in species other than *D.melanogaster* produces siRNAs of predominantly 21 nt in length. The estimates of siRNA size vary in the literature between 21 and 25 nt (Hamilton and Baulcombe, 1999; Hammond *et al.*, 2000; Hutvágner *et al.*, 2000; Parrish *et al.*, 2000; Yang *et al.*, 2000; Zamore *et al.*, 2000; Elbashir *et al.*, 2001b).

In a recent study of the effect of siRNA length in mammalian cells (primary mouse embryonic fibroblasts, 293 and HeLa cells), duplexes of 21–27 nt siRNAs with 2 nt 3′ overhangs were directed against different co-transfected reporter genes (Caplen *et al.*, 2001). Duplexes of 22 and 23 nt siRNAs were found to be slightly more efficient in triggering sequence-specific gene silencing than 21 nt siRNA duplexes. In our hands, using the dual luciferase assay system in HeLa cells, 21 nt siRNA duplexes with 2 nt 3′ overhang are 2- to 3-fold more efficient than 20 or 22–25 nt siRNA duplexes (data not shown), therefore recapitulating the results obtained from the *D.melanogaster* biochemical system. In contrast to the *D.melanogaster* system, siRNA duplexes >23 nt in length are still triggering some RNAi in HeLa cells and also in *C.elegans* (Caplen *et al.*, 2001). However, it remains to be determined whether the RNA strands finally incorporated into the active endonuclease complex are of the initially provided length. It is possible that exonucleases present in *C.elegans* and mammalian cells trim longer siRNAs to their optimum length and that these exonucleases are absent from *D.melanogaster* lysate.

The functional anatomy of long dsRNAs as a trigger for RNAi was analysed previously in *C.elegans* (Parrish *et al.*, 2000). Activation of RNAi by injection of long dsRNA requires at least two steps: dsRNA processing by dicer RNase III and siRNP or RISC formation. Substitution of one of the strands of the long dsRNA by DNA abolished RNAi and even the substitution of C by dC or U by dT in only one of the strands caused a substantial decrease in RNAi. Because introduction of 2′-fluoro modifications into long RNA had no effect, it was suggested that an A-form double helical structure was important for triggering RNAi (Parrish *et al.*, 2000). We have been able to substitute eight ribose residues of a siRNA duplex by 2′-deoxyribose residues without substantial reduction of RNAi, although it should be noted the 2′-deoxy modifications were clustered at the 3′ end of the siRNAs, including the 2 nt 3′ overhangs. It is possible that the four 2′-deoxy modifications, which are located in the paired region at the end of the helix, do not affect the overall A-form helical structure and do not strongly compromise RISC formation. Complete modification of one or both siRNA strands by 2′-deoxyribose, however, abolished RNAi. Interestingly, substitution by 2′-*O*-methylribose, which adopts the ribose sugar pucker, also abolished RNAi, probably because methylation of the 2′-hydroxyls blocked hydrogen bond formation or introduced steric hindrance.

It was recently demonstrated that a 5′-phosphate on the target-complementary strand of a siRNA duplex is required for siRNA function and that ATP is used to maintain the 5′-phosphates of the siRNAs (Nykänen *et al.*, 2001). However, 5′-phosphorylation of fully 2′-deoxy- or 2′-*O*-methyl-modified siRNA strands was not able to restore RNAi (data not shown). Unmodified siRNA duplexes with free 5′-hydroxyls and 2 nt 3′ overhangs are readily phosphorylated in *D.melanogaster* embryo lysate (Nykänen *et al.*, 2001). In this respect, it should be noted that our reported RNAi efficiencies were determined by pre-incubating the siRNA duplexes for 15 min in *D.melanogaster* lysate before adding target and control mRNAs, thus providing sufficient time for 5′-phosphorylation of siRNA duplexes to occur. Comparison of the RNAi efficiencies of 5′-phosphorylated and 5′-non-phosphorylated siRNAs (for duplexes shown in Figures 1E, F and 2C) did not reveal any sizeable differences (data not shown).

Conclusions

We have performed an extensive analysis of the length, sequence and structure of siRNA duplexes in *D.melanogaster* embryo lysate. Duplexes of 21 nt siRNAs with 2 nt 3′ overhangs were shown to be the most efficient triggers of RNAi-based mRNA degradation. The target recognition is a highly sequence-specific process, although not all positions of a guide siRNA contribute equally to specificity. These results are important for the design of efficient siRNAs in order to silence genes in *D.melanogaster* and provide a basis for similar studies in other organisms.

Materials and methods

RNA preparation and RNAi assay

Chemical RNA synthesis, annealing and luciferase-based RNAi assays were performed as described previously (Tuschl *et al.*, 1999; Zamore *et al.*, 2000; Elbashir *et al.*, 2001b). Synthetic RNAs were gel purified after deprotection. The formation of siRNA duplexes was verified by agarose gel electrophoresis using 4% NuSieve GTG agarose (BMA, Rockland, ME) in 0.5× TBE buffer. All siRNA duplexes were directed against firefly luciferase and the luciferase mRNA sequence was derived from pGEM-luc (DDBJ/EMBL/GenBank accession No. X65316) as described (Tuschl *et al.*, 1999). The siRNA duplexes were incubated in a *D.melanogaster* RNAi/translation reaction for 15 min prior to addition of mRNAs. Translation-based RNAi assays were performed at least in triplicate.

For mapping of sense target RNA cleavage, a 177 nt transcript was generated, corresponding to the firefly luciferase sequence between positions 113 and 273 relative to the start codon, followed by the 17 nt complement of the SP6 promoter sequence (Elbashir *et al.*, 2001b). For mapping of antisense target RNA cleavage, a 166 nt transcript was produced from a template, which was amplified from plasmid sequence by PCR using the 5′ primer TAATACGACTCACTATAGAGCCCATATCGTTTCATA (T7 promoter underlined) and 3′ primer AGAG-

GATGGAACCGCTGG. The target sequence corresponds to the complement of the firefly luciferase sequence between positions 50 and 215 relative to the start codon. Guanylyl transferase labelling was performed as described previously (Zamore *et al.*, 2000). For mapping of target RNA cleavage, 100 nM siRNA duplex was incubated with 5–10 nM target RNA in *D.melanogaster* embryo lysate under standard conditions (Zamore *et al.*, 2000) for 2 h at 25°C. The reaction was stopped by the addition of 8 vols of proteinase K buffer [200 mM Tris–HCl pH 7.5, 25 mM EDTA, 300 mM NaCl, 2% (w/v) SDS]. Proteinase K (dissolved in water; Merck) was added to a final concentration of 0.6 mg/ml. The reactions were then incubated for 15 min at 65°C, extracted with phenol/chloroform/isoamyl alcohol (25:24:1) and precipitated with 3 vols of ethanol. Samples were loaded on 6% sequencing gels. Length standards were generated by partial RNase T1 digestion and partial base hydrolysis of the cap-labelled sense or antisense target RNAs.

Acknowledgements

We acknowledge Heike Taubner and Jutta Meyer for technical assistance, Phil Zamore for critical comments on the manuscript and H.Jäckle and R.Lührmann for support. This work was funded by a BMBF Biofuture grant, No. 0311856.

References

Ambros,V. (2000) Control of developmental timing in *Caenorhabditis elegans*. *Curr. Opin. Genet. Dev.*, **10**, 428–433.

Bass,B.L. (2000) Double-stranded RNA as a template for gene silencing. *Cell*, **101**, 235–238.

Bernstein,E., Caudy,A.A., Hammond,S.M. and Hannon,G.J. (2001) Role for a bidentate ribonuclease in the initiation step of RNA interference. *Nature*, **409**, 363–366.

Caplen,N.J., Parrish,S., Imani,F., Fire,A. and Morgan,R.A. (2001) Specific inhibition of gene expression by small double-stranded RNAs in invertebrate and vertebrate systems. *Proc. Natl Acad. Sci. USA*, **98**, 9742–9747.

Carthew,R.W. (2001) Gene silencing by double-stranded RNA. *Curr. Opin. Cell Biol.*, **13**, 244–248.

Cerutti,L., Mian,N. and Bateman,A. (2000) Domains in gene silencing and cell differentiation proteins: the novel PAZ domain and redefinition of the piwi domain. *Trends Biochem. Sci.*, **25**, 481–482.

Clemens,J.C., Worby,C.A., Simonson-Leff,N., Muda,M., Maehama,T., Hemmings,B.A. and Dixon,J.E. (2000) Use of double-stranded RNA interference in *Drosophila* cell lines to dissect signal transduction pathways. *Proc. Natl Acad. Sci. USA*, **97**, 6499–6503.

Cogoni,C. and Macino,G. (2000) Post-transcriptional gene silencing across kingdoms. *Curr. Opin. Genet. Dev.*, **10**, 638–643.

Dalmay,T., Hamilton,A., Rudd,S., Angell,S. and Baulcombe,D.C. (2000) An RNA-dependent RNA polymerase gene in *Arabidopsis* is required for posttranscriptional gene silencing mediated by a transgene but not by a virus. *Cell*, **101**, 543–553.

Elbashir,S.M., Harborth,J., Lendeckel,W., Yalcin,A., Weber,K. and Tuschl,T. (2001a) Duplexes of 21-nucleotide RNAs mediate RNA interference in mammalian cell culture. *Nature*, **411**, 494–498.

Elbashir,S.M., Lendeckel,W. and Tuschl,T. (2001b) RNA interference is mediated by 21 and 22 nt RNAs. *Genes Dev.*, **15**, 188–200.

Fire,A. (1999) RNA-triggered gene silencing. *Trends Genet.*, **15**, 358–363.

Fire,A., Xu,S., Montgomery,M.K., Kostas,S.A., Driver,S.E. and Mello,C.C. (1998) Potent and specific genetic interference by double-stranded RNA in *Caenorhabditis elegans*. *Nature*, **391**, 806–811.

Fraser,A.G., Kamath,R.S., Zipperlen,P., Martinez-Campos,M., Sohrmann,M. and Ahringer,J. (2000) Functional genomic analysis of *C. elegans* chromosome I by systematic RNA interference. *Nature*, **408**, 325–330.

Gönczy,P. *et al.* (2000) Functional genomic analysis of cell division in *C. elegans* using RNAi of genes on chromosome III. *Nature*, **408**, 331–336.

Grishok,A. *et al.* (2001) Genes and mechanisms related to RNA interference regulate expression of the small temporal RNAs that control *C. elegans* developmental timing. *Cell*, **106**, 23–34.

Hamilton,A.J. and Baulcombe,D.C. (1999) A species of small antisense RNA in posttranscriptional gene silencing in plants. *Science*, **286**, 950–952.

Hammond,S.M., Bernstein,E., Beach,D. and Hannon,G.J. (2000) An RNA-directed nuclease mediates post-transcriptional gene silencing in *Drosophila* cells. *Nature*, **404**, 293–296.

Hammond,S.M., Boettcher,S., Caudy,A.A., Kobayashi,R. and Hannon,G.J. (2001a) Argonaute2, a link between genetic and biochemical analyses of RNAi. *Science*, **293**, 1146–1150.

Hammond,S.M., Caudy,A.A. and Hannon,G.J. (2001b) Post-transcriptional gene silencing by double-stranded RNA. *Nature Rev. Genet.*, **2**, 110–1119.

Hutvágner,G., Mlynarova,L. and Nap,J.P. (2000) Detailed characterization of the posttranscriptional gene-silencing-related small RNA in a GUS gene-silenced tobacco. *RNA*, **6**, 1445–1454.

Hutvágner,G., McLachlan,J., Bálint,É., Tuschl,T. and Zamore,P.D. (2001) A cellular function for the RNA interference enzyme dicer in small temporal RNA maturation. *Science*, **293**, 834–838.

Jacobsen,S.E., Running,M.P. and Meyerowitz,M.E. (1999) Disruption of an RNA helicase/RNase III gene in *Arabidopsis* causes unregulated cell division in floral meristems. *Development*, **126**, 5231–5243.

Knight,S.W. and Bass,B.L. (2001) A role for the RNase III enzyme DCR-1 in RNA interference and germ line development in *C. elegans*. *Science*, **293**, 2269–2271.

Lam,G. and Thummel,C.S. (2000) Inducible expression of double-stranded RNA directs specific genetic interference in *Drosophila*. *Curr. Biol.*, **10**, 957–963.

Maeda,I., Kohara,Y., Yamamoto,M. and Sugimoto,A. (2001) Large-scale analysis of gene function in *Caenorhabditis elegans* by high-throughput RNAi. *Curr. Biol.*, **11**, 171–176.

Matsuda,S., Ichigotani,Y., Okuda,T., Irimura,T., Nakatsugawa,S. and Hamaguchi,M. (2000) Molecular cloning and characterization of a novel human gene (HERNA) which encodes a putative RNA-helicase. *Biochim. Biophys. Acta*, **1490**, 163–169.

Moss,E.G. (2000) Non-coding RNAs: lightning strikes twice. *Curr. Biol.*, **10**, R436–R439.

Mourrain,P. *et al.* (2000) *Arabidopsis SGS2* and *SGS3* genes are required for posttranscriptional gene silencing and natural virus resistance. *Cell*, **101**, 533–542.

Nykänen,A., Haley,B. and Zamore,P.D. (2001) Nucleotide cofactor requirements and small interfering RNA conformation in the RNA interference pathway. *Cell*, **107**, 309–321.

Olsen,P.H. and Ambros,V. (1999) The lin-4 regulatory RNA controls developmental timing in *Caenorhabditis elegans* by blocking LIN-14 protein synthesis after the initiation of translation. *Dev. Biol.*, **216**, 671–680.

Palauqui,J.C., Elmayan,T., Pollien,J.M. and Vaucheret,H. (1997) Systemic acquired silencing: transgene-specific post-transcriptional silencing is transmitted by grafting from silenced stocks to non-silenced scions. *EMBO J.*, **16**, 4738–4745.

Parrish,S., Fleenor,J., Xu,S., Mello,C. and Fire,A. (2000) Functional anatomy of a dsRNA trigger: differential requirement for the two trigger strands in RNA interference. *Mol. Cell*, **6**, 1077–1087.

Pasquinelli,A.E. *et al.* (2000) Conservation of the sequence of *let-7* heterochronic regulatory RNA. *Nature*, **408**, 86–89.

Piano,F., Schetterdagger,A.J., Mangone,M., Stein,L. and Kemphues,K.J. (2000) RNAi analysis of genes expressed in the ovary of *Caenorhabditis elegans*. *Curr. Biol.*, **10**, 1619–1622.

Ray,A., Lang,J.D., Golden,T. and Ray,S. (1996) Short integument (*SIN1*), a gene required for ovule development in *Arabidopsis*, also controls flowering time. *Development*, **122**, 2631–2638.

Reinhart,B.J., Slack,F.J., Basson,M., Pasquinelli,A.E., Bettinger,J.C., Rougvie,A.E., Horvitz,H.R. and Ruvkun,G. (2000) The 21-nucleotide let-7 RNA regulates developmental timing in *Caenorhabditis elegans*. *Nature*, **403**, 901–906.

Sharp,P.A. (2001) RNA interference 2001. *Genes Dev.*, **15**, 485–490.

Smardon,A., Spoerke,J., Stacey,S., Klein,M., Mackin,N. and Maine,E. (2000) EGO-1 is related to RNA-directed RNA polymerase and functions in germ-line development and RNA interference in *C. elegans*. *Curr. Biol.*, **10**, 169–178.

Stark,G.R., Kerr,I.M., Williams,B.R., Silverman,R.H. and Schreiber,R.D. (1998) How cells respond to interferons. *Annu. Rev. Biochem.*, **67**, 227–264.

Tuschl,T. (2001) RNA interference and small interfering RNAs. *ChemBioChem*, **2**, 239–245.

Tuschl,T., Zamore,P.D., Lehmann,R., Bartel,D.P. and Sharp,P.A. (1999) Targeted mRNA degradation by double-stranded RNA *in vitro*. *Genes Dev.*, **13**, 3191–3197.

Ui-Tei,K., Zenno,S., Miyata,Y. and Saigo,K. (2000) Sensitive assay of

RNA interference in *Drosophila* and Chinese hamster cultured cells using firefly luciferase gene as target. *FEBS Lett.*, **479**, 79–82.

Voinnet,O. (2001) RNA silencing as a plant immune system against viruses. *Trends Genet.*, **17**, 449–459.

Voinnet,O., Vain,P., Angell,S. and Baulcombe,D.C. (1998) Systemic spread of sequence-specific transgene RNA degradation in plants is initiated by localized introduction of ectopic promoterless DNA. *Cell*, **95**, 177–187.

Waterhouse,P.M., Wang,M.B. and Lough,T. (2001) Gene silencing as an adaptive defence against viruses. *Nature*, **411**, 834–842.

Wightman,B., Ha,I. and Ruvkun,G. (1993) Posttranscriptional regulation of the heterochronic gene lin-14 by lin-4 mediates temporal pattern formation in *C. elegans*. *Cell*, **75**, 855–862.

Yang,D., Lu,H. and Erickson,J.W. (2000) Evidence that processed small dsRNAs may mediate sequence-specific mRNA degradation during RNAi in *Drosophila* embryos. *Curr. Biol.*, **10**, 1191–1200.

Zamore,P.D., Tuschl,T., Sharp,P.A. and Bartel,D.P. (2000) RNAi: double-stranded RNA directs the ATP-dependent cleavage of mRNA at 21 to 23 nucleotide intervals. *Cell*, **101**, 25–33.

Received August 23, 2001; revised October 10, 2001; accepted October 16, 2001

TAB 5

ACADEMIC PRESS

Methods 26 (2002) 199–213

METHODS

www.academicpress.com

Analysis of gene function in somatic mammalian cells using small interfering RNAs

Sayda M. Elbashir,[a,1] Jens Harborth,[b,1] Klaus Weber,[b,*] and Thomas Tuschl[a,*]

[a] *Department of Cellular Biochemistry, Max-Planck-Institute for Biophysical Chemistry, Am Fassberg 11, D-37077 Göttingen, Germany*
[b] *Department of Biochemistry and Cell Biology, Max-Planck-Institute for Biophysical Chemistry, Am Fassberg 11, D-37077 Göttingen, Germany*

Accepted 29 January 2002

Abstract

RNA interference (RNAi) is a highly conserved gene silencing mechanism that uses double-stranded RNA (dsRNA) as a signal to trigger the degradation of homologous mRNA. The mediators of sequence-specific mRNA degradation are 21- to 23-nt small interfering RNAs (siRNAs) generated by ribonuclease III cleavage from longer dsRNAs. Twenty-one-nucleotide siRNA duplexes trigger specific gene silencing in mammalian somatic cells without activation of the unspecific interferon response. Here we provide a collection of protocols for siRNA-mediated knockdown of mammalian gene expression. Because of the robustness of the siRNA knockdown technology, genomewide analysis of human gene function in cultured cells has now become possible.

Keywords: RNA interference; Small interfering RNA; Posttranscriptional gene silencing; Knockdown; Double-stranded RNA

1. Introduction

Mammalian gene function has been determined traditionally by methods such as disruption of murine genes, the introduction of transgenes, the molecular characterization of human hereditary diseases, and targeting of genes by antisense or ribozyme techniques. In addition, microinjection of specific antibodies into cultured cells or binding of antibodies to cell surface-exposed receptors may provide information on the function of the targeted protein. A new alternative to these reverse genetic approaches has now become available with the discovery of small interfering RNAs, which are able to trigger RNA interference in mammalian somatic cells [1,2].

RNA interference (RNAi) is a sequence-specific posttranscriptional gene silencing mechanism, which is triggered by double-stranded RNA and causes degradation of mRNAs homologous in sequence to the dsRNA [3,4]. Although RNAi has been observed in a wide range of eukaryotes, including plants, protists, filamentous fungi, and invertebrate and vertebrate animals [5–10], it has only recently become possible to silence human genes in cultured somatic cells [1]. The detection of RNAi in somatic mammalian cells has been hampered by the presence of a number of dsRNA-triggered pathways that mediate nonspecific suppression of gene expression [11–14]. dsRNA is a potent inducer of type I interferon (IFN) synthesis and is the activator of two classes of IFN-induced enzymes: PKR, the dsRNA-dependent protein kinase, and 2′,5′-oligoadenylate synthetases, whose products activate the latent ribonuclease RNase L. These nonspecific responses to dsRNA are not triggered by dsRNA shorter than 30 bp including siRNA duplexes that resemble in length and structure the natural processing products from long dsRNAs [1,2,15]. The most predominant processing products are duplexes of 21- and 22-nt RNAs with symmetric 2-nt 3′ overhangs, which are also the most efficient mediators of mRNA degradation [16].

One of the enzymes involved in processing long dsRNAs to siRNA duplexes is the RNase III enzyme Dicer, which was characterized in extracts prepared

* Corresponding authors. Fax: +49-551-201-1197.
E-mail addresses: office.weber@mpibpc.gwdg.de (K. Weber), ttuschl@mpibpc.gwdg.de (T. Tuschl).
[1] Authors contributed equally to this review.

1046-2023/02/$ - see front matter
PII: S1046-2023(02)00023-3

from insect cells [17], *Caenorhabditis elegans* embryos [18], and mammalian cultured cells [19]. In mammalian cells, it was also shown that Dicer localizes to the cytoplasm, which provides evidence that RNAi is a predominantly cytoplasmic process [19]. Dicer has an N-terminal RNA helicase domain, a PAZ domain [20], two RNase III domains, and a C-terminal dsRNA-binding motif. A PAZ domain is also present in Argonaute2, which is a component of the mRNA-degrading sequence-specific endonuclease complex of *Drosophila melanogaster Schneider 2* cells [21]. This siRNA-bound endonuclease complex was also referred to as RNA-induced silencing complex (RISC) [22]. Dicer and Argonaute2 appear to interact in S2 cells, probably through their PAZ domains, but RISC and Dicer activities could be separated and RISC was unable to process dsRNA to siRNAs, suggesting that Dicer is not a component of RISC [21,22]. Possibly, the interaction between Dicer and Argonaute2 facilitates siRNA incorporation into RISC [21]. The catalytic subunit of RISC remains to be identified. A schematic illustration of the mechanism of RNAi is shown in Fig. 1.

In *D. melanogaster* lysate, RISC is readily assembled onto synthetic siRNA duplexes and is highly effective in degrading homologous mRNAs [16,23]. In vivo, siRNA duplexes are easily introduced into *D. melanogaster* or human somatic cells by transfection with cationic liposomes [1]. When siRNAs are directed against endogenous genes, expression of the corresponding gene

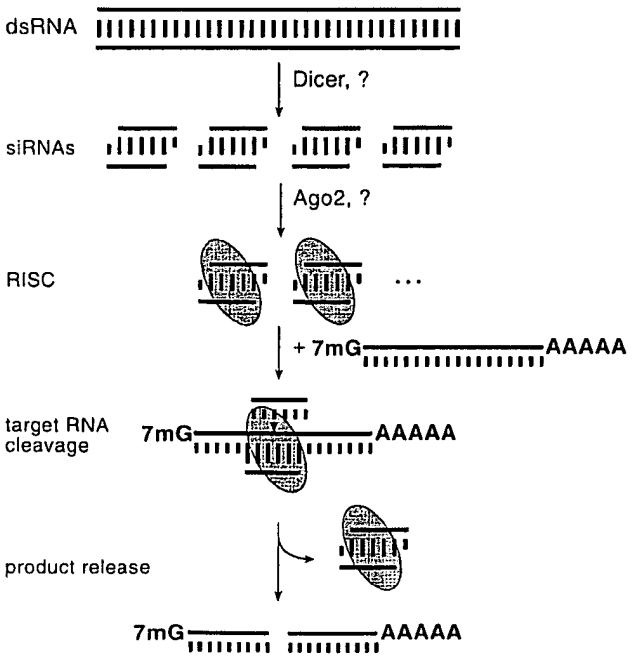

Fig. 1. Model for RNA interference. dsRNA is processed to 21- to 23-nt siRNA duplexes by Dicer RNase III and presumably other factors. The siRNA duplexes are incorporated into RISC, which targets homologous mRNAs for degradation. Ago2 and yet to be characterized proteins participate in RISC formation.

products is knocked down as expected. This technique can be applied to any protein-coding gene, as validated recently by examining the knockdown phenotypes of 20 different gene products in human somatic cells [24]. In a different report, siRNAs were successfully used to knockdown human Dicer protein, which revealed a new cellular function of Dicer for let-7 RNA precursor processing [25]. Furthermore, siRNAs were successfully used to establish a function for the human vacuolar protein Tsg101 for HIV (human immunodeficiency virus) budding [26]. Knockdown of this cellular protein arrested HIV-1 budding and this defect could be rescued by transfection of a plasmidborne, RNAi-resistant version of Tsg101. This combination of siRNA knockdown and plasmid rescue experiments will become extremely valuable for functional analysis of mutant protein-coding constructs. Further applications of siRNAs for specific gene silencing in cultured mammalian cells have been published recently [15,27–31].

Here we present detailed protocols to produce and evaluate siRNA-induced protein knockdowns in mammalian somatic cells. The method is useful for reverse genetic analysis of mammalian gene function in any aspect of general cell biology, such as cell cycle, gene expression, metabolic pathways, or the cytoskeleton. The method is also suitable for high-throughput analysis of gene function, provided that highly transfectable cell lines are used and that single-cell based assays, e.g., immunofluorescence, are applied for phenotypic screening.

2. Selection of siRNA sequences for targeting of mRNAs

The design of siRNA duplexes for interfering with the expression of a specific gene requires knowledge of the accurate target sequence, i.e., of at least a 20-nt segment of its encoded mRNA. Intronic sequences contained in pre-mRNAs should not be targeted, because incompletely spliced mRNAs are normally retained in the nucleus and RNAi is believed to occur predominantly, if not exclusively, in the cytoplasm. Sequence information about mature mRNAs may be extracted from EST databases (www.ncbi.nlm.nih.gov or www.ebi.ac.uk) or can be predicted from genomic sequences using gene prediction programs. However, the limited quality of single-pass EST sequence data or gene predictions should be kept in mind.

The analysis of siRNA function in *D. melanogaster* embryo lysates indicated that siRNA duplexes composed of 21-nt sense and 21-nt antisense strands, paired in a manner to have a 2-nt 3′ overhang, are the most efficient triggers of sequence-specific mRNA degradation in this system [23]. Preliminary analysis of the length dependence of siRNAs in mammalian cells suggests that this may also be true in mammalian systems, although differences in efficiencies as a function of

siRNA length are less pronounced than in the fly biochemical system (Ref. [2], and Section 4).

The target RNA cleavage reaction guided by siRNAs is highly sequence-specific. However, not all positions of a siRNA contribute equally to target recognition [23]. Mismatches in the center of the siRNA duplex are most critical and essentially abolish target RNA cleavage. In contrast, the 3′ nucleotide of the siRNA strand (position 21) that is complementary to the single-stranded target RNA does not contribute to specificity of target recognition. As may be expected, the sequence of the unpaired 2-nt 3′ overhang of the siRNA strand with the same polarity as the target RNA is not critical for target RNA cleavage as only the antisense siRNA strand guides target recognition. Thus, only the penultimate position of the antisense siRNA (position 20) needs to match the targeted sense mRNA [23].

Selection of the targeted region is currently a trial-and-error process, but with the likelihood of 80–90% success given a large enough random selection of target genes [24]. In every single case, however, the half-life of the targeted gene product, its abundance, or the regulation of its expression may have to be considered. For example, in an attempt to knock down the strongly expressed and stable intermediate filament protein vimentin, only two of four randomly selected siRNAs were effective [24]. We prefer to select target regions such that siRNA sequences may contain uridine residues in the 2-nt overhangs (Fig. 2A). Uridine residues in the 2-nt 3′ overhang can be replaced by 2′-deoxythymidine without loss of activity, which significantly reduces costs of RNA synthesis and may also enhance nuclease resistance of siRNA duplexes when applied to mammalian cells [23]. Another rationale for designing siRNA duplexes with symmetric TT overhangs is to ensure that the sequence-specific endonuclease complex (RISC) is formed with an approximately equal ratio of sense to antisense target RNA-cleaving complexes [16,23].

It may also be desirable to design siRNA sequences in a manner that may allow the later expression of siRNAs from plasmids or in transgenic animals, should such technology become available. Efficient expression of small ribozymes or antisense RNAs using polymerase III promoters was previously demonstrated [32,33]. Because RNA transcription is primed by 5′-guanosine triphosphate, it would require the selection of siRNA sequences starting with 5′-guanosine residues.

It was recently demonstrated that a 5′-phosphate on the target-complementary strand of a siRNA duplex is required for siRNA function and that ATP is used to maintain the 5′-phosphates of the siRNAs [34]. However, siRNA duplexes with free 5′-hydroxyls and 2-nt 3′ overhangs are readily phosphorylated in *D. melanogaster* embryo lysates [34] and also in extracts prepared from human HeLa cells (J. Martinez and T. Tuschl, unpublished). As expected, comparison of the mammalian RNAi efficiencies of 5′-phosphorylated and non-phosphorylated siRNAs did not reveal any sizable differences (J. Harborth, S. Elbashir, unpublished). Thus, siRNAs synthesized or purchased without a 5′-phosphate group can be used in knockdown experiments.

Finally, we believe that the secondary structure of the target mRNA does not have a strong effect on silencing, as judged by the success rate of the essentially randomly chosen siRNA duplexes. A more comprehensive evaluation of all the parameters to be considered for siRNA selection remains to be performed, perhaps best on a therapeutically relevant target. Therefore, our

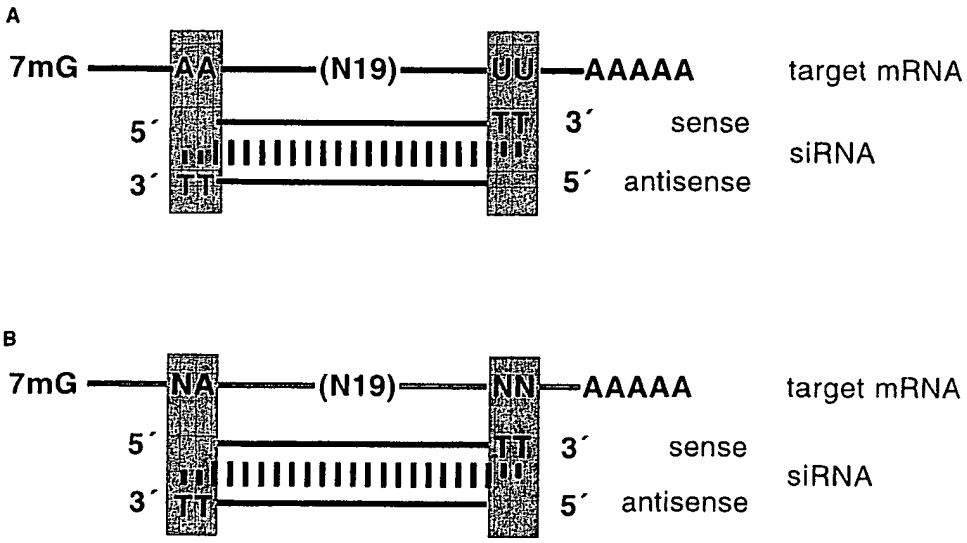

Fig. 2. Selection of siRNA duplexes. (A) The design of siRNA duplexes for target mRNAs that contain the sequence AA(N19)UU. (B) The design of siRNA duplexes in the absence of AA(N19)UU target sequences. As long as one adenosine is present in the targeted region, siRNA duplexes with 3′-TT overhangs can be used without effect on specificity of target recognition or RNAi efficiency.

"personal" set of rules is only a historic starting point and it is not intended to discourage anybody from further experimentation.

2.1. Protocol 1: selection of siRNA sequences

1. Select the target region from the open reading frame of a given cDNA sequence preferably 50 to 100 nt downstream of the start codon. Avoid 5′ or 3′ untranslated regions (UTRs) or regions close to the start codon as these may be richer in regulatory protein binding sites. It is conceivable that UTR-binding proteins and/or translation initiation complexes could interfere with binding of RISC to the target RNA. However, if it is desired to rescue a knockdown phenotype by reintroduction of a plasmid coding for a mutant or tagged form of the targeted gene, it may be favorable to target regions in the UTRs. Preparation of rescue constructs by deletion of terminal untranslated sequences is easier than the introduction of silent mutations within the targeted region of a coding segment. Which of the approaches works best remains to be examined.
2. Search for sequences 5′-AA(N19)UU, where N is any nucleotide, in the mRNA sequence and choose those with approximately 50% G/C content (Fig. 2A). Nevertheless, 32 to 79% G/C content has also worked well in our hands. Highly G-rich sequences should be avoided because they tend to form G-quartet structures. If there are no 5′-AA(N19)UU motifs present in the target mRNA, search for 5′-AA(N21) or 5′-NA(N21) (Fig. 2B). Independent of the selection procedure described in Fig. 2, synthesize the sense siRNA as 5′-(N19)TT, and the sequence of the antisense siRNA as 5′-(N′19)TT, where N′19 denotes the reverse complement sequence of N19. N19 and N′19 indicate ribonucleotides; T indicates 2′-deoxythymidine.
3. Blast-search (www.ncbi.nlm.nih.gov/BLAST) the selected siRNA sequences against EST libraries or mRNA sequences of the respective organism to ensure that only a single gene is targeted.
4. It may be advisable to synthesize several siRNA duplexes to control for the specificity of the knockdown experiments; those siRNA duplexes that are effective for silencing should produce exactly the same phenotype. Furthermore, a nonspecific siRNA duplex may be needed as control. It is possible to reverse the sequence of an effective siRNA duplex or to use a siRNA duplex, which is targeting a gene absent from the selected model organism, e.g., GFP or luciferase. We have previously used a siRNA duplex targeting firefly luciferase as a control for targeting endogenous genes in mammalian cells since the firefly luciferase gene was not present in the targeted cells [1].
5. If the siRNA does not work, first verify that the target sequence and the cell line used are derived from the same organism. According to a recent study, there is quite a high probability for not having the right cell line [35]. Finally, make sure that the mRNA sequence used for selection of the siRNA duplexes is reliable; it could contain sequencing errors, mutations (e.g., in cancer cells) or polymorphisms.

3. Preparation of siRNA duplexes

Twenty-one-nucleotide RNAs are preferably chemically synthesized using appropriately protected ribonucleoside phosphoramidites and a conventional DNA/RNA synthesizer. Synthesis protocols are adapted to RNA reagents [36]. Suppliers of RNA synthesis reagents are Proligo (Hamburg, Germany, www.proligo.com), Dharmacon Research (Lafayette, CO, www.dharmacon.com), Pierce Chemical (part of Perbio Science, Rockford, IL, www.perbio.com), Glen Research (Sterling, VA, www.glenres.com), ChemGenes (Ashland, MA, www.chemgenes.com), and Cruachem (Glasgow, UK, www.cruachem.com). Most conveniently, siRNAs are obtained from commercial RNA oligonucleotide synthesis suppliers, which sell RNA synthesis products of different quality and costs. In general, 21-nt RNAs are not too difficult to synthesize and are readily provided in a quality suitable for RNAi.

The following custom RNA synthesis companies are entitled to provide siRNAs with a license for target validation. A typical 0.2-μmol-scale RNA synthesis provides about 1 mg of RNA, which is sufficient for 1000 transfection experiments using a 24-well tissue culture plate format.

3.0.1. Dharmacon (www.dharmacon.com)

Dharmacon currently offers three siRNA options for the custom synthesis of siRNA oligonucleotides. (Dharmacon also offers a range of presynthesized siRNA duplexes.) Option A offers water-soluble, stable, 2′-protected RNA, which is readily deprotected in aqueous buffers after arrival. The 2′ protection ensures the RNA is not degraded before use. The pair of RNA oligonucleotides can be simultaneously 2′-deprotected and annealed in the same reaction as a further precaution against degradation. The siRNA duplex can then be readily desalted via ethanol precipitation directly from the aqueous 2′-deprotection/annealing reaction [37]. After deprotection and annealing, the RNA pellet is dissolved in 400 μl buffer. To ethanol precipitate, adjust the solution to 0.3 M NaCl by addition of 26 μl 5 M NaCl. Finally, add 1500 μl absolute ethanol and vortex. After 1–2 h incubation of the sample on dry ice or at −20 °C, collect the RNA pellet by centrifugation. Remove all

liquid and redissolve the pellet in 200–400 μl sterile water. Determine the concentration by UV spectroscopy (1 A_{260} unit is equivalent to 32 μg RNA) and continue with annealing (see below). Alternatively, the pair of RNA oligonucleotides can be simultaneously 2′-deprotected and annealed in the same reaction as a further precaution against degradation. The siRNA duplex can then be readily desalted via ethanol precipitation directly from the aqueous 2′-deprotection/annealing reaction [37]. It should be noted that the crude RNA products are more than 85% full-length, which makes gel purification of siRNAs for knockdown applications unnecessary. Option B provides the RNA fully deprotected, desalted, and aliquoted in 50-nmol amounts. Redissolve the shipped RNA pellet in water and continue with siRNA annealing (see below). Option C provides the siRNAs as the purified duplex with a purity >97%. Redissolve the shipped RNA duplex pellet in water and continue directly with transfection (see below). This final option guarantees the duplex is properly formed and ready for transfection. It is also possible to order the RNA with duplexing but no purification with either Option A or Option B.

3.0.2. Xeragon Inc. (www.xeragon.com)

Xeragon offers siRNAs in two ready-to-use options and a variety of off-the-shelf siRNA duplexes for common gene targets. Option 1 offers crude siRNAs that are fully deprotected and desalted (NAP-10 Sephadex G-25 and ethanol precipitation) and which are more than 85% pure. Option 2 provides siRNAs that are ion-exchange HPLC-purified and are more than 97% pure. Both options include a choice for free annealing and come with a quality HPLC-trace done on the actual duplex if annealing was requested. Otherwise the quality is shown in two individual chromatograms. Both options are ready for transfection. The sterile buffer to dilute the siRNAs is provided. It is recommended that siRNA duplexes lyophilized for shipment be dissolved in annealing buffer and reheated to 95 °C for 1 min followed by 1 h at 37 °C incubation (as described below). This procedure disrupts higher aggregates, which may have formed in the lyophilization process.

3.0.3. Genset Oligos (www.gensetoligos.com)

Genset Oligos offers fully deprotected and desalted siRNAs delivered in dried form and ready for resuspension. The siRNAs are supplied in either single strand or duplex format and are more than 85% pure. Genset Oligos also offers siRNAs at higher grades of purity (PAGE, RP-HPLC purification). All shipped siRNAs are systematically controlled by PAGE and certified for gene silencing applications. The protocol for siRNA annealing is posted on Genset Oligo's Web site.

3.0.4. Ambion (www.ambion.com)

Ambion has developed a transcription-based method for construction of siRNA available as The Silencer siRNA Construction Kit. Ambion also offers the traditional custom chemical synthesis service for siRNA and supplies fully deprotected and desalted siRNAs, with optional PAGE purification and delivered in dry form along with RNase-free water and 5× annealing buffer. A central Web-based resource for RNAi and siRNA methodologies, along with links to additional siRNA-related products and services, can be found on Ambion's Web site.

Several other synthesis companies may provide 21-nt RNAs without a license for siRNA applications. However, it should be noted that the application of RNAs as siRNAs requires a license, which is included when purchasing RNA from licensed providers listed above, or can be provided as in-house research licenses from the MIT licensing office (Cambridge, MA) or Garching Innovation (Munich, Germany).

3.1. Protocol 2: annealing of siRNAs to produce siRNA duplexes

1. Prepare 2× annealing buffer (200 mM potassium acetate, 4 mM magnesium acetate, 60 mM Hepes–KOH, pH 7.4).
2. To prepare 140 μl of a 20 μM siRNA duplex solution, combine 70 μl 2× annealing buffer, x μl sense siRNA (20 μM final concentration), y μl antisense oligonucleotide (20 μM final concentration), and $70 - x - y$ μl sterile water.
3. Incubate for 1 min at 90 °C, followed by 1 h at 37 °C. After use, store the solution frozen at −20 °C. The siRNA duplex solution can be freeze–thawed many times and does not require any further heat-shock treatments. As general advice, it is recommended that RNA solutions be kept on ice as much as possible to reduce the rate of RNA hydrolysis.
4. For quality control, separately load 1 μl 20 μM sense and antisense siRNA and 0.5 μl 20 μM siRNA duplex onto 4% NuSieve GTG agarose gels (BMA, Rockland, ME, www.bmaproducts.com). For loading of the samples, it is helpful to first dilute the samples with a few microliters of 0.5× TBE buffer (45 mM Tris base, 45 mM boric acid, 1 mM Na_2 EDTA) and sucrose loading buffer [38]. Run the gel in 0.5× TBE buffer at 80 V for 1 h. Note that NuSieve agarose is a low-melt agarose and it may melt if electrophoresis is performed with too high an electric current. The RNA bands are visualized under UV light after ethidium bromide staining. Preferably, the ethidium bromide is added to the 4% gel/0.5× TBE solution at a concentration of 0.04% mg/l prior to casting of the gel. An example is illustrated in Fig. 3.

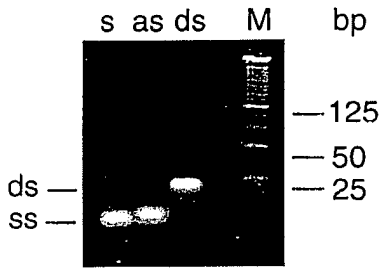

Fig. 3. Analysis of siRNA duplex formation. Single-stranded (ss) sense RNA (s), antisense RNA (as), and annealed siRNA duplexes (ds) were separated on 4% NuSieve agarose gels. A 25-bp DNA ladder (M) was loaded as marker. The bands were visualized by UV light after ethidium bromide staining. The siRNA duplex was used for targeting lamin A/C mRNA [1].

4. Determination of RNAi activity of mammalian cells by co-transfection of luciferase reporter plasmids and siRNA duplexes

Before siRNAs are applied to knock down an endogenous gene, it may be important to establish if the studied cells are susceptible to RNAi. It may be possible that some cell lines have lost the ability to perform RNAi or that cells derived from certain tissues do not support RNAi. We developed a rapid and reliable protocol to examine transfectable cell lines for the ability to perform RNAi [1]. Reporter plasmids, encoding firefly (*Photinus pyralis*) and sea pansy (*Renilla reniformis*) luciferase (Fig. 4A), were cotransfected into cells with specific or control siRNAs (Fig. 4B). Following a 1-day incubation period, cells were lysed and luciferase activity was monitored. The sensitive luciferase assay combined with the siRNA cotransfection provide a reliable readout even at low transfection efficiencies. Using this assay, we demonstrated that siRNAs trigger silencing in HeLa (human cervix carcinoma) S3 (Fig. 4C, D) and HeLa SS6, COS-7 (African green monkey kidney), NIH/3T3 (mouse fibroblast), HEK 293 (human embryonic kidney), CHO (Chinese hamster ovary) (Fig. 4E), A431 (human epidermoid carcinoma) (Fig. 4F), and SKBR3 (human breast tumor) (Fig. 4G) cells. Instead of luciferase constructs, green fluorescent protein (GFP)-encoding plasmids may be transfected together with GFP and control siRNAs. The GFP-based assay may be most suitable for quantification by fluorescence-activated cell sorting (FACS). Please note that transfection reagents change the autofluorescence of cells, which must be controlled for by mock transfection.

4.1. Protocol 3: cell culture and preparation of cells in 24-well plates

1. Grow various mammalian cell lines, e.g., HeLa S3, HeLa SS6, COS7, NIH/3T3, HEK 293, CHO, A431, and SKBR3, in a 5% CO_2 humidified incubator at 37 °C in Dulbecco's modified Eagle's medium (DMEM) (Life Technologies, No. 41966-029, www.lifetech.com) supplemented with 10% fetal bovine serum (FBS) (Life Technologies, No. 10500-064), 100 units/ml penicillin, and 100 μg/ml streptomycin (BioChrom, No. A2212, www.biochrom.com). For general advice on cell culture, see [39]. Passage cells regularly to maintain exponential growth. Do not exceed a passage number of 30 after thawing the stock culture. The number of passages may affect DNA and siRNA transfection efficiencies. Aliquots of cells of low passage number may be stored frozen and can be thawed at convenience.
2. One day (24 h) before plasmid/siRNA transfection, trypsinize 90% confluent cells grown in a 175-ml cell culture flask with 10 ml trypsin–EDTA (Life Technologies, No. 25300-054). Dilute the cell suspension 1:5 with fresh DMEM medium without antibiotics, and transfer 500-μl aliquots into each well of a 24-well plate. If immunofluorescence assays are planned, cells should be grown on coverslips, which are placed at the bottom of the 24-well plates prior to addition of the cell suspension. Twenty-four hours after seeding the cells, a confluency of 50–80% should be reached, which corresponds to 3×10^4–1×10^5 cells per well depending on the cell line and its doubling time.

4.2. Protocol 4: cotransfection of luciferase reporter plasmids with siRNA duplexes

The protocol below is based on a published procedure [1]. Two applications are illustrated in Figs. 4 and 5. The quantities of reagents given below are calculated for the transfection of one well of a 24-well plate.

1. The day before transfection, follow protocol 3 for culturing cells in 24-well plates.
2. Mix 1.0 μg pGL2-Control plasmid (Promega, No. E1611) or 1 μg pGL3-Control plasmid (Promega, No. E1741) with 0.1 μg pRL-TK plasmid (Promega, No. E2241, www.promega.com) and 0.21 μg siRNA duplex (0.75 μl 20 μM annealed duplex, see protocol 2) with 50 μl OPTI-MEM 1 medium (Life Technologies, No. 31985-047). Reporter plasmids may be amplified in XL-1 Blue (Stratagene, No. 200249, www.stratagene.com) and purified using the Qiagen EndoFree maxi plasmid kit (www.qiagen.com).
3. In a separate tube, add 2 μl Lipofectamine 2000 (Invitrogen, No. 11668-019, www.invitrogen.com) to 50 μl Opti-Mem 1. Mix the tube gently by inverting, not by vortexing. Incubate the suspension for 5 min at room temperature without movement.
4. Combine the solution from step 2 with the suspension from step 3. Mix gently by inverting the tube and incubate for 20–25 min at room temperature to allow for formation of liposome complexes. Do not exceed a 30-min incubation time.

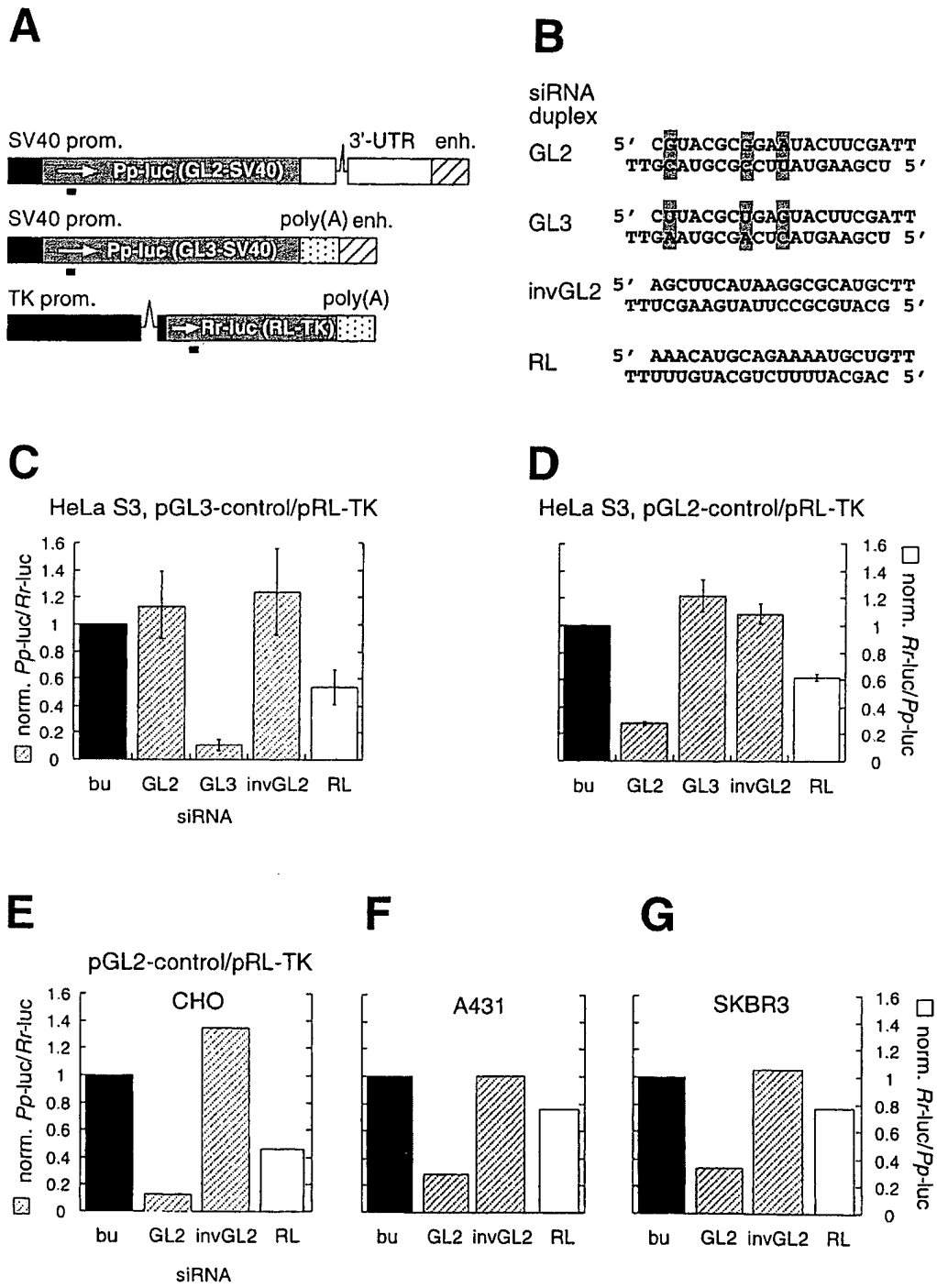

Fig. 4. Detection of RNAi in mammalian cells by cotransfection of reporter constructs. (A) Reporter constructs. The firefly (*Pp*-luc) and sea pansy (*Rr*-luc) luciferase reporter-gene regions from plasmids pGL2-Control, pGL3-Control, and pRL-TK are illustrated. The promoter, enhancer and poly (A) region are indicated. The sequences of GL2 and GL3 luciferase are 95% identical but completely unrelated to that of RL. The region targeted by the siRNA duplexes is indicated as a black bar below the coding region. (B) siRNA duplexes targeting GL2, GL3, and RL luciferase. GL2 and GL3 differ by only three single-nucleotide substitutions. As nonspecific control, a duplex with the inverted GL2 (invGL2) sequence was included. The 2-nt 3′ overhang of 2′-deoxythymidine is indicated as TT. (C–G) RNA interference measurements. Ratios of target to control luciferase were normalized to that of a buffer control (bu, black bars); patterned bars indicate ratios of firefly (*Pp*-luc) GL2 or GL3 luciferase to sea pansy (*Rr*-luc) RL luciferase (left axis); white bars indicate RL to GL2 or GL3 ratios (right axis). The cell line used for the interference experiment is indicated at the top of each plot. Cotransfection of plasmids was performed with 0.21 μg siRNA duplex/well for HeLa cells (C, D) and with 0.84 μg for the other cell lines tested (E–G); see also protocol 4.

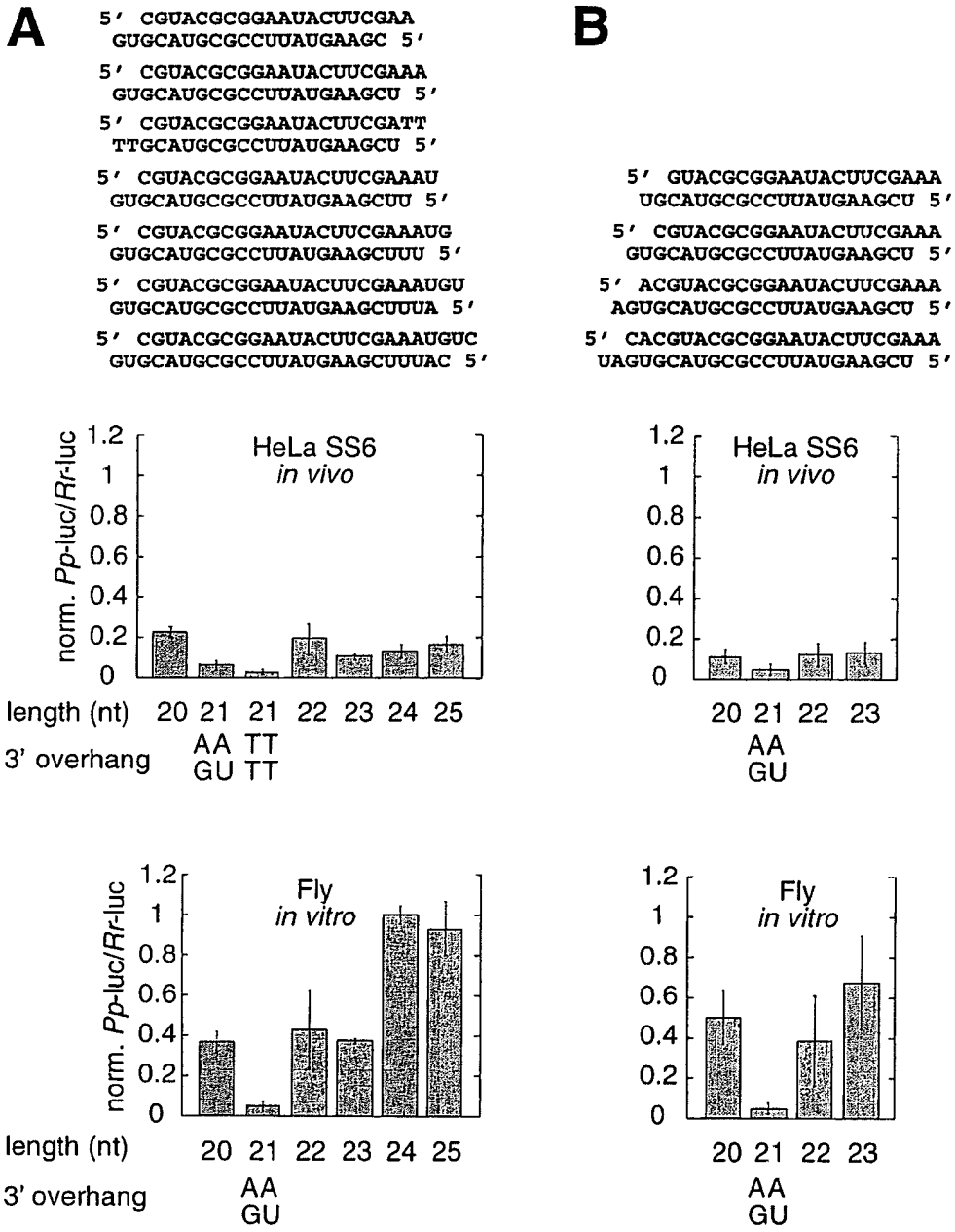

Fig. 5. Variation of the length of siRNA duplexes with preserved 2-nt 3′ overhangs. The siRNA duplexes were extended to the 3′ side of the sense siRNA (A) or the 5′ side of the sense siRNA (B). The siRNA duplex sequences and the respective interference ratios are indicated. For HeLa SS6 cells, siRNA duplexes (0.84 μg) targeting GL2 luciferase were transfected together with pGL2-Control and pRL-TK plasmids (protocol 4). For comparison, the in vitro RNAi activities of siRNA duplexes tested in *D. melanogaster* lysate are indicated [23].

5. Add the liposome complexes to the well without replacing the growth medium and mix gently for 15 s by gently rocking the plate. Incubate the plate for 20–48 h at 37 °C in the incubator (see above). If cytotoxic effects are to be expected from the transfection reagent, it is possible to change the growth medium 5 h after transfection.
6. To monitor luciferase activity, lyse cells and measure luciferase expression subsequently by the dual luciferase assay (Promega, No. E1960) according to the manufacturer's instructions.

Remark. To estimate the transfection efficiency it is convenient to cotransfect a GFP-coding plasmid together with 0.21 μg of a siRNA duplex noncognate to GFP (e.g., invGL2, Fig. 4B) and to count the GFP-expressing cells by fluorescence microscopy. Transfection efficiencies for most cell lines described above range from 70 to 90%.

5. Knockdown of the expression of endogenous genes by siRNA duplexes

We examined silencing of many different genes expressed in cultured mammalian cells by duplexes of 21-nt siRNAs [1,24]. Knockdown of proteins of various subcellular localizations, functions, or expression levels was achieved. The majority of knockdown experiments were performed in human HeLa cells, but we also knocked down proteins in SV40 transformed rat fibroblasts and mouse 3T3 cells. Knockdown of proteins was frequently associated with impaired cell growth or altered cell morphology, which was monitored by phase-contrast microscopy. If no alterations in cell growth or cell morphology were observed, immunofluorescence or Western blotting was performed to analyze the depletion of the target protein. When no antibodies are available, the levels of the targeted mRNA may be monitored by reverse transcription polymerase chain reaction (RT-PCR) [25]. Examples of knockdown cells and characterization of the associated phenotypes are shown in Figs. 6–12.

Exogenous delivery of siRNA duplexes to mammalian cells was carried out with the transfection reagent Oligofectamine (Invitrogen, No. 12252-011, www.invitrogen.com), which was developed for the delivery of short oligonucleotides. Transfection efficiencies with Oligofectamine were near 90%. A new siRNA transfection reagent, TransIT-TKO (Mirus, No. MIR 2150, www.genetransfer.com) has recently become available. Cells did not take up siRNA duplexes in the absence of transfection reagents. Knockdown phenotypes were apparent 1–3 days posttransfection, but depended on the efficiency of the siRNA duplex and/or the abundance and/or the lifetime (turnover) of the targeted proteins [24]. To control for the specificity of the knockdown, we transfected cultures with a siRNA duplex targeting firefly luciferase (GL2, Fig. 4B) or buffer, both of which have no detectable effect on cell growth or morphology.

5.1. Protocol 5: transfection of siRNA duplexes

The quantities of reagents given below are calculated for the transfection of one well of a 24-well plate.

1. The day before transfection, follow closely protocol 3, but dilute the cell suspension after trypsination of the stock culture 1:10 rather than 1:5 before transferring to the 24-well plate. A higher dilution is necessary to obtain the recommended confluency of 50% for Oligofectamine transfection.
2. Mix 3 μl 20 μM siRNA duplex (0.84 μg, 60 pmol) with 50 μl Opti-Mem 1.
3. In a separate tube, add 3 μl Oligofectamine or 3.5 μl of TransIT-TKO to 12 μl Opti-Mem 1. Mix gently and incubate for 7–10 min at room temperature.
4. Combine the solutions prepared in steps 2 and 3 and mix gently by inversion, not by vortexing. Incubate for 20–25 min at room temperature to allow for formation of liposome complexes; the solution will turn turbid. Then add 32 μl fresh Opti-Mem 1 to obtain a final volume of 100 μl and mix gently by inversion. The addition of 32 μl optiMEM is optional and serves only to adjust the total volume of cell culture medium to 600 μl after transfection.
5. Add the 100-μl liposome complexes to the well without replacing the growth medium and mix gently for 30 s by gently rocking the plate. Incubate the plate for 2–3 days at 37 °C in the incubator.

6. Detection of siRNA-mediated specific gene silencing

Growth arrest of transfected cells is easily monitored by phase-contrast microscopy. Cells grown and transfected on coverslips are mounted on slides in Hepes-buffered DMEM (pH 7.3) supplemented with 10% fetal calf serum (FCS) (Sigma, No. F-7521) and examined with a microscope for example equipped with a Plan-Neofluar 25×/0.8 objective. Cells arrested in mitosis round up and show condensed chromosomes while apoptotic cells have micronucleated, shriveled nuclei.

The preferred way of detecting specific gene knockdowns is to use a specific antibody recognizing the targeted gene product. Antibodies to many cellular proteins can be purchased commercially, for example, from Abcam (www.abcam.com), Novocastra (www.novocastra.co.uk), Progen (www.progen.com), Santa Cruz Biotechnology (www.scbt.com), Sigma (www.sigma-aldrich.com), and BD Transduction Laboratories (www.translab.com). As primary antibodies, murine monoclonal antibodies or rabbit polyclonal antibodies are commonly used. The concentration of primary antibodies is critical for the immunofluorescence assay as too strong immunofluorescence staining obstructs the quantification of the knockdown effect. Therefore, subsaturating concentrations of antibodies have to be used, which should be determined in a titration series. Monoclonal antibodies supplied as overgrown hybridoma supernatants are applied anywhere between 1:1 and 1:1000 dilutions. Monoclonal antibodies supplied as ascites fluid can often be diluted up to 1:10,000. Polyclonal antibodies should be used only after affinity purification. Secondary antibodies directed against IgGs of the primary mouse or rabbit antibody are best purchased as reagents coupled to fluorescent dyes such as fluorescein isothiocyanate (FITC), rhodamine, Cy3, Alexa 488 (Dianova, Hamburg, Germany, www.dianova.de; MolecularProbes, Eugene, OR,

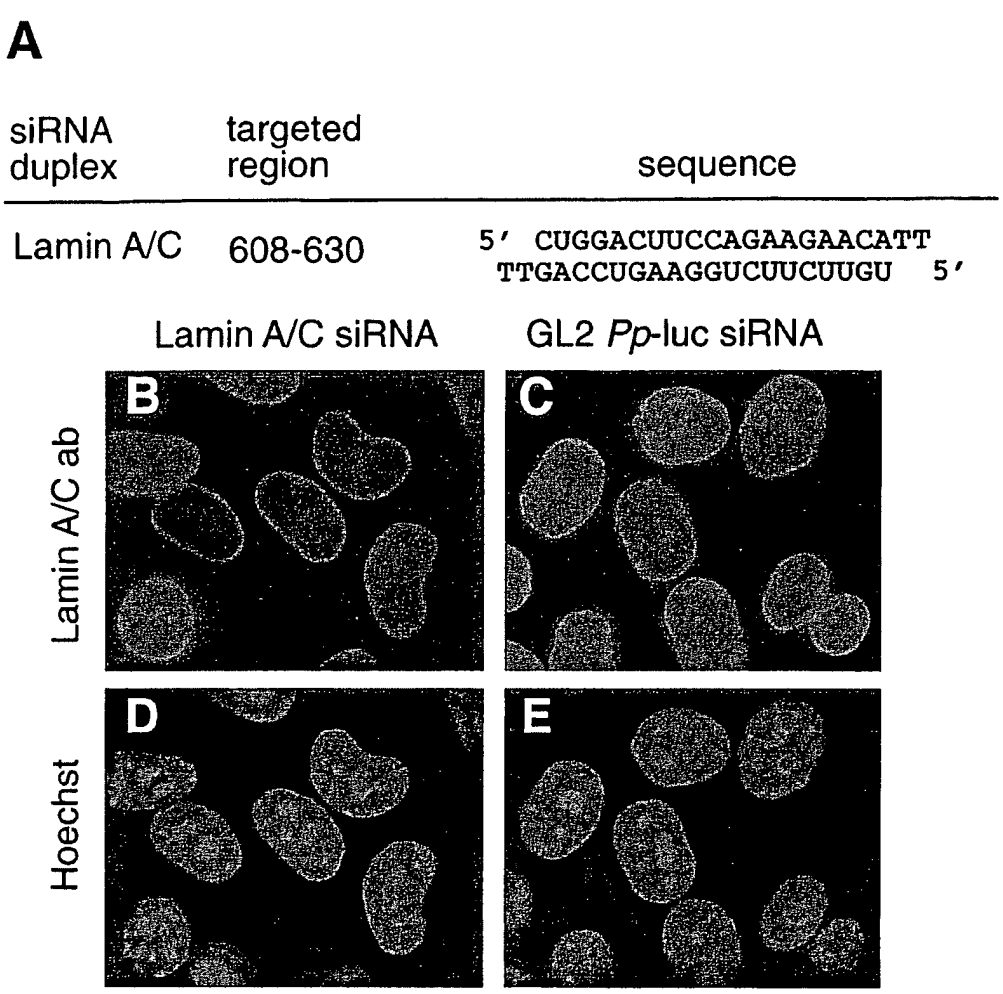

Fig. 6. Knockdown of lamin A/C protein. (A) Lamin A/C siRNA duplex. The targeted region of lamin A/C mRNA is indicated with respect to the start codon (pos. 1). HeLa SS6 cells were transfected with either lamin A/C siRNA (B, D) or GL2 Pp-luc control siRNA duplex (C, E) according to protocol 5. Knockdown of lamin A/C was monitored as described in protocol 6 using lamin A/C antibody 636 (Santa Cruz Biotechnology, No. sc-7292; or Novocastra, No. NCL-LAM-A/C) The bright cell located at the bottom left-hand corner of (B) was not transfected.

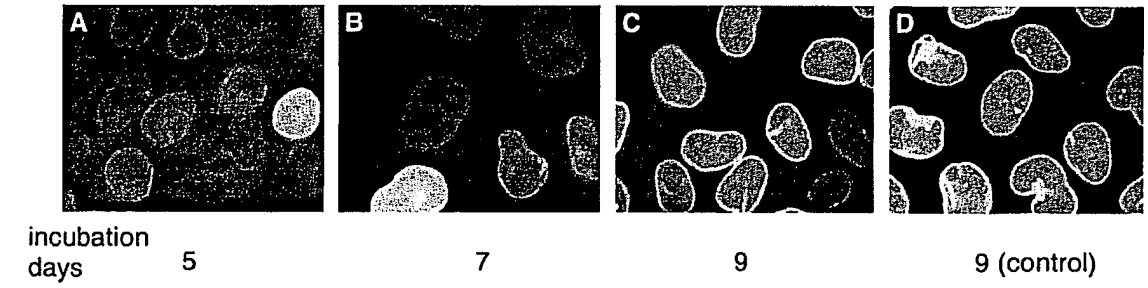

Fig. 7. Recovery of lamin A/C knockdown cells. HeLa SS6 cells were transfected with the lamin A/C siRNA duplex (protocol 5) and fixed and stained with lamin A/C-specific antibody at the indicated time points (protocol 6). (D) Cells transfected with a control GL2 luciferase siRNA duplex. Cells were split every second or third day to maintain exponential growth. Although the majority of cells has recovered from the knockdown 9 days posttransfection, a few cells still display reduced lamin A/C levels (C).

www.probes.com). The working conditions of the secondary antibodies are also established by titration series. Typical dilutions are between 1:40 and 1:100 for FITC- and rhodamine-conjugated antibodies, 1:600 for the Cy3-conjugated antibodies, and 1:100–1:200 for the Alexa-conjugated antibodies. It is also important to

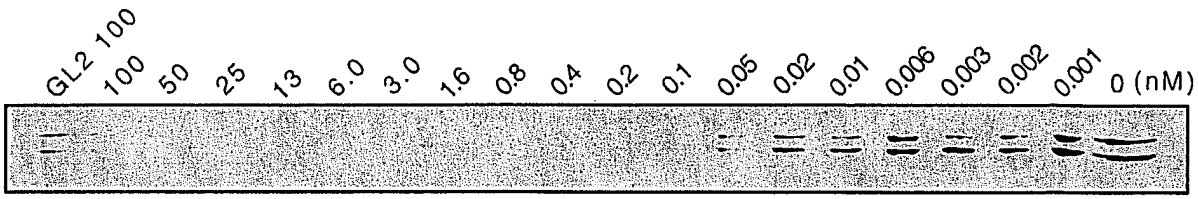

Fig. 8. Western blot analysis of HeLa SS6 cells transfected with various concentrations of lamin A/C siRNA duplex. Transfection of siRNA duplex was performed according to protocol 5 and the amount of duplex was varied from 0.84 μg to 8.4 pg, which corresponds to a final duplex concentration in the medium of 100 nM–1 pM, respectively. Cells transfected with buffer or 100 nM GL2 Pp-luc siRNA duplex served as control. Western blotting was performed according to protocol 7.

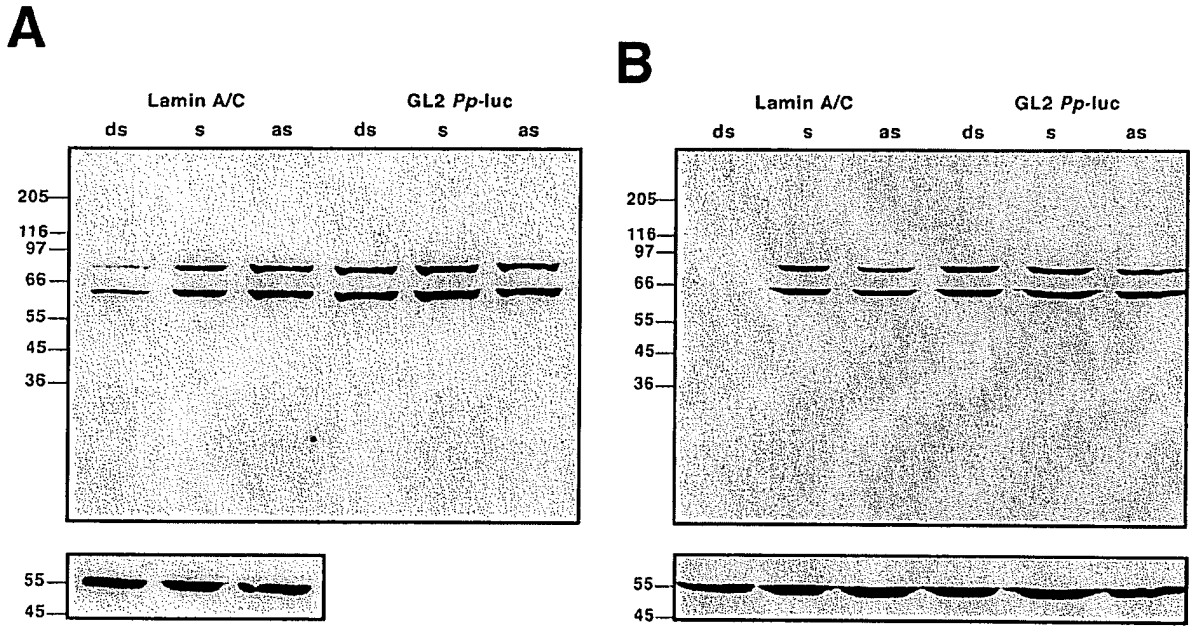

Fig. 9. Double-stranded siRNAs are required for gene silencing. HeLa SS6 cells were transfected with either duplex siRNA (ds) or single-stranded sense (s) or antisense (as) siRNA according to protocol 5. For transfection, 8.4 ng (A) or 0.84 μg (B) of sense, antisense, or dsRNA were used, which corresponds to 1 or 100 nM final siRNA duplex concentration and 2 or 200 nM single-stranded siRNA concentration. As nonspecific control, GL2 *Pp*-luc siRNAs were used. Western blotting was performed according to protocol 7, harvesting cells 2 days posttransfection. Following lamin A/C detection by ECL, the blot was stripped and reprobed with vimentin antibody to control for loading (see bottom).

verify that the second antibody does not bind unless the primary antibody has bound first.

6.1. Protocol 6: immunofluorescence detection of protein knockdowns

1. Fix and permeabilize the knockdown cells. Methanol fixation is suitable for the detection of many cellular proteins, but the optimal fixation procedure may have to be established experimentally for each individual protein [39,40]. We recommend beginning tests with methanol fixation, which preserves the ultrastructure of the cell and sufficiently permeabilizes the cells for penetration of the antibody. Remove the coverslips carrying the knockdown cells (see protocol 5) from the 24-well plate with tweezers (Dumont No. 7). Place the coverslips on a ceramic rack and incubate in methanol chilled to −10 °C for 6 min.
2. Wash the methanol-fixed coverslips three times in phosphate-buffered saline (PBS: 137 mM NaCl, 7 mM Na_2HPO_4, 1.5 mM KH_2PO_4, 2.7 mM KCl, pH 7.1) and touch with filter paper to remove excess PBS. Place the coverslips in a wet chamber with cells facing up. A wet chamber is prepared by soaking filter paper in water and placing it into a 13-cm-diameter Petri dish. It is important that specimens do not dry out during the entire procedure.
3. Add 20 μl of appropriately diluted primary antibody on top of the coverslip without touching the cells. Dilute antibodies with PBS buffer containing 0.5 mg/ml BSA (Sigma, No. A-9706) and 0.02% sodium azide. Make sure the solution is spread evenly over the entire surface of the coverslip. Transfer the

A

siRNA duplex	targeted region	sequence
NuMA	3988-4010	5′ GGCGUGGCAGGAGAAGUUCTT TTCCGCACCGUCCUCUUCAAG 5′

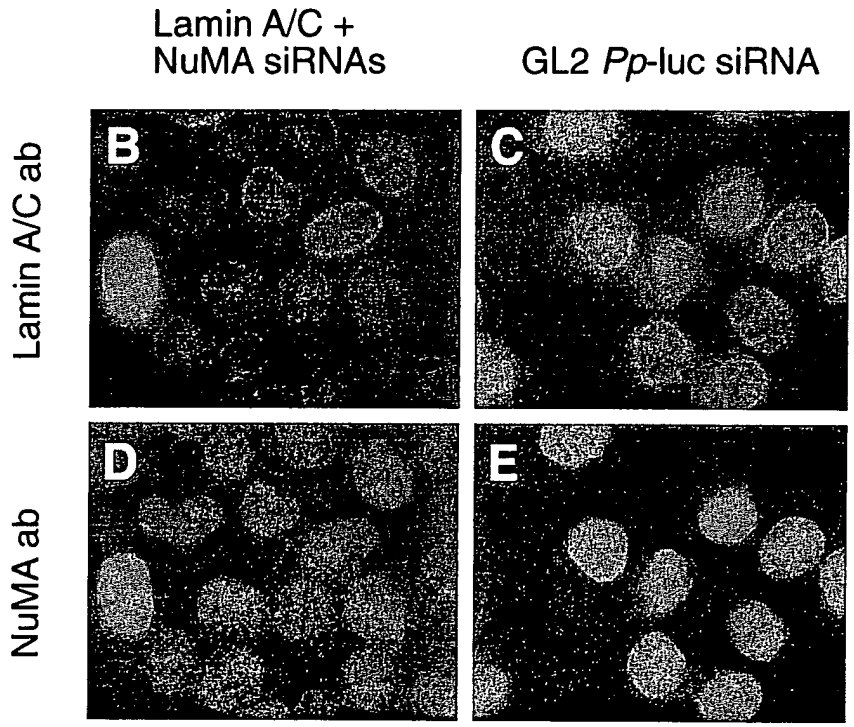

Fig. 10. Double knockdown of lamin A/C and NuMA in HeLa SS6 cells. (A) NuMA siRNA duplex. Cells transfected with 0.42 μg lamin A/C and 0.42 μg NuMA siRNA duplexes (B, D) and with 0.84 μg of GL2 luciferase siRNA duplex control (C, E) according to protocol 5. Two days after transfection, cells were examined with lamin A/C (B, C) or NuMA antibodies (D, E). Primary antibodies for lamin A/C (mouse monoclonal) and NuMA (affinity purified polyclonal [41]) were applied together, followed by simultaneous incubation of the secondary antibodies (Cy3 anti-mouse, Alexa 488 anti-rabbit) according to protocol 7. The majority of cells shows reduced expression of both target proteins; the single bright cell lighting up in (B) and (D) was nontransfected.

closed wet chamber to a 37 °C incubator and incubate for 45–60 min.

4. Place the coverslips again on the ceramic rack and wash them three times for 5 min with PBS. Touch with filter paper to remove excess PBS and transfer the coverslips back to the wet chamber.
5. Add 20 μl of appropriately diluted, fluorescently labeled secondary antibody. Incubate the wet chamber again for 45 min at 37 °C.
6. Repeat step 4.
7. Visualize the cell nuclei by chromatin staining. Add 20 μl 1 μM Hoechst 33342 (bisbenzimide, Serva No. 15091, www.serva.com) solution in PBS on top of the coverslip and incubate for 4 min.
8. Repeat step 4.
9. Mount two coverslips per slide by placing the coverslips with the cells facing downward on a drop of Moviol mounting medium (Hoechst, www.hoechst.com). Place a piece of filter paper on top of the slide and press gently on top of the paper to remove excess mounting medium. Coverslips are glued to the slide using clear nail polish.
10. Examine immunofluorescence staining and take pictures using an upright light microscope, e.g., Zeiss

A

siRNA duplex	targeted region	sequence
V1	346-368	5′ CUACAUCGACAAGGUGCGCTT TTGAUGUAGCUGUUCCACGCG 5′
V2	1145-1167	5′ UACCAAGACCUGCUCAAUGTT TTAUGGUUCUGGACGAGUUAC 5′
V3	863-885	5′ GAAUGGUACAAAUCCAAGUTT TTCUUACCAUGUUUAGGUUCA 5′
V4	1037-1059	5′ AUGGAAGAGAACUUUGCCGTT TTUACCUUCUCUUGAAACGGC 5′

B

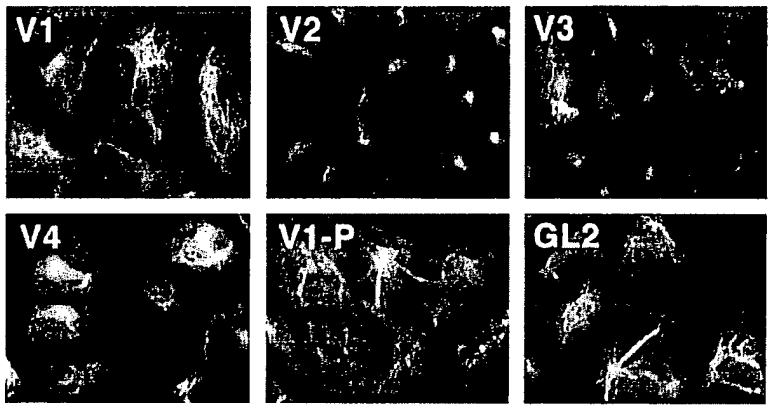

C

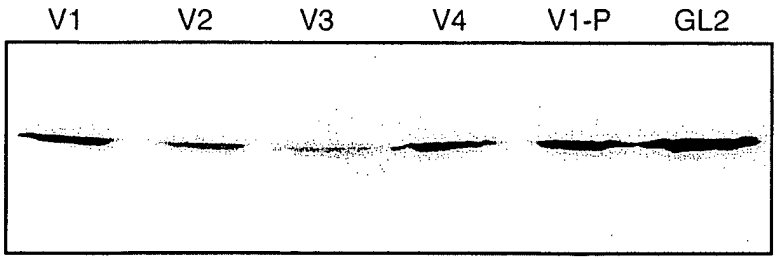

Fig. 11. Knockdown of the abundant cytoskeletal intermediate filament protein vimentin and comparison of the efficiency of different siRNA duplexes. (A) Sequences of vimentin siRNA duplex. (B) Immunofluorescence detection of vimentin 3 days posttransfection of HeLa SS6 cells. siRNA duplexes V1 and V4 are not efficient enough to suppress vimentin expression. 5′-Phosphorylation of siRNA duplex V1 (V1-P) has no effect. As control, transfection with GL2 luciferase siRNA duplex (GL2) was performed. Vimentin protein was detected with vimentin V9 antibody (Novocastra, No. NCL-VIM-V9) as described in protocol 6. (C) Western blot analysis of HeLa SS6 cells 3 days posttransfection with vimentin siRNA duplexes according to protocol 7. In agreement with the immunofluorescence results (B) V3 appears to be the most efficient siRNA duplex. Some of the residual vimentin has to be accounted for by incomplete transfection.

Axiophot with a F Fluar 40×/1.30 oil objective and MetaMorph Imaging Software (Universal Imaging Corp., West Chester, PA). Use identical exposure times for photographing the silenced and the control-treated cells. Alternatively, laser scanning microscopes may be used.

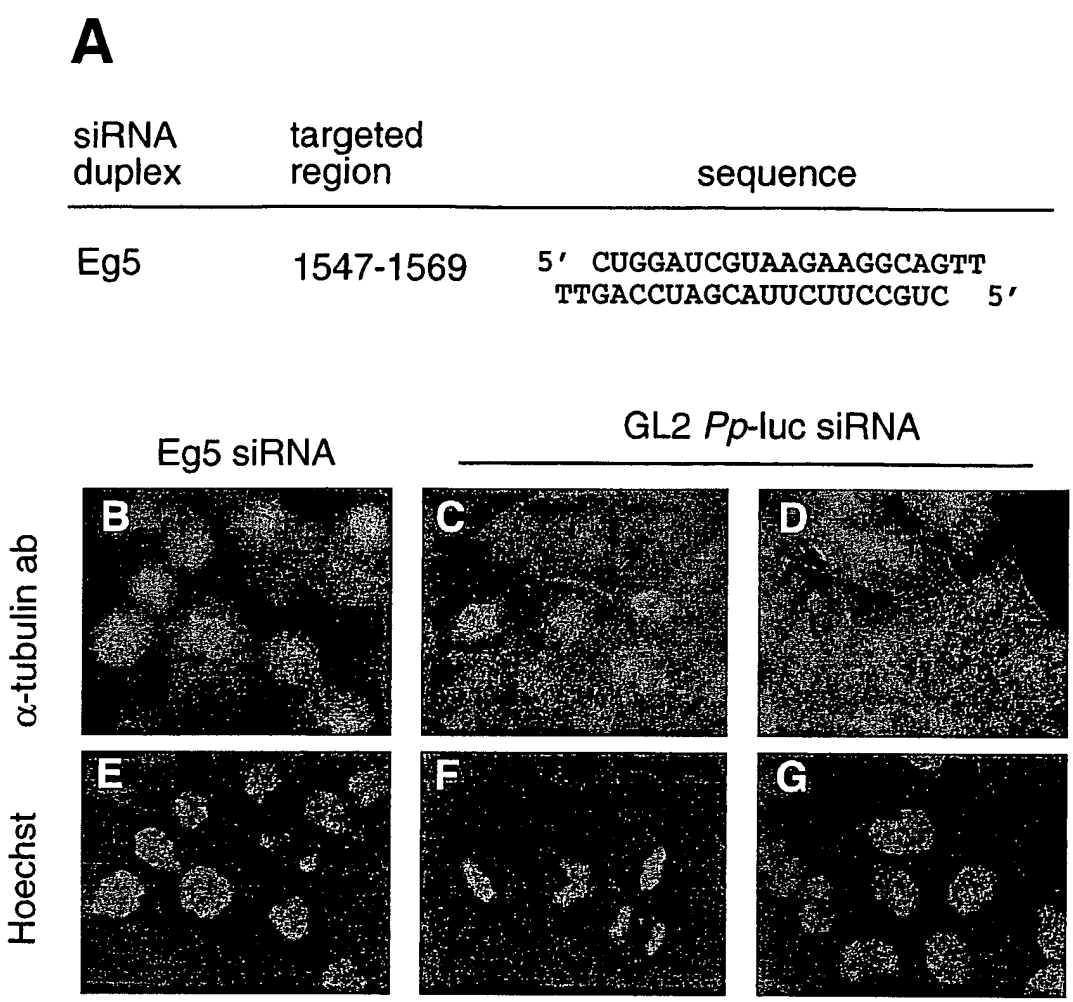

Fig. 12. Knockdown of the kinesin-related motor protein Eg5 causes mitotic defects. (A) Eg5 siRNA duplex. HeLa SS6 cells were transfected with Eg5 siRNA (B, E) or GL2 luciferase control siRNA duplexes (C, D, F, G). Two days posttransfection, spindle formation was analyzed by staining cells for α-tubulin with α-tubulin antibody (Sigma, No. T-9026) (B–D). Nuclear chromatin was stained with Hoechst dye (E–G). Eg5 siRNAs triggered aberrant mitotic arrest [24] with monoastral microtubular arrays (B). This phenotype was previously observed by alternative methods such as antibody microinjection [42] or application of the small molecule inhibitor monastrol [43]. In control experiments applying GL2 siRNAs, normal bipolar spindles were observed during mitosis (C, F) or normal microtubules during interphase (D, G).

6.2. Protocol 7: detection of protein knockdown by Western blotting

1. Remove the tissue culture medium from the siRNA-treated cells cultivated in 24-well plates. Rinse the cells once with 200 μl PBS and add 200 μl trypsin–EDTA (Life Technologies, No. 25300-054). Incubate for 1 min at 37 °C, suspend the cells and add 800 μl DMEM medium to quench the trypsin.
2. Transfer the suspended cells to a chilled 1.5-ml microfuge tube. Collect the cells by centrifugation at 3000 rpm (700*g*) for 4 min at 4 °C. Resuspend the cell pellet in ice-cold PBS and centrifuge again.
3. Remove the supernatant and add 25 μl of hot (90 °C) 2× concentrated Laemmli sodium dodecyl sulfate (SDS) sample buffer (Bio-Rad, No. 161-073, www.bio-rad.com) to the cell pellet obtained from one well of a 24-well plate. Incubate the sample for 3 min in a boiling water bath and vortex.
4. Separate the proteins by SDS–polyacrylamide gel electrophoresis using an appropriate acrylamide concentration to resolve the appropriate molecular weight of the targeted protein [38]. We have separated proteins on minigels that were run at constant 10 mA.
5. Transfer proteins onto nitrocellulose membrane (Protran BA85 0.45 mm, Schleicher & Schuell, No. 10401196, www.s-und-s.de). Our minigels were electroblotted onto the membrane using a Bio-Rad Trans-Blot cell at 333 mA for 30 min in the cold room. As transfer buffer, 25 mM Tris, 192 mM glycine, 0.01% SDS, 20% methanol was used.
6. Verify the protein transfer by Ponceau S (Sigma) staining of the transfer membrane.

7. Incubate the membrane in blocking solution (5% milk powder in TBST (0.2% Tween 20, 20 mM Tris–HCl, 150 mM NaCl, pH 7.4)) for 1 h at 37 °C.
8. Replenish the blocking solution with fresh blocking solution and add the antibody in the appropriate dilution. Incubate 1–2 h at 37 °C.
9. Wash the blot four times with TBST for 10 min.
10. For enhanced chemiluminescence (ECL) detection, incubate the blot with either horseradish peroxidase (HRP)-conjugated rabbit anti-mouse or HRP- conjugated swine anti-rabbit antibodies (Dako Diagnostika, Hamburg, Germany, www.dako.com) at a dilution of 1:20,000 as described in step 7.
11. Repeat step 8.
12. Perform ECL detection according to the protocol described by Amersham–Pharmacia (www.amersham.co.uk).

7. Concluding remarks

Small interfering RNAs (siRNAs) have become powerful reagents for triggering gene-specific silencing in mammalian cultured cells. siRNAs can be used to assess whether a gene is essential or nonessential, and specific gene silencing can be rapidly documented by immunofluorescence microscopy or Western blotting provided that specific antibodies to the targeted proteins are available. Silencing persists for several cell generations and even major cellular proteins such as vimentin have been knocked down. Simultaneous knockdown of two different proteins in the same cell population is possible. The highly efficient siRNA duplexes provide a novel tool for genomewide analysis of gene function in mammalian cells and may become useful for therapeutic applications.

Acknowledgments

We thank M. Osborn and D.J. Arndt-Jovin for reagents, M. Osborn, T. Achsel, R. Rauhut, J. Martinez, A. Patkaniowska, M. Hoßbach, and M. Mitkowski for critical comments on the manuscript, and W. Lendeckel and H.-J. Dehne for technical assistance.

References

[1] S.M. Elbashir, J. Harborth, W. Lendeckel, A. Yalcin, K. Weber, T. Tuschl, Nature 411 (2001) 494–498.
[2] N.J. Caplen, S. Parrish, F. Imani, A. Fire, R.A. Morgan, Proc. Natl. Acad. Sci. USA 98 (2001) 9742–9747.
[3] A. Fire, S. Xu, M.K. Montgomery, S.A. Kostas, S.E. Driver, C.C. Mello, Nature 391 (1998) 806–811.
[4] M.K. Montgomery, S. Xu, A. Fire, Proc. Natl. Acad. Sci. USA 95 (1998) 15502–15507.
[5] R.W. Carthew, Curr. Opin. Cell Biol. 13 (2001) 244–248.
[6] S.M. Hammond, A.A. Caudy, G.J. Hannon, Nat. Rev. Genet. 2 (2001) 110–119.
[7] P.A. Sharp, Genes Dev. 15 (2001) 485–490.
[8] T. Tuschl, ChemBioChem 2 (2001) 239–245.
[9] P.M. Waterhouse, M.B. Wang, T. Lough, Nature 411 (2001) 834–842.
[10] P.D. Zamore, Nat. Struct. Biol. 8 (2001) 746–750.
[11] M.J. Clemens, A. Elia, J. Interferon Cytokine Res. 17 (1997) 503–524.
[12] G.R. Stark, I.M. Kerr, B.R. Williams, R.H. Silverman, R.D. Schreiber, Annu. Rev. Biochem. 67 (1998) 227–264.
[13] M. Kumar, G.G. Carmichael, Microbiol. Mol. Biol. Rev. 62 (1998) 1415–1434.
[14] G. Geiss, G. Jin, J. Guo, R. Bumgarner, M.G. Katze, G.C. Sen, J. Biol. Chem. 276 (2001) 30178–30182.
[15] V. Bitko, S. Barik, BMC Microbiol. 1 (2001) 34.
[16] S.M. Elbashir, W. Lendeckel, T. Tuschl, Genes Dev. 15 (2001) 188–200.
[17] E. Bernstein, A.A. Caudy, S.M. Hammond, G.J. Hannon, Nature 409 (2001) 363–366.
[18] R.F. Ketting, S.E. Fischer, E. Bernstein, T. Sijen, G.J. Hannon, R.H. Plasterk, Genes Dev. 15 (2001) 2654–2659.
[19] E. Billy, V. Brondani, H. Zhang, U. Muller, W. Filipowicz, Proc. Natl. Acad. Sci. USA 98 (2001) 14428–14433.
[20] L. Cerutti, N. Mian, A. Bateman, Trends Biochem. Sci. 25 (2000) 481–482.
[21] S.M. Hammond, S. Boettcher, A.A. Caudy, R. Kobayashi, G.J. Hannon, Science 293 (2001) 1146–1150.
[22] S.M. Hammond, E. Bernstein, D. Beach, G.J. Hannon, Nature 404 (2000) 293–296.
[23] S.M. Elbashir, J. Martinez, A. Patkaniowska, W. Lendeckel, T. Tuschl, EMBO J. 20 (2001) 6877–6888.
[24] J. Harborth, S.M. Elbashir, K. Bechert, T. Tuschl, K. Weber, J. Cell Sci. 114 (2001) 4557–4565.
[25] G. Hutvágner, J. McLachlan, É. Bálint, T. Tuschl, P.D. Zamore, Science 93 (2001) 834–838.
[26] J.E. Garrus et al., Cell 107 (2001) 55–65.
[27] N. Ancellin, C. Colmont, J. Su, Q. Li, N. Mittereder, S.S. Chae, S. Steffansson, G. Liau, T. Hla, J. Biol. Chem. 10 (2001) 10.
[28] X. Bai, D. Zhou, J.R. Brown, B.E. Crawford, T. Hennet, J.D. Esko, J. Biol. Chem. 276 (2001) 48189–48195.
[29] D. Cortez, S. Guntuku, J. Qin, S.J. Elledge, Science 294 (2001) 1713–1716.
[30] L. Li, J. Mao, L. Sun, W. Liu, D. Wu, J. Biol. Chem. 12 (2001) 12.
[31] L.M. Martins et al., J. Biol. Chem. 277 (2002) 439–444.
[32] P.D. Good et al., Gene Ther. 4 (1997) 45–54.
[33] J. Ohkawa, K. Taira, Hum. Gene Ther. 11 (2000) 577–585.
[34] A. Nykänen, B. Haley, P.D. Zamore, Cell 107 (2001) 309–321.
[35] J.R. Masters et al., Proc. Natl. Acad. Sci. USA 98 (2001) 8012–8017.
[36] F. Eckstein, Oligonucleotides and Analogues, second ed., Oxford University Press, Oxford, UK, 1991.
[37] M.L. Deras, K. Vandenburgh, S.A. Scaringe, submitted.
[38] J. Sambrook, E. Fritsch, T. Maniatis, Molecular Cloning, second ed., Cold Spring Harbor Laboratory Press, Plainview, NY, 1989.
[39] D.L. Spektor, R.D. Goldman, L.A. Leinwand, Cells: A Laboratory Manual, Cold Spring Harbor Laboratory Press, Plainview, NY, 1989.
[40] J.E. Celis, Cell Biology: A Laboratory Handbook, vol. 2, Academic Press, San Diego, CA, 1998.
[41] J. Harborth, J. Wang, C. Gueth-Hallonet, K. Weber, M. Osborn, EMBO J. 18 (1999) 1689–1700.
[42] A. Blangy, H.A. Lane, P. d'Herin, M. Harper, M. Kress, E.A. Nigg, Cell 83 (1995) 1159–1169.
[43] T.U. Mayer, T.M. Kapoor, S.J. Haggarty, R.W. King, S.L. Schreiber, T.J. Mitchison, Science 286 (1999) 971–974.

TAB 6

BMC Microbiology

BioMed Central

Research article

Phenotypic silencing of cytoplasmic genes using sequence-specific double-stranded short interfering RNA and its application in the reverse genetics of wild type negative-strand RNA viruses

Vira Bitko and Sailen Barik*

Address: Department of Biochemistry and Molecular Biology (MSB 2370), University of South Alabama, College of Medicine, 307 University Blvd., Mobile, AL 36688-0002, USA

E-mail: Vira Bitko - vbitko@jaguar1.usouthal.edu; Sailen Barik* - sbarik@jaguar1.usouthal.edu

*Corresponding author

Published: 20 December 2001

BMC Microbiology 2001, 1:34

Received: 23 November 2001

Accepted: 20 December 2001

This article is available from: http://www.biomedcentral.com/1471-2180/1/34

Abstract

Background: Post-transcriptional gene silencing (PTGS) by short interfering RNA has opened up new directions in the phenotypic mutation of cellular genes. However, its efficacy on non-nuclear genes and its effect on the interferon pathway remain unexplored. Since directed mutation of RNA genomes is not possible through conventional mutagenesis, we have tested sequence-specific 21-nucleotide long double-stranded RNAs (dsRNAs) for their ability to silence cytoplasmic RNA genomes.

Results: Short dsRNAs were generated against specific mRNAs of respiratory syncytial virus, a nonsegmented negative-stranded RNA virus with a cytoplasmic life cycle. At nanomolar concentrations, the dsRNAs specifically abrogated expression of the corresponding viral proteins, and produced the expected mutant phenotype *ex vivo*. The dsRNAs did not induce an interferon response, and did not inhibit cellular gene expression. The ablation of the viral proteins correlated with the loss of the specific mRNAs. In contrast, viral genomic and antigenomic RNA, which are encapsidated, were not directly affected.

Conclusions: Synthetic inhibitory dsRNAs are effective in specific silencing of RNA genomes that are exclusively cytoplasmic and transcribed by RNA-dependent RNA polymerases. RNA-directed RNA gene silencing does not require cloning, expression, and mutagenesis of viral cDNA, and thus, will allow the generation of phenotypic null mutants of specific RNA viral genes under normal infection conditions and at any point in the infection cycle. This will, for the first time, permit functional genomic studies, attenuated infections, reverse genetic analysis, and studies of host-virus signaling pathways using a wild type RNA virus, unencumbered by any superinfecting virus.

Background

Over the last decade, RNA interference (RNAi), mediated by short interfering double-stranded RNA molecules (siRNA or dsRNA), has been gradually recognized as a major mechanism of post-transcriptional gene silencing (PTGS) in species as diverse as plants, *Drosophila*, and *C. elegans*[1]. Recently, 21-nucleotide long dsRNA molecules corresponding to specific mRNA sequences, when introduced into mammalian cells in culture, have been shown to be highly effective in degrading the cognate mRNAs

and thus abrogating the expression of the corresponding proteins [2]. Although the exact mechanism of PTGS is currently unknown and is an area of intense research, the successful use of this phenomenon in cultured mammalian cells has raised the exciting prospect that it can be used as a simple strategy for phenotypic ablation of mammalian gene function *ex vivo* without the time-consuming and expensive construction of transgenic animals.

So far, the genes targeted for siRNA-mediated PTGS have been cellular in origin and thus, the mRNAs were transcribed in the nucleus by cellular DNA-dependent RNA polymerase. In contrast, the vast majority of RNA genomes are transcribed exclusively in the cytoplasm. For example, transcription of RNA viral genomes, with the exception of retroviral RNA, is catalyzed by a virally encoded RNA-dependent RNA polymerase (RdRP) [3]. It remains untested whether the siRNA-mediated PTGS will work on mRNAs that never went through the nucleus. Interestingly, because of the potency of siRNA in some organisms, it has been proposed that they may be replicated by a cellular RdRP activity, although this has been debated [4]. Furthermore, since dsRNA is known to be a potent inducer of the interferon pathway [5,6], it is important to know whether this also occurs in cells in which antisense dsRNA has been introduced.

To answer these questions, we have used a nonsegmented negative-strand RNA (NNR) virus as a test target for RNA-mediated inhibition. We reasoned that, if successful, our studies would additionally contribute a reliable and simple technology for specific gene silencing in cytoplasmic RNA viruses. Traditionally, structure-function analyses of RNA genomes, including those of RNA viruses, have relied on spontaneous mutants found in natural isolates or chemically mutagenized stocks [7]. Mutations in either case are essentially unpredictable and must be mapped by elaborate techniques such as classical complementation analyses or direct sequencing of the genome. Since conventional site-directed mutagenesis requires a DNA template, direct mutational analysis of selected RNA genes is not an option. These obstacles have been largely circumvented by the use of cloned viral cDNA that is then altered by standard DNA-based site-directed mutagenesis procedures [8,9]. Originally designed for influenza virus minigenomes [10], such cDNA-based "reverse genetics" strategy has been adopted in a large number of NNR viruses, including vesicular stomatitis virus (VSV), respiratory syncytial virus (RSV), and measles, to name a few [11–14]. Recently, extension of this approach has resulted in the cloning of full-length viral cDNA capable of producing infectious recombinant virus particles upon transcription.

Despite its revolutionary effect on RNA viral reverse genetics, however, the cDNA-based strategy is not without limitations. First, as implied above, cloning and recombinant expression of the viral genomic RNA and all the viral proteins in the right proportion constitute a long and arduous task, daunting to an average laboratory. The problem is particularly acute for NNR viruses, which have large RNA genomes [8,9]. The 10–15 kb long RNA genomes of these viruses require specific sequences at the 5' and 3' termini for transcription and replication, and must be properly encapsidated by the nucleocapsid protein (N) in order to be recognized by the viral RdRP [15,16]. Thus, any recombinant technology must be able to faithfully reproduce these features of the genome. Moreover, the functional viral RdRP, as detailed later for RSV, is a complex holoenzyme composed of viral as well as cellular proteins [17–23]. Second, many NNR viral genomes and proteins are currently expressed from vaccinia-based cDNA clones, which generally requires superinfection by vaccinia virus [22,23]. Unfortunately, vaccinia virus itself is a major modulator of cellular signaling, including MAP kinase pathways and the actin cytoskeleton [24–26]. It is, therefore, virtually impossible to study the interaction between cellular signaling pathways and NNR viruses in cells that are also superinfected by vaccinia virus [24–26]. Third, mutations in the recombinant DNA are "permanent", and thus, the mutational phenotype cannot be switched on at pre-determined time points in infection. For example, if a viral gene product has essential roles both early and late in infection, its mutational inactivation will fail to reveal the late function, since the mutant virus will never proceed beyond the early stage.

A member of the *Paramyxoviridae* family, RSV is a major causative agent of childhood respiratory disease and asthma [27]. Pediatric RSV disease claims about a million lives annually, and no reliable antiviral or vaccine currently exists [27,28]. A need to understand the molecular genetics of the virus and the function of the various gene products has thus been appreciated. Since our laboratory is interested in deciphering the temporal signaling pathways in host-RSV interaction and the role of RSV gene products in the process, we have sought potential alternatives to the cDNA-based approach that might allow us to study the effect of functional loss of a specific RSV gene product during the course of a standard virus infection in cell culture. Using two different RSV gene mRNAs as targets, and another NNR virus (VSV) as well as cellular mRNAs as controls, we show that synthetic dsRNA molecules are highly efficient and specific silencers of cytoplasmic RNA viral gene expression. We also provide the first direct evidence that the 21-nt long dsRNAs do not activate a general interferon response. Our results thus offer a mechanism of specific and direct ablation of RNA-based gene expression and a quicker and simpler alternative to cDNA-based reverse genetics of RNA viruses.

Results

Ablation of viral gene expression by dsRNA against RSV P mRNA

The RNA genome of RSV is about 15 kb long and contains 11 documented protein-coding genes [13]. Three viral proteins are minimally required to reconstitute the functional transcription complex of NNR viruses [3]: the nucleocapsid protein (N) that wraps the negative-strand genome RNA and its full-length complement, the positive-strand antigenome RNA, thus converting them into highly nuclease-resistant, chromatin-like templates; the large protein (L), which is the major subunit of the RdRP; and the phosphoprotein (P), which is the smaller subunit of RdRP and an essential transcription factor of L [19–22]. In RSV, optimal transcription, although not replication, additionally requires the transcription antitermination protein M2-1 [13]. In addition, cellular actin, and to a lesser extent, profilin, are also required for viral transcription [17,18].

The overall steps of a NNR viral macromolecular synthesis in the infected cell are relevant for this paper, and are briefly described here [3]. The L protein is believed to encode the basic RNA polymerization function, and binds to the viral promoter at the 3' end of the genomic RNA to initiate transcription. However, the P protein is essential for the RdRP holoenzyme to exit the promoter and to form a closed complex that is capable of sustained elongation [20]. The preformed RdRP brought in by the infecting viral nucleocapsids catalyzes the first rounds of transcription, known as primary transcription. In its "transcription mode", the viral RdRP starts and stops at the beginning and end, respectively, of each viral gene, and this results in the synthesis of individual gene mRNAs. Unlike the full-length genomic and antigenomic RNA, the mRNAs are 5'-capped, 3'-polyadenylated, and do not bind N protein. Translation of these mRNAs results in *de novo* synthesis of viral proteins. The availability of large quantities of N protein then allows encapsidation of nascent leader RNA by N. This leads to the switching of the RdRP to the "replication mode", resulting in the synthesis of full-length, encapsidated anti-genomic RNA, which is in turn replicated into more genomic RNA [15]. Thus, the very requirement of N for replication ensures that all full-length genomic and antigenomic RNA are wrapped with N protein, i.e., encapsidated [15]. The new pool of replicated genomic RNA serves as templates for secondary transcription. It should be obvious from the foregoing that the *de novo* macromolecular synthesis accounts for the major burst of viral protein and RNA in the infected cell. Specifically, if the *de novo* synthesis of the essential subunits of viral RdRP – such as L or P – is inhibited, it will abolish the bulk of viral transcription and replication, and hence, viral translation [3].

To test the effectiveness of the anti-P dsRNA, we transfected the dsRNA into A549 cells, and infected the cells with RSV. Subsequently, the amount of intracellular P protein was directly monitored by immunoblot analysis using anti-P antibody. Results presented in Fig. 1 show a nearly 90% reduction of P protein using as little as 10 nM dsRNA. Although we have not tested lower amounts of dsRNA for P, the severe loss of P protein at 10 nM dsRNA and only a slightly greater loss with higher dsRNA concentrations (Fig. 1) suggest that it may be possible to cause substantial ablation of P protein at dsRNA concentrations even below 10 nM.

The phenotypic effect of loss of P was further examined by measuring progeny viral titer, overall viral protein synthesis, and syncytium formation, as described under Materials and Methods. Yield of progeny virus in 20 nM dsRNA-treated cells was found to be reduced by 10 fold, and was reduced by at least 10^4 fold at 100 and 300 nM dsRNA (data not shown). *De novo* viral protein synthesis was measured by metabolic labeling with S^{35}-Met/Cys followed by immunoprecipitation. As shown in Fig. 1, all viral proteins detectable in the precipitate were drastically diminished in the dsRNA-treated cells, as would be expected in the event of a loss of the P protein. The inhibition of viral growth was further reflected in the essentially complete loss of cell fusion (syncytia) in the treated cells (Fig. 2). In fact, the RSV-infected anti-P dsRNA-treated cells were morphologically indistinguishable from control uninfected ones even at 5 days post-infection, which was the longest time period for which they were observed. The presence of equal amounts of actin in all the samples confirmed that the observed inhibition of viral proteins is not due to a general degradation of proteins.

The specificity of dsRNA activity was further tested by using a dsRNA against cellular lamin A/C that was earlier shown to specifically abrogate lamin A/C synthesis in a variety of cultured cell lines [2]. As shown in Fig. 1 (lane 'La'), the anti-lamin dsRNA, while abrogating lamin protein (data not shown) had no effect on RSV protein synthesis. Furthermore, a mismatched anti-P dsRNA in which the lowercase A-U base pair (see the dsRNA sequences in Materials and Methods) was altered to a G-C pair also failed to inhibit viral translation (data not shown), confirming that a perfect match is needed for the dsRNA effect, hence its extreme specificity of action.

Lack of syncytium in RSV-infected cells treated with anti-F dsRNA

Fusion of the infected cells is a hallmark of all Paramyxoviruses including RSV (as also in some other viruses, such as HIV), and the resultant mass of fused cells is referred as a syncytium, from which respiratory syncytial virus derives its middle name. The fusion protein F is by far the

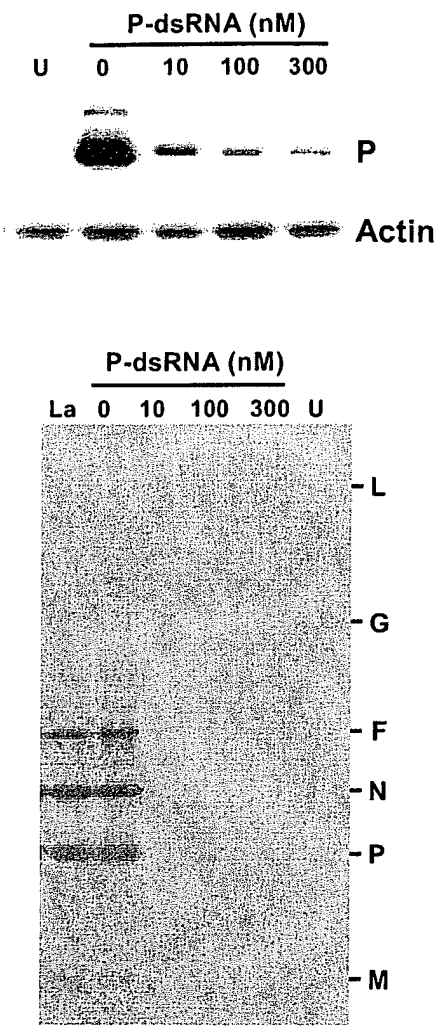

Figure 1
Ablation of RSV P protein by anti-P dsRNA. Transfection of A549 cells with 0 (no dsRNA), 10, 100, or 300 nM dsRNA and infection with RSV were carried out as described under Materials and Methods. Lane 'U' indicates control, uninfected cells. Top: Immunoblot (Western) of total cell extracts was performed with either rabbit anti-P or monoclonal anti-actin antibody (Boehringer-Mannheim), as indicated. Bottom: Viral protein synthesis in dsRNA-treated cells was measured by standard immunoprecipitation procedures as described previously [17]. Infected A549 cells (or uninfected control, lane 'U') were metabolically labeled with ^{35}S-(methionine plus cysteine) at 18 h post-infection, followed by lysis of the cells, precipitation with anti-RSV antibody, and analysis of the labeled proteins by SDS-PAGE and autoradiography. 'La' represents treatment with 100 nM anti-lamin A/C dsRNA. The different viral protein bands are so indicated.

most important viral glycoprotein that is central to the cell fusion activity [29]. Since the P and F proteins have such diverse roles in viral life cycle, we decided to investigate the effect of dsRNA on F as a second test gene, and also to compare and contrast the two respective phenotypes.

First, to test the effectiveness of the anti-F dsRNA intracellularly, we probed the infected cell monolayer with anti-F antibody by indirect immunofluorescence (Fig. 3). Results clearly demonstrated the abundant synthesis of F protein as cytoplasmic fluorescence in cells that were not treated with dsRNA; the nuclei of the same cells could be visualized by staining with DAPI. In contrast, cells treated with just 3 nM anti-F dsRNA showed a substantial loss of F stain. At 20 nM dsRNA, F protein was undetectable.

Second, immunoblot analysis (Fig. 4, top panel) revealed that anti-F dsRNA, at concentrations as low as 20 nM, produced a severe reduction in F protein levels. Again, no effect was seen on cellular profilin, ruling out a general protein loss. The anti-F dsRNA also had no effect on P protein levels, suggesting that such dsRNAs do not activate a general antiviral response that might abrogate all viral mRNA translation. This was further corroborated by the direct measurement of *de novo* viral protein synthesis by metabolic labeling (Fig. 4, bottom panel). Results showed that the synthesis of F only was affected while all other viral proteins were translated in normal amounts, which is in agreement with the notion that F has little or no role in intracellular viral macromolecular synthesis.

Finally, the phenotype of F protein loss was tested by examining syncytia formation, and as presented in Fig. 2, no syncytia could be discerned in anti-F dsRNA-treated cells (Panel B). However, a cytopathic effect was still visible, which is most likely the result of intracellular replication of the virus. This demonstrates an interesting contrast with the anti-P dsRNA (Panel C), which inhibited all viral gene expression, and therefore, the resultant monolayer exhibited essentially the same appearance as the uninfected one (Panel D).

Direct measurement of intracellular F mRNA by semi-quantitative RT-PCR showed a nearly 15-fold loss caused by anti-F dsRNA (Fig. 5, top panel). Similar RT-PCR of viral genomic RNA, viral P mRNA, or cellular actin mRNA revealed essentially no reduction, suggesting that the dsRNA did not activate a general antiviral response, and did not directly target genomic RNA. Together, these results directly demonstrate that the dsRNAs promote ablation of the specific mRNA target, which most likely underlies the loss of the respective proteins.

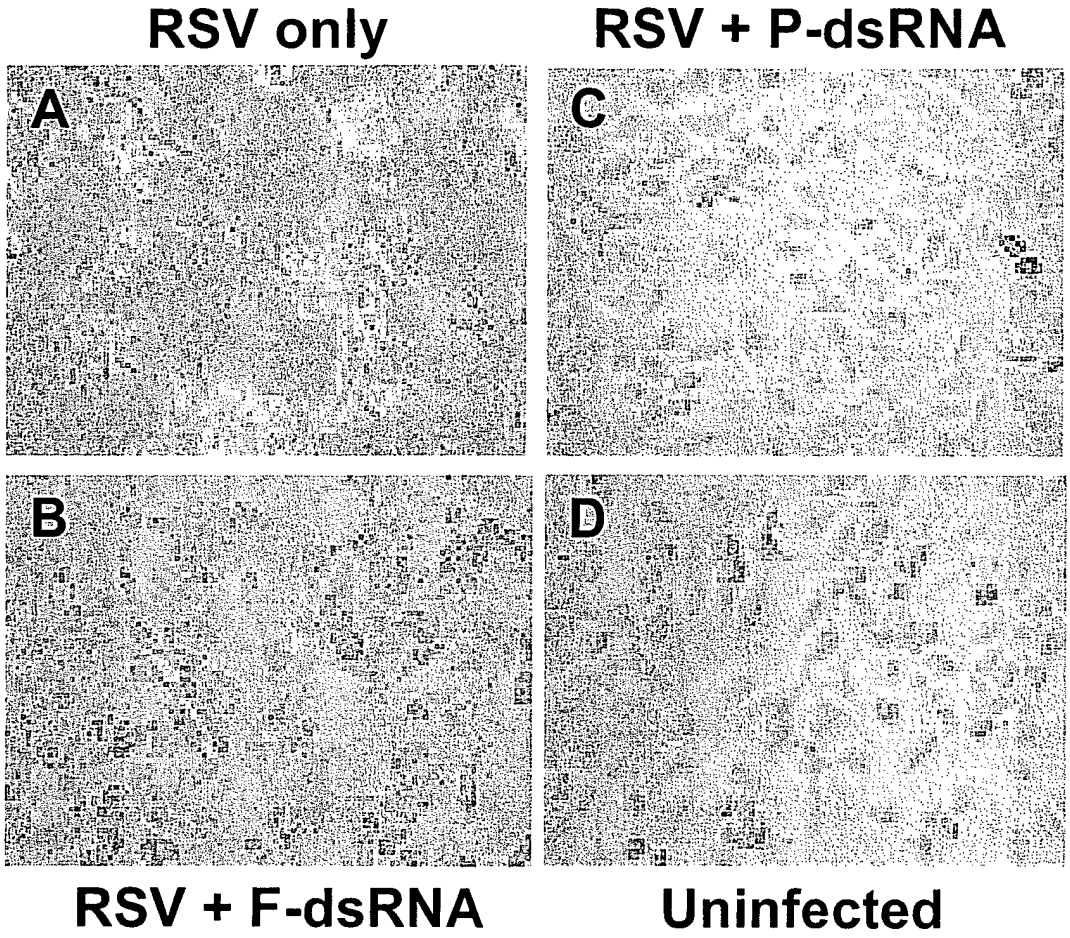

Figure 2
Effect of dsRNA on the cell fusion activity of RSV. A549 monolayers were transfected with 20 nM of anti-P or anti-F dsRNA and infected with RSV as described under Materials and Methods. At 40 h p.i., the monolayers were examined under a Nikon TS100F phase-contrast microscope at 40× magnification and digitally photographed with a Nikon Coolpix 995 camera. Note the syncytia in 'A', cytopathic effect without syncytia in 'B', and monolayers that appear unaffected and identical in 'C' and 'D'.

Anti-RSV dsRNAs do not activate an interferon response

As mentioned before, cytoplasmic dsRNA can trigger a series of signaling reactions that lead to interferon (IFN) synthesis [5,6]. In the "interferon response", dsRNA molecules activate protein kinase PKR and 2',5'-oligonucleotide synthetase. One of the effects of PKR is to phosphorylate the α subunit of the general translation initiation factor eIF-2, which constitutes a major mechanism for global translation arrest. The 2', 5'-oligonucleotide synthetase activates RNase L that in turn catalyses non-specific degradation of mRNA. Since NNR viruses co-opt the cellular translation machinery, the interferon response thus causes severe inhibition of viral translation. Interestingly, the IFN response requires long dsRNA [5,6], and it has been conjectured that the improved specificity of the 21-nucleotide long dsRNA in cultured mammalian cells is probably due to their inability to activate the IFN response [2]. We provide several lines of direct and indirect evidence that the dsRNAs described here did not activate a general IFN response. First, the in-

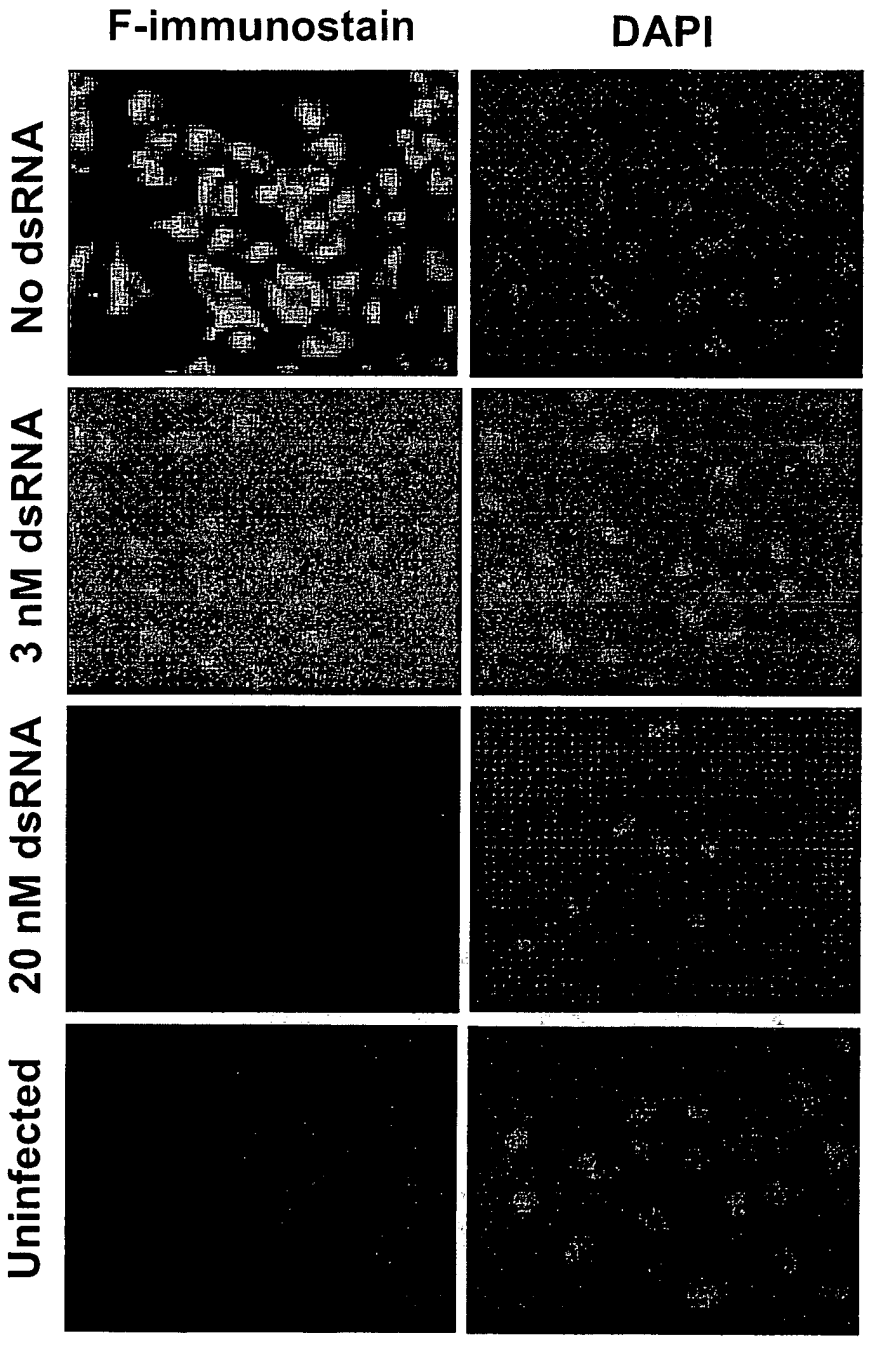

Figure 3
Ablation of RSV F by anti-F dsRNA. Anti-F dsRNA, RSV infection, and immunostaining of A549 monolayer were performed as described under Materials and Methods. Right panel shows the nuclear staining of the same cells using DAPI (Blue). Note the substantial reduction of F (Green) with as low as 3 nM anti-F dsRNA, and reduction to background levels by 20 nM dsRNA.

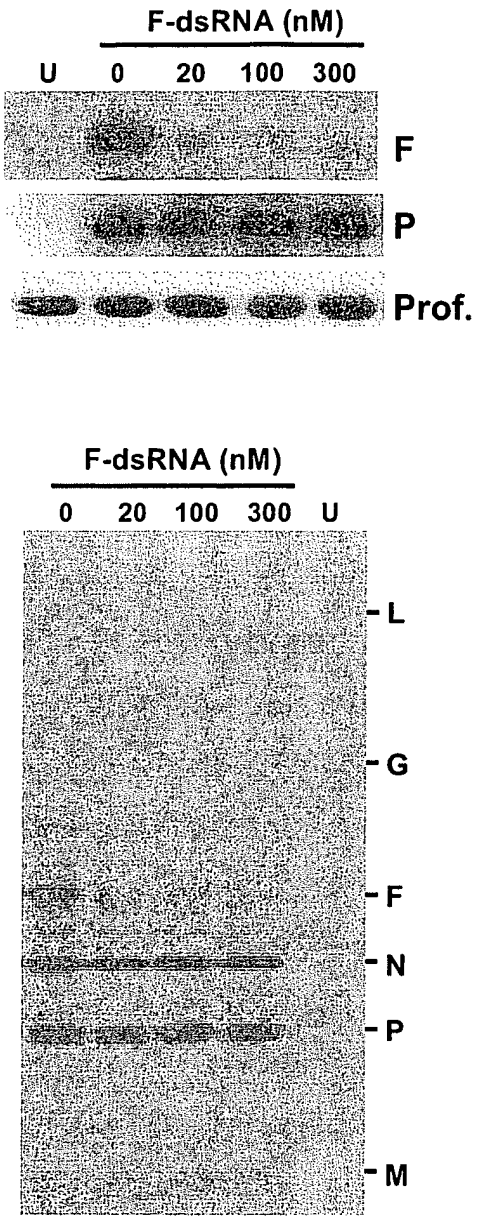

Figure 4
Specificity of anti-F dsRNA. Experiments were done essentially as described for Fig. 2. A549 cells were transfected with the indicated amounts of anti-F dsRNA followed by infection by RSV as described under Materials and Methods. Top: Immunoblot of total cell extracts to detect RSV F, RSV P, and profilin; Bottom: Autoradiograph showing immunoprecipitated metabolically ^{35}S-labeled RSV proteins. 'U' represents uninfected cells. Note the specific loss of F protein, but no effect on other proteins.

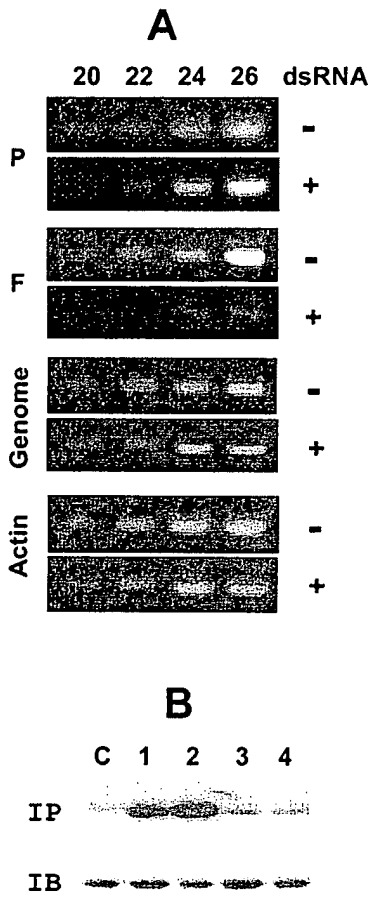

Figure 5
Induction of target mRNA degradation but not interferon response by dsRNA. Panel A: Semi-quantitative RT-PCR to measure the indicated RSV gene mRNA and genomic RNA in A549 cells were performed as described under Materials and Methods. Where indicated (labeled '+'), anti-F dsRNA was used at a concentration of 20 nM. PCR samples were taken at the end of the number of cycles indicated on top (20, 22, 24, and 26). Actin mRNA was also quantitated as a control. Note that in dsRNA-untreated cells (labeled '-') the F band is visible even at 20 cycles, whereas in the treated cells, appearance of a comparable intensity required 4 additional PCR cycles, i.e., 16-fold more amplification. Panel B: Assay of eIF-2α phosphorylation. Metabolic ^{32}P-labeling and immunoprecipitation (IP) analysis of eIF-2 have been described in Materials and Methods. An autoradiograph of the gel is shown. The cells were treated with no RNA (lane C), 100 nM thapsigargin (lane 1), 100 nM A23178 (lane 2), 50 nM anti-P dsRNA (lane 3), or 50 nM anti-F dsRNA (lane 4). Note the increased phosphorylation of eIF-2 in lanes 1 and 2 only. The immunoblot (IB) shows that the total amount of eIF-2α protein was not affected by the treatments.

hibitory effect of each dsRNA was gene-specific (Figs. 1, 2, 4). Second, growth of VSV is known to be highly sensitive to IFN, however, its replication in A549 cells was not affected by any of the dsRNAs described here (data not shown). Lastly, elevated phosphorylation of eIF-2α has been used as a diagnostic marker of IFN response [30]. We, therefore, examined the phosphorylation status of eIF-2α in A549 cells following transfection with these dsRNAs. Results (Fig. 5, bottom panel) showed no increase in phosphorylation. In positive controls, A549 cell treated with calcium mobilizers (thapsigargin or A23178) did increase eIF-2 phosphorylation, as has been shown earlier [30]. These results provide the first direct evidence that the 21-nt long double-stranded siRNAs fail to trigger interferon response in mammalian cells, and hence, can be used as specific antiviral agents.

Discussion

In this communication, we establish 21-nucleotide long double-stranded interfering RNA as a viable tool to ablate specific cytoplasmic RNAs, as exemplified by the mRNAs of a RNA virus. The major findings are: (i) The ablation is highly efficient: nanomolar concentrations of dsRNA can lead to a 10–20 fold reduction of the corresponding protein. The two RSV mRNAs that we have targeted here, namely P and F, are relatively abundant viral mRNAs. In fact, they respectively represent the 4th and 5th most abundant viral mRNAs in the infected cell. Thus, we predict that an even lower concentration of dsRNA, perhaps in the sub-nanomolar range, might be able to destroy NNR viral mRNAs that are rarer, such as those of RSV M2 and L proteins. This is currently being tested. It is to be noted that a chemical is generally considered a promising pharmaceutical if it is effective at sub-micromolar concentrations, (ii) The effect is highly specific: dsRNA against one viral mRNA did not affect other viral mRNAs or the cellular genes tested here. In this regard, dsRNA generally surpasses the standard antisense technology based on oligodeoxynucleotides (ODNs), whose specificity has often been debated. Moreover, since the most potent antisense ODNs rely on the degradation of target RNA by RNase H [31], which is a predominantly nuclear enzyme, this mechanism is not available to RNA viruses that are strictly cytoplasmic. (iii) Lack of interferon response: We provide direct experimental evidence that the 21-nt dsRNA does not trigger an IFN response, which is an advantage because an IFN response would have caused a general and non-specific inhibition of all cap-dependent translation [5]. (iv) Regulation any time: Although we have not tested this specifically, one can, in principle, transfect the virus-infected cell with dsRNA at any time point during infection. This will allow ablation of a specific protein at different times in infection and allow one to determine if the same "mutation" may have early and late phenotypes. In addition, this will allow mutational analysis of essential genes, genetic deletion of which may result in a nonviable virus. In this regard, the dsRNA technique is akin to a temperature-shift experiment using a temperature-sensitive mutant virus, however, as implied earlier, conditional lethal mutations are not available for the vast majority of viral genes. (v) Ease of use: The dsRNA approach is relatively simple to design, and its application in cell culture only requires the standard transfection technology that already exists. (vi) Multiple targets: It is also possible to deplete multiple cellular or viral gene mRNAs in any combination, either simultaneously or in a temporal order, and thus ask questions about the interaction between the phenotypes. (vii) Normal infection environment: As we have contended, a major benefit of this approach in viral reverse genetics is that one can start with standard wild type virus (or even a relatively uncharacterized field isolate) with no requirements of recombinant expression, and thus, the cellular milieu is only minimally perturbed, if at all.

Lastly, the lack of effect of the anti-F dsRNA on viral genome replication deserves special attention. As described earlier (in the beginning of the Results section), intracellular NNR viral replication generates both negative- and positive-strand full-length genomic RNA, each of which should find complementarity to the appropriate strand of the anti-F dsRNA. In general, genome-length RNAs of both positive and negative sense could, therefore, be potential targets for RNA interference, resulting in severe inhibition of replication. We speculate that the genomic and antigenomic RNA of NNR viruses escape the onslaught of dsRNA because they are tightly wrapped with the nucleocapsid protein N, which makes them inaccessible to the dsRNA and/or the RNAi silencing complex (RISC). As mentioned before, the N-encapsidated genome-length RNAs are indeed extremely resistant to nucleases, to the extent that formation of such nuclease-resistant RNA products is in fact considered a defining criterion for viral replication *in vitro* and *in vivo*[32]. While the resistance of the viral genomic RNA to dsRNA has important ramifications for antiviral therapy, it is also clear that the dsRNA approach cannot be used against *cis*-acting NNR viral genomic sequences such as the intergenic regions, for which the cDNA-based approach will continue to be the method of choice [16]. It is obvious that a creative combination of the two techniques will lead to exciting possibilities in the reverse genetics of RNA viruses and in the antiviral regimen.

Conclusions

Properly designed synthetic 21-nucleotide long double-stranded RNA (dsRNA) molecules can effectively and specifically abrogate translation of target RNAs without activating a general interferon response. When applied against mRNAs of cytoplasmic RNA viruses, the dsRNAs

caused degradation of the specific viral mRNA and resultant ablation of the specific viral protein. The technique is quick, simple, and can be used against wild type RNA viruses in standard tissue culture at any point in the infection cycle. Post-transcriptional gene silencing by such dsRNA molecules should facilitate the reverse genetics and functional genomics of RNA genomes.

Materials and methods

Double-stranded RNA

The following dsRNA sequences with 3'-dT extensions were synthesized against RSV P, RSV F, and cellular lamin A/C mRNA sequences (Accession numbers M11486, M22643, and X03444, respectively), following the design recommendations of Tuschl and coworkers [2]:

P: 5' CGAUAAUAUaACUGCAAGATT 3'

3' TTGCUAUUAUAuUGACGUUCU 5'

F: 5' UGCUGUAACAGAAUUGCAGTT 3'

3' TTACGACAUUGUCUUAACGUC 5'

Lamin: 5' CUGGACUUCCAGAAGAACATT 3'

3' TTGACCUGAAGGUCUUCUUGU 5'

The two T's at the 3'-end of all RNAs were 2'-deoxythymidines. The dT residues most likely provided stability against RNases [2], since they produced a more reproducible and sustained effect at a substantially lower concentration, compared to RNAs that contained all ribonucleotides but an otherwise identical sequence (data not shown). All oligonucleotide were synthesized by Dharmacon Research (Lafayette, CO) using their recommended 2'-ACE protection chemistry, and then gel-purified. Deprotection of the RNA and hybridization of the two strands were carried out according to the manufacturer's protocol. In the mutant dsRNA (for P), the lowercase a-u base pair was changed to g-c (see Results).

Transfection with dsRNA and RSV infection

The dsRNAs were introduced in cells essentially as described [2]. Briefly, A549 cells were propagated in standard MEM (Life Technologies) supplemented with 10% fetal bovine serum (FBS) and penicillin-streptomycin. Twenty-four h before transfection, cells were trypsinized and transferred to 12-well plates. Transfection with dsRNAs was carried out with OligofectAMINE Reagent (Life Technologies) in OPTIMEM I (Life Technologies) as described by the manufacturer for adherent cell lines. Indicated amounts of dsRNA, formulated into liposomes, were applied per well, and the final volume was 500 µl per well. Cells were incubated for 6 h after transfection, and then infected with RSV Long strain at an m.o.i. of 4 [17,33], and FBS was added back to 1% to supplement the growth of the virus. A second transfection was performed after 5 h of infection and FBS was again restored to 1% in 12 h after second transfection. At 40 to 48 h after the first transfection, cells were photographed, or processed for immunostaining (see below), RNA isolation, or immunoblot, as and where indicated.

Indirect immunofluorescence

Rabbit anti-F antibody was raised against a synthetic peptide, and was a kind gift from Dr. James E. Crowe, Jr. (Vanderbilt University, TN). Rabbit polyclonal antibody against RSV-P protein has been described [21]. Indirect immunofluorescence and nuclear staining with DAPI was performed essentially as described previously [33]. A549 cells in monolayer, grown on cover slips, were washed in PBS and fixed in ice-cold 10% trichloracetic acid for 15 min, followed by successive washes in cold 70%, 90% and absolute ethanol for 3 min each. After one more PBS washing, the fixed cells were incubated for 45 min at room temperature with anti-P or anti-F protein antibody in PBS. Thereafter, cells were washed three times for 5 min in PBS and incubated for 45 min at room temperature with TRITC- or FITC-conjugated anti-rabbit IgG secondary antibody (Sigma) diluted 1:75. Nonspecific binding was eliminated by three washes in PBS. Where mentioned, nuclei were stained with DAPI (Sigma) after the final PBS wash. Cells were visualized and the images digitally captured in an Olympus BMAX Epifluorescence microscope using a 100× oil-immersion objective and appropriate filters [12,33].

Ex vivo phosphorylation assay

Metabolic labeling of cells and immunoprecipitation was performed essentially as described previously [21,30]. In brief, confluent monolayers of A549 cells were transfected with appropriate dsRNA (at 20 nM final) as described above, and at 8 hr post-transfection, were washed with a phosphate-free buffer (120 mM NaCl, 5 mM KCl, 1.5 mM $MgCl_2$, 0.25 mM $CaCl_2$, 25 mM $NaHCO_3$, 20 mM HEPES [pH 7.4]) and labeled with ^{32}P-orthophosphate (500 µCi/ml) (Amersham) in Dulbecco-modified Eagle MEM lacking both phosphate and pyruvate. Where mentioned, thapsigargin or A23178 was used at final concentrations of 100 nM, and was added to the cells 15 min before addition of the ^{32}P-containing medium containing the same concentration of the drugs. After a 1 h labeling period, all cells were washed with phosphate-buffered saline without Ca^{2+} and Mg^{2+} and disrupted as described previously to obtain the total lysate. The eIF-2 was precipitated with a polyclonal antibody against human eIF-2α (C-20) (Santa Cruz Biotech) in the presence of protein G-Sepharose (Amersham) for 1 h at 10°C, and then processed as described previously [21]. The immunoprecipitates were

subjected to SDS-PAGE followed by autoradiography to examine eIF-2 phosphorylation.

To monitor total eIF-2α in the cell, a parallel A549 monolayer was treated identically except that the labeled orthophosphate was omitted. Portions of the total cell lysate were analyzed by SDS-PAGE followed by immunoblot with anti-eIF-2α antibody. All immunoblots (Western blots) were performed essentially as described [17]. Thapsigargin and A23178 were from Sigma-Aldrich.

Reverse transcription-PCR (RT-PCR)

Quantitation of specific mRNAs by RT-PCR was done essentially as described [34]. Briefly, total RNA was isolated from trypsinized cell monolayers using the Quickprep Micro™ mRNA purification kit from Pharmacia Biotech (Piscataway, NJ). Equal amounts of total RNA were subjected to reverse transcription using the *C. therm.* RT system (Roche Molecular Biochemicals, Indianapolis, IN) at 65°C for 1 hr in the presence of 5 units of RNasin (Promega), followed by PCR through increasing number of cycles. The primers were based on RSV (*Acc#* M74568) and actin (X00351) sequences, and are as follows (sense and antisense, respectively):

P: $^{5'}$CCCTTTTCTAAACTATACAAAGAAACC$^{3'}$ and $^{5'}$AGCAGATGTAGGTCCTGCACTTG$^{3'}$;

F: $^{5'}$AGTGTAATGGAACAGATGCCAAGG$^{3'}$ and $^{5'}$GCAGGACCTTAGATACAGCAGTG$^{3'}$;

RSV genomic RNA:
$^{5'}$AATGACCAATTATATGAATCAATTATCTG$^{3'}$ and $^{5'}$GTTGACCAGGAATGTAAATGTGGC$^{3'}$;

β-actin: $^{5'}$CCTCACCCTGAAGTACCCCATC$^{3'}$ and $^{5'}$GCCGTGGTGGTGAAGCTGTAGC$^{3'}$. The RT-PCR products were 198, 274, 307, and 420 bp long, respectively, for these mRNAs. The amount of RNA was optimized for the individual genes, and PCR samples were withdrawn at 20, 22, 24, and 26 cycles of amplification and analyzed by standard agarose gel electrophoresis followed by ethidium bromide staining.

Acknowledgements

We thank Dr. James E. Crowe for the anti-F antibody. This research was supported in part by a National Research Service Award (to V.B.) from the National Institute of Allergy and Infectious Diseases, NIH. The technical assistance of Anja Oldenburg is appreciated.

References

1. Hammond SM, Caudy AA, Hannon GJ: **Post-transcriptional gene silencing by double-stranded RNA.** *Nat Rev Genet* 2001, **2**:110-119
2. Elbashir SM, Harborth J, Lendeckel W, Yalcin A, Weber K, Tuschl T: **Duplexes of 21-nucleotide RNAs mediate RNA interference in cultured mammalian cells.** *Nature* 2001, **411**:494-498
3. Banerjee AK, Barik S, De BP: **Gene expression of nonsegmented negative-strand RNA viruses.** *Pharmacol Ther* 1991, **51**:47-70
4. Cogoni C, Macino G: **Post-transcriptional gene silencing across kingdoms.** *Curr Opin Genet Dev* 2000, **10**:638-643
5. Geiss G, Jin G, Guo J, Bumgarner R, Katze MG, Sen GC: **A comprehensive view of regulation of gene expression by double-stranded RNA-mediated cell signaling.** *J Biol Chem* 2001, **276**:30178-30182
6. Kumar M, Carmichael GG: **Antisense RNA: function and fate of duplex RNA in cells of higher eukaryotes.** *Microbiol Mol Biol Rev* 1998, **62**:1415-1434
7. Crowe JE Jr, Bui PT, London WT, Davis AR, Hung PP, Chanock RM, Murphy BR: **Satisfactorily attenuated and protective mutants derived from a partially attenuated cold-passaged respiratory syncytial virus mutant by introduction of additional attenuating mutations during chemical mutagenesis.** *Vaccine* 1994, **12**:691-699
8. Pekosz A, He B, Lamb RA: **Reverse genetics of negative-strand RNA viruses: Closing the circle.** *Proc Natl Acad Sci USA* 1999, **96**:8804-8806
9. Marriott AC, Easton AJ: **Reverse genetics of the *Paramyxoviridae*.** *Adv Virus Res* 1999, **53**:321-340
10. Luytjes W, Krystal M, Enami M, Pavin JD, Palese P: **Amplification, expression, and packaging of foreign gene by influenza virus.** *Cell* 1989, **59**:1107-1113
11. Whelan SP, Ball LA, Barr JN, Wertz GT: **Efficient recovery of infectious vesicular stomatitis virus entirely from cDNA clones.** *Proc Natl Acad Sci USA* 1995, **92**:8388-8392
12. Lawson N, Stillman E, Whitt M, Rose J: **Recombinant vesicular stomatitis viruses from DNA.** *Proc Natl Acad Sci USA* 1995, **92**:4477-4481
13. Collins PL, Hill MG, Camargo E, Grosfeld H, Chanock RM, Murphy BR: **Production of infectious human respiratory syncytial virus from cloned cDNA confirms an essential role for the transcription elongation factor from the 5' proximal open reading frame of the M2 mRNA in gene expression and provides a capability for vaccine development.** *Proc Natl Acad Sci USA* 1995, **92**:11563-11567
14. Radecke F, Spielhofer P, Schneider H, Kaelin K, Huber M, Dotsch C, Christiansen G, Billeter MA: **Rescue of measles viruses from cloned DNA.** *EMBO J* 1995, **14**:5773-5784
15. Wertz GM, Howard MB, Davis N, Patton J: **The switch from transcription to replication of a negative-strand RNA virus.** *Cold Spring Harb Symp Quant Biol* 1987, **52**:367-371
16. Pattnaik AK, Ball LA, LeGrone A, Wertz GW: **The termini of VSV DI particle RNAs are sufficient to signal RNA encapsidation, replication, and budding to generate infectious particles.** *Virology* 1995, **206**:760-764
17. Burke E, Dupuy L, Wall C, Barik S: **Role of cellular actin in the gene expression and morphogenesis of human respiratory syncytial virus.** *Virology* 1998, **252**:137-148
18. Burke E, Mahoney NM, Almo SC, Barik S: **Profilin is required for optimal actin-dependent transcription of respiratory syncytial virus genome RNA.** *J Virol* 2000, **74**:669-675
19. Barik S, McLean T, Dupuy LC: **Phosphorylation of Ser232 directly regulates the transcriptional activity of the P protein of human respiratory syncytial virus: phosphorylation of Ser237 may play an accessory role.** *Virology* 1995, **213**:405-412
20. Dupuy LC, Dobson S, Bitko V, Barik S: **Casein kinase 2-mediated phosphorylation of respiratory syncytial virus phosphoprotein P is essential for the transcription elongation activity of the viral polymerase; phosphorylation by casein kinase I occurs mainly at Ser215 and is without effect.** *J Virol* 1999, **73**:8384-8392
21. Mazumder B, Barik S: **Requirement of casein kinase II-mediated phosphorylation for the transcriptional activity of human respiratory syncytial viral phosphoprotein P: transdominant negative phenotype of phosphorylation-defective P mutants.** *Virology* 1994, **205**:104-111
22. Yu Q, Hardy RW, Wertz GW: **Functional cDNA clones of the human respiratory syncytial (RS) virus N, P, and L proteins support replication of RS virus genomic RNA analogs and define minimal trans-acting requirements for RNA replication.** *J Virol* 1995, **69**:2412-2419
23. Grosfeld H, Hill MG, Collins PL: **RNA replication by respiratory syncytial virus (RSV) is directed by the N, P, and L proteins; transcription also occurs under these conditions but re-**

quires RSV superinfection for efficient synthesis of full-length mRNA. *J Virol* 1995, **69**:5677-5686
24. de Magalhaes JC, Andrade AA, Silva PN, Sousa LP, Ropert C, Ferreira PC, Kroon EG, Gazzinelli RT, Bonjardim CA: **A mitogenic signal triggered at an early stage of vaccinia virus infection: implication of MEK/ERK and protein kinase A in virus multiplication.** *J Biol Chem* 2001, **276**:38353-38360
25. Dramsi S, Cossart P: **Intracellular pathogens and the actin cytoskeleton.** *Annu Rev Cell Dev Biol* 1998, **14**:137-166
26. Frischknecht F, Moreau V, Rottger S, Gonfloni S, Reckmann I, Superti-Furga G, Way M: **Actin-based motility of vaccinia virus mimics receptor tyrosine kinase signalling.** *Nature* 1999, **401**:926-929
27. Falsey AR, Walsh EE: **Respiratory syncytial virus infection in adults.** *Clin Microbiol Rev* 2000, **13**:371-384
28. Kahn JS: **Respiratory syncytial virus vaccine development.** *Curr Opin Pediatr* 2000, **12**:257-262
29. Gonzalez-Reyes L, Ruiz-Arguello MB, Garcia-Barreno B, Calder L, Lopez JA, Albar JP, Skehel JJ, Wiley DC, Melero JA: **Cleavage of the human respiratory syncytial virus fusion protein at two distinct sites is required for activation of membrane fusion.** *Proc Natl Acad Sci USA* 2001, **98**:9859-9864
30. Srivastava SP, Davies MV, Kaufman RJ: **Calcium depletion from the endoplasmic reticulum activates the double-stranded RNA-dependent protein kinase (PKR) to inhibit protein synthesis.** *J Biol Chem* 1995, **270**:16619-16624
31. Bennett CF, Cowsert LM: **Application of antisense oligonucleotides for gene functionalization and target validation.** *Curr Opin Mol Ther* 1999, 1:359-371
32. Moyer SA, Smallwood-Kentro S, Haddad A, Prevec L: **Assembly and transcription of synthetic vesicular stomatitis virus nucleocapsids.** *J Virol* 1991, **65**:2170-2178
33. Bitko V, Barik S: **An endoplasmic reticulum-specific stress-activated caspase (caspase-12) is implicated in the apoptosis of A549 epithelial cells by respiratory syncytial virus.** *J Cell Biochem* 2001, **80**:441-454
34. Fuchs B, Zhang K, Schabel A, Bolander ME, Sarkar G: **Identification of twenty-two candidate markers for human osteogenic sarcoma.** *Gene* 2001, **278**:245-252

TAB 7

Malaria Journal

BioMed Central

Research

Characterisation and expression of a PP1 serine/threonine protein phosphatase (PfPP1) from the malaria parasite, *Plasmodium falciparum:* demonstration of its essential role using RNA interference

Rajinder Kumar, Brian Adams, Anja Oldenburg, Alla Musiyenko and Sailen Barik*

Address: Department of Biochemistry and Molecular Biology (MSB 2370), University of South Alabama, College of Medicine, 307 University Blvd., Mobile, AL 36688-0002, U.S.A

E-mail: Rajinder Kumar - rkumar@usamail.usouthal.edu; Brian Adams - badams@bbl.usouthal.edu; Anja Oldenburg - anja.oldenburg@gmx.net; Alla Musiyenko - musiyenkoalla@hotmail.com; Sailen Barik* - sbarik@jaguar1.usouthal.edu

*Corresponding author

Published: 26 April 2002

Malaria Journal 2002, 1:5

Received: 9 February 2002
Accepted: 26 April 2002

This article is available from: http://www.malariajournal.com/content/1/1/5

Abstract

Background: Reversible protein phosphorylation is relatively unexplored in the intracellular protozoa of the *Apicomplexa* family that includes the genus *Plasmodium*, to which belong the causative agents of malaria. Members of the PP1 family represent the most highly conserved protein phosphatase sequences in phylogeny and play essential regulatory roles in various cellular pathways. Previous evidence suggested a PP1-like activity in *Plasmodium falciparum*, not yet identified at the molecular level.

Results: We have identified a PP1 catalytic subunit from *P. falciparum* and named it PfPP1. The predicted primary structure of the 304-amino acid long protein was highly similar to PP1 sequences of other species, and showed conservation of all the signature motifs. The purified recombinant protein exhibited potent phosphatase activity *in vitro*. Its sensitivity to specific phosphatase inhibitors was characteristic of the PP1 class. The authenticity of the PfPP1 cDNA was further confirmed by mutational analysis of strategic amino acid residues important in catalysis. The protein was expressed in all erythrocytic stages of the parasite. Abrogation of PP1 expression by synthetic short interfering RNA (siRNA) led to inhibition of parasite DNA synthesis.

Conclusions: The high sequence similarity of PfPP1 with other PP1 members suggests conservation of function. Phenotypic gene knockdown studies using siRNA confirmed its essential role in the parasite. Detailed studies of PfPP1 and its regulation may unravel the role of reversible protein phosphorylation in the signalling pathways of the parasite, including glucose metabolism and parasitic cell division. The use of siRNA could be an important tool in the functional analysis of *Apicomplexan* genes.

Background

Reversible protein phosphorylation is gaining recognition as a potentially important mechanism of post-translational regulation in protozoan parasites, especially those belonging to the *Apicomplexan* family. The dephosphorylation of phosphoproteins is universally catalyzed by protein phosphatases that are classified into two major functional groups, protein tyrosine phosphatase (PTP) and protein serine/threonine phosphatase (PP) although enzymes with various degrees of dual-specificity are also encountered [1-5]. The majority of Ser/Thr phosphatases belong to three classical groups, namely PP1, PP2A, and PP2B (calcineurin), and possess similar primary structures in their catalytic cores [2,3,6]. PP1, in particular, exhibits an extremely high degree of sequence conservation through evolution, and its orthologs and isoforms are found in all eukaryotic cells [6,7]. In various organisms, PP1 regulates such diverse cellular processes as cell cycle progression, protein synthesis, carbohydrate metabolism, transcription, and neuronal signaling [3,7], underscoring its profound importance in biology. The PP1 and PP2A phosphatases are differentially affected by natural toxins such as okadaic acid (OA) and microcystin-LR. For example, the characteristic IC_{50} values for OA fall in the range: PP2A, 1-5 nM, PP1, 20-80 nM, whereas PP2B is highly resistant to both [2,3,7]. In contrast, tautomycin affects PP1 and PP2A nearly equally, but fails to inhibit other phosphatases [8].

In the past few years, a number of phosphatase activities and putative sequences have been reported in *P. falciparum*[9]. These include a PP2A [10], a PP2B-like activity [10], a unique chimeric PP2C [11], two putative sexual-stage phosphatases - PPα [12] and PPβ [13], and a tetratricopeptide repeat-containing phosphatase, PP5 [14]. Preliminary studies revealed the presence of a protein phosphatase activity in crude extracts of RBC-grown *P. falciparum* that exhibited toxin-sensitivity resembling that of PP1 [15]. Uninfected RBC, in contrast, possessed mainly a PP2A-like activity. Because of its potential importance in a variety of signalling pathways of the parasite, we have turned our attention to defining the PP1 phosphatase and its regulation in *P. falciparum*.

In this communication, we report the exact sequence of a PP1 cDNA in *P. falciparum*, the corresponding gene sequence in *P. falciparum* chromosome 14, the enzymatic properties of the recombinant enzyme, and its inhibition by mammalian physiological PP1-inhibitors, namely, inhibitor-1 (I-1) and inhibitor-2 (I-2). Post-transcriptional gene silencing using synthetic short interfering RNA (siRNA) molecules has been recently used to ablate specific mRNAs and thus, produce phenotypic mutations in specific genes [16,17]. We have adopted this technology to knockdown specific gene products in RNA viruses that are obligatory intracellular parasites [18]. In the present study, we have successfully used a similar strategy to generate phenotypic PP1-deficient *P. falciparum* parasites.

Results and Discussion

Identification of the PfPP1 cDNA sequence

Various pairs of oligodeoxynucleotide primers were designed on the basis of the PlasmoDB-predicted mRNA sequence (Gene chr14_1.phat_133), and employed in reverse transcription-PCR (RT-PCR) amplification using Pf3D7 total mRNA as template. Based on the prediction, primers 5' ATGGCATTAGAAATAGATATAGATAATG 3' (primer A in Fig. 1, the start codon in bold) and 5' TTATTTCCGACAAAAAGAAATATATGG 3' were first tested, but no product was obtained. Since there was no other ATG within a reasonable distance upstream that was in the same reading frame, we proceeded on the assumption that the 3'-end of the mRNA might be different. Thus, the second primer was replaced by a series of nested primers (based on the genomic sequence), each of which was paired with primer A in RT-PCR. The combination of primer A and the primer 5' TTTTTTAATTTGCTGCTTTCTTTTTTTCC 3' (Fig. 1) eventually produced a RT-PCR product that was cloned into pGEM-T vector and sequenced. The cDNA sequence contained a 915-nucleotide long open reading frame corresponding to a polypeptide 304 amino acid in length and ending with a TAA stop codon.

Comparison of the cDNA sequence with the genomic sequence (in Chromosome 14 at TIGR) revealed that the coding sequence is divided into five exons, of which the first two are the largest and contain most of the catalytic core of the phosphatase (Fig. 1 and 2). The intron sequences are pronouncedly more AT-rich than exons, and contained homopolymeric repeats, a feature which, in our experience, is common in *Plasmodium* genes.

BLAST analysis of the predicted primary structure of the protein revealed its clear identity with the PP1 class (Fig. 2). It is to be mentioned that among all the Ser/Thr phosphatases, PP1 has been subjected to the most extensive structure-function analysis [19-26]. In fact, it was one of the first phosphatases for which the three-dimensional structure was solved [26,27]. A representative alignment in Fig. 2 demonstrates the high sequence conservation between the human and *Plasmodium* PP1 sequences. The catalytic core of all members of the PP1 and PP2 families are very conserved, and roughly corresponds to residues 5-260 of PfPP1 (Fig. 2). This region contains all the signature motifs and conserved residues that have been shown to be important for the fundamental steps of catalysis, including substrate binding, metal ion coordination, and interaction with the phosphate group [19,26-28]. It is to be noted that at 304 amino acid residues, PfPP1 is the

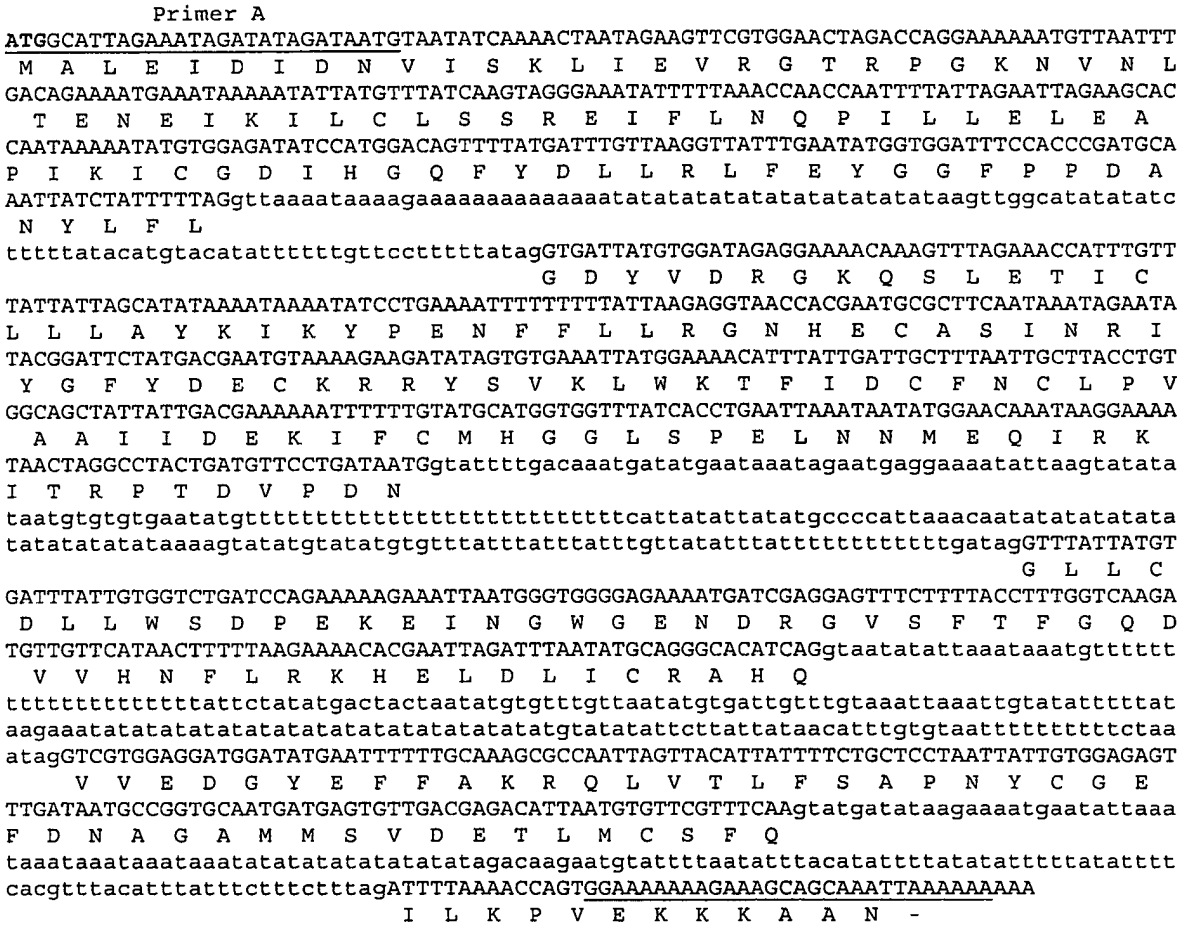

Figure 1
PfPP1 gene structure. The exon and intron sequences of PfPP1 gene are shown in capital and small letters, respectively. Underlined primers were used in RT-PCR to amplify the PP1 ORF, and have been described under Results. The amino acid sequence of PfPP1 is in single-letter codes below the coding sequence.

shortest PP1 known to date, and lacks a short proline-rich stretch at the C-terminal end (Fig. 2).

Expression and catalytic properties of PfPP1

In order to characterize the PfPP1 cDNA we subcloned it into pET-15b such that the protein is expressed with an N-terminal $(His)_6$-tag. As shown in Fig. 3, a protein band of approximately 37,000 Mr was produced from the pET-15b-PfPP1 clone, which is in agreement with the predicted molecular weight of 34,904 of PfPP1 and roughly another 2,000 added for the $(His)_6$ region of pET-15b (Novagen: Madison, WI). The protein specifically reacted with a monoclonal anti-His antibody and also with a polyclonal antibody against full-length human PP1 (Transduction Laboratories: Lexington, KY). The recombinant protein was purified through nickel-chelation chromatography and tested for phosphatase activity. It dephosphorylated the small substrate *p*NPP, as well as histone, labelled at Ser residues. Interestingly, it also showed decent activity on a Tyr-phosphorylated synthetic peptide. The V_{max} values (μmol Pi liberated / mg enzyme/ min) against these three substrates (pNPP, phosphoserine-histone, phosphotyrosine peptide) were, respectively: 12 +2, 8 +1, and 2 +0.5. An equivalent protein fraction, obtained from *E. coli* containing vector alone (without insert), showed no activity against any of these substrates. It has

```
Plasmodium      --MALEIDIDNVISKLIEVRGTRPGKNVNLTENEIKILCLSSREIFLNQPILLELEAPIK 58
Human           MSDSEKLNLDSIIGRLLEVQGSRPGKNVQLTENEIRGLCLKSREIFLSQPILLELEAPLK 60
                      *::*.:* :*:**:*:******:******: ***.******.**********:*

Plasmodium      ICGDIHGQFYDLLRLFEYGGFPPDANYLFLGDYVDRGKQSLETICLLLAYKIKYPENFFL 118
Human           ICGDIHGQYYDLLRLFEYGGFPPESNYLFLGDYVDRGKQSLETICLLLAYKIKYPENFFL 120
                ********:**************::************************************

Plasmodium      LRGNHECASINRIYGFYDECKRRYSVKLWKTFIDCFNCLPVAAIIDEKIFCMHGGLSPEL 178
Human           LRGNHECASINRIYGFYDECKRRYNIKLWKTFTDCFNCLPIAAIVDEKIFCCHGGLSPDL 180
                ************************.:****** *******:***:****** ******:*

Plasmodium      NNMEQIRKITRPTDVPDNGLLCDLLWSDPEKEINGWGENDRGVSFTFGQDVVHNFLRKHE 238
Human           QSMEQIRRIMRPTDVPDQGLLCDLLWSDPDKDVQGWGENDRGVSFTFGAEVVAKFLHKHD 240
                ..*****:* *******:***********:*:  ************** :** :**:**:

                                        β12    loop       β13
Plasmodium      LDLICRAHQVVEDGYEFFAKRQLVTLFSAPNYCGEFDNAGAMMSVDETLMCSFQILKPVE 298
Human           LDLICRAHQVVEDGYEFFAKRQLVTLFSAPNYCGEFDNAGAMMSVDETLMCSFQILKPAD 300
                ************************************************************::

Plasmodium      KKK-----AAN------------------------ 304
Human           KNKGKYGQFSGLNPGGRPITPPR--NSAKAKK---- 330
                *.*
```

Figure 2
PfPP1 sequence comparison. The predicted sequences of *Plasmodium* PP1 (this study) and human PP1 alpha (P08129) catalytic subunits were aligned using the CLUSTALW program at the European Bioinformatics Institute (EMBL) server, and later refined by visual inspection. The amino acid residue numbers are shown on the right. Residues are marked as: non-conservative replacement (.); conservative replacement (:), and identical (*). Residues important in I-2 interaction are highlighted in gray: E52, E54; D164, E165, and K166.

been recently shown that rabbit PP1, expressed in *E. coli*, also possessed Tyr phosphatase activity. In contrast, native PP1 isolated from rabbit muscle or expressed in Sf9 insect cells contained only Ser/Thr phosphatase activity but no Tyr phosphatase activity [24]. It was concluded that this apparent difference might be due to subtle changes in protein folding in eukaryotic versus prokaryotic cellular environments. It remains to be seen whether this is a general feature of all PP1.

To obtain biochemical evidence for the identity of the recombinant PfPP1, we tested the effect of specific phosphatase inhibitors and selected mutations on the phosphatase activity. Mutation of Asn122 to Asp by site-directed mutagenesis destroyed the phosphatase activity, confirming the essential role of this residue of PP1 in catalysis [19]. PfPP1 was inhibited by NaF, inorganic orthophosphate, and pyrophosphate at respective IC_{50} values of 2.5 mM, 10 mM, and 90 μM (data not shown). Similar values were recently obtained for *Arabidopsis* PP1 [8]. PfPP1 was also inhibited by tautomycin, I-1, I-2, and OA with IC_{50} values of 0.8, 400, 7, and 100 nM, respectively (Fig. 4). These values are comparable to those obtained with various PP1 isoforms recombinantly expressed in *E. coli*[25,29]. The sensitivity of PfPP1 to these natural toxins is consistent with the fact that the loop sequence between the β12 and β13 regions plays a direct role in binding these toxins [23,26], and this sequence is entirely conserved in PfPP1 (Fig. 2). Recently, a few additional residues that are closer to the N-terminus in the PP1 sequence have also been shown to be important in the interaction with I-2 [24]; in PfPP1 numbers, these residues are: E52, E54, and D164, E165, K166 (Fig. 2). In yeast PP1 (Glc7p), the double mutant E52A/E54A and the triple mutant D164A/E165A/K166A showed IC_{50} values for I-2 that were respectively 8 and 300 times the wild type enzyme values [24]. As shown in Fig. 4, a similar loss of inhibition by I-2 was also observed when the corresponding muta-

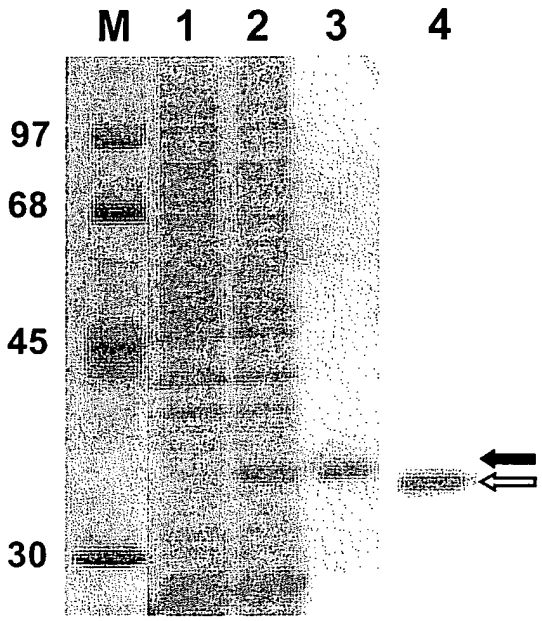

Figure 3
Recombinant expression of PfPP1 in bacteria. The following proteins / extracts were analyzed by SDS-PAGE followed by staining with Coomassie Brilliant Blue R250: approximately 30 μg (protein) of total extract [14] of IPTG-induced *E. coli* BL21(DE3) containing the RIG plasmid and pET-15-PfPP1 (lane 2) or pET-15 without insert (lane 1); 4 μg of the purified recombinant $(His)_8$-tagged PfPP1 (lane 3). Lane 4 shows an immunoblot in which 80 μg of 100,000 × g extract of Pf [10] was probed using a PP1 antibody described under Materials and Methods. Parasitic PfPP1 and the recombinant His-tagged PfPP1 bands are indicated by open and closed arrowheads, respectively. Protein markers (lane M) are indicated by Mr in thousands.

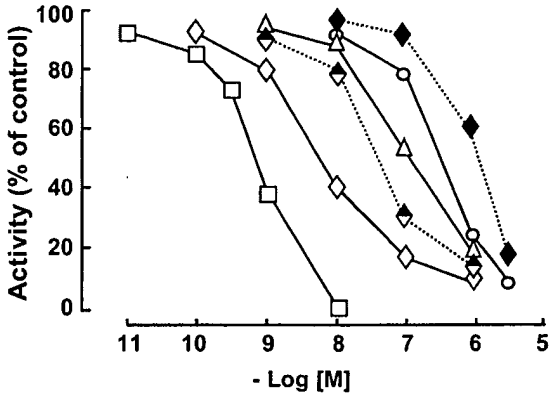

Figure 4
PfPP1 dose response to inhibitors. Inhibition assays for recombinant PfPP1 were performed using ^{32}P-phosphorylase *a* as substrate essentially as described [14]. The inhibitors and the symbols are: tautomycin (square), inhibitor-2 (diamond), OA (triangle), and I-1 (circle). The half-closed and fully closed diamonds represent I-2 against the double mutant (E52A/E54A) and triple mutant (D164A/E165A/K166A) enzymes, respectively. Activities are expressed as percentage of the inhibitor-free reaction. As shown, the X-axis represents negative logarithm of molar concentration of the inhibitors.

tions were introduced into PfPP1, although they did not affect the catalytic activity (specific activity) (data not shown). Together, these results provide experimental confirmation of the catalytic identity of PfPP1.

Expression of native PfPP1

As mentioned earlier, inhibition studies using OA and calyculin A suggested the existence of a PP1-like activity in *P. falciparum* extracts [15]. However, our attempts to purify the native PfPP1 enzyme by chromatographic procedures resulted in only small amounts of activity, probably due to rapid inactivation during fractionation. To determine if PfPP1 is expressed in *Plasmodium*, we have, therefore, taken an immunological approach. First, cell-free extracts of different erythrocytic stages of *P. falciparum* were subjected to Western blot using a monoclonal antibody that was raised against nearly full-length human PP1 and showed a broad species specificity (see Materials and Methods). As shown in Fig. 5A, a major band of the expected size of 35 k was observed in all stages including gametes. A peptide antibody, specific for human PP1 (Materials and Methods), did not detect the band. The gametogenesis was confirmed by the appearance of Pfg27, an early gamete-specific protein [30]. Having demonstrated that the monoclonal antibody was specific for PP1, we used it in an attempt to inhibit PfPP1 activity *in vitro*. At optimal concentrations, the antibody almost completely inhibited (90% inhibition) recombinant PfPP1 (including its Tyr phosphatase activity), and also inhibited the phosphatase activity of the *P. falciparum* extract by about 70% (data not shown). Under the same conditions, the human-specific antibody had no effect. Finally, it has been shown that affinity resins containing immobilized microcystin specifically bind toxin-sensitive phosphatases such as PP1 and PP2A [31]. Thus, we passed soluble cytosolic Pf extract through microcystin-Sepharose, and the bound proteins were analyzed on SDS-PAGE followed by immunoblot using the anti-PP1 antibody. The blot revealed that the 35 kDa PfPP1 polypeptide indeed specifically bound to microcystin (Fig. 5B), correlating the antigenic reactivity of PfPP1 with its affinity for the toxin. Pre-incubation of the

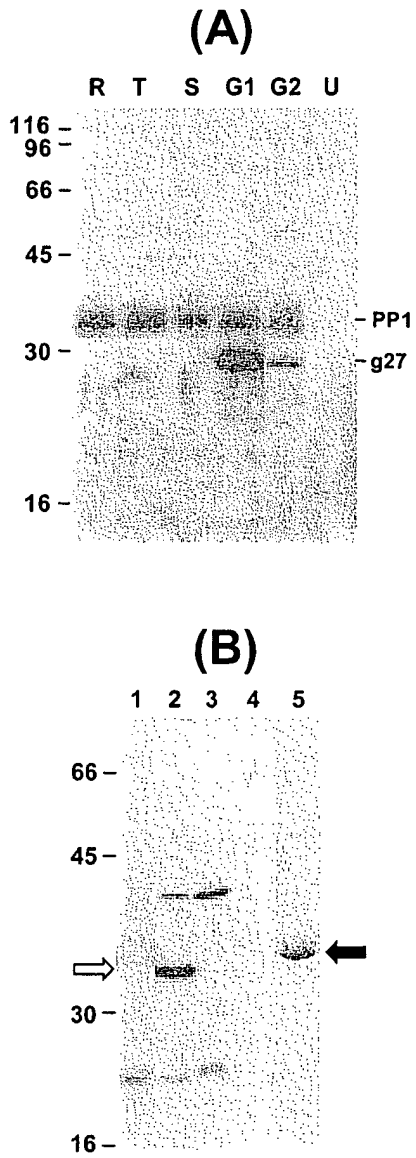

Figure 5
Constitutive expression of parasitic PfPP1. (A) Western blot: Total protein (80 μg) from the ring (R), Trophozoite (T), schizont (S), and early (G1) and late (G2) sexual stages of Pf were probed with a mixture of anti-PP1 and anti-Pfg27 antibodies as described [14]. (B) Microcystin-sepharose chromatography: About 500 μg of the following extracts was subjected to microcystin affinity chromatography and the bound proteins analyzed by Western blot using PP1 antibody: extract of uninfected RBC processed identically (lane 1); Pf extract (lane 2); Pf extract pre-incubated with 1 μM microcystin-LR at room temperature for 5 min (lane 3); unbound fraction (a double-pass flow-through from the column) (lane 4). Recombinant His-tagged PfPP1 is displayed in lane 5 for comparison. The native and recombinant PP1 bands are marked by open and closed arrows, respectively. Sizes of protein standards are indicated on the left. Two non-PP1 proteins are also seen in the blot in panel B. The ~25 kDa band (common in lanes 1, 2, and 3) is evidently a RBC protein. The ~40 kDa band (lanes 2, 3), on the other hand, is a *Plasmodium* protein, since it is absent in the RBC fraction. We speculate that these proteins non-specifically bound to the Sepharose matrix, since they could not be competed out by microcystin (lane 3).

extract with microcystin specifically prevented binding of PfPP1 to the column.

Generation of phenotypic PfPP1 mutants by PTGS using RNAi

RNA interference (RNAi), mediated by short interfering double-stranded RNA molecules (siRNA or dsRNA), is now recognized as a major mechanism of post-transcriptional gene silencing (PTGS) in essentially all eukaryotes [16]. Recently, the technique has been successfully applied to cultured mammalian cells, whereby introduction of 21-nucleotide long synthetic dsRNA molecules corresponding to specific mRNA sequences effectively and specifically degraded the cognate mRNAs and abrogated the expression of the corresponding proteins [17,18]. This prompted us to test a similar approach to knockdown PfPP1 function in the erythrocytic *P. falciparum* stages. Our initial attempts with standardized transfection procedures using OligofectAMINE (Life Technologies: Bethesda, MD) with the dsRNA did not produce an appreciable loss of PfPP1. We then resorted to the electroporation procedure originally developed for DNA transfection in *Plasmodium* by Wellems and co-workers [32], as detailed under Materials and Methods. A representative set of results shown in Fig. 6 clearly demonstrates loss of PfPP1 by the RNAi procedure, while the control PP2A was not significantly affected. Loss of PfPP1 resulted in concomitant inhibition of parasite growth as evidenced by the drastic reduction in ^{3}H-hypoxanthine incorporation. These results suggest that PfPP1 plays an essential role in *Plasmodium* replication. The facts that the parasite culture was asynchronous, i.e., contained all three major stages (ring, trophozoite, and schizont) (data not shown) and that the effect of dsRNA was severe, suggest that PfPP1 is required for cell cycle progression at all stages of the parasite. This is further supported by the expression of PP1 protein in all the parasitic stages (Fig. 5). Taken together, this is consistent with the established role of PP1 in eukaryotic DNA synthesis and cell cycle progression, as discussed below.

PP1 is one of the major protein phosphatases found in all eukaryotic cells. The activity of the catalytic subunit of PP1 is controlled by its interaction with a large number of regulatory subunits, many of which also target it to specific subcellular compartments [7,24,33]. The major ones include the glycogen-targeting subunits (G_M, G_L) [34], myofibrillar-targeting subunit (M_{110}) [34], nuclear inhibitor of PP1 (NIPP-1) [35], PP1 nuclear targeting subunit (PNUTS) [36,37], mitosis-regulating subunit Sds22 [38–40], ribosomal protein L5 [41] and small cytosolic inhibitory proteins, I-1, I-2, and DARRP-32 (Dopamine and cAMP-regulated phosphoprotein, Mr 32,000) [7,23,25]. The physiological role of many of these interactions has been revealed in recent studies. A temperature-sensitive mutant of the yeast PP1 (Glc7), for example, exhibits a

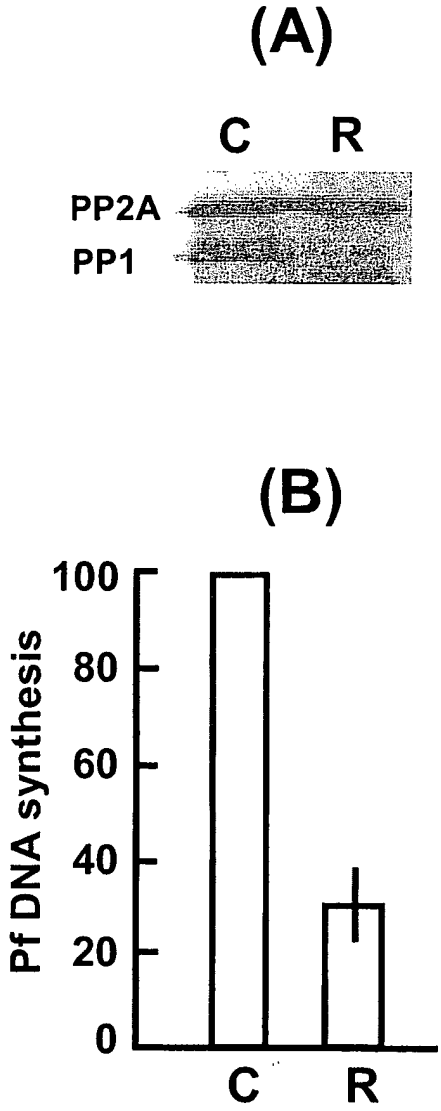

Figure 6
Inhibition of parasite growth and abrogation of PfPP1 expression by interfering dsRNA. The dsRNA sequences, and electroporation procedure have been described under Materials and Methods. Infected RBC were transfected with dsRNA against PfPP1 (R) or luciferase (C). Western blot (A) shows loss of PfPP1 by the dsRNA, but no effect on the control PfPP2A. The PP1 monoclonal and PP2A peptide antibodies have been described in Materials and Methods. Hypoxanthine incorporation assay (B) shows an approximately 70% inhibition of parasitic DNA synthesis in PP1-depleted cells, compared to the luciferase antisense-treated control.

block in the M phase of the cell division cycle, and elevated expression of Sds22 suppresses this defect [38]. Structure-function analysis of recombinant mammalian PP1 has recently begun to map specific residues involved in interaction with other molecules. Interestingly, all these residues are conserved in PfPP1, and a few examples are presented here. Co-crystal structure of PP1 and a G_M peptide [42], as well as mutagenesis studies [43] of the yeast PP1 ortholog, Glc7, have demonstrated a role of specific PP1 residues in PP1-G_M interaction. In the PfPP1 sequence, these residues are: I167, L241, F255, L264, C289, and F291 (Fig. 2). As mentioned, the β12-loop-β13 region, important in interaction with natural toxins [23], is fully conserved in PfPP1 (Fig. 2). Two residues, recently shown to be important for interaction with DARPP-32 [22], are also conserved in PfPP1; these are: Met288 and Cys289 (Fig. 2). We have provided experimental evidence of an important role of a number of invariant residues of PfPP1 in the interaction with I-2 (Fig. 2 and 4). Based on such overwhelming conservation of functionally important residues, we propose that orthologs of many of these PP1-interacting proteins may also exist in *Plasmodium* and function in similar roles. The use of recombinant PfPP1 and protein-protein interaction techniques should aid in characterizing these physiological regulatory subunits of PfPP1. Our ability to generate PP1-deficient *P. falciparum* parasites will allow us to study the "mutant" phenotype in further detail and understand the role of this highly conserved phosphatase in malarial biochemistry and pathophysiology. These studies are in progress.

As mentioned earlier, Li and Baker [12] described a putative phosphatase DNA sequence in *Plasmodium*, the mRNA of which was detected in the sexual stages of the parasite. The predicted protein, named PPα, was 889 amino acid long, and contained a unique N-terminal extension of about 500 amino acids. The C-terminal 345 amino acids, containing the putative catalytic domain, had 5 unique peptide stretches that were called "inserts". When these inserts were omitted from the alignment, the rest of the sequence showed significant similarity with PP1 phosphatases [12]. Clearly, further studies are needed to identify the PPα protein and characterize its potentially interesting identity.

While our manuscript was being written, McRobert and McConkey [44] achieved similar success in using the RNAi strategy to ablate dihydroorotate dehydrogenase (DHODH) of *P. falciparum*. Although the protein level was not directly monitored, the loss of DHODH mRNA was confirmed by RT-PCR. This resulted in inhibition of parasite growth, consistent with the role of DHODH in pyrimidine biosynthesis, essential for parasite DNA replication. These authors introduced the double-stranded RNA by electroporation also, using conditions very similar to ours. Thus, although the exact mechanism of the RNA uptake remains to be elucidated, the electroporation procedure must have allowed the dsRNA to traverse the various erythrocytic and parasitic membranes to enter the parasitic cells.

The success in ablating PfPP1 is particularly gratifying to us on a number of accounts. As mentioned, PP1 is a highly conserved enzyme, and toxin-sensitive Ser/Thr phosphatase activities are also found in erythrocytes [15]. Thus, use of PP1 inhibitors, such as okadaic acid or tautomycin (Fig. 4) would affect the parasite as well as the host, making conclusions difficult. The dsRNA, in contrast, is known to be extremely specific for its intended target, such that a single nucleotide mismatch prevents its action [17]. This has allowed us to create specific phenotypic loss of PfPP1. Moreover, RNAi will permit the ablation of essential gene products, at any time point in infection, or on a desired parasitic stage following synchronization. Lastly, traditional genetic manipulation in eukaryotes, including the *Apicomplexa*, is a relatively difficult and elaborate procedure [45,46]. Thus, we believe that the RNAi strategy will become a powerful and convenient tool in *Plasmodium* functional genomics, particularly in the studies of phylogenetically conserved signalling molecules.

Conclusion

P. falciparum contains a PP1 protein phosphatase that is virtually identical to its orthologs in other species in both sequence and biochemical properties. Based on the established physiological role of PP1 in other organisms such as mammals and yeast, PfPP1 may regulate a variety of parasitic pathways, including glycogen metabolism, glucose repression, and cell cycle progression. Indeed, the successful use of RNA interference to ablate PfPP1 confirms its essential role on parasitic growth. The catalytic subunit of PfPP1 is expressed in all the erythrocytic stages of the parasite and is specifically inhibited by mammalian physiological inhibitors, inhibitor-1 and inhibitor-2. Thus, an in-depth study of PfPP1 and its interacting subunits may shed light on the regulation of the relevant pathways in this clinically important family of parasites.

Materials and methods

Materials

Histone and the catalytic subunit of PKA were purchased from Sigma (St. Louis, MO), and rabbit I-2, the *v-abl* protein tyrosine kinase, and its peptide substrate EAIYAAPFAKKK were from New England Biolabs (Bedford, MA). Okadaic acid (OA) and recombinant I-1 [22] were kind gifts from R. Honkanen and S. Shenolikar (Duke University), respectively. The monoclonal anti-PP1 antibody was raised against a 25.6 kDa fragment of human PP1α (residue 5–226), and was purchased from Transduction Laboratories (Lexington, KY). This antibody reacts with all

mammalian and avian PP1 tested, but does not react with other PP classes. The other PP1 antibody (a kind gift from R. Honkanen) was specific for human PP1, and was raised in rabbit against a synthetic peptide corresponding to the last 13 residues of human PP1 (PITPPRNSAKAKK; Fig. 2). The anti-PfPP2A antibody was raised in rabbit against the peptide MLIFKDTPDSRNSIKN, corresponding to residue 285–300 of the previously described PfPP2A [10]. The RIG plasmid was kindly provided by W. Hol (University of Washington, Howard Hughes Medical Institute) [47]. Monoclonal antibody against the early sexual-stage *P. falciparum* antigen Pfg27 [30] was a generous gift from N. Kumar (Johns Hopkins University, Baltimore, MD). Microcystin-coupled sepharose was purchased from Upstate Biotechnology, Inc. (Lake Placid, NY).

Amplification, cloning, and mutagenesis of PfPP1 cDNA

Total RNA was isolated from asynchronous *P. falciparum* 3D7 cells grown in human A-positive erythrocytes essentially as before [48,49]. Various pairs of primers were designed on the basis of the relevant sequences of chromosome 14. T_m values of the primers were in the range of 65–72°C in order to achieve high specificity in reverse transcription (RT) as well as PCR. RT reaction was carried out at 60°C for 1.5 hrs using the C. therm. polymerase kit (Roche Molecular Biochemicals, Cat. No. 2016311). The RT reaction was incorporated into PCR, carried out using a mixture of Taq (Roche) and Pfu (Stratagene) polymerases (20:1) to ensure high fidelity [50]. Elongation in PCR was performed at 62°C. The various products were gel-purified and cloned in pGEM-T by "TA cloning" (Promega, WI). The clones were initially screened by restriction analysis and finally confirmed by sequencing.

All site-directed mutagenesis were performed using the megaprimer procedure [51], and the mutations were confirmed by sequencing. DNA sequencing was carried out by cycle sequencing using the PRISM Big Dye Terminator sequencing kit and AmpliTaq DNA polymerase (Perkin-Elmer, Division of PE/ABI).

Expression and assay of recombinant PfPP1 phosphatase

Growth and induction of *E. coli* BL21(DE3) containing pET-15b-PfPP1 and the RIG plasmid were carried out using procedures described earlier [14,48], except that the culture was grown at 18°C in the presence of 2 mM $MnCl_2$, and IPTG concentration was lowered to 0.4 mM. The $(His)_6$-tagged PfPP1 expressed from pET-15b-PfPP1 was purified through Ni^{+2}-chelation chromatography [14] as described by the manufacturer (Novagen), with 1 mM $MnCl_2$ being present in all the buffers. The imidazole-eluted His-tagged PfPP1 was dialyzed against 50 mM Tris-Cl (pH 7.5), 100 mM NaCl, 25% glycerol, 1 mM DTT (buffer A), and stored in small portions at -80°C.

Phosphatase activities were assayed essentially as described [14,19,52]. Unless otherwise mentioned, 80 µl reactions contained 2 mM of $MnCl_2$ and requisite amount of recombinant enzyme in buffer A. Where mentioned, OA was directly added to the reaction. When I-2 was used, it was pre-incubated with PfPP1 at 32°C for 30 min. I-1 was prephosphorylated by PKA in a standard kinase reaction containing 200 µM γ-thiophosphorylated ATP. ^{32}P-labelled histone was prepared by phosphorylation with PKA in the presence of γ-^{32}P [ATP] essentially as described, followed by removal of the free ATP by gel filtration [19,52]. The resultant phosphohistone is exclusively phosphorylated at Ser residues [53]. ^{32}P-labeled peptide EAI(Yp)AAPFAKKK, phosphorylated at the single Tyr residue by $pp43^{v\text{-}abl}$ kinase, was prepared essentially as described [19,52]. Phosphatase reactions were initiated by the addition of the substrate. The liberated ^{32}P was quantitated by a phosphomolybdate extraction assay as described previously [14]. Reactions were followed with time, and results were corrected by subtraction of the corresponding values from an enzyme-free reaction.

Analysis of native PfPP1

P. falciparum 3D7 was grown on A-positive human erythrocytes in the presence of homologous serum as described earlier [48,49]. When needed, cultures were synchronized in two steps [49,54]: (i) schizonts were purified by flottation over 65% (v/v) Percoll (Pharmacia) followed by incubation with fresh erythrocytes (5% haematocrit); (ii) the cultures were then left to mature into rings and treated with 5% D-sorbitol for 15 min at 37°C. The purity of individual stages was greater than 95% as confirmed by microscopic observation of a stained thin smear of the culture. Sexual stage parasite was generated as described [30].

Transfection by inhibitory dsRNA

The following 21-mer RNA molecules, corresponding to the underlined sequence in Fig. 1, were synthesized as described [18] and deprotected according to the manufacturer's protocol (Dharmacon Research, Lafayette, CO):

Sense: (5') GAGGUAACCACGAAUGCGCdTdT (3')

Antisense: (5') GCGCAUUCGUGGUUACCUCdTdT (3')

The negative control luciferase RNA was the same as the double-stranded GL3 RNA described previously [17]. The RNAs were annealed *in vitro* to form double-stranded RNA (dsRNA) [18] and electroporation was carried out essentially as described [32]. In brief, 3 µg dsRNA in 800 µl of incomplete cytomix [32] was added to infected RBC (at 10–15% parasitemia), and electroporation was performed using a Bio-Rad Gene Pulsar unit at settings of 200 Ω, 2 kV, and 25 µF. Control cells were identically electro-

porated without RNA. The cells were then grown in 12-well plates in triplicate wells, and measurement of ^{3}H-hypoxanthine incorporation was carried out at 24 hr post-electroporation using standard procedures [49], except that parasites were liberated with saponin, pelleted, and counts in the pellet measured following solubilization. Parasites from unlabelled but otherwise identical cultures were analyzed in Western blot using a mixture of anti-PP1 and anti-PfPP2A antibodies (see Materials and Methods).

Acknowledgements

This research was supported in part by a grant (AI45803) from the National Institute of Allergy and Infectious Diseases, National Institutes of Health, USA. S. B. is a recipient of a Burroughs Wellcome New Initiatives in Malaria Research Award. We sincerely thank the members of the Malaria Genome Project and the PlasmoDB web site for providing free access to the sequences. Thanks are also due to Dr. Wim G. J. Hol for the RIG plasmid, Dr. Richard E. Honkanen for OA and the monospecific human PP1 antibody, Dr. Shirish Shenolikar for I-1, Dr. Nirbhay Kumar for the antibody against Pfg27, Dr. David McGee (Department of Microbiology and Immunology) for the use of his Bio-Rad Gene Pulser instrument, and Dr. Tin Cao for expert help in DNA sequencing.

References

1. Graves JD, Krebs EG: **Protein phosphorylation and signal transduction.** *Pharmacol Ther* 1999, **82**:111-121
2. Cohen PT: **Novel protein serine/threonine phosphatases: variety is the spice of life.** *Trends Biochem Sci* 1997, **22**:245-251
3. Wera S, Hemmings BA: **Serine/threonine protein phosphatases.** *Biochem J* 1995, **311**:17-29
4. Fischer EH: **Cell signaling by protein tyrosine phosphorylation.** *Adv Enzyme Regul* 1999, **39**:359-369
5. Guan KL, Dixon JE: **Bacterial and viral protein tyrosine phosphatases.** *Semin Cell Biol* 1993, **4**:389-396
6. Barton GJ, Cohen PT, Barford D: **Conservation analysis and structure prediction of the protein serine/threonine phosphatases. Sequence similarity with diadenosine tetraphosphatase from *Escherichia coli* suggests homology to the protein phosphatases.** *Eur J Biochem* 1994, **220**:225-237
7. Bollen M, Stalmans W: **The structure, role, and regulation of type 1 protein phosphatases.** *Crit Rev Biochem Mol Biol* 1992, **27**:227-281
8. Stubbs MD, Tran HT, Atwell AJ, Smith CS, Olson D, Moorhead GB: **Purification and properties of *Arabidopsis thaliana* type 1 protein phosphatase (PP1).** *Biochim Biophys Acta* 2001, **1550**:52-63
9. Wyler DJ: **Malaria: overview and update.** *Clin Infect Dis* 1993, **16**:449-456
10. Dobson S, May T, Berriman M, Del Vecchio C, Fairlamb AH, Chakrabarti D, Barik S: **Characterization of protein Ser/Thr phosphatases of the malaria parasite, *Plasmodium falciparum* : inhibition of the parasitic calcineurin by cyclophilin-cyclosporin complex.** *Mol Biochem Parasitol* 1999, **99**:167-181
11. Mamoun CB, Sullivan DJ Jr, Banerjee R, Goldberg DE: **Identification and characterization of an unusual double serine/threonine protein phosphatase 2C in the malaria parasite *Plasmodium falciparum*.** *J Biol Chem* 1998, **273**:11241-11247
12. Li JL, Baker DA: **A putative protein serine/threonine phosphatase from *Plasmodium falciparum* contains a large N-terminal extension and five unique inserts in the catalytic domain.** *Mol Biochem Parasitol* 1998, **95**:287-295
13. Li JL, Baker DA: **Protein phosphatase beta, a putative type-2A protein phosphatase from the human malaria parasite *Plasmodium falciparum*.** *Eur J Biochem* 1997, **249**:98-106
14. Dobson S, Kar B, Kumar R, Adams B, Barik S: **A novel tetratricopeptide repeat (TPR) containing PP5 serine/threonine protein phosphatase in the malaria parasite, *Plasmodium falciparum*.** *BMC Microbiol* 2001, **1**:31
15. Yokoyama D, Saito-Ito A, Asao N, Tanabe K, Yamamoto M, Matsumura T: **Modulation of the growth of *Plasmodium falciparum* in vitro by protein serine/threonine phosphatase inhibitors.** *Biochem Biophys Res Commun* 1998, **247**:18-23
16. Hammond SM, Caudy AA, Hannon GJ: **Post-transcriptional gene silencing by double-stranded RNA.** *Nat Rev Genet* 2001, **2**:110-119
17. Elbashir SM, Harborth J, Lendeckel W, Yalcin A, Weber K, Tuschl T: **Duplexes of 21-nucleotide RNAs mediate RNA interference in cultured mammalian cells.** *Nature* 2001, **411**:494-498
18. Bitko V, Barik S: **Phenotypic silencing of cytoplasmic genes using sequence-specific double-stranded short interfering RNA and its application in the reverse genetics of wild type negative-strand RNA viruses.** *BMC Microbiol.* 2001, **1**:34
19. Ansai T, Dupuy LC, Barik S: **Interactions between a minimal protein serine/threonine phosphatase and its phosphopeptide substrate sequence.** *J Biol Chem* 1996, **271**:24401-24407
20. Zhang J, Zhang Z, Brew K, Lee EY: **Mutational analysis of the catalytic subunit of muscle protein phosphatase-1.** *Biochemistry* 1996, **35**:6276-6282
21. Zhang L, Lee EY: **Mutational analysis of substrate recognition by protein phosphatase 1.** *Biochemistry* 1997, **36**:8209-8214
22. Connor JH, Quan HQ, Ramaswamy NT, Zhang L, Barik S, Zheng J, Cannon JP, Lee EYC, Shenolikar S: **Inhibitor-1 interaction domain that mediates the inhibition of protein phosphatase-1.** *J Biol Chem* 1998, **273**:27716-27724
23. Connor JH, Kleeman T, Barik S, Honkanen RE, Shenolikar S: **Importance of the β12-β13 loop in protein phosphatase-1 catalytic subunit for inhibition by toxins and mammalian protein inhibitors.** *J Biol Chem* 1999, **274**:22366-22372
24. Connor JH, Frederick D, Huang H, Yang J, Helps NR, Cohen PT, Nairn AC, DePaoli-Roach A, Tatchell K, Shenolikar S: **Cellular mechanisms regulating protein phosphatase-1. A key functional interaction between inhibitor-2 and the type 1 protein phosphatase catalytic subunit.** *J Biol Chem* 2000, **275**:18670-18675
25. Watanabe T, Huang HB, Horiuchi A, da Cruze Silva EF, Hsieh-Wilson L, Allen PB, Shenolikar S, Greengard P, Nairn AC: **Protein phosphatase 1 regulation by inhibitors and targeting subunits.** *Proc Natl Acad Sci U S A* 2001, **98**:3080-3085
26. Goldberg J, Huang HB, Kwon YG, Greengard P, Nairn AC, Kuriyan J: **Three-dimensional structure of the catalytic subunit of protein serine/threonine phosphatase-1.** *Nature* 1995, **376**:745-753
27. Egloff M-P, Cohen PTW, Reinemer P, Barford D: **Crystal structure of the catalytic subunit of human protein phosphatase 1 and its complex with tungstate.** *J Mol Biol* 1995, **254**:942-959
28. Zhuo S, Clemens JC, Stone RL, Dixon JE: **Mutational analysis of a Ser/Thr phosphatase. Identification of residues important in phosphoesterase substrate binding and catalysis.** *J Biol Chem* 1994, **269**:26234-26238
29. Endo S, Connor JH, Forney B, Zhang L, Ingebritsen TS, Lee EY, Shenolikar S: **Conversion of protein phosphatase 1 catalytic subunit to a Mn(2+)-dependent enzyme impairs its regulation by inhibitor 1.** *Biochemistry* 1997, **36**:6986-6992
30. Lobo CA, Konings RN, Kumar N: **Expression of early gametocyte-stage antigens Pfg27 and Pfs16 in synchronized gametocytes and non-gametocyte producing clones of *Plasmodium falciparum*.** *Mol Biochem Parasitol* 1994, **68**:151-154
31. Moorhead G, MacKintosh RW, Morrice N, Gallagher T, MacKintosh C: **Purification of type 1 protein (serine/threonine) phosphatases by microcystin-Sepharose affinity chromatography.** *FEBS Lett* 1994, **356**:46-50
32. Wu Y, Sifri CD, Lei HH, Su XZ, Wellems TE: **Transfection of *Plasmodium falciparum* within human red blood cells.** *Proc Natl Acad Sci USA* 1995, **92**:973-977
33. Aggen JB, Nairn AC, Chamberlin R: **Regulation of protein phosphatase-1.** *Chem Biol* 2000, **7**:R13-23
34. Johnson DF, Moorhead G, Caudwell FB, Cohen P, Chen YH, Chen MX, Cohen PT: **Identification of protein-phosphatase-1-binding domains on the glycogen and myofibrillar targetting subunits.** *Eur J Biochem* 1996, **239**:317-325
35. Beullens M, Van Eynde A, Vulsteke V, Connor J, Shenolikar S, Stalmans W, Bollen M: **Molecular determinants of nuclear protein phosphatase-1 regulation by NIPP-1.** *J Biol Chem* 1999, **274**:14053-14061
36. Allen PB, Kwon YG, Nairn AC, Greengard P: **Isolation and characterization of PNUTS, a putative protein phosphatase 1 nuclear targeting subunit.** *J Biol Chem* 1998, **273**:4089-4095
37. Kreivi JP, Trinkle-Mulcahy L, Lyon CE, Morrice NA, Cohen P, Lamond AI: **Purification and characterisation of p99, a nuclear modu-**

lator of protein phosphatase 1 activity. *FEBS Lett* 1997, **420**:57-62
38. Ohkura H, Yanagida M: ***S. pombe* gene sds22+ essential for a midmitotic transition encodes a leucine-rich repeat protein that positively modulates protein phosphatase-1.** *Cell* 1991, **64**:149-157
39. MacKelvie SH, Andrews PD, Stark MJ: **The *Saccharomyces cerevisiae* gene SDS22 encodes a potential regulator of the mitotic function of yeast type 1 protein phosphatase.** *Mol Cell Biol* 1995, **15**:3777-3785
40. Renouf S, Beullens M, Wera S, Van Eynde A, Sikela J, Stalmans W, Bollen M: **Molecular cloning of a human polypeptide related to yeast sds22, a regulator of protein phosphatase-1.** *FEBS Lett* 1995, **375**:75-78
41. Hirano K, Ito M, Hartshorne DJ: **Interaction of the ribosomal protein, L5, with protein phosphatase type 1.** *J Biol Chem* 1995, **270**:19786-19790
42. Egloff MP, Johnson DF, Moorhead G, Cohen PT, Cohen P, Barford D: **Structural basis for the recognition of regulatory subunits by the catalytic subunit of protein phosphatase 1.** *EMBO J* 1997, **16**:1876-1887
43. Wu X, Tatchell K: **Mutations in yeast protein phosphatase type 1 that affect targeting subunit binding.** *Biochemistry* 2001, **40**:7410-7420
44. McRobert L, McConkey GA: **RNA interference (RNAi) inhibits growth of *Plasmodium falciparum*.** *Mol Biochem Parasitol* 2002, **119**:273-278
45. Wellems TE, Su XZ, Ferdig M, Fidock DA: **Genome projects, genetic analysis, and the changing landscape of malaria research.** *Curr Opin Microbiol* 1999, **2**:415-419
46. Reynolds MG, Oh J, Roos DS: ***In vitro* generation of novel pyrimethamine resistance mutations in the *Toxoplasma gondii* dihydrofolate reductase.** *Antimicrob Agents Chemother* 2001, **45**:1271-1277
47. Baca AM, Hol WG: **Overcoming codon bias: a method for high-level over-expression of *Plasmodium* and other AT-rich parasite genes in *Escherichia coli*.** *Int J Parasitol* 2000, **30**:113-118
48. Barik S, Taylor RE, Chakrabarti D: **Identification, cloning, and mutational analysis of the casein kinase 1 cDNA of the malaria parasite, *Plasmodium falciparum*. Stage-specific expression of the gene.** *J Biol Chem* 1997, **272**:26132-26138
49. Bracchi-Ricard V, Barik S, DelVecchio C, Doerig C, Chakrabarti R, Chakrabarti D: **PfPK6, a novel cyclin-dependent kinase/mitogen-activated protein kinase-related protein kinase from *Plasmodium falciparum*.** *Biochem J* 2000, **347**:255-263
50. Barnes WM: **PCR amplification of up to 35-kb DNA with high fidelity and high yield from lambda bacteriophage templates.** *Proc Natl Acad Sci USA* 1994, **91**:2216-2220
51. Barik S: **Site-directed mutagenesis by PCR: substitution, insertion, deletion, and gene fusion.** *Methods in Neurosciences* 1995, **26**:309-323
52. Barik S: **Expression and biochemical properties of a protein serine/threonine phosphatase encoded by bacteriophage lambda.** *Proc Natl Acad Sci USA* 1993, **90**:10633-10637
53. Ganguly S, Singh M: **Purification and characterization of a protein phosphatase from winged bean.** *Phytochemistry* 1999, **52**:239-246
54. Lambros C, Vanderberg JP: **Synchronization of *Plasmodium falciparum* erythrocytic stages in culture.** *J Parasitol* 1979, **65**:418-420

TAB 8

Nucleic Acids Research, 2002, Vol. 30, No. 8 1757–1766

Positional effects of short interfering RNAs targeting the human coagulation trigger Tissue Factor

Torgeir Holen, Mohammed Amarzguioui, Merete T. Wiiger, Eshrat Babaie and Hans Prydz*

The Biotechnology Centre of Oslo, University of Oslo, Gaustadalleen 21, N-0349 Oslo, Norway

Received January 2, 2002; Revised and Accepted February 22, 2002

ABSTRACT

Chemically synthesised 21–23 bp double-stranded short interfering RNAs (siRNA) can induce sequence-specific post-transcriptional gene silencing, in a process termed RNA interference (RNAi). In the present study, several siRNAs synthesised against different sites on the same target mRNA (human Tissue Factor) demonstrated striking differences in silencing efficiency. Only a few of the siRNAs resulted in a significant reduction in expression, suggesting that accessible siRNA target sites may be rare in some human mRNAs. Blocking of the 3′-OH with FITC did not reduce the effect on target mRNA. Mutations in the siRNAs relative to target mRNA sequence gradually reduced, but did not abolish mRNA depletion. Inactive siRNAs competed reversibly with active siRNAs in a sequence-independent manner. Several lines of evidence suggest the existence of a near equilibrium kinetic balance between mRNA production and siRNA-mediated mRNA depletion. The silencing effect was transient, with the level of mRNA recovering fully within 4–5 days, suggesting absence of a propagative system for RNAi in humans. Finally, we observed 3′ mRNA cleavage fragments resulting from the action of the most effective siRNAs. The depletion rate-dependent appearance of these fragments argues for the existence of a two-step mRNA degradation mechanism.

INTRODUCTION

Studies on silencing of transgenes in plants and RNA antisense mechanisms in *Caenorhabditis elegans* have recently led to a general opportunity for suppression of gene expression by double-stranded RNA (dsRNA) through a process termed RNA interference (RNAi) (1,2). In *C.elegans* and *Drosophila*, dsRNA has already become an established tool for functional genomics (3–7) and dsRNA has been used for genomic screens of whole chromosomes in *C.elegans* (8–10). Genetic screens in different species, along with sequence similarity studies and biochemical evidence, have partly elucidated the RNAi mechanism. The dsRNA is processed to 21–25 nt short interfering RNA (siRNA) with 2 nt 3′-overhangs by the RNase III-like protein Dicer in the initiating step of RNAi (11). These cleavage products are subsequently utilised by the RNA-induced silencing complex (RISC) in the recognition and cleavage of the corresponding mRNA (12,13). In *Drosophila* embryo lysates one constituent of this complex is the PAZ/PIWI protein AGO-2 (14). Unwinding of the siRNAs to single-stranded RNA in the active RISC appears to be a prerequisite for cleavage (15) and suggests the participation of a helicase in the RNAi process. Recently, a RNA-dependent RNA polymerase (RdRP) activity has been proposed to be involved in production of secondary siRNAs in both *Drosophila* and *C.elegans* (16,17). The process involves extension of a mRNA-primed antisense strand from the primary siRNA and cleavage of the secondary dsRNA by Dicer. For extensive reviews of siRNAs and RNAi developments see Tuschl (18), Sharp (19), Zamore (20) and Nishikura (21).

In mammals, long dsRNAs result in non-specific suppression of gene expression at the translational level, mediated in part through activation of the protein kinase PKR (22). This problem was circumvented with the recent discovery that chemically synthesised siRNAs avoid this non-specific response (23). In two separate studies (23,24), siRNAs have been employed in human cells to target non-human transgene transcripts like GFP, EGFP, CAT, firefly luciferase and sea pansy (*Renilla*) luciferase. siRNA was also used against endogenous human proteins like lamin A/C, lamin B1, nuclear mitotic apparatus protein (NuMA) and vimentin (23). Interestingly, *Renilla* luciferase and vimentin protein were not efficiently targeted in some human cells. In a subsequent report (25), siRNA was used against a human homologue of the RNAi component Dicer to demonstrate its involvement in the maturation of let-7 stRNA, which belongs to a group of short RNAs involved in temporal control of expression through interference with translation (26,27). Very recently, siRNA was also used to knock down expression of HtrA2 (28). Concomitant abrogation of the apoptotic response to UV exposure demonstrated the potential of siRNA as a tool for functional genomics in human cells.

Careful review of the data implies that certain siRNA species have limited efficiency. Sites on mRNA targets are differentially accessible to ribozymes and oligodeoxynucleotides (29). We therefore wanted to test whether a position effect might be a significant factor for the observed siRNA limitations. siRNAs were designed to target a wide range of sites within the mRNA of human Tissue Factor (TF). TF is the most potent trigger of blood coagulation (30) and the demonstration of

*To whom correspondence should be addressed. Tel: +47 22 84 05 32; Fax: +47 22 84 05 01; Email: hans.prydz@biotek.uio.no

The authors wish it to be known that, in their opinion, the first two authors should be regarded as joint First Authors

specific depletion of TF expression by RNAi would be of importance. In this study we report a target position dependence of siRNA efficacy in human cells. In a time-consuming reaction, a 10-fold depletion of TF mRNA and 5–10-fold depletion of TF protein and procoagulant activity were achieved with the most effective siRNA species. The appearance of mRNA cleavage fragments suggests a two-step model for the siRNA-mediated cleavage and degradation process.

MATERIALS AND METHODS

siRNA preparation

Twenty-one nucleotide RNAs were chemically synthesised using phosphoramidites (Pharmacia and ABI). Deprotected and desilylated synthetic oligoribonucleotides were purified by reverse phase HPLC. Ribonucleotides were annealed at 10 μM in 500 μl of 10 mM Tris–HCl, pH 7.5, by boiling and gradual cooling in a water bath. Successful annealing was confirmed by non-denaturing polyacrylamide gel electrophoresis. siRNA species were designed targeting sites within human protein serine kinase H1 (PSKH1) (accession no. AJ272212) and human TF (accession no. M16553) mRNAs.

Cell culture

HeLa, Cos-1 and 293 cells were maintained in Dulbecco's minimal essential medium (DMEM) supplemented with 10% foetal calf serum (Gibco BRL). The human keratinocyte cell line HaCaT was cultured in serum-free keratinocyte medium (Gibco BRL) supplemented with 2.5 ng/ml epidermal growth factor and 25 μg/ml bovine pituitary extract. All cell lines were regularly passaged at sub-confluence and plated 1 or 2 days before transfection. Lipofectamine-mediated transient co-transfections were performed in triplicate in 12-well plates with 0.40 μg/ml plasmid (0.38 μg/ml reporter and 20 ng/ml control) and typically 30 nM siRNA (0.43 μg/ml) essentially as described (29). Luciferase acitivity levels were measured in 25 μl of cell lysate 24 h after transfection using the Dual Luciferase assay (Promega). Serial transfections were performed by transfecting initially with 100 nM siRNA, followed by transfection with reporter and internal control plasmids 24 h before harvest time points. For northern analyses and coagulation assays, HaCaT cells in 6-well plates were transfected with 100 nM siRNA in serum-free medium. For endogenous targets, Lipofectamine 2000™ was used for higher transfection efficiency. Poly(A) mRNA was isolated 24 h after transfection using Dynabeads oligo$(dT)_{25}$ (Dynal). Isolated mRNA was fractionated for 16–18 h on 1.3% agarose/formaldehyde (0.8 M) gels and blotted onto nylon membranes (MagnaCharge; Micron Separations Inc.). Membranes were hybridised with random primed TF (position 61–1217 in cDNA) and GAPDH (1.2 kb) cDNA probes in PerfectHyb hybridisation buffer (Sigma) as recommended by the manufacturer.

TF activity and antigen

For TF activity measurements HaCaT cell monolayers were washed three times with ice-cold barbital-buffered saline, pH 7.4 (BBS, 3 mM sodium barbital, 140 mM NaCl) and scraped into BBS. Immediately after harvesting and homogenisation the activity was measured in a one-stage clotting assay using normal citrated platelet-poor plasma mixed from two donors and 10 mM $CaCl_2$. The activity was related to a standard (31,32). One unit (U) of TF corresponds to 1.5 ng TF as determined in the TF ELISA (31,33). The activity was normalised to the protein content in the cell homogenates, as measured by the Bio-Rad Bradford or DC assays. TF antigen was quantified using the Imubind Tissue Factor ELISA kit (American Diagnostica, Greenwich, CT). The samples were left to thaw at 37°C and homogenised. An aliquot of each homogenate (100 μl) was diluted in phosphate-buffered saline containing 1% BSA and 0.1% Triton X-100. This sample was then added to the ELISA well and the procedure from the manufacturer followed. The antigen levels were normalised to the total protein content in the cell homogenates.

RESULTS

The efficiency of siRNAs is dependent on mRNA target position

We synthesised four siRNAs against each of two mRNAs of interest (Fig. 1A), human TF (30) and human PSKH1 (34), the sites chosen on each gene being the two most accessible (hTF372i, hTF478i, PSK314i and PSK546i) and the two least accessible (hTF167i, hTF562i, PSK566i and PSK739i) to ribozyme-mediated inhibition (29; M.Amarzguioui, T.Holen, E.Babaie and H.Prydz, unpublished data). The initial analysis of TF siRNA efficacy was performed in HeLa cells transiently co-transfected with siRNA (Fig. 1A) and a luciferase fusion construct, TF–LUC (Fig. 1B), using the Dual Luciferase system. The siRNAs had potent and specific inhibitory effects in the co-transfection assays. The best candidates, hTF167i and hTF372i, gave only 10–15% residual luciferase activity in HeLa cells (Fig. 1C). This level of inhibition is similar to results from previous studies using luciferase reporter plasmid systems (23,24). A possible positional effect was found, as hTF562i showed only an intermediate effect and hTF478i had very low activity. This pattern of activity was also found in Cos-1, 293 and HaCaT cells (Fig. 1C), with siRNAs from different synthetic batches and at various transfection concentrations. The siRNAs caused the same degree of inhibition over a concentration range of 1–100 nM in the co-transfection assay (see below).

To further investigate the positional effect, we synthesised several series of siRNAs against new target sites. Of the siRNAs against TF in this second series, the siRNA targeting the translation initiation site (hTF77i) and the 3′-end of the coding region (hTF929i) were both essentially inactive (Fig. 1C). Of the two others, targeting heavily base paired regions as predicted by MFold (35,36), one (hTF256i) demonstrated intermediate activity while the other (hTF459i) had low activity. Again, siRNAs targeting different positions on mRNA thus differed in activity.

We decided to explore the accessibility of the region surrounding the target site of our best siRNA, hTF167i, at a higher resolution. A third series of siRNAs (hTF158i, hTF161i, hTF164i, hTF170i, hTF173i and hTF176i) was synthesised, targeting sites shifted at both sides of hTF167 in increments of 3 nt. Each of these shared 18 of 21 nt with its neighbours (Fig. 2A). Surprisingly enough, we found that despite the minimal sequence and position differences between these siRNAs, they displayed a wide range of activities (Fig. 2B).

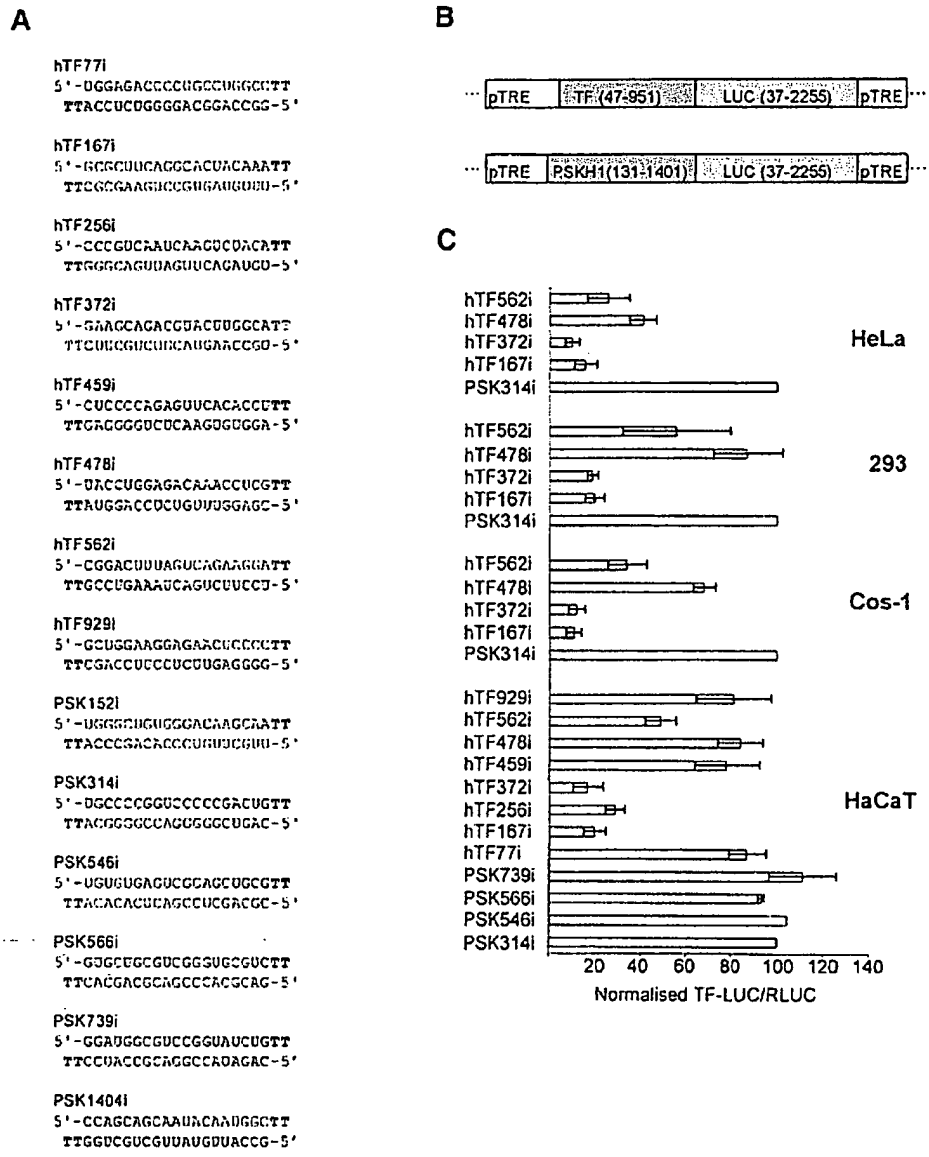

Figure 1. siRNAs, reporter constructs and RNA interference in transgene expression. (**A**) The sense (top) and antisense (bottom) strands of siRNA species, each targeting a site within mRNA for human TF (accession no. M16553) or human protein serine kinase H1 (PSKH1) (accession no. AJ272212), are shown. siRNAs were synthesised with 2 nt deoxythymidine 3′-overhangs and were numbered according to the position of the first nucleotide of the sense strand (numbering as in the GenBank entries). (**B**) Luciferase reporter constructs. The coding regions of PSKH1 and TF were cloned in-frame with the firefly luciferase (LUC) gene, into the cloning vector pTRE (accession no. U89931), producing the fusion constructs PSKH1–LUC (accession no. AF416988) and TF–LUC (accession no. AF416989). Numbering of the fusion constructs refers to that of the respective GenBank entries for PSKH1 and TF and to the pGL3-Enhancer plasmid (Promega) for LUC. TF–LUC was generated from PSKH1–LUC by PCR. The plasmid pcDNA3-Rluc (accession no. AF416990), encoding *Renilla* luciferase (RLUC), was used as an internal control (not shown). All plasmids were sequenced enough to confirm correct cloning. (**C**) RNA interference by siRNAs in reporter gene co-transfection assays. Cells were co-transfected with siRNA (30 nM) and a mixture of reporter (TF–LUC) and internal control (RLUC) plasmids. Ratios of LUC to RLUC expression were normalised to levels in cells transfected with a representative irrelevant siRNA, PSK314i.

There was a gradual change away from the full activity of hTF167i that was more pronounced for the upstream siRNAs. The two siRNAs hTF158i and hTF161i were shifted only 9 and 6 nt away from hTF167i, respectively, yet their activity was severely diminished. These results suggested that a local protein factor(s) on the mRNA caused the positional effect. However, we cannot exclude that other factors, such as sequence-dependent mRNA product release or differential efficiency of 5′ siRNA phosphorylation (15), may influence the efficacy of the siRNAs.

siRNAs cause position-dependent depletion of endogenous mRNA

Although fast and convenient, the co-transfection assay involves the use of forced expression of reporter genes, which causes difficulties of interpretation. A more direct approach is

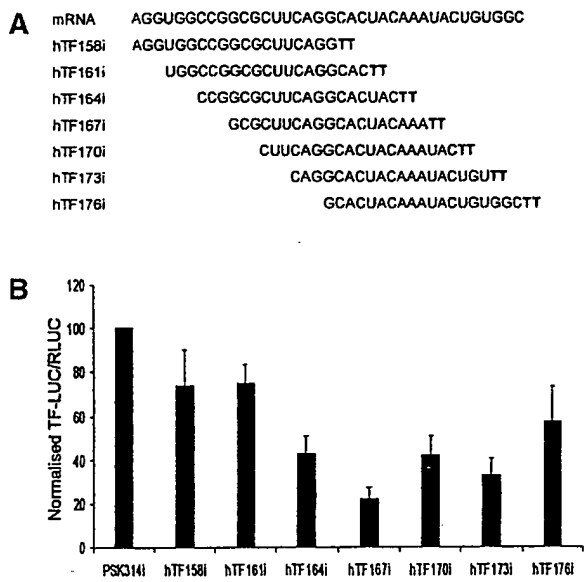

Figure 2. Investigation of siRNA position dependence at codon level resolution. (A) Sequences (sense strand only) of the new series of siRNAs, targeting sites surrounding hTF167. Deoxynucleotide overhangs are indicated in bold. The siRNAs were shifted in increments of 3 nt to either side of hTF167i. (B) Efficacy of the siRNAs in standard co-transfection assays in HaCaT cells. Different synthetic batches of the hTF167i siRNA showed similar efficacy. Results are averages of at least three independent experiments, each in triplicate.

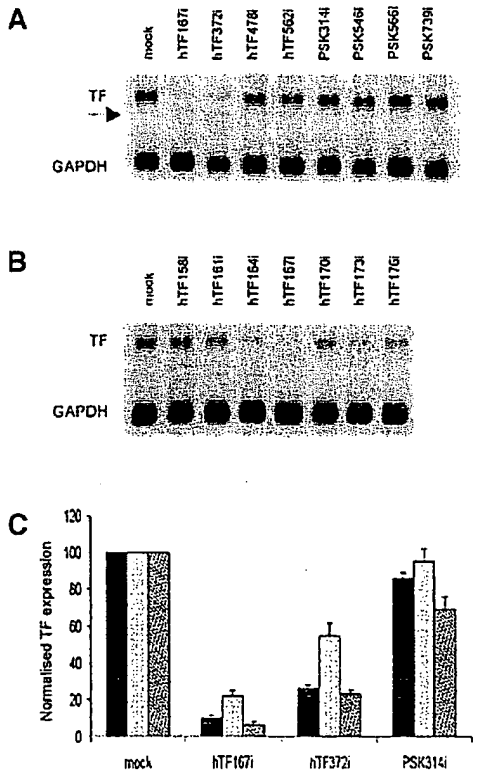

Figure 3. siRNA-mediated reduction in endogenous TF expression. (A and B) Northern analysis of TF mRNA after transfection of HaCaT cells with siRNA (100 nM). GAPDH was used as a control. The arrow indicates cleavage fragments resulting from siRNA action. (C) Effect of siRNAs on steady-state mRNA levels (filled bars), procoagulant activity (dotted bars) and TF protein (antigen) expression (hatched bars). For measurement of procoagulant activity and antigen, cells were harvested 48 h after siRNA transfection to accommodate the 7–8 h half-life of TF protein (31). Data are from a representative experiment in triplicate.

to measure the effect of transfected siRNA on expression of endogenous TF mRNA, which is expressed constitutively in the human keratinocyte cell line HaCaT. The two best TF siRNAs in the co-transfection assay, hTF167i and hTF372i, demonstrated strong activity. Normalised TF mRNA expression was reduced to 10 ± 1.2 and $26 \pm 2.6\%$, respectively (Fig. 3A). Experimental reproducibility was generally higher for the northern analysis than for the co-transfection assay. The third best siRNA in co-transfection assays, hTF256i, also resulted in significant depletion of TF mRNA levels (57% residual expression; data not shown). The remaining TF siRNAs of the first two series (hTF77i, hTF459i, hTF478i, hTF562i and hTF929i), along with the control PSKH1 siRNAs, did not show any significant activity as measured by northern assay (Fig. 3A).

Interestingly, cleavage products, whose sizes were consistent with primary cleavage at the target sequences, were clearly visible below the depleted main band, though *in vitro* cleavage assays of mRNA based on RNA interference have so far not succeeded in mammalian systems (37). Our observations provide convincing evidence that siRNAs deplete the steady-state mRNA level by cleaving the mRNA. The demonstration of a cleavage product has another interesting implication. Uncapped mRNA should be quickly degraded (38,39) following cleavage and similar cleavage fragments have to our knowledge not been reported with ribozymes, DNA enzymes or RNase H-competent antisense oligos. The fact that we can observe the cleavage product implies stabilisation of a mRNA intermediate following cleavage. We defer further discussion of this matter to a later section.

There was a good, but not perfect, correlation between siRNA efficacy in the two assays. siRNAs with only intermediate activity in co-transfection assays were unable to deplete endogenous mRNA levels. Differences in activity between active siRNAs on the endogenous target were more pronounced than on transgene expression, although the activity rank order was generally conserved between the two assay systems. This observation was found to also be true for the series of siRNAs close to hTF167i. The previously demonstrated sharp boundary between active and inactive siRNAs was seen on endogenous TF mRNA (Fig. 3B), only more pronounced. For the series hTF158i–hTF167i activity increased from no mRNA depletion to 90% depletion over an interval of only 9 nt. Thus, the positional effect is demonstrated using two different versions of the same mRNA, with the results on the endogenous TF mRNA being clearer.

The TF cDNA shows an abrupt change in GC content in the region 152–198, falling from 84 to 15% for a 19 bp window. Further analysis of results from other siRNAs and their target sequences showed a slight bias of doubtful biological significance towards a correlation of higher activity and lower GC content (23,25,28; data not shown). A total of six PSKH1 siRNAs from two synthesis series had moderate to no activity

in co-transfection assays and limited effects in northern assays (data not shown). As the expression levels of PSKH1–LUC and endogenous PSKH1 mRNA regularly appeared to be lower than the corresponding hTF mRNAs (data not shown), an overabundance of target mRNA in this case was not a likely explanation for the lower silencing efficiency. We have, however, observed a correlation between the expression level and degree of silencing of the TF–LUC reporter gene. Retransfection of siRNA-transfected cells (3 days after initial transfection) with increasing amounts of the reporter gene plasmid resulted in reduced silencing with higher plasmid concentrations (data not shown). The generally lower activity of the PSKH1 siRNAs is consistent with the previously mentioned GC content bias, as the PSKH1 mRNA has a very high overall GC content (60%). No relationship between MFold-predicted mRNA structures and the potency of the siRNA was found, as siRNAs targeting sites of similar predicted secondary structures (hTF167i versus hTF478i, hTF383i versus hTF562i and hTF256i versus hTF459i) demonstrated very different activities. There was also no correlation with previous results obtained with ribozymes (29; M.Amarzguioui, T.Holen, E.Babaie and H.Prydz, unpublished data).

Inhibition of TF function by siRNAs

The effect of the siRNAs on TF protein levels and activity was assessed. Clotting, triggered by TF, was measured 48 h after transfection of HaCaT cells with selected siRNAs. The two best siRNAs, hTF167i and hTF372i, reduced the procoagulant activity of cell extracts 5- and 2-fold relative to mock-transfected cells, while the irrelevant control siRNA PSK314i had no effect on procoagulant activity (Fig. 3C). A TF-specific siRNA that was inactive in other assays (hTF478i) likewise had no effect on procoagulant activity (data not shown). Thus, a positional dependence of siRNA activity was also demonstrated in this assay. The difference in activity of the two best siRNAs also correlated well with their demonstrated efficacy in depleting mRNA. When TF antigen was measured in an ELISA assay, the reduction in antigen was essentially proportional to the reduction in mRNA (Fig. 3C) for both hTF167i and hTF372i.

We have demonstrated siRNA positional dependence in four different TF mRNA-dependent test systems. The low activity of the majority of the siRNAs may be due to non-accessibility of mRNA for cleavage, caused by higher order RNA structures or protein coverage, as suggested in a previous report (23). Prediction of secondary structures of mRNA by MFold did not provide an explanation for the position dependence (data not shown). The GC content of a region might affect its general accessibility to siRNAs indirectly through the effect on protein coverage or mRNA unwinding. It might be significant that our three best siRNAs all lie within one region of generally low GC content, with the best (hTF167i) at the edge of a deep valley of low GC content. At present, however, the factors determining the differences in siRNA efficiency remain unclear.

Competitive effects of siRNAs

The use of a single species of siRNA to target a mRNA is not a biologically relevant situation, as cells would normally encounter multiple siRNAs produced from long dsRNAs by the RNase III-like Dicer (11–14). We asked whether the complexes involved in cleaving the mRNA might have evolved to utilise multiple siRNA species, for instance through a mechanism of allosteric stimulation of RISC, and thus not work as efficiently with single siRNAs. Specifically, we wanted to know whether combinations of siRNAs would result in increased activity through synergism or addition. Testing this concept by co-transfecting various combinations of two or three siRNAs, no addition or synergism could be discerned. On the contrary, co-transfecting with an active and inactive siRNA revealed a sequence-independent competitive effect, reducing the activity of the most effective siRNA. When mixing saturating concentrations of active siRNA (hTF167i) with inactive control siRNA (PSK314i) at different ratios, a shifted dose-dependence curve was obtained (Fig. 4A). In the absence of competitor, the siRNA effect of 10 nM hTF167i was the same as that of 30 nM, yet when combining 10 nM hTF167i with 20 nM PSK314i the activity was significantly diminished. At lower ratios of active to competitor siRNA the competitive effect was progressively stronger. Investigating the generality of this competition effect beyond this siRNA pair (hTF167i versus PSK314i), we demonstrated the ability of PSK314i to interfere with the function of hTF256i and hTF372i (Fig. 4B) and that other irrelevant siRNAs (PSK546i and PSK739i) competed equally well (Fig. 4C). Furthermore, the competitive effect was also demonstrated on endogenous TF mRNA, antigen and procoagulant activity (Fig. 4D). The order of siRNA transfection did not affect hTF167i activity in competition experiments, suggesting that the initial binding of siRNAs is reversible (data not shown).

The time course of siRNA silencing

Northern analysis of cells harvested 4, 8, 24 and 48 h after the start of transfection showed maximum siRNA silencing after 24 h (Fig. 5A). There seemed to be a difference in the apparent depletion rate, as hTF167i reduced the mRNA level more than hTF173i at each time point. Similar observations were made for modified versions of hTF167i with attenuated final mRNA depletion (see below). We noted that siRNA-induced target degradation was incomplete, as a level of ~10% of the target mRNA remained even with the most effective siRNAs. This may be due to the presence of a fraction of mRNA in a protected compartment, e.g. in spliceosomes, in other nuclear locations or in non-transfected/unsilenced cells. In view of the above data and data from competition experiments, however, part of the non-degraded fraction may be explained by a kinetically determined balance between transcription and degradation, the latter being a time-consuming process (Fig. 5A).

Uptake of siRNA

To investigate the uptake of siRNAs following transfection, a FITC-tagged version of the most effective siRNA, hTF167i–FITC, was synthesised. After uptake of hTF167i–FITC by HaCaT cells, a characteristic spotty distribution was seen (Fig. 5B), as in earlier transfection experiments with FITC-tagged oligos and ribozymes. The spots are assumed to be cationic lipid micelles (containing hTF167i–FITC) that have fused with the cells. We were unable to find cells that did not display such spots and thus assume that siRNA transfection of cells is close to 100%. siRNA uptake reached its maximum and levelled off after transfection for 2–4 h. There was no evidence for uptake of siRNA in the absence of transfection agent. Cells incubated in the

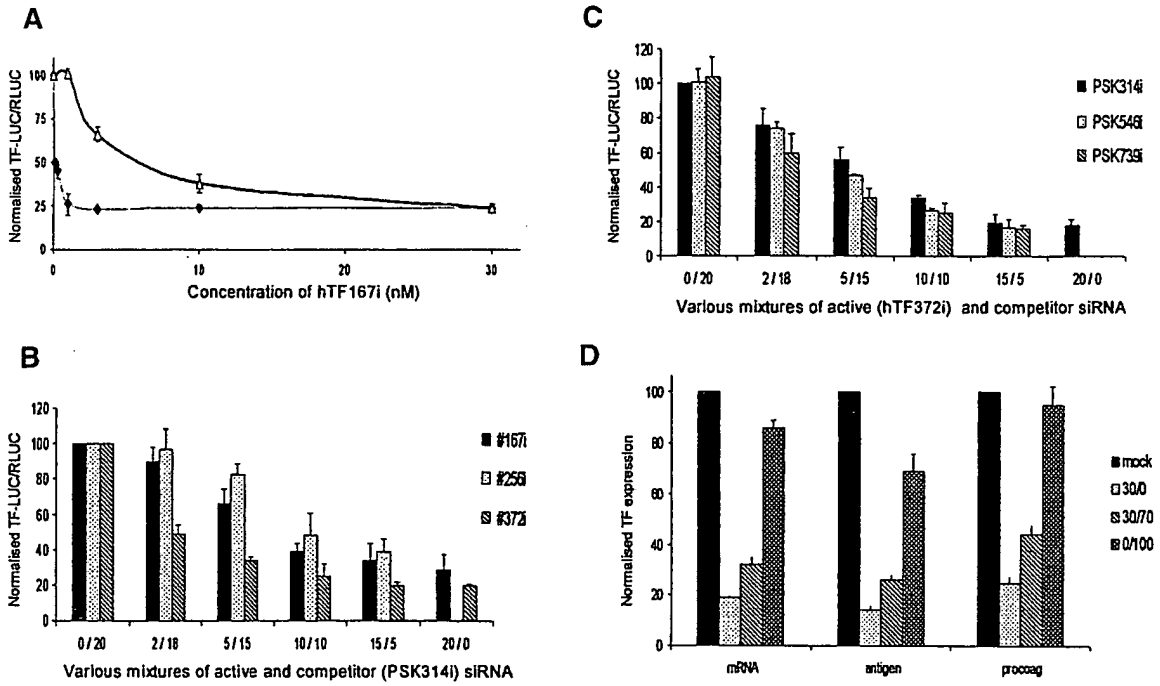

Figure 4. RNA interference by active siRNA is inhibited by the presence of inactive siRNAs. Ordinates show normalised reporter gene activity as a percent of control. (A) Dose dependence of active siRNA (hTF167i) in the absence (closed diamonds) and presence (open triangles) of irrelevant siRNA (PSK314i). At each concentration of hTF167i, normalised LUC/RLUC was standardised to levels in cells co-transfected with PSK314i to rule out the possibility of non-specific dose-dependent effects of siRNAs. In samples with mixtures of hTF167i and PSK314i, the total concentration of siRNA was kept constant at 30 nM by adding PSK314i to the indicated concentrations of hTF167i. (B) Competitive inhibition by PSK314i of various active siRNAs. (C) Competitive inhibition of hTF372i-mediated RNAi by different irrelevant siRNAs. Increasing concentrations of active siRNA (0, 2, 5, 10 and 20 nM) were mixed with competitor siRNA (20, 18, 15, 10 and 0 nM) to a final concentration of 20 nM. (D) Competitive inhibition of RNAi on endogenous TF expression by PSK314i. HaCaT cells were transfected with 30 nM hTF167i in the absence (30/0) or presence (30/70) of 70 nM PSK314i as competitor. Inactive siRNA at 100 nM (0/100) was included as a control. Complexations with Lipofectamine 2000™ were performed in parallel for northern (cells harvested after 24 h), procoagulant and antigen assays (cells harvested after 48 h). Activities and expression levels were standardised to mock-transfected cells.

presence of siRNA without liposomes did not exhibit any inhibition following transfection with reporter plasmid the next day (data not shown). Furthermore, when co-culturing siRNA-transfected cells with cells transfected with reporter plasmids, no transfer of siRNA silencing between cells was detected (data not shown), contrary to earlier reports of medium-mediated silencing in *Drosophila* S2 cells (40). We found no evidence of transfer of siRNA between cells or via the medium, thus the siRNAs seem to be taken up by cells exclusively via lipid micelles. The escape of siRNA from these lipid micelles might contribute to the slow action of siRNAs.

Persistence of siRNA silencing

Experiments in plants (41,42) and nematodes (1,43) have suggested the existence of a system whereby certain siRNA genes are involved in the heritability of RNAi-induced phenotypes. To investigate the existence of such propagators in mammalian cell lines we measured the persistence of siRNA silencing in HaCaT cells transfected at very low cell density to allow 5–10-fold cell culture expansion over a 5 day period. In an experiment based on serial transfection of reporter constructs (Fig. 5C), there was a gradual recovery of expression between 2 and 5 days post-transfection. The time-dependence of the siRNA effect on endogenous TF mRNA was similar (Fig. 5C). The level of TF mRNA in mock-transfected control cells declined gradually during this experiment, in what appeared to be cell expansion-dependent down-regulation of expression. Interestingly, the procoagulant activity showed little indication of recovering to control levels in transfected cells (Fig. 5C). Similar observations were made with hTF372i and with a combination of hTF167i, hTF372i and hTF562i (data not shown). The cause for this TF phenotype remains unknown.

Tolerance of RNAi for mismatches and modifications

The use of 2 nt deoxythymidine 3′-overhangs in these studies prompted the question of whether such overhangs might affect the efficiency of the siRNA. We synthesised a siRNA with deoxynucleotide overhangs able to base pair with the target mRNA (hTF167i-BO, Fig. 6A). Its activity was indistinguishable from that of the siRNA with non-base pairing overhangs (Fig. 6B and C). Another version of this siRNA with ribonucleotide base pairing overhangs had identical silencing activity on endogenous mRNA expression (data not shown). The same observation was made for siRNAs targeting the sites hTF173, hTF256, hTF372, hTF478 and hTF562 (data not shown). Although these modifications in the overhangs appeared to have no effect on initial silencing activity, they might affect the persistence of siRNA silencing through their differential ability to serve as templates for a putative

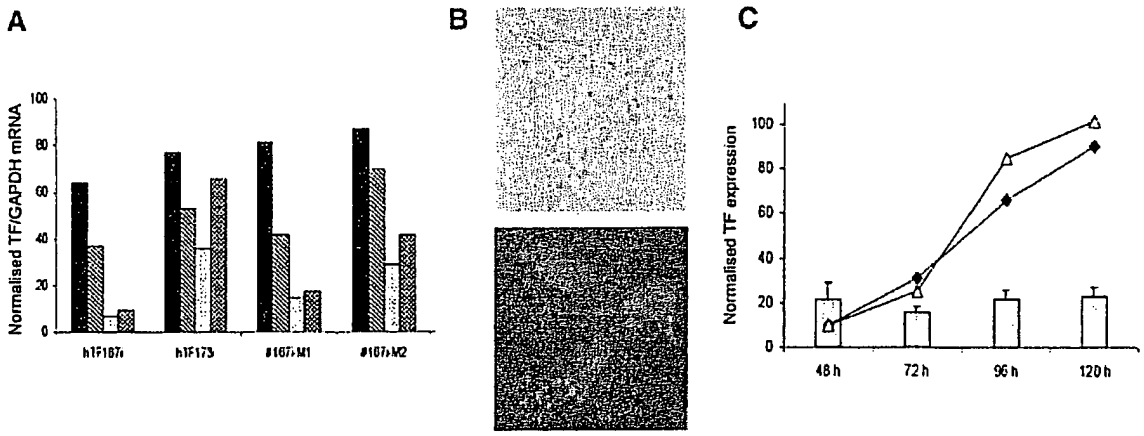

Figure 5. Time dependence of siRNA-mediated RNAi. (A) Time-course of mRNA silencing. Cells were transfected with 100 nM siRNA and harvested for mRNA isolation 4, 8, 24 and 48 h after initiation of transfection. Expression levels were normalised to GAPDH and standardised to mock-transfected cells at all time points. (B) Fluorescence and phase contrast microscopy of cells transfected with FITC-tagged hTF167i (hTF167i–FITC). (Lower) FITC signal (green) and Hoechst staining of nuclei (blue). HaCaT cells grown on coverslips were transfected for 4 h, incubated for a further 20 h, washed in PBS, fixed in methanol, mounted with DAKO mounting medium containing Hoechst reagent (2 μg/ml) and subjected to fluorescence microscopy (magnification ×40). (C) Persistence of siRNA silencing effect in HaCaT cells determined in a serial transfection experiment (open triangles) and by northern (closed diamonds) and procoagulant (bars) assays. In all experiments cells were harvested 48, 72, 96 and 120 h after initial transfection of 100 nM hTF167i. For the northern and procoagulation assays expression levels were standardised to mock-transfected cells as described. In the serial transfection assay cells were retransfected with the two reporter constructs 24, 48, 72 and 96 h after siRNA transfection and harvested 24 h later in each case. Normalised luciferase expression was standardised to levels in PSK314i-transfected cells.

siRNA-regenerating RdRP (16). Northern and serial transfection time-course experiments, however, revealed no significant differences in silencing between the three different versions of hTF167i, or the two versions of hTF372i, at any time up to at least 120 h (Fig. 6D and data not shown). We further tested the effect of blocking the 3′-OH position by a FITC group, thereby negating the possibility of primer extension of the siRNA antisense oligo by a putative RdRP. The activity of hTF167i–FITC was only marginally lower than the wild-type (Fig. 6B and C). The combined results indicate that some degree of modification can be introduced in the overhangs without compromising siRNA efficacy. Furthermore, the high level of activity of the 3′-OH blocked hTF167i–FITC demonstrates that initial mRNA depletion does not occur through the recently reported RdRP-dependent degradative PCR mechanism (16) in human cells. Any hypothetical human RdRP must have little effect on the persistence of siRNA-mediated silencing.

We next investigated the tolerance of the RNAi system for mismatches in the siRNA relative to the mRNA target. Low or no tolerance for mismatches would make siRNAs a valuable tool for allele-specific degradation of the aberrant mRNA in various dominant negative disorders resulting from single base pair mutations. We therefore made mutant siRNAs containing either one (hTF167i-M1) or two (hTF167i-M2) central mismatches relative to the target (Fig. 6A). The mismatches (G/G and GC/GC) were chosen to be maximally disruptive. The single mismatch reduced the effect of siRNA moderately in both co-transfection and northern assays. The double mutant, however, had almost no activity in the co-transfection assay, while still reducing mRNA levels to 30%. We interpret the gradual loss of activity in the mutants as further circumstantial evidence of a near equilibrium kinetic balance between mRNA synthesis/processing and mRNA degradation. A more direct test of the near equilibrium model was to compare the rate of mRNA depletion for 'mutated' and wild-type versions of hTF167i. A clear difference in depletion rate caused by active and mutant siRNAs was seen (Fig. 5A). As predicted by the model based on rates of decay and transcription, there was an apparent correlation between the rate and extent of depletion.

A similar mismatch tolerance was recently reported for siRNAs in *Drosophila* embryos (44). In another study, however, no tolerance for even a single central mutation was seen in a *Drosophila* embryo lysate assay (45). The *in vivo* system differs from the *in vitro* one in having continual mRNA production. Thus, if we assume a range of siRNA cleavage rates, all siRNAs that have so low cleavage activity that their contribution would be insignificant compared to the rate of mRNA turnover *in vivo* could possibly still significantly deplete mRNA *in vitro*. The siRNAs with high cleavage activity *in vivo* would, on the other hand, as we observed with hTF167i, lose their activity gradually when mutated.

In contrast to hTF167i-wt, hTF167i-M2 did not produce a detectable cleavage fragment. Furthermore, the appearance of a cleavage fragment with hTF167i-wt was dose dependent. It is present at saturating (30–100 nM) but not at sub-saturating (10 nM) concentrations (Fig. 6E). No cleavage fragment was seen with hTF173i, which shares 13 of 19 nt of its target sequence with hTF167i, but exhibits a reduced depletion rate compared to the latter (Fig. 5A). Combined, these observations suggest that the appearance of a cleavage product is dependent on a high enough rate of the initial cleavage step to saturate a secondary nuclease.

We annealed combinations of hTF167i wild-type and mismatched strands (Fig. 6A), producing imperfect siRNAs with 1 or 2 bp bulges. These bulges were found to have little effect on activity, with the important determinant for activity being the state of the antisense strand. Thus hTF167i-wt/M1 and hTF167i-wt/M2, containing a mutated antisense strand,

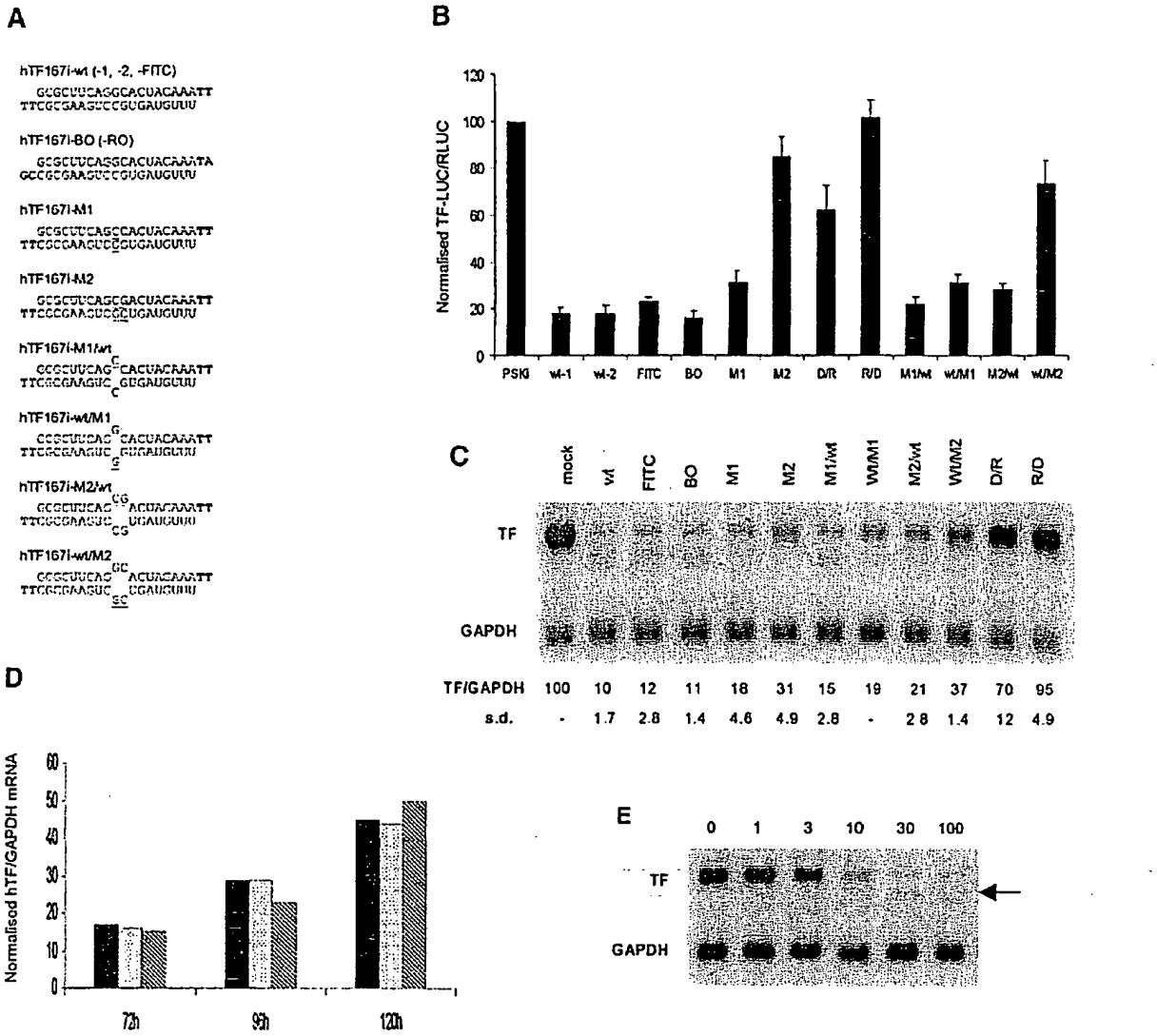

Figure 6. Tolerance of RNAi for modifications and mutations. (A) Sequence of modified and mutated siRNAs targeting hTF167. Two different batches of wild-type hTF167i (wt-1 and wt-2) were synthesised. Modified versions were prepared with a FITC tag on the 3′-OH of the 3′ nucleotide of the antisense strand (hTF167i–FITC) or with target mRNA base pairing overhangs consisting of either deoxyribonucleotides (hTF167i-BO) or ribonucleotides (hTF167i-RO). The siRNAs hTF167i-M1 and hTF167i-M2 have one (G→C) and two (GC→CG) central mismatches (underlined) relative to target mRNA, respectively. By combining sense and antisense strands of wild-type siRNA with partially complementary strands of the M1 and M2 mutants, imperfect siRNAs with 1 and 2 bp bulges were prepared in which the mutation relative to the wild-type siRNA was either in the sense (M1/wt and M2/wt) or antisense (wt/M1 and wt/M2) strand. (B) Standard co-transfections with modified/mutated siRNAs (30 nM). DNA(sense)/RNA(antisense) (D/R) and RNA/DNA (R/D) hybrid versions of hTF167i were included. (C) Northern analysis of RNAi by the hTF167i variants (100 nM). GAPDH-normalised expression ± SD is indicated. (D) Northern time-course experiment. Cells were transfected with 100 nM siRNA. Normalised mRNA levels are shown for hTF167i-wt (filled bars), hTF167i-BO (dotted bars) and hTF167i-RO (hatched bars). TF mRNA was normalised to GAPDH and standardised to levels in mock-transfected cells at each time point. (E) Concentration dependence (nM) of mRNA depletion by hTF167i-wt. Complexation with Lipofectamine™ was performed in one batch for all samples and complexes diluted in medium as appropriate immediately before addition to cells. The arrow indicates cleavage fragments.

behaved essentially as the non-bulged mutants and were less active than the corresponding hTF167i-M1/wt and hTF167i-M2/wt, with the modification in the sense strand (Fig. 6B and C). This strand bias has previously been seen with dsRNA in *C.elegans* (46) and emphasises that the principal role of the sense strand is to protect the antisense strand, as a single-stranded RNA of this size is degraded very rapidly *in vivo* (25). Another role has been uncovered recently whereby the identity of the sense strand is checked by gateway kinases before allowing incorporation into the RISC complex and subsequent unwinding of the siRNA (15). This is consistent with our results with DNA/RNA hybrids of hTF167i. These chimeras exhibited low or no activity in both assays (Fig. 6B and C), in agreement with recent observations in *Drosophila* (44). The strand bias was still apparent, however, with DNA being less detrimental to activity when

present in the sense (hTF167i-D/R) than in the antisense (hTF167i-R/D) strand. Finally, competition experiments demonstrated that mismatched and bulged siRNAs of low activity could compete with hTF167i as well as inactive siRNAs and competition by DNA-containing double-stranded oligos was only slightly impaired (data not shown). The process which this sequence-independent competition inhibits is not presently known.

DISCUSSION

The biological functions of RNAi seem to be control of viruses and transposons (47–50). In a study of certain aspects of the RNAi mechanism we have revealed some current limitations to the use of siRNAs as tools in functional genomics and lead compounds in drug development. We find that siRNA efficacy is highly dependent on target position. Despite this limitation, we identified one siRNA that specifically and efficiently inhibited expression of the target gene at the levels of mRNA, protein and function. The levels of TF mRNA and protein were reduced 10-fold, while TF-dependent procoagulant activity was depleted 5-fold. The effect was transient, as the mRNA levels as well as transgene expression fully recovered after 4–5 days. Our results suggest that susceptible siRNA target sites in some human genes may be rare.

We have demonstrated that inactive siRNAs compete with active siRNAs in a reversible and sequence-independent manner (Fig. 4). Mutants and other non-standard siRNAs were also able to compete. Taken together, these observations indicate lack of discrimination at one or more initial steps in the degradative process.

Even the most effective siRNAs acted relatively slowly in mRNA depletion following transfection, with the optimum effect observed after 24 h, and in no case was there total depletion of TF mRNA. Several lines of evidence suggest that this is caused by the existence of a near equilibrium kinetic balance between siRNA-mediated cleavage of mRNA and mRNA transcription and processing. These include the concentration dependence of siRNA efficacy (i.e. the increased residual mRNA or reporter gene level) in the presence of a competitor (Fig. 4), the difference in depletion rate among active siRNAs targeting different sites (Fig. 5A) and the gradual reduction in depletion rate for mutated siRNAs (Fig. 5A). We further demonstrate that RNAi to a certain degree tolerates siRNA:mRNA mismatches, with 1 and 2 bp mismatches only partially reducing the rate and extent of depletion.

The gradual recovery of gene expression within 4–5 days of transfection (Fig. 5C) constitutes evidence against the presence of a propagative system in humans maintaining the siRNA-based silencing over time. A recent report of RNAi in *C.elegans* demonstrates the need for continual siRNA production by RdRP homologues (17). Two of these RdRPs (rrf-1 and rrf-3) are intimately involved in synthetic siRNA-mediated silencing, as this pathway is abolished in a rrf-1 negative strain, while the rrf-3 negative strain actually seemed to enhance synthetic siRNA silencing. This propagative system was also proposed to operate in *Drosophila* (16), where, as in humans, RdRP homologues have not yet been identified. In both cases the mechanism seems to be production of dsRNA from mRNA by siRNA priming, with secondary siRNAs being produced by Dicer. This degradative PCR-like system was recently nominated as the mRNA degrading complex itself (16). Results from a third report (15), however, show that Dicer is ATP dependent while RISC is not. Our data with a 3′-OH blocked siRNA, which cannot be utilised as a primer by a putative RdRP, constitutes direct evidence that the proposed degradative PCR mechanism is not essential for initial mRNA depletion *in vivo* in human cells.

Finally, we observed cleavage fragments resulting from siRNA action. These cleavage fragments appeared only in the presence of a high rate of mRNA depletion. Thus, we see a cleavage fragment with wild-type hTF167i, but not with the slower hTF173i (Figs 3A and B and 5A). A double mutant of hTF167i, which results in a 3-fold increase in residual mRNA levels (Fig. 6C) and has a lower depletion rate than the wild-type (Fig. 5A), also does not produce a cleavage fragment. Even with wild-type hTF167i, the cleavage fragment disappears when the concentration of the siRNA is reduced to sub-saturating levels, resulting in less extensive cleavage of mRNA (Fig. 6E). These observations suggest that degradation is performed in at least two separate steps. We hypothesise that mRNA is cleaved in the first step by RISC. The cleaved mRNA is subsequently degraded by an exonuclease similar to that implicated in RNAi by genetic evidence in *C.elegans* (47). The accumulation of a cleavage product as seen in our northern gels would require the second step to be rate determining when RISC operates at full speed.

ACKNOWLEDGEMENTS

The authors wish to express their gratitude to Gaute Brede for valuable suggestions. This work was supported by grants from the Norwegian Cancer Society, Health and Rehabilitation and the Research Council of Norway (RCN) to H.P. T.H. is a fellow of the RCN.

REFERENCES

1. Fire,A., Xu,S., Montgomery,M.K., Kostas,S.A., Driver,S.E. and Mello,C.C. (1998) Potent and specific genetic interference by double-stranded RNA in *Caenorhabditis elegans*. *Nature*, **391**, 806–811.
2. Hamilton,A.J. and Baulcombe,D.C. (1999) A species of small antisense RNA in posttranscriptional gene silencing in plants. *Science*, **286**, 950–952.
3. Parrish,J., Li,L., Klotz,K., Ledwich,D., Wang,X. and Xue,D. (2001) Mitochondrial endonuclease G is important for apoptosis in *C. elegans*. *Nature*, **412**, 90–94.
4. Clemens,J.C., Worby,C.A., Simoson-Leff,N., Muda,M., Maehama,T., Hemmings,B.A. and Dixon,J.E. (2000) Use of double-stranded RNA interference in *Drosophila* cell lines to dissect signal transduction pathways. *Proc. Natl Acad. Sci. USA*, **97**, 6499–6503.
5. Kennerdell,J.R. and Carthew,R.W. (1998) Use of dsRNA-mediated genetic interference to demonstrate that frizzled and frizzled 2 act in the wingless pathway. *Cell*, **95**, 1017–1026.
6. Karabinos,A., Schmidt,H., Harborth,J., Schnabel,R. and Weber,K. (2001) Essential roles for four cytoplasmic intermediate filament proteins in *Caenorhabditis elegans* development. *Proc. Natl Acad. Sci. USA*, **89**, 7863–7868.
7. Longman,D., Johnstone,I.L. and Cáceres,J.F. (2000) Functional characterization of SR and SR-related genes in *Caenorhabditis elegans*. *EMBO J.*, **19**, 1625–1637.
8. Fraser,A.G., Kamath,R.S., Zipperlen,P., Martinez-Campos,M., Sohrmann,M. and Ahringer,J. (2000) Functional genomic analysis of *C. elegans* chromosome I by systematic RNA interference. *Nature*, **408**, 325–330.
9. Gonczy,P., Echeverri,G., Oegema,K., Coulson,A., Jones,S.J., Copley,R.R., Duperon,J., Oegema,J., Brehm,M , Cassin,E. *et al.* (2000)

Functional genomic analysis of cell division in *C. elegans* using RNAi of genes on chromosome III. *Nature*, **408**, 331–336.
10. Hanazawa,M., Mochii,M., Ueno,N., Kohara,Y. and Iino,Y. (2001) Use of cDNA subtraction and RNA interference screens in combinations reveals genes required for germ-line development in *Caenorhabditis elegans*. *Proc. Natl Acad. Sci. USA*, **98**, 8686–8691.
11. Bernstein,E., Caudy,A.A., Hammond,S.M. and Hannon,G.J. (2001) Role for a bidentate ribonuclease in the initiation step of RNA interference. *Nature*, **409**, 363–366.
12. Hammond,S.M., Bernstein,E., Beach,D. and Hannon,G.J. (2000) An RNA-directed nuclease mediates post-transcriptional gene silencing in *Drosophila* cells. *Nature*, **404**, 293–296.
13. Elbashir,S.M., Lendeckel,W. and Tuschl,T. (2001) RNA interference is mediated by 21 and 22 nt RNAs. *Genes Dev.*, **15**, 188–200.
14. Hammond,S.M., Boettcher,S., Caudy,A.A., Kobayashi,R. and Hannon,G.J. (2001) Argonaute2, a link between genetic and biochemical analyses of RNAi. *Science*, **293**, 1146–1150.
15. Nykänen,A., Haley,B. and Zamore,P.D. (2001) ATP requirements and small interfering RNA structure in the RNA interference pathway. *Cell*, **107**, 309–321.
16. Lipardi,C., Wei,Q. and Paterson,B.M. (2001) RNAi as random degradative PCR: siRNA primers convert mRNA into dsRNAs that are degraded to generate new siRNAs. *Cell*, **107**, 297–307.
17. Sijen,T., Fleenor,J., Simmer,F., Thijssen,K.L., Parrish,S., Timmons,L., Plasterk,R.H. and Fire,A. (2001) On the role of RNA amplification in dsRNA-triggered gene silencing. *Cell*, **107**, 465–476.
18. Tuschl,T. (2001) RNA interference and small interfering RNAs. *Chembiochem*, **2**, 239–245.
19. Sharp,P.A. (2001) RNA interference—2001. *Genes Dev.*, **15**, 485–490.
20. Zamore,P.D. (2001) RNA interference: listening to the sound of silence. *Nature Struct. Biol.*, **8**, 746–750.
21. Nishikura,K. (2001) A short primer on RNAi: RNA-directed RNA polymerase acts as a key catalyst. *Cell*, **107**, 415–418.
22. Stark,G.R., Kerr,I.M., Williams,B.R., Silverman,R.H. and Schreiber,R.D. (1998) How cells respond to interferons. *Annu. Rev. Biochem.*, **67**, 227–264.
23. Elbashir,S.M., Harborth,J., Lendeckel,W., Yalcin,A., Weber,K. and Tuschl,T. (2001) Duplexes of 21-nucleotide RNAs mediate RNA interference in cultured mammalian cells. *Nature*, **411**, 494–498.
24. Caplen,N.J., Parrish,S., Imani,F., Fire,A. and Morgan,R.A. (2001) Specific inhibition of gene expression by small double-stranded RNAs in invertebrate and vertebrate systems. *Proc. Natl Acad. Sci. USA*, **98**, 9742–9747.
25. Hutvagner,G., McLachlan,J., Pasquinelli,A.E., Bálint,É., Tuschl,T. and Zamore,P.D. (2001) A cellular function for the RNA-interference enzyme Dicer in the maturation of the let-7 small temporal RNA. *Science*, **293**, 834–838.
26. Lee,R.C., Feinbaum,R.L. and Ambros,V. (1993) The *C. elegans* heterochronic gene lin-4 encodes small RNAs with antisense complementarity to lin-14. *Cell*, **75**, 843–854.
27. Reinhart,B.J., Slack,F.J., Basson,M., Pasquinelli,A.E., Bettinger,J.C., Rougvie,A.E., Horvitz,H.R. and Ruvkun,G. (2000) The 21-nucleotide let-7 RNA regulates developmental timing in *Caenorhabditis elegans*. *Nature*, **403**, 901–906.
28. Martins,L.M., Iaccarino,I., Tenev,T., Gschmeissner,S., Totty,N.F., Lemoine,N.R., Savopoulos,J., Gray,C.W., Creasy,C.L., Dingwall,C. *et al.* (2002) The serine protease Omi/HtrA2 regulates apoptosis by binding through a reaper-like motif. *J. Biol. Chem.*, **277**, 439–444.
29. Amarzguioui,M., Brede,G., Babaie,E., Grotli,M., Sproat,B. and Prydz,H. (2000) Secondary structure prediction and *in vitro* accessibility of mRNA as tools in the selection of target sites for ribozymes. *Nucleic Acids Res.*, **28**, 4113–4124.
30. Camerer,E., Kolsto,A.B. and Prydz,H. (1996) Cell biology of tissue factor, the principal initiator of blood coagulation. *Thromb. Res.*, **81**, 1–41.
31. Wiiger,M.T., Pringle,S., Pettersen,K.S., Narahara,N. and Prydz,H. (2000) Effects of binding of ligand (FVIIa) to induced tissue factor in human endothelial cells. *Thromb. Res.*, **98**, 311–321.
32. Hvatum,M. and Prydz,H. (1966) Studies on tissue thromboplastin. *Biochim. Biophys. Acta*, **130**, 92–101.
33. Camerer,E., Pringle,S., Skartlien,A.H., Wiiger,M., Prydz,K., Kolsto,A.B. and Prydz,H. (1996) Opposite sorting of tissue factor in human umbilical vein endothelial cells and Madin-Darby canine kidney epithelial cells. *Blood*, **88**, 1339–1349.
34. Brede,G., Solheim,J., Troen,G. and Prydz,H. (2000) Characterization of PSKH1, a novel human protein serine kinase with centrosomal, Golgi and nuclear localization. *Genomics*, **70**, 82–92.
35. Zuker,M., Mathews,D.H. and Turner,D.H. (1999) Algorithms and thermodynamics for RNA secondary structure prediction: a practical guide. In Barciszewski,J. and Clark,B.F.C (eds), *RNA Biochemistry and Biotechnology*. Kluwer Academic Publishers, Dordrecht, The Netherlands, pp. 11–43.
36. Mathews,D.H., Sabina,J., Zuker,M. and Turner,D.H. (1999) Expanded sequence dependence of thermodynamic parameters improves prediction of RNA secondary structure. *J. Mol. Biol.*, **288**, 911–940.
37. Tuschl,T., Zamore,P.D., Lehmann,R., Bartel,D.P. and Sharp,P.A. (1999) Targeted mRNA degradation by double-stranded RNA *in vitro*. *Genes Dev.*, **13**, 3191–3197.
38. Gao,M., Wilusz,C.J., Peltz,S.W. and Wilusz,J. (2001) A novel mRNA-decapping activity in HeLa cytoplasmic extracts is regulated by AU-rich elements. *EMBO J.*, **20**, 1134–1143.
39. Evdokimova,V., Ruzanov,P., Imataka,H., Raught,B., Svitkin,Y., Ovchinnikov,L.P. and Sonenberg,N. (2001) The major mRNA-associated protein YB-1 is a potent 5′ cap-dependent mRNA stabilizer. *EMBO J.*, **20**, 5491–5502.
40. Caplen,N.J., Fleenor,J., Fire,A. and Morgan,R.A. (2000) dsRNA-mediated gene silencing in cultured *Drosophila* cells: a tissue culture model for the analysis of RNA interference. *Gene*, **252**, 95–105.
41. Vance,V. and Vaucheret,H. (2001) RNA silencing in plants—defense and counterdefense. *Science*, **292**, 2277–2280.
42. Waterhouse,P.M., Wang,M.B. and Lough,T. (2001) Gene silencing as an adaptive defence against viruses. *Nature*, **411**, 834–842.
43. Grishok,A., Tabara,H. and Mello,C.C. (2000) Genetic requirements for inheritance of RNAi in *C. elegans*. *Science*, **287**, 2494–2497.
44. Boutla,A., Delidakis,C., Livadaras,I., Tsagris,M. and Tabler,M. (2001) Short 5′-phosphorylated double-stranded RNAs induce RNA interference in *Drosophila*. *Curr. Biol.*, **11**, 1776–1780.
45. Elbashir,S.M., Martinez,J., Patkaniowska,A., Lendeckel,W. and Tuschl,T. (2001) Functional anatomy of siRNAs for mediating efficient RNAi in *Drosophila melanogaster* embryo lysate. *EMBO J.*, **20**, 6877–6888.
46. Parrish,S., Fleenor,J., Xu,S., Mello,C. and Fire,A. (2000) Functional anatomy of a dsRNA trigger: differential requirement for the two trigger strands in RNA interference. *Mol. Cell*, **6**, 1077–1087.
47. Ketting,R.F., Haverkamp,T.H., van Luenen,H.G. and Plasterk,R.H. (1999) Mut-7 of *C. elegans*, required for transposon silencing and RNA interference, is a homolog of Werner syndrome helicase and RNaseD. *Cell*, **99**, 133–141.
48. Tabara,H., Sarkissian,M., Kelly,W.G., Fleenor,J., Grishok,A., Timmons,L., Fire,A. and Mello,C.C. (1999) The rde-1 gene, RNA interference and transposon silencing in *C. elegans*. *Cell*, **99**, 123–132.
49. Wu-Scharf,D., Jeong,B., Zhang,C. and Cerutti,H. (2000) Transgene and transposon silencing in *Chlamydomonas reinhardtii* by a DEAH-box RNA helicase. *Science*, **290**, 1159–1162.
50. Djikeng,A., Shi,H., Tschudi,C. and Ullu,E. (2001) RNA interference in *Trypanosoma brucei*: cloning of small RNAs provides evidence for retroposon-derived 24–26-nucleotide RNAs. *RNA*, **7**, 1522–1530.

TAB 9

siRNA function in RNAi: A chemical modification analysis

YA-LIN CHIU and TARIQ M. RANA
Department of Biochemistry and Molecular Pharmacology, University of Massachusetts Medical School, Worcester, Massachusetts 01605, USA

ABSTRACT

Various chemical modifications were created in short-interfering RNAs (siRNAs) to determine the biochemical properties required for RNA interference (RNAi). Remarkably, modifications at the 2′-position of pentose sugars in siRNAs showed the 2′-OHs were not required for RNAi, indicating that RNAi machinery does not require the 2′-OH for recognition of siRNAs and catalytic ribonuclease activity of RNA-induced silencing complexes (RISCs) does not involve the 2′-OH of guide antisense RNA. In addition, 2′ modifications predicted to stabilize siRNA increased the persistence of RNAi as compared with wild-type siRNAs. RNAi was also induced with chemical modifications that stabilized interactions between A–U base pairs, demonstrating that these types of modifications may enhance mRNA targeting efficiency in allele-specific RNAi. Modifications altering the structure of the A-form major groove of antisense siRNA–mRNA duplexes abolished RNAi, suggesting that the major groove of these duplexes was required for recognition by activated RISC*. Comparative analysis of the stability and RNAi activities of chemically modified single-stranded antisense RNA and duplex siRNA suggested that some catalytic mechanism(s) other than siRNA stability were linked to RNAi efficiency. Modified or mismatched ribonucleotides incorporated at internal positions in the 5′ or 3′ half of the siRNA duplex, as defined by the antisense strand, indicated that the integrity of the 5′ and not the 3′ half of the siRNA structure was important for RNAi, highlighting the asymmetric nature of siRNA recognition for initiation of unwinding. Collectively, this study defines the mechanisms of RNAi in human cells and provides new rules for designing effective and stable siRNAs for RNAi-mediated gene-silencing applications.

Keywords: RNAi; siRNA; human; nucleotide modification; GFP

INTRODUCTION

The evolutionarily conserved phenomenon RNA interference (RNAi), the process by which specific mRNAs are targeted for degradation by complementary short-interfering RNAs (siRNAs), has increasingly become a powerful tool for genetic analysis and is likely to become a potent therapeutic approach for gene silencing (for review, see Hammond et al. 2001; McManus and Sharp 2002). Consequently, understanding the mechanism of RNAi has become critical for developing the most effective RNAi methodologies for both laboratory and clinical applications. The general mechanism of RNAi involves the cleavage of double-stranded RNA (dsRNA) to short 21–23-nt siRNAs. This processing event is catalyzed by Dicer, a highly conserved, dsRNA-specific endonuclease that is a member of the RNase III family (Hammond et al. 2000; Zamore et al. 2000; Bernstein et al. 2001; Hamilton et al. 2002; Provost et al. 2002; Zhang et al. 2002). Processing by Dicer results in siRNA duplexes that have 5′-phosphate and 3′-hydroxyl termini, and subsequently, these siRNAs are recognized by the RNA-induced silencing complex (RISC; Hammond et al. 2000). Active RISC complexes (RISC*) promote the unwinding of the siRNA through an ATP-dependent process, and the unwound antisense strand guides RISC* to the complementary mRNA (Nykanen et al. 2001). The targeted mRNA is then cleaved by RISC* at a single site that is defined with regard to where the 5′-end of the antisense strand is bound to the mRNA target sequence (Hammond et al. 2000; Elbashir et al. 2001b). For RNAi-mediated mRNA cleavage and degradation to be successful, 5′-phosphorylation of the antisense strand must occur, and the double helix of the antisense-target mRNA duplex must be in the A form (Chiu and Rana 2002).

One highlighted difference between mammalian RNAi and RNAi in other eukaryotes is the lack of an amplification system for long-term persistence of RNAi in mammalian cells. For example, in *Drosophila*, ~35 molecules of dsRNA can silence ~1000 copies of the targeted mRNA per cell and can persist over the course of many generations (Kennerdell

Reprint requests to: Tariq M. Rana, Chemical Biology Program, Department of Biochemistry and Molecular Pharmacology, University of Massachusetts Medical School, 364 Plantation Street, Worcester, MA 01605, USA; e-mail: tariq.rana@umassmed.edu; fax: (508) 856-6696.

Article and publication are at http://www.rnajournal.org/cgi/doi/10.1261/rna.5103703.

and Carthew 1998; Zamore 2001). In mammalian cells, RNAi only persists effectively for an average of ~66 h before the siRNA is likely diluted out over the course of several cell divisions (Chiu and Rana 2002). The amplification that is seen in flies and other lower eukaryotes can potentially be attributed to three factors. One is that the conversion of long trigger dsRNA to smaller 21–23-nt siRNAs by Dicer adds a degree of RNAi amplification, whereas in mammalian cells long trigger dsRNA invokes the interferon response that activates the protein kinase PKR (Stark et al. 1998). This suggests that only siRNA transfections successfully trigger RNAi in mammalian cells without other side effects, and thus, no amplification would take place through the processing of longer RNAs. A second factor in amplification is the presence of RNA-dependent RNA polymerase (RdRP), which has been found in plants, worms, fungi, and flies (Cogoni and Macino 1999; Dalmay et al. 2000; Sijen et al. 2001). RdRP has been postulated to amplify target mRNA, through a random, degradative PCR model (Lipardi et al. 2001; Nishikura 2001; Sijen et al. 2001), into dsRNA, which can be targeted by Dicer. However, no RdRP homologs have been found in mammalian cells, and the 3′-OH that is required for RdRP-dependent degradative PCR is not required for RNAi in mammalian cells (Chiu and Rana 2002; Schwarz et al. 2002; Stein et al. 2003), indicating that PCR-based amplification likely does not occur in mammals. A third factor in amplification may be the high enzymatic turnover rate of RISC* during the targeting and cleavage of mRNA (Hutvagner and Zamore 2002), which may add a degree of amplification to RNAi induction in all eukaryotes, including mammals. However, as the persistence of RNAi occurs for only a short period of time, finding methods for increasing the longevity of siRNAs in human cells will be fundamental for applying RNAi to laboratory and therapeutic applications.

To address this issue of siRNA stability for prolonging the duration of dsRNA-mediated gene silencing and to further dissect the mechanism of RNAi in human cells, various chemically modified nucleotides predicted to affect siRNA stability were incorporated into siRNAs to study whether specific modifications increased or decreased the efficacy and persistence of RNAi in vivo. The most important of these modifications was to the 2′-OH of the ribonucleotide that distinguishes RNA from DNA and is required for the nucleophilic attack occurring during the hydrolysis of the RNA backbone, the reaction catalyzed by degradative RNases. Our results showed that the 2′-OH was not required for RNAi, indicating that structural rather than chemical properties of siRNA–mRNA duplexes were the key to inducing RNAi and that RISC* did not require the 2′-OH for ribonuclease activity. 2′-modified siRNAs also increased the persistence of RNAi in human cells. Modifications that stabilized base-pairing interactions were also incorporated into the antisense strand of siRNAs and were able to initiate RNAi, signifying that this class of chemical modifications could be used to increase the targeting efficiency of siRNAs for mRNA target sequences and for allele-specific inhibition of gene expression.

Other chemical modifications affected the formation of the major groove of the A-form helix of the antisense-siRNA–target-mRNA duplex, and potentially disrupted H-bonds or sterically hindered protein contacts, most probably preventing the RISC* complex from stably interacting with the dsRNA duplex. These modifications completely abolished RNAi, demonstrating that an intact major groove in the A-form helix and stable RNA–protein interactions were required for RNAi in human cells. Finally, previous observations of psorelan cross-linked siRNAs implied that unwinding of siRNA occurred from the 5′-end of the antisense strand and that complete unwinding may not be necessary for effective RNAi (Chiu and Rana 2002). By using mismatched or chemically modified nucleotides on either the 3′ or 5′ half of the antisense strand within the siRNA duplex, we have shown here that RNAi depended on the integrity of the 5′, and not the 3′, half of the siRNA duplex, as defined by the antisense strand. Altogether, these results gave insight into the essential biochemical properties of functional siRNAs and how specific changes in the siRNA structure can affect the efficacy of RNAi. Furthermore, these studies present new methodologies for improving the stability and utility of siRNAs for future RNAi applications.

RESULTS

2′-OH is not required for siRNA to enter the RNAi pathway

Previous results showed that RNAi effects typically peaked between 42 and 54 h posttransfection, and targeted gene expression started to be restored by 66 h posttransfection (Chiu and Rana 2002). To determine if the duration of RNAi could be prolonged by increasing the half-life of siRNAs, various chemical modifications were made to nucleotides that affected siRNA stability. These modified siRNAs were then tested in an improved dual fluorescence reporter assay based on the original assay developed previously (Chiu and Rana 2002). Briefly, GFP and RFP were constitutively expressed from pEGFP-C1 and pDsRed2-N1, respectively. EGFP mRNA was targeted for RNAi using a 21-nt siRNA targeted to nucleotides 238–258 of the EGFP mRNA (Fig. 1A). The fluorescence intensity ratio of target (GFP) to control (RFP) fluorophores was determined in the presence of siRNA duplexes and normalized to that observed in the mock-treated cells. The sequence of EGFP siRNA and EGFP mRNA, the specific mRNA cleavage site, plus the structures of the chemically modified nucleotides are diagrammed in Figure 1. As outlined previously, the cleavage site was defined precisely 11 nt downstream of the target position complementary to the 3′-most nucleotide of

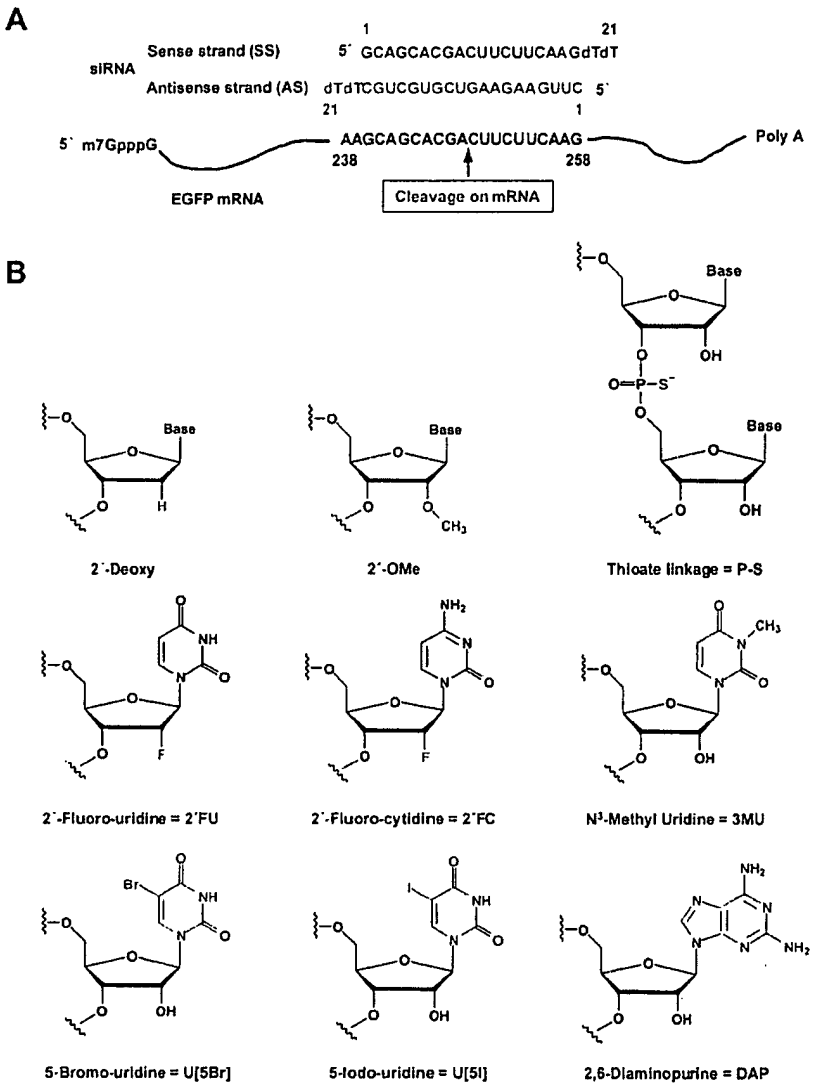

FIGURE 1. Structures of EGFP siRNA and chemical modifications. (*A*) Graphical representation of dsRNAs used for targeting EGFP mRNA. EGFP was encoded by the pEGFP-C1 reporter plasmid. siRNAs were synthesized with 2-nt deoxythymidine overhangs at the 3'-end. The position of the first nucleotide of the mRNA target site is indicated relative to the start codon of EGFP mRNA. The sequence of the antisense strand of siRNA is exactly complementary to the mRNA target site. (*B*) Structure and nomenclature of chemical modifications.

the antisense guide siRNA (Elbashir et al. 2001a). The specific chemical modifications, the particular siRNA strand(s) where modifications were made, and the effect of the chemically modified siRNA on RNAi activity are summarized in Table 1. The RNAi activity of siRNAs was evaluated with eight different siRNA concentrations (ranging from 1 to 200 nM). Each experiment was completed in duplicate and repeated twice.

The effects of modifying the 2'-OH of nucleotides on RNAi were studied by replacing uridine and cytidine in the antisense strand of siRNA with 2'-fluoro-uridine (2'-FU) and 2'-fluoro-cytidine (2'-FC), respectively, which have a fluoro group at the 2'-position in place of the 2'-OH (Fig. 1B). Where these modified 2'-FU, 2'-FC nucleotides reside in the siRNA sequence are highlighted in red in Figure 2A. Addition of a 2'-fluoro group should increase the stability of the siRNA by making the siRNAs less recognizable to RNases, thereby providing siRNAs protection from degradation (see below). When measured in the dual fluorescence assay, 2'-FU, 2'-FC siRNAs, modified only in the sense strand, only in the antisense strand, or in both strands, all showed decreased EGFP fluorescence when normalized to non-targeted RFP fluorescence that was comparable to the normalized decrease seen with wild-type siRNAs (Fig. 2; Table 1, rows 1–4). These results indicated that the 2'-OH was not required for RNAi and that nucleotides modified with 2'-fluoro groups could be used in siRNA constructs to successfully induce RNAi-mediated gene silencing.

To support the conclusion that the 2'-OH was not required for RNAi, adenine and guanine deoxynucleotides that inherently have 2'-H in place of the 2'-OH (Fig. 1B) were incorporated into the sense, antisense, or both strands of 2'-FU, 2'-FC-modified EGFP siRNAs to determine their effect on RNAi (Fig. 2A; green nucleotides). When 2'-FU, 2'-FC nucleotides were incorporated into the EGFP siRNA antisense strand with guanine and adenine deoxynucleotides at positions 9, 10, and 13, which base pair with nucleotides lining the cleavage site (Fig. 2A), EGFP RNAi effects were almost indistinguishable from wild-type levels (Fig. 2B; Table 1, row 5). This same antisense construct base-paired to 2'-FU, 2'-FC-modified sense strands also showed considerable EGFP silencing at ~64% (Table 1, row 6). In addition, siRNAs that had the entire antisense strand replaced with 2'-FU, 2'-FC, dATP, and dGTP nucleotides still showed moderate levels of RNAi activity at ~42%, or ~44% if the sense strand was also modified with 2'-FU, 2'-FC (Table 1, rows 7,8). All together, these results demonstrated that a 2'-OH group was not required for RNAi-mediated degradation and, even more specifically, was not required for nucleotides base-paired with nucleotides lining the mRNA cleavage site. There was, however, a limit on the extent to

TABLE 1. RNA interference mediated by chemically modified siRNAs

Row no.	EGFP siRNA	Sense strand	Antisense strand	RNAi activity (%)	RNAi activity (+ or −)
1	DS (WT)	Unmodified	Unmodified	93 ± 0.70	++++
2	SS/AS-2′-FU, FC	Unmodified	2′-FU, FC	83 ± 3.48	++++
3	SS-2′-FU, FC/AS	2′-FU, FC	Unmodified	92 ± 0.98	++++
4	DS-2′-FU, FC	2′-FU, FC	2′-FU, FC	83 ± 0.01	++++
5	SS/AS-2′-FU, FC + (9, 10, 13) dA, dG	Unmodified	2′-FU, FC + (9, 10, 13) dA, dG	85 ± 2.10	++++
6	SS-2′-FU, FC/AS-2′-FU, FC + (9, 10, 13) dA, dG	2′-FU, FC	2′-FU, FC + (9, 10, 13) dA, dG	64 ± 2.89	+++
7	SS/AS-2′-FU, FC + dA, dG	Unmodified	2′-FU, FC + dA, dG	42 ± 1.66	++
8	SS-2′-FU, FC/AS-2′-FU, FC + dA, dG	2′-FU, FC	2′-FU, FC + dA, dG	44 ± 0.60	++
9	SS/AS-Deoxy	Unmodified	Deoxy	0 ± 5.97	−
10	SS-Deoxy/AS	Deoxy	Unmodified	38 ± 2.95	+
11	DS-Deoxy	Deoxy	Deoxy	0 ± 0.01	−
12	SS/AS-2′-OMe	Unmodified	2′-OMe	16 ± 4.41	−
13	SS-2′-OMe/AS	2′-OMe	Unmodified	25 ± 1.75	+
14	DS-2′-OMe	2′-OMe	2′-OMe	0 ± 0.01	−
15	SS/AS-P-S	Unmodified	P-S	42 ± 6.03	++
16	SS-P-S/AS	P-S	Unmodified	62 ± 0.07	+++
17	DS-P-S	P-S	P-S	47 ± 0.03	++
18	SS/AS-2′-FU, FC + P-S	Unmodified	2′-FU, FC + P-S	22 ± 0.03	+
19	SS/AS-U[5Br]	Unmodified	U[5Br]	70 ± 1.88	+++
20	SS/AS-U[5I]	Unmodified	U[5I]	59 ± 11.2	+++
21	SS/AS-DAP	Unmodified	DAP	51 ± 0.57	++
22	SS-2′-FU, FC/AS-U[5Br]	2′-FU, FC	U[5Br]	31 ± 1.88	+
23	SS-2′-FU, FC, FC/AS-U[5I]	2′-FU, FC	U[5I]	42 ± 5.02	++
24	SS-2′-FU, FC/AS-DAP	2′-FU, FC	DAP	35 ± 7.69	+
25	SS/AS-3MU	Unmodified	3MU	0 ± 6.65	−
26	SS/AS-(11) 3MU	Unmodified	(11) 3MU	0 ± 1.71	−
27	SS/AS-(1, 2) mm	Unmodified	(1, 2) mm	35 ± 5.69	+
28	SS/AS-(18, 19) mm	Unmodified	(18, 19) mm	77 ± 2.00	+++
29	SS/AS-2′-FU, FC + (1-13) dA, dG	Unmodified	2′-FU, FC + (1-13) dA, dG	43 ± 0.09	++
30	SS-2′-FU, FC/AS-2′-FU, FC + (1-13) dA, dG	2′-FU, FC	2′-FU, FC + (1-13) dA, dG	45 ± 2.23	++
31	SS/AS-2′-FU, FC + (9-19) dA, dG	Unmodified	2′-FU, FC + (9-19) dA, dG	91 ± 0.36	++++
32	SS-2′-FU, FC/AS-2′-FU, FC + (9-19) dA, dG	2′-FU, FC	2′-FU, FC + (9-19) dA, dG	64 ± 0.42	+++

Summary of the specific chemical modifications analyzed, the particular siRNA strand(s) modified, and the effect of the chemically modified siRNA on RNAi activity in HeLa cells. RNAi activity was quantified by the dual fluorescence assay and is presented as the inhibition efficiency of target gene (EGFP) expression when cells were treated with 50 nM modified siRNAs. For comparison, the RNAi activity of unmodified, or wild-type, duplex siRNA (DS) normalized to 93% was designated (++++). Modified siRNAs assigned (++++) showed >80% RNAi activity, (+++) showed 60%–80%, (++) showed 40%–60%, and (+) showed 20%–40%. Modified siRNAs showing <20% RNAi activity were considered nonfunctional (–) in the RNAi pathway. Each experiment measuring RNAi activity of siRNAs was completed in duplicate and repeated twice.

which deoxynucleotides could substitute for ribonucleotides because replacing the entire siRNA sense strand with deoxynucleotides decreased EGFP gene silencing to ~38% inhibition, and replacing either the antisense strand or both strands entirely with deoxynucleotides completely abolished EGFP RNAi (Fig. 2B; Table 1, rows 9–11). Nonetheless, these results collectively showed that nucleotides with either 2′-F or 2′-H groups can selectively replace ribonucleotides within the siRNA sequence to effectively induce RNAi.

An interesting result was seen by modifying the 2′-OH to a bulky methyl group to create 2′-OMe nucleotides that were incorporated into sense, antisense, or both strands of EGFP siRNAs (Fig. 1B). This modification was hypothesized to improve RNAi efficacy because 2′-OMe groups are thought to increase RNA stability by inducing an altered RNA conformation that is more resistant to nucleases (Cummins et al. 1995). This modification is also thought to increase RNA affinity for RNA targets and improve hybridization kinetics (Majlessi et al. 1998). Despite these potential benefits, 2′-OMe nucleotides incorporated into either the sense or antisense strand greatly diminished EGFP gene silencing to ~25% or ~16%, respectively, whereas double-stranded 2′-OMe-modified siRNAs completely abolished RNAi (Table 1, rows 12–14). These results indicated that the methyl group, as a bulky group, may severely limit the interactions between siRNAs, target mRNAs, and the RNAi machinery required for successfully mediating RNAi. It is worth noting that because the bulkiness of the methyl group would likely be the cause of decreased RNAi activity rather than the actual lack of the 2′-OH specifically, these studies still supported the conclusion that the 2′-OH was not required for RNAi.

In a final analysis of modifications that may potentially increase siRNA stability without disrupting RNAi potency,

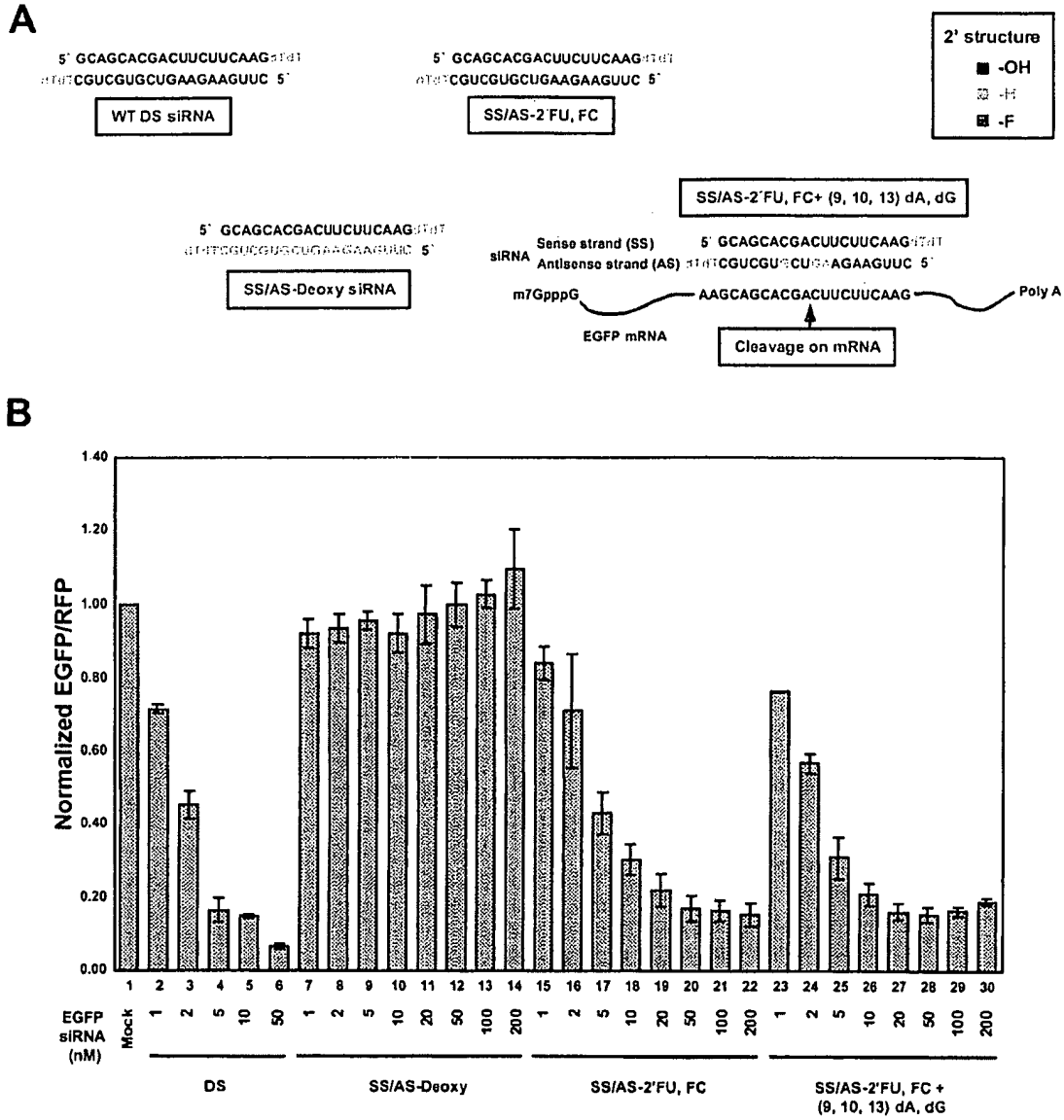

FIGURE 2. siRNA 2′-OH is not required to guide mRNA cleavage. (*A*) Sequence and structure of siRNA duplexes with modification at the 2′-position of the sugar unit. Nucleotides with 2′-hydroxyl groups (-OH) are black. Nucleotides with 2′-deoxy groups (-H) are cyan. Nucleotides with 2′-fluoro groups (-F) are red. The cleavage site on the target mRNA is also shown (red arrow). (*B*) Ratios of normalized GFP to RFP fluorescence intensity in lysates from modified siRNA-treated HeLa cells. The fluorescence intensity ratio of target (GFP) to control (RFP) fluorophores was determined in the presence of EGFP siRNA duplexes with modifications at the 2′-position of the sugar unit. Normalized ratios at <1.0 indicate specific RNA interference effects. For comparison, results from unmodified duplex siRNA-treated cells are included.

a thioate linkage (P–S) was integrated into the backbone of the EGFP siRNA strand(s). P–S linkages were previously used in antisense methodology for increasing resistance to ribonucleases (for review, see Stein 1996) and, therefore, were postulated to enhance the stability of siRNAs. Incorporating the P–S linkages into the double-stranded siRNA sense strand led to moderate levels of RNAi activity (62% inhibition), whereas P–S linkages in either the antisense or both strands of the siRNAs led to just less than ~50% RNAi-induced inhibition (Table 1, rows 15–17). These results implied that the P–S modifications did not prohibit RNAi-mediated degradation and only moderately affected the efficiency of RNAi. Interestingly, incorporating 2′-FU, 2′-FC modifications into the antisense strand in addition to the added P–S linkages showed lower levels of EGFP gene silencing (Table 1, row 18), indicating that there was a synergistic effect that decreased but did not inhibit RNAi-mediated degradation when both the 2′-F groups and the

P–S linkages were incorporated into siRNAs.

Stability of modified siRNAs and the persistence of their RNAi activity in vitro and in vivo

As the above experiments showed that siRNAs modified with stabilizing 2′-FU, 2′-FC groups could effectively mediate RNAi to levels comparable to wild type, it was necessary to show that these modifications did in fact enhance siRNA stability. To measure the stability of siRNA in cell extracts, unmodified or 2′-FU, 2′-FC-modified EGFP antisense strand siRNAs 5′-labeled with [γ-^{32}P]ATP were annealed with sense strand siRNAs to form duplex siRNAs, which were then incubated in HeLa cell extracts. At various time points, siRNAs were extracted, analyzed on a 20% polyacrylamide gel containing 7 M urea, and visualized by phosphorimager analysis. Smaller siRNA degradation products were visualized in this analysis (data not shown), indicating that the lost of intact siRNA observed during these experiments was not caused by dephosphorylation of siRNAs. The top panel (a) of Figure 3A shows the stability of the various 2′-FU, 2′-FC-modified siRNAs as compared with wild-type siRNAs over time. Wild-type double-stranded siRNAs showed a steady loss of intact siRNAs over the course of the experiment, with only ~7% of the original concentration of intact siRNAs remaining after 1 h in extract (Fig. 3A[a], dark blue line). Intact modified or unmodified single-stranded antisense siRNAs were quickly lost over the time course and were virtually undetectable by 30 min in extract (Fig. 3A[a], black and red lines). This result showed that single-stranded modified siRNA was as susceptible to degradation as wild-type siRNA, indicating that single-stranded siRNAs, modified or unmodified, are inherently less stable than duplex siRNA. Double-stranded siRNAs with 2′-FU, 2′-FC modifications in either the antisense strand or both strands remained predominantly intact over the course of the experiment with ~68% or ~81%, respec-

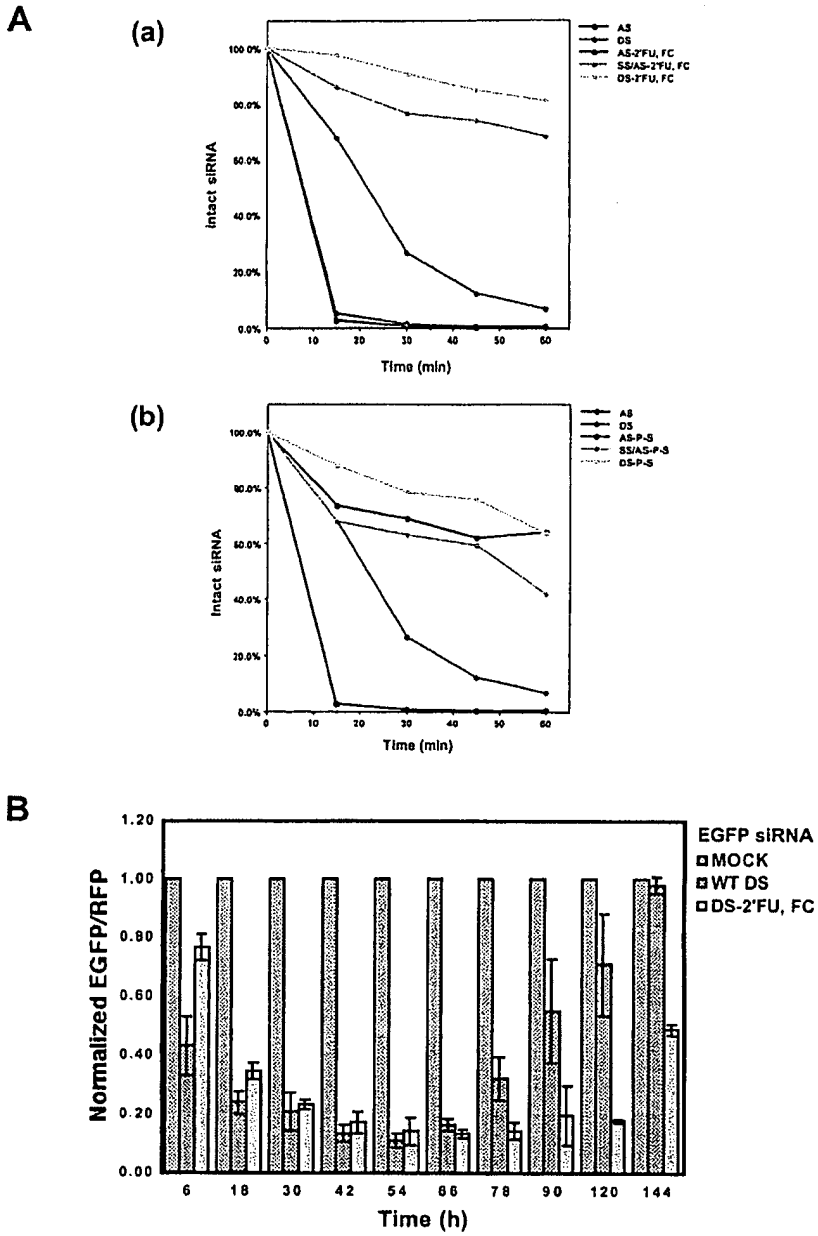

FIGURE 3. Extending the half-life of siRNA duplexes prolongs the persistence of RNA interference in vivo. (*A*) Comparing the stability of unmodified siRNAs with siRNAs containing 2′-fluoro-uridine and 2′-fluoro-cytidine (2′-FU, 2′-FC) modifications (*a*) and thioate linkage (P–S) modifications (*b*). Unmodified or modified EGFP antisense strand siRNAs (AS) were 5′-labeled with [γ-^{32}P]ATP by T4 polynucleotide kinases. Duplex siRNAs were formed by annealing equal molar ratios of sense-strand (SS) siRNAs with the 5′-^{32}P-labeled antisense strand. To analyze siRNA stability in HeLa cell extract, 50 pmole of siRNA was incubated with 500 μg of HeLa cell extract in 50 μL of reaction mixture containing 20 mM HEPES (pH 7.9), 100 mM KCl, 10 mM NaCl, 2 mM $MgCl_2$, and 10% glycerol. At various time points, siRNAs were extracted and analyzed on 20% polyacrylamide gels containing 7 M urea followed by phosphorimage analysis (Fugi). (*B*) Kinetics of RNAi effects of duplex siRNA with 2′-fluoro-uridine and 2′-fluoro-cytidine modification in HeLa cells over a 144-h time course. The fluorescence intensity ratio of target (GFP) to control (RFP) protein was determined in the presence of unmodified dsRNA (blue bars) and duplex siRNA with 2′-fluoro-uridine and -cytidine modifications (DS-2′-FU, 2′-FC, cyan bar) and normalized to the ratio observed in the presence of mock-treated cells (red bars). Normalized ratios at <1.0 indicated specific RNA interference.

tively, of the original siRNA population remaining intact throughout the duration of the experiment (Fig. 3A[a], green and light blue lines). These results indicated that the 2′-FU, 2′-FC modifications did, indeed, increase the stability of the siRNAs upon exposure to extract and that having these modifications in both strands provided the siRNAs with the most stability.

In a similar experiment, the stability of P–S-modified EGFP siRNAs was evaluated. Unmodified, double-stranded antisense siRNAs showed about the same rate of siRNA loss as described in the above experiment (Fig. 3A[b], dark blue lines). However, P–S-modified single-stranded antisense siRNAs demonstrated a markedly increased rate of stability over the course of the experiment, showing ~63% of the original siRNAs remaining intact after 1 h in extract as compared with 0% intact for single-stranded unmodified antisense siRNAs (Fig. 3A[b], black and red lines). The stability of double-stranded siRNAs with P–S modifications in both strands was comparable to the stability seen with the modified single-stranded antisense strand, with ~63% of the original siRNA population remaining intact after 1 h (Fig. 3A[b], light blue lines). Double-stranded siRNAs with P–S modifications in only the antisense strand showed weaker but still significant stability with ~42% of the original siRNA population remaining intact through 1 h in extract (Fig. 3A[b], green lines). These results showed that the P–S modifications increased the stability of the siRNAs and, most notably, increased the stability of both single- and double-stranded siRNAs.

These in vitro results indicated that siRNA stability is prolonged by these different modifications; however, it is important to note that these experiments address the general stability of siRNA in the context of endonucleases present in whole-cell extracts. Therefore, these experiments cannot distinguish whether the endonucleases affecting siRNAs in the in vitro assay would necessarily affect the stability of these various siRNAs in vivo. To address whether increased stability seen with modified siRNAs prolonged the duration of RNAi in vivo, RNAi, induced by unmodified and 2′-FU, 2′-FC-modified double-stranded EGFP siRNAs, was assayed in the dual fluorescence reporter assay over a period of 144 h. To visualize RNAi effects over an even longer period of time, HeLa cells were transfected with modified or unmodified siRNA and, 36 h later, transfected with dual fluorescence reporter plasmids; RNAi activity persisted but was tapering by 168 h (data not shown). Also, growth of cells containing modified siRNAs was comparable to cells containing wild-type siRNA, indicating that modified siRNAs were not affecting cell division (data not shown). Although 2′-FU, 2′-FC-modified EGFP siRNAs were slower to show RNAi effects by 6–18 h, maximal RNAi effects occurred by 42 h posttransfection for both modified and unmodified siRNAs. The maximal activity for both siRNAs was also in the same range, with both showing ~85%–90% inhibition of GFP expression. However, the RNAi effects observed over the period of 66–120 h revealed that the effect of modified siRNAs was much more persistent than that of unmodified siRNAs. By 120 h posttransfection, the effect of modified siRNAs still remained at ~80% inhibition of GFP expression but the effect of unmodified siRNAs had dropped to less than ~40% inhibition. Similarly, prolonged RNAi activity was observed with 2′-FU, 2′-FC-modified siRNAs targeting endogenous human Cyclin T1 mRNA when compared with wild-type siRNAs targeting Cyclin T1 (see Discussion; Y.L. Chiu and T.M. Rana, unpubl.). Altogether, these results strongly indicated that there was a direct link between the duration of the RNAi effects and siRNA stability in human cells. Furthermore, these results showed conclusively that siRNAs stabilized by chemical modifications, like the 2′-FU, 2′-FC modifications, can be used to effectively induce and significantly prolong RNAi-mediated gene silencing in vivo.

Modified siRNAs that stabilize A–U base-pair interactions can induce RNAi

In addition to incorporating modifications that affected the stability of siRNAs, nucleotides chemically modified to strengthen the base-pair interactions between two complementary bases were analyzed. In theory, increasing the stability of base-pair interactions may increase the targeting efficiency of siRNAs to target mRNA sequences. Increasing targeting efficiency may then induce more robust RNAi effects with siRNAs that are weaker at binding to their target sequence or have mismatched sequences, and thus, are not showing a high degree of RNAi. This type of approach may also be used to significantly inhibit expression of one allele over another when both alleles are present in the same cell. To bolster base-pairing interactions, 5-bromo-uridine (U[5Br]), 5-iodo-uridine (U[5I]), or 2,6-diaminopurine (DAP; Fig. 1B), which are modified nucleotides known to increase the association constant between A–U base pairs (Saenger 1984), were incorporated into siRNAs and tested in the dual fluorescence report assay. Double-stranded siRNAs having U[5Br], U[5I], or DAP modifications incorporated into the antisense strand were capable of inducing RNAi activity at levels of ~70% for U[5Br], ~59% for U[5I], and ~51% for DAP (Fig. 4; Table 1, rows 19–21). Interestingly, when 2′-FU, 2′-FC stabilizing modifications in the sense strand were combined with these modifications in the antisense strand, gene silencing was not as efficient as wild type in inducing RNAi. EGFP gene silencing was 31% for the 2′-FU, 2′-FC-modified sense siRNA base-paired with U[5Br]-modified, ~42% for U[5I]-modified, or ~35% for DAP-modified antisense siRNAs (Fig. 4; Table 1, rows 22–24). These results indicated that enhancing the interactions between base pairs through these siRNA modifications was a viable option for increasing mRNA targeting efficiency, but that there was a limit to how stable the base-pairing

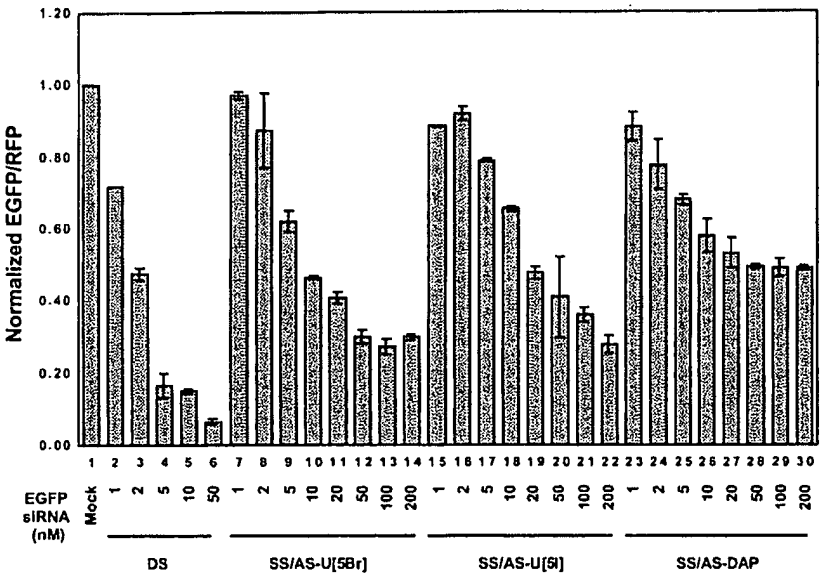

FIGURE 4. RNA interference mediated by siRNAs harboring modifications that stabilize base-pairing interactions. 5-Bromo-uridine (U[5Br]) or 5-iodo-uridine (U[5I]) replaced uridine or 2,6-diaminopurine (DAP) replaced adenine in siRNAs to stabilize base-pairing interactions. The activity of siRNAs with base modifications was quantified by the dual fluorescence assay. For comparison, results from unmodified duplex siRNA (DS, lanes 2–6)-treated cells are included.

interactions can be made before they interfere with siRNA unwinding (see Discussion).

The major groove of the A-form helix is required for RNAi

Previously, the A-form helix was shown to be required for the mechanism of RNAi, as 2-nt bulges that distort A-form helices between antisense siRNAs and target mRNAs abolished RNAi (Chiu and Rana 2002). To test whether the major groove of the A-form helix was required for RNAi, siRNAs were modified with N^3-methyl uridine (3MU) nucleotides that remove an H-bond donor at N^3-H. Structurally, the bulky N^3-methyl group would jut into the major groove of the A-form helix, potentially introducing a steric clash between base pairs. In addition, the presence of 3MU in the major groove may also introduce a steric clash between RNA and RNA-interacting proteins (Saenger 1984). Therefore, both steric hindrance and the loss of an H-bond donor by the addition of the N^3-methyl group should destabilize RNA–protein interactions in the major groove. 3MU-modified EGFP siRNAs introduced into HeLa cells completely abolished RNAi (Table 1, row 25). RNAi was also abolished if only one 3MU modification was introduced specifically at U11 of the antisense strand, which is one of the nucleotides that base pairs with A248 of the target EGFP mRNA cleavage site (Fig. 1A; Table 1, row 26). These results indicated that disrupting the functional groups of the major groove of the A-form helix formed by the antisense strand and its target mRNA specifically at the cleavage site inhibited RNAi. These data also indicated that the major groove was required for mediating RNAi and for RNA–RISC interactions that subsequently lead to mRNA cleavage.

Structural integrity of the 5′ half of siRNA duplex, as defined by the antisense strand, is important for mediating RNAi

Previous data using psoralen photochemistry suggested that complete unwinding of the siRNA duplex was not required for RNAi in vivo because psoralen cross-linked siRNAs did not completely abolish gene silencing (Chiu and Rana 2002). In describing these results, it was proposed that a single cross-linking event occurring near the 3′-end of the antisense strand still allowed for the initial unwinding of duplex siRNAs from the 5′-end, freeing enough of the nucleotides in the antisense strand to hybridize to the target mRNA and induce RNAi, even if unwinding was not complete. If this were the case, then unwinding of siRNAs must start from the 5′-end of the antisense strand, a conclusion supported by the fact that blocking either the 3′-end of the antisense siRNA strand or the 5′-end of the sense siRNA strand had no significant effect on RNAi activity (Chiu and Rana 2002).

If this 5′-to-3′ unwinding model was correct, sequences within the 3′ half of the siRNA duplex as defined by the antisense siRNA strand should be changeable without significantly interfering with RNAi. To test this hypothesis, EGFP siRNAs with mismatched base pairs at either the internal 5′ (nt 1, 2) or 3′ (nt 18, 19) positions within the duplex were introduced into the antisense strand (Fig. 5A, purple box, purple nucleotides). siRNAs with mismatches near the 5′ half of the duplex structure showed only ~35% inhibition in the dual fluorescence reporter assay, whereas mismatches at the 3′ half retained a significant level of gene silencing at ~77% (Fig. 5B; Table 1, rows 27–28). These results strongly indicated that the integrity at the 5′ half of the duplex, as defined by the antisense strand, was functionally more important than that at the 3′ half.

To explore this idea even further, 2′-FU, 2′-FC plus dATPs, dGTPs were incorporated within internal positions within the antisense-strand siRNAs predominantly at the 5′ (nt 1–13) or predominantly within the 3′ half (nt 9–19; Fig. 5A, red and cyan nucleotides). In the dual fluorescence

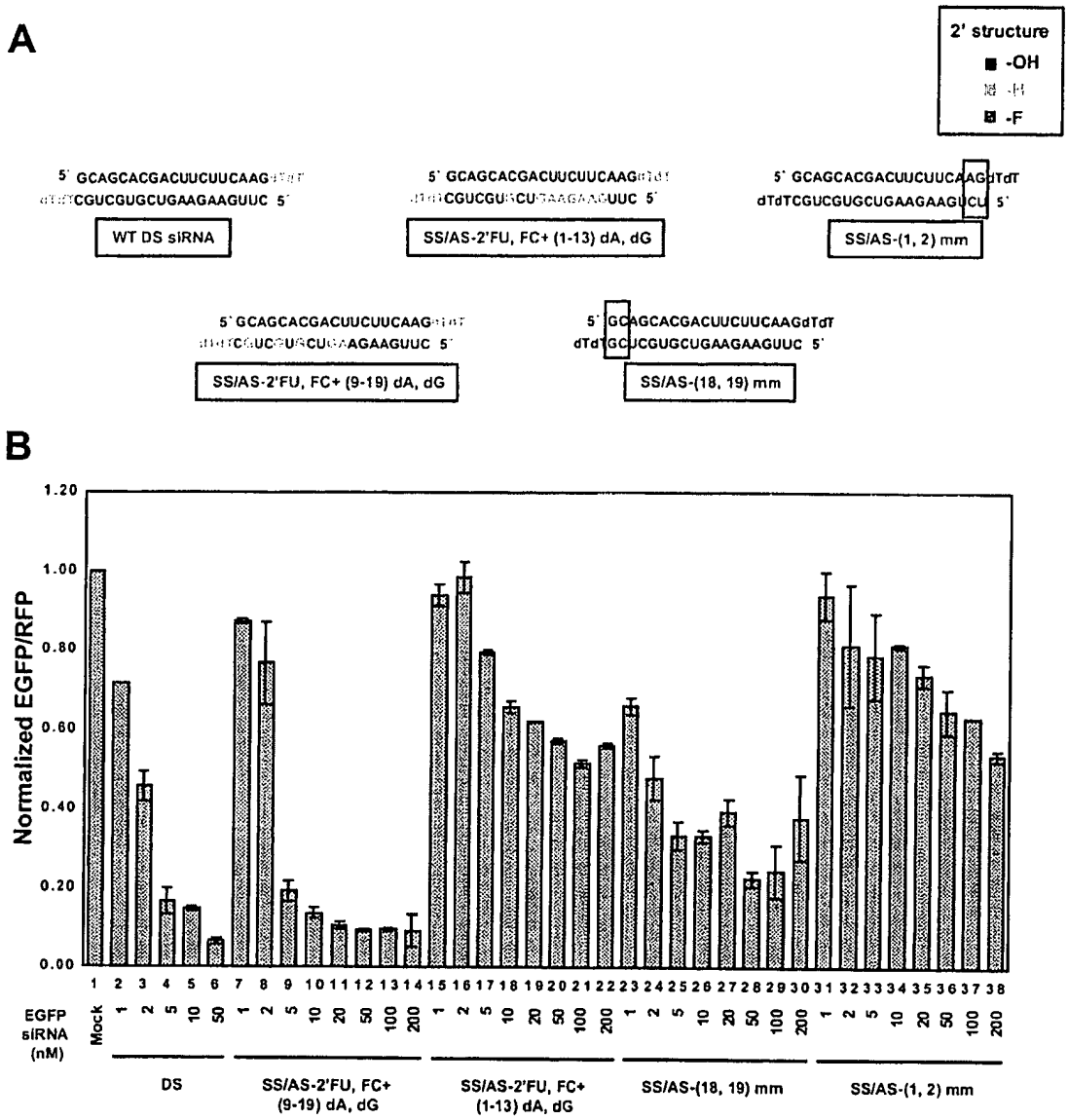

FIGURE 5. Structural integrity of the 5′ half of siRNA duplexes, as defined by the antisense strand, was functionally more important than at the 3′ half. (*A*) Graphical description of asymmetric requirement of duplex siRNA structure. The structure of unmodified (WT DS) siRNA duplexes, siRNAs with 2′-fluoro-uridine and 2′-fluoro-cytidine, 2′-deoxy modification at the 3′ half (SS/AS-2′-FU, 2′-FC + [9–19] dA, dG) or 5′ half (SS/AS-2′-FU, 2′-FC + [1–13] dA, dG) of the antisense strand, and siRNA duplexes with mismatches within the antisense 3′ half (SS/AS-[18,19] mm) or 5′ half (SS/AS-[1,2] mm) of the siRNA duplex are shown here. (*B*) Results from cells treated with duplex siRNAs with asymmetrically modified siRNA duplexes. For comparison, results from unmodified duplex siRNAs (DS, lanes *2–6*)-treated cells are included.

reporter assay, predominantly 5′-modified antisense (AS-2′-FU, 2′-FC + [1–13] dA, dG) EGFP siRNAs were only moderately effective, inducing RNAi at ~43%, or at 45% if the sense strand was also modified to 2′-FU, 2′-FC (Fig. 5B; Table 1, rows 29,30). However, predominantly 3′-modified and 5′-unmodified antisense (AS-2′-FU, 2′-FC + [9–19] dA, dG) siRNAs significantly induced RNAi activity at ~91%, or at 64% if the sense strand was also modified to 2′-FU, 2′-FC (Fig. 5B; Table 1, rows 31,32). These contrasting results indicated that sequence structure within the 5′ region of the antisense strand was more sensitive to modification than in the 3′region. All together, these data indicated that recognition of siRNA duplexes by an as-yet-unidentified RNA helicase occurs asymmetrically with the structure of the antisense 5′-end of the duplex preferentially distinguished from the 3′-end during the initiation of unwinding.

Modified siRNAs enter into the RNAi pathway in vitro

Although the dual fluorescence reporter assay did detect changes in EGFP gene expression with the modified siRNAs

created herein, it was possible that gene silencing was being induced by a mechanism other than RNAi-mediated degradative pathways. To test whether the targeted mRNA was, indeed, being cleaved upon exposure to modified siRNAs, an in vitro RNAi assay was performed to measure the cleavage of a ^{32}P-cap-labeled mRNA target upon incubation with modified siRNAs and HeLa cytoplasmic extract. Cleavage products were resolved on an 8% polyacrylamide-7 M urea gel. Mock-treated mRNAs did not show an observable cleavage product (Fig. 6, lane 1), but wild-type and all modified siRNAs that displayed gene silencing effects in vivo showed clearly visible cleavage products in vitro (Fig. 6, lanes 2,8–11,14–17). Furthermore, modified siRNAs that did not show any marked gene-silencing effects in vivo did not show any distinct cleavage products in the in vitro assay (Fig. 6, lanes 1,6,7,12,13), implying that the cleavage events observed were specifically dependent on functional siRNAs. These in vitro results provided a strong correlation between the in vivo gene silencing observed with the modified siRNAs and target mRNA degradation, indicating that the modified siRNAs were distinctly targeting mRNAs for cleavage and subsequent degradation through the in vivo RNAi pathway.

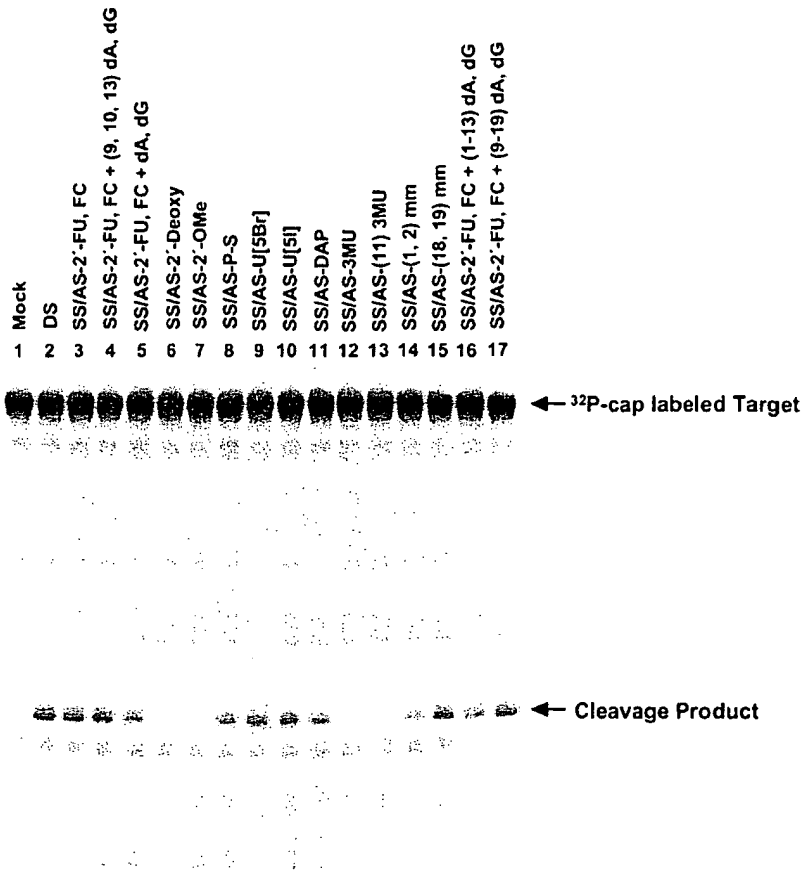

FIGURE 6. For analysis of siRNA-mediated target mRNA cleavage in vitro, 10 nM cap-labeled target EGFP mRNA was incubated with 100 nM siRNA and HeLa cytoplasmic extracts, as described in Materials and Methods. Reaction products were resolved on an 8% polyacrylamide-7 M urea gel. Arrows indicate the capped target EGFP mRNA and the 5′ cleavage product, which were expected to be 124 nt and 55 nt, respectively. The identity of the cleavage product was assigned according to RNase T1 partial digestion and a molecular weight marker of RNA (data not shown). The 3′ fragment is unlabeled, and therefore, invisible.

DISCUSSION

RNAi has moved toward the forefront of reverse genetic analysis in human cells for characterizing loss of gene function phenotypes and establishing connections between gene structure and function. In light of its versatility, understanding the detailed mechanism behind the RNAi phenomenon and developing methods to extend the limits of its current capabilities is crucial for implementing this methodology even further into the laboratory and therapeutic realms. By introducing various chemical modifications into siRNAs and measuring their effects on RNAi, this study revealed new insights into the mechanism of RNAi and outlined new approaches for increasing the efficacy of RNAi in vivo in human cells for use in future applications.

From these data, a more complete picture of the stepwise process of RNAi can be envisioned and is depicted in Figure 7. In the first step of RNAi induction, the 5′-ends of the siRNA duplex are phosphorylated, resulting in the formation of an siRNA–RISC complex. The data presented here showing the asymmetric nature of unwinding then indicate an ATP-dependent event during which siRNA is unwound from the 5′-end of the antisense strand and RISC is activated. Following RISC activation, the antisense strand of the unwound siRNA guides the siRNA–RISC* complex to the target mRNA. The guide antisense strand base pairs with the target mRNA, forming an A-form helix, and the RISC* protein complex recognizes the major groove of the A-form

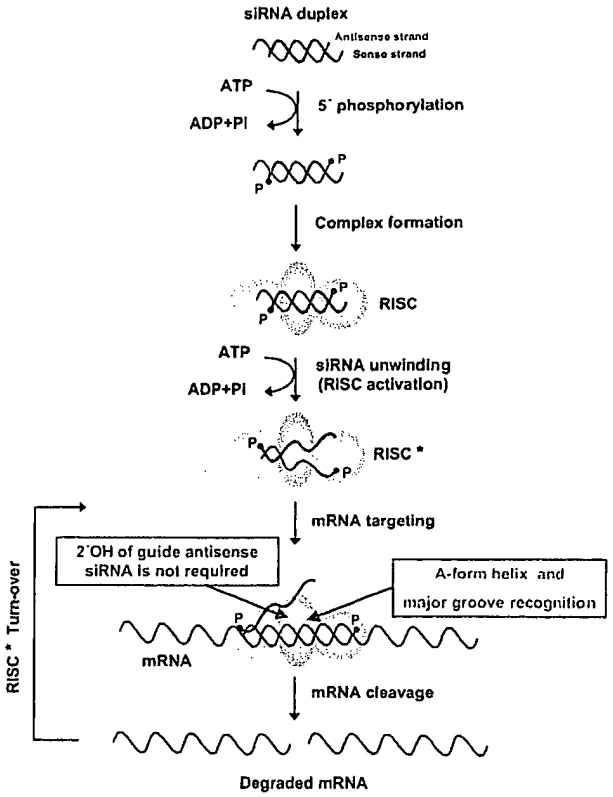

FIGURE 7. Model for RNAi in human cells highlighting the requirement of the A-form helix and major groove for mRNA cleavage with the steps not requiring the RNA 2′-OH of the guide antisense siRNA. See text for details.

helix, an event that occurs independently of the RNA 2′-OH of the guide antisense siRNA. In the final step of this process, the target mRNA is cleaved by RISC*, which is another event that occurs independently of the 2′-OH of the guide antisense siRNA. RISC* is then recycled to catalyze another cleavage event.

The requirement for the A-form helix supercedes the requirement for the 2′-OH in RNAi

Several important mechanistic findings were presented here that not only more clearly defined the mechanism of the RNAi pathway, but will also increase the utility of RNAi in various applications. Our results showing that the 2′-OH was not essential for RNAi have several important implications for the structural and catalytic elements required for the RNAi pathway. Remarkable functional implications were that the RNAi machinery does not require the 2′-OH for recognition of siRNAs, and the catalytic ribonuclease activity of RISC does not involve 2′-OH groups of the guide antisense RNA. Another consequence of this discovery was that a variety of chemical groups, including fluoro or deoxy groups, could substitute for the 2′-OH in siRNAs, indicating that no distinguishing chemical specificity was required for RNAi at the 2′-position. These findings would imply that other properties of the siRNA–mRNA duplexes, such as core structural elements, were essential for siRNA. If helical structure was the key to RNAi induction, then the A-form helix that forms between siRNAs and the target mRNA would, indeed, be required for RNAi, as was previously shown (Chiu and Rana 2002). Furthermore, the 2′-fluoro or combined 2′-fluoro, deoxy-modified antisense siRNAs lacking the 2′-OH would have to competently form an A-form helix to induce RNAi as shown here. This will likely turn out to be the case because 2′-fluoro-modified RNA–RNA hybrids were previously reported to exhibit an A-form helical conformation (Cummins et al. 1995; Luy and Marino 2001), lending significant merit to the idea that helical structure strongly influences RNAi efficiency. Still another implication of these particular results was that alternate chemical groups at the 2′-position that allow the A-form helix to be retained but help siRNAs evade recognition by RNases can increase siRNA stability and prolong RNAi effects induced in vivo.

It was previously shown in *Caenorhabditis elegans* and *Drosophila* extracts that completely substituting one or both siRNA strands with deoxynucleotides abolished RNAi (Parrish et al. 2000; Elbashir et al. 2001b), and those observations were consistent with the data presented here. The failure of true DNA–RNA hybrids to induce RNAi most plausibly relates to the argument that structure, and thus the A-form helix, was an essential determinant for RNAi induction. Based on circular dichroism spectra, DNA–RNA hybrids displayed characteristics that were intermediate between A- and B-form helices (Cummins et al. 1995). Following the contention that the A-form helix was an absolute requirement for RNAi induction, 2′-deoxy siRNA–mRNA target duplexes would not be recognized by the RNAi machinery because they would not be forming the proper A-form helical structure. Therefore, RNAi would not be induced by DNA–RNA hybrids, as has been observed. It is also worth mentioning that microRNAs (miRNAs) induce posttranscriptional gene silencing (PTGS) through the same pathway as RNAi but, ultimately, only inhibit translation machinery instead of inducing RNA degradation, the event that defines RNAi. The only observable difference between the two mechanisms is that RNAi requires the A-form helix, but miRNA-induced PTGS does not, as miRNAs often mismatch with their target mRNAs, forming a bulge that would distort the helical structure. This would indicate that the differences between the miRNA-induced silencing mechanism and siRNA-mediated RNAi may solely be attributable to differences in RNA–RNA helical structure, and further support a model in which helical structure was the sole determinant for whether RNAi was induced.

It was also previously reported that replacement of uridine with 2′-FU, corresponding to one-fourth of the bases of long dsRNAs, elicited RNAi effects in *C. elegans*, whereas

deoxycytodine incorporated into long dsRNAs diminished RNAi effects (Parrish et al. 2000). However, exactly where these modified nucleotides fell within the sequence structure of RNAi-inducing siRNAs and whether these modified nucleotides in the longer RNAs corresponded to the mRNA cleavage site or major groove after being processed to siRNAs was not clear. It has also been reported that siRNAs in which 3′ overhangs and two of the 3′-end ribonucleotides were replaced with deoxyribonucleotides retained RNAi activity upon exposure to *Drosophila* extracts (Elbashir et al. 2001b). Presumably, replacing two of the 3′-end base-paired nucleotides with deoxynucleotides would not disrupt the overall A-form structure of the siRNA–mRNA duplex required for RNAi and would thereby allow RNAi induction.

Neither analyses in *C. elegans* nor in *Drosophila* extracts ascertained whether there was a distinct requirement for the 2′-OH for cleavage-site recognition and the cleavage event itself during RNAi induction. The results presented here demonstrated that exclusively using 2′-FU, 2′-FC modifications in siRNAs and selectively substituting in deoxyribonucleotides for nucleotides base-paired with the nucleotides lining the mRNA cleavage site, or even replacing the entire sequence of siRNA with a combination of 2′-fluoro- and 2′-deoxynucleotides, elicited RNAi induction. Therefore, it has now been definitively established that recognition of the mRNA-target cleavage site and subsequent cleavage did not require the 2′-OH of the antisense siRNA to induce RNAi. As a final point, the inhibitory RNAi effects seen with the bulky 2′-OMe modification, which was also shown previously with *Drosophila* (Elbashir et al. 2001b), did demonstrate that there were steric constraints on the types of 2′ modifications that would be amenable for inducing RNAi. As 2′-OMe modifications probably did not disrupt the A-form helix of the siRNA–mRNA duplex (Cummins et al. 1995), the methyl group may be sterically interfering with protein–RNA interactions, thereby preventing RNAi. Nevertheless, steric constraints notwithstanding, this analysis conclusively showed that the nonessential nature of the 2′-position could very much be exploited for improving the efficacy of RNAi in a variety of applications.

Improving the efficacy of RNAi using chemical modifications

Modifications like the 2′-fluoro and P–S linkages both increased the half-life of siRNAs upon exposure to cytoplasmic extracts, and in vivo studies with 2′-FU, 2′-FC siRNAs showed that increasing the half-life of siRNAs did, in fact, prolong the effects of RNAi. In addition, we have observed similar prolonged RNAi activity with silencing lasting over 90 h using these same modifications in siRNAs targeting the endogenous target, human Cyclin T1 (Y.L. Chiu and T.M. Rana, unpubl.). These observations demonstrated that the siRNA modifications studied here can be used to effectively silence endogenous human genes over prolonged periods of time. Our results also indicated that short-lived RNAi effects usually observed in human cells were caused at least in part by the degradation of siRNAs. Our findings that the stabilizing siRNA modifications still allowed for a substantial level of RNAi induction showed that these modifications will be invaluable for studying the phenotypic effects of prolonged gene silencing in cell culture or in increasing the long-term in vivo effects of siRNAs in clinical applications. Interestingly, the P–S-modified, single-stranded antisense strand did not show increased RNAi effects in the dual fluorescence reporter assay used here (data not shown), despite showing significantly increased stability (Fig. 3A[a]). Similarly, single-stranded antisense siRNAs modified with 2′-OMe or 2′-FU, 2′-FC did not cause RNAi efficiently (data not shown). This strongly indicated that siRNA stability was not the main reason that single-stranded antisense RNAi was not as effective in inducing RNAi as dsRNA. Nonetheless, creating P–S modifications in the siRNA backbone showed that stabilizing the siRNA backbone did not inhibit RNAi and signified that using chemical modifications that stabilized phosphate linkages was a viable option for prolonging RNAi effects.

Another option for increasing the efficacy of RNAi was uncovered by the analysis of modifications that should enhance base-pairing interactions between antisense siRNA and targeted mRNA. DAP is a naturally occurring nucleobase that sometimes replaces adenine in phages like the cyanophage S-2L (Kirnos et al. 1977). Incorporation of DAP into RNA strands promotes the formation of three H-bonds between DAP and uridine, increasing the stability of interactions seen between A–U base pairs (Bailly and Waring 1998). U[5Br] and U[5I] have also been shown to have higher association constants when base-paired to A residues than to unmodified uridine (Saenger 1984). When any of these modifications were incorporated into siRNAs, RNAi was still quite efficient, indicating that modifications that stabilize base-pairing interactions can be used in designing siRNAs for various applications. It was also notable that siRNAs with 2′-fluoro modifications introduced into sense strands and base-paired with the DAP, U[Br], or U[5I] antisense strands had decreased RNAi efficiency. 2′-fluoro modifications have been shown to significantly increase the melting temperature between base pairs (Cummins et al. 1995). Consequently, the stabilizing effect on base-pairing interactions when both the 2′-fluoro and DAP, U[Br], or U[5I] modifications were present may have actually hindered the unwinding of the siRNA duplex. These results indicated that the lower rates of siRNA unwinding account for the observed decrease in RNAi activity.

Despite some minor limitations on how much the base-pair interactions can be stabilized, an application for using these types of modifications would be to increase the targeting efficiency of one mRNA sequence over another closely homologous but not identical sequence. Precedent

for this type of sequence discrimination was set by Haaima et al. (1997), who showed that DAP improved the ability of an oligomer to discriminate against mismatches. Translated to an RNAi application, these modifications may be useful for specifically targeting a mutant mRNA in a population of both mutant and wild-type mRNAs to recover a recessive wild-type phenotype. These modifications may also be useful in increasing binding affinity between target mRNAs and siRNAs that appear to have weak gene-silencing effects.

Other structural determinants for RNAi induction

Another structural facet of the RNAi mechanism was uncovered using the 3MU modification, which showed that the major groove of the A-form helix was required for RNAi. This finding builds on previous data showing that the A-form helix was required for RNAi (Chiu and Rana 2002). Together, these results indicated that the specific structure of the A-form helical RNA that forms the major groove and contains the mRNA cleavage site was important for recognition by the RNAi machinery. Conceivably, RNA–RISC* contacts depend on the structural integrity of the major groove for precise interactions and, ultimately, to initiate cleavage of the target. By disrupting the major groove, RISC* may no longer be able to interact or only weakly interacts with the siRNA–mRNA target duplex, thereby preventing mRNA cleavage. Alternatively, RISC* might still be able to interact with the destabilized RNA helix but not recognize the cleavage site within the major groove as the catalytic site if the conformation of the RNA helix and more specifically the major groove were altered.

The other structural property of siRNAs defined by these analyses was the asymmetric nature of siRNA unwinding. Initiation of siRNA unwinding from the 5′-end was previously indicated from the ability of single cross-linked siRNAs to still induce RNAi (Chiu and Rana 2002). By using mismatched or modified nucleotides on either the 3′ or 5′ half of the antisense strand within the siRNA duplex, it was shown here that RNAi depended on the integrity of the 5′, and not the 3′, half of the siRNA duplex, as defined by the antisense strand. Previous studies from our laboratory and from other groups have observed that mutations or modifications at the 3′-end overhang of the antisense strands are well-tolerated (Chiu and Rana 2002; Martinez et al. 2002; Amarzguioui et al. 2003; Holen et al. 2003). However, it is important to note that these studies did not address the role of nucleotides and the structure of siRNA at internal sequence positions. Here, we have specifically demonstrated the significance of nucleotides within the RNA duplex and their role in defining the structure of siRNA required for RNAi in vivo. These results indicated that, like RISC*, the RNA helicase, which has not yet been identified, also recognizes structural properties of the siRNA duplex as opposed to specific sequences of the RNA strands. This recognition appears to be asymmetric, with the structure of the antisense 5′ half of siRNA duplexes favored over the 3′ half, and is similar to how restriction enzymes can preferentially cleave the DNA backbone asymmetrically within a palindromic sequence. Further structural analysis of siRNAs to define what properties within the antisense 5′ half of the duplex contribute to the asymmetric nature of the duplex should help elucidate the specific structural elements required for duplex recognition by the RNA helicase for siRNA unwinding.

Our results showing that the modified siRNAs displayed effective RNAi in vivo and in vitro was also significant as it confirmed that the observed gene silencing was mediated by the RNAi pathway. These results also indicated that using chemical modifications that allow for efficient RNAi induction should work in the design of any given siRNA to increase its stability and capacity to specifically induce RNAi in vivo. Using these chemical modifications should take the field of RNAi quite a large step forward beyond the limits presently imposed by unmodified siRNAs with respect to long-term RNAi induction and targeting efficiency. One can imagine numerous applications for all of the chemical modifications used in this analysis, from studying prolonged RNAi effects on multiple genes in human cell cultures to opening up the door for long-term RNAi efficacy in therapeutic realms for curing a variety of genetic diseases.

From the data presented here, the mechanism of RNAi has been further elucidated and the groundwork for incorporating RNAi successfully into therapeutic realms has been laid out. We hope that future studies using the insight garnered here will not only help direct studies for further dissection of the mechanism of RNAi but will lead to new discoveries about gene function and facilitate the introduction of RNAi into vital clinical applications.

MATERIALS AND METHODS

siRNA preparation

The sequences of EGFP target-specific siRNA duplexes were designed as previously described (Chiu and Rana 2002). The 21-nt RNAs were chemically synthesized as 2′-bis(acetoxyethoxy)-methyl ether-protected oligonucleotides by Dharmacon. Synthetic oligonucleotides were deprotected, annealed, and purified; successful duplex formation was confirmed by 20% nondenaturing polyacrylamide gel electrophoresis (Chiu and Rana 2002).

Culture and transfection of cells

HeLa cells were maintained at 37°C in Dulbecco's modified Eagle's medium (DMEM, Invitrogen) supplemented with 10% fetal bovine serum (FBS), 100 units/mL penicillin, and 100 μg/mL streptomycin (Invitrogen). Cells were regularly passaged at subconfluence and plated 16 h before transfection at 70% confluency. Lipofectamine (Invitrogen)-mediated transient cotransfections of reporter plasmids and siRNAs were performed in duplicate 6-well plates. A transfection mixture containing 0.16 μg of pEGFP-C1

and 0.33 μg of pDsRed2-N1 reporter plasmids (Clontech), various amounts of siRNA (1.0–200 nM), and 10 μL of lipofectamine in 1 mL of serum-reduced OPTI-MEM (Invitrogen) was added to each well. Cells were incubated in the transfection mixture for 6 h and further cultured in antibiotic-free DMEM. Cells were treated under the same conditions without siRNA for mock experiments. At various time intervals, the transfected cells were washed twice with phosphate-buffered saline (PBS, Invitrogen), flash-frozen in liquid nitrogen, and stored at −80°C for reporter gene assays.

Improved dual fluorescence assay

In an improved dual fluorescence reporter assay, EGFP-C1 encoded enhanced green fluorescence protein (GFP) and DsRed2-N1 encoded red fluorescence protein DsRed2 (RFP), a DsRed variant that has been engineered for faster maturation and lower unspecific aggregation. The extinction coefficient of DsRed2 is 43,800 M^{-1} cm^{-1}, and the quantum yield is 0.55, a significant quantitative increase when compared with the DsRed1 vector used in the dual fluorescence assay (Chiu and Rana 2002). To quantify RNAi effects, cell lysates were prepared from siRNA duplex-treated cells at 42 h posttransfection, as described previously (Chiu and Rana 2002). Then 240 μg of total cell lysate in 160 μL of reporter lysis buffer was measured by fluorescence spectrophotometry (Photo Technology International). The slit widths were set at 4 nm for both excitation and emission. All experiments were carried out at room temperature. GFP fluorescence in cell lysates was detected by exciting at 488 nm and recording from 498 to 650 nm. The spectrum peak at 507 nm represents the fluorescence intensity of GFP. RFP fluorescence in the same cell lysates was detected by exciting at 568 nm and recording from 588 to 650 nm. The spectrum peak at 583 nm represents the fluorescence intensity of RFP. The fluorescence intensity ratio of target (GFP) to control (RFP) fluorophores was determined in the presence of siRNA duplexes and normalized to that observed in the mock-treated cells. Normalized ratios at <1.0 indicated specific interference.

Study of duplex siRNA stability in HeLa cell lysate

Unmodified or modified EGFP antisense strand siRNAs were 5′-labeled with [γ-^{32}P]ATP (3000 Ci/mM; ICN) by T4 polynucleotide kinases (New England Biolabs) at 37°C for 1 h and chase-kinased by adding 1 mM ATP at 37°C for 15 min. Free ATP and kinases were removed by the QIAGEN nucleotide removal kit. RNA was then purified by 20% polyacrylamide gel containing 7 M urea. Duplex siRNAs were formed by annealing equal molar ratios of unmodified or modified sense-strand siRNAs with the 5′-^{32}P-labeled antisense strand. Duplex formation was confirmed by 20% PAGE under native condition. We incubated 50 pmole of duplex siRNAs labeled at the 5′-end of the antisense strand with 500 μg of HeLa whole-cell extract in a 50-μL reaction mixture containing 20 mM HEPES (pH 7.9), 100 mM KCl, 10 mM NaCl, 2 mM $MgCl_2$, and 10% glycerol. At various time points, 8-μL aliquots were mixed with 16 μL of loading buffer (0.01% bromophenol blue, 0.01% xylene cyanol, 98% formaldehyde, and 5 mM EDTA). The products were then denatured by heating at 95°C for 10 min and analyzed on 20% polyacrylamide gel containing 7 M urea followed by phosphorimage analysis (Fugi).

Preparation of HeLa cells cytoplasmic extract

Cytoplasm from HeLa cells was prepared following the Dignam protocol for isolation of HeLa cell nuclei (Dignam et al. 1983). The cytoplasmic fraction was dialyzed against cytoplasmic extract buffer (20 mM HEPES at pH 7.9, 100 mM KCl, 200 μM EDTA, 500 μM DTT, 500 μM PMSF, 2 mM $MgCl_2$, 10% glycerol). The extract can be stored frozen at −70°C after quick-freezing in liquid nitrogen. The protein concentration of HeLa cytoplasmic extract varied between 4 and 5 mg/mL as determined by a Biorad protein assay kit.

Preparation of cap-labeled target mRNA

For mapping of the target RNA cleavage, a 124-nt EGFP transcript, corresponding to nucleotides 195–297 relative to the start codon followed by the 21-nt complement of the SP6 promoter sequence, was amplified from template pEGFP-C1 by PCR using the 5′ primer GCCTAATACGACTCACTATAGGACCTACGGCGTGCA GTGC (T7 promoter underlined) and the 3′ primer TTGATTTAG GTGACACTATAGATGGTGCGCTCCTG-GACGT (SP6 promoter underlined). His-tagged mammalian capping enzyme was expressed in *Escherichia coli* from a plasmid generously provided by Stewart Shuman (Molecular Biology Program, Sloan-Kettering Institute, New York) and purified to homogeneity. Guanylyltransferase labeling was performed by incubating 1 nmole of transcripts with 50 pmole of His-tagged mammalian capping enzyme in the 100-μL capping reaction containing 50 mM Tris-HCl (pH 8.0), 5 mM DTT, 2.5 mM $MgCl_2$, 1 U/μL RNasin RNase inhibitor (Promega), and [α-^{32}P]GTP at 37°C for 1 h. Reactions were chased for 30 min by supplementing GTP concentration to 100 μM. Cap-labeled target mRNAs were resolved on 10% polyacrylamide-7 M urea gel and purified.

In vitro target mRNA cleavage assay

siRNA-mediated cleavage of target mRNA in human cytoplasmic extract was performed as described (Martinez et al. 2002) with some modifications. siRNA duplexes were preincubated in HeLa cytoplasmic extract at 37°C for 15 min prior to addition of the 124-nt cap-labeled target mRNA generated as described above. After addition of all components, the final concentrations were 500 nM siRNA, 50 nM target mRNA, 1 mM ATP, 0.2 mM GTP, 1 U/μL RNasin, 30 μg/mL creatine kinase, 25 mM creatine phosphate, and 50% S100 extract. Incubation was continued for 1.5 h. Cleavage reactions were stopped by the addition of 8 volumes of proteinase K buffer (200 mM Tris-HCl at pH 7.5, 25 mM EDTA, 300 mM NaCl, and 2% [w/v] SDS). Proteinase K, dissolved in 50 mM Tris-HCl (pH 8.0), 5 mM $CaCl_2$, and 50% glycerol, was added to a final concentration of 0.6 mg/mL. Reaction products were extracted with phenol/chloroform/isoamyl alcohol (25:24:1), chloroform, and precipitated with 3 volumes of ethanol. Samples were separated on 8% polyacrylamide-7 M urea gels.

ACKNOWLEDGMENTS

We thank Tamara J. Richman for assistance in editing and critical evaluation of the work. We also thank B. Cullen, C. Mello, and P. Zamore for useful discussions and S. Shuman for kindly providing

reagents. This work was supported by grants from the NIH (AI41404, AI45466, and AI43198).

The publication costs of this article were defrayed in part by payment of page charges. This article must therefore be hereby marked "advertisement" in accordance with 18 USC section 1734 solely to indicate this fact.

Received May 28, 2003; accepted June 16, 2003.

REFERENCES

Amarzguioui, M., Holen, T., Babaie, E., and Prydz, H. 2003. Tolerance for mutations and chemical modifications in a siRNA. *Nucleic Acids Res.* **31:** 589–595.

Bailly, C. and Waring, M.J. 1998. The use of diaminopurine to investigate structural properties of nucleic acids and molecular recognition between ligands and DNA. *Nucl. Acids Res.* **19:** 4309–4314.

Bernstein, E., Caudy, A.A., Hammond, S.M., and Hannon, G.J. 2001. Role for a bidentate ribonuclease in the initiation step of RNA interference. *Nature* **409:** 363–366.

Chiu, Y.L. and Rana, T.M. 2002. RNAi in human cells: Basic structural and functional features of small interfering RNA. *Mol. Cell* **10:** 549–561.

Cogoni, C. and Macino, G. 1999. Gene silencing in *Neurospora crassa* requires a protein homologous to RNA-dependent RNA polymerase. *Nature* **399:** 166–169.

Cummins, L.L., Owens, S.R., Risen, L.M., Lesnik, E.A., Freier, S.M., McGee, D., Guinosso, C.J., and Cook, P.D. 1995. Characterization of fully 2′-modified oligoribonucleotide hetero- and homoduplex hybridization and nuclease sensitivity. *Nucleic Acids Res.* **23:** 2019–2024.

Dalmay, T., Hamilton, A., Rudd, S., Angell, S., and Baulcombe, D.C. 2000. An RNA-dependent RNA polymerase gene in *Arabidopsis* is required for posttranscriptional gene silencing mediated by a transgene but not by a virus. *Cell* **101:** 543–553.

Dignam, J.D., Lebovitz, R.M., and Roeder, R.G. 1983. Accurate transcription initiation by RNA polymerase II in a soluble extract from isolated mammalian nuclei. *Nucleic Acids Res.* **11:** 1475–1489.

Elbashir, S.M., Lendeckel, W., and Tuschl, T. 2001a. RNA interference is mediated by 21- and 22-nucleotide RNAs. *Genes & Dev.* **15:** 188–200.

Elbashir, S.M., Martinez, J., Patkaniowska, A., Lendeckel, W., and Tuschl, T. 2001b. Functional anatomy of siRNAs for mediating efficient RNAi in *Drosophila melanogaster* embryo lysate. *EMBO J.* **20:** 6877–6888.

Haaima, G., Hansen, H.F., Christensen, L., Dahl, O., and Nielsen, P.E. 1997. Increased DNA binding and sequence discrimination of PNA oligomers containing 2,6-diaminopurine. *Nucleic Acids Res.* **25:** 4639–4643.

Hamilton, A., Voinnet, O., Chappell, L., and Baulcombe, D. 2002. Two classes of short interfering RNA in RNA silencing. *EMBO J.* **21:** 4671–4679.

Hammond, S.M., Bernstein, E., Beach, D., and Hannon, G.J. 2000. An RNA-directed nuclease mediates post-transcriptional gene silencing in *Drosophila* cells. *Nature* **404:** 293–296.

Hammond, S.M., Caudy, A.A., and Hannon, G.J. 2001. Post-transcriptional gene silencing by double-stranded RNA. *Nat. Rev. Genet.* **2:** 110–119.

Holen, T., Amarzguioui, M., Babaie, E., and Prydz, H. 2003. Similar behaviour of single-strand and double-strand siRNAs suggests they act through a common RNAi pathway. *Nucleic Acids Res.* **31:** 2401–2407.

Hutvagner, G. and Zamore, P.D. 2002. A microRNA in a multiple-turnover RNAi enzyme complex. *Science* **297:** 2056–2060.

Kennerdell, J.R. and Carthew, R.W. 1998. Use of dsRNA-mediated genetic interference to demonstrate that frizzled and frizzled 2 act in the wingless pathway. *Cell* **95:** 1017–1026.

Kirnos, M.D., Khudyakov, I.Y., Alexandrushkina, N.I., and Vanyushin, B.F. 1977. 2-Aminoadenine is an adenine substituting for a base in S-2L cyanophage DNA. *Nature* **270:** 369–370.

Lipardi, C., Wei, Q., and Paterson, B.M. 2001. RNAi as random degradative PCR: siRNA primers convert mRNA into dsRNAs that are degraded to generate new siRNAs. *Cell* **107:** 297–307.

Luy, B. and Marino, J.P. 2001. Measurement and application of ^{1}H–^{19}F dipolar couplings in the structure determination of 2′-fluoro-labeled RNA. *J. Biomol. NMR* **20:** 39–47.

Majlessi, M., Nelson, N.C., and Becker, M.M. 1998. Advantages of 2′-*O*-methyl oligoribonucleotide probes for detecting RNA targets. *Nucleic Acids Res.* **26:** 2224–2229.

Martinez, J., Patkaniowska, A., Urlaub, H., Luhrmann, R., and Tuschl, T. 2002. Single-stranded antisense siRNAs guide target RNA cleavage in RNAi. *Cell* **110:** 563–574.

McManus, M.T. and Sharp, P.A. 2002. Gene silencing in mammals by small interfering RNAs. *Nat. Rev. Genet.* **3:** 737–747.

Nishikura, K. 2001. A short primer on RNAi: RNA-directed RNA polymerase acts as a key catalyst. *Cell* **107:** 415–418.

Nykanen, A., Haley, B., and Zamore, P.D. 2001. ATP requirements and small interfering RNA structure in the RNA interference pathway. *Cell* **107:** 309–321.

Parrish, S., Fleenor, J., Xu, S., Mello, C., and Fire, A. 2000. Functional anatomy of a dsRNA trigger: Differential requirement for the two trigger strands in RNA interference. *Mol. Cell* **6:** 1077–1087.

Provost, P., Dishart, D., Doucet, J., Frendewey, D., Samuelsson, B., and Radmark, O. 2002. Ribonuclease activity and RNA binding of recombinant human Dicer. *EMBO J.* **21:** 5864–5874.

Saenger, W. 1984. Forces stabilizing association between bases: hydrogen bonding and base stacking. In *Principles of nucleic acid structure* (ed. C.R. Cantor), pp. 116–158. Springer-Verlag, New York.

Schwarz, D.S., Hutvagner, G., Haley, B., and Zamore, P.D. 2002. Evidence that siRNAs function as guides, not primers, in *Drosophila* and human RNAi pathways. *Mol. Cell* **10:** 537–548.

Sijen, T., Fleenor, J., Simmer, F., Thijssen, K.L., Parrish, S., Timmons, L., Plasterk, R.H., and Fire, A. 2001. On the role of RNA amplification in dsRNA-triggered gene silencing. *Cell* **107:** 465–476.

Stark, G.R., Kerr, I.M., Williams, B.R., Silverman, R.H., and Schreiber, R.D. 1998. How cells respond to interferons. *Annu. Rev. Biochem.* **67:** 227–264.

Stein, C.A. 1996. Phosphorothioate antisense oligodeoxynucleotides: Questions of specificity. *Trends Biotechnol.* **14:** 147–149.

Stein, P., Svoboda, P., Anger, M., and Schultz, R.M. 2003. RNAi: Mammalian oocytes do it without RNA-dependent RNA polymerase. *RNA* **9:** 187–192.

Zamore, P.D. 2001. RNA interference: Listening to the sound of silence. *Nat. Struct. Biol.* **8:** 746–750.

Zamore, P.D., Tuschl, T., Sharp, P.A., and Bartel, D.P. 2000. RNAi: Double-stranded RNA directs the ATP-dependent cleavage of mRNA at 21 to 23 nucleotide intervals. *Cell* **101:** 25–33.

Zhang, H., Kolb, F.A., Brondani, V., Billy, E., and Filipowicz, W. 2002. Human Dicer preferentially cleaves dsRNAs at their termini without a requirement for ATP. *EMBO J.* **21:** 5875–5885.

TAB 10

Fully 2′-Modified Oligonucleotide Duplexes with Improved in Vitro Potency and Stability Compared to Unmodified Small Interfering RNA

Charles R. Allerson,*,† Namir Sioufi,‡ Russell Jarres,‡ Thazha P. Prakash,† Nishant Naik,† Andres Berdeja,§ Lisa Wanders,§ Richard H. Griffey,† Eric E. Swayze,† and Balkrishen Bhat†

Departments of Medicinal Chemistry, Antisense Lead Identification, and Research Chemistry, Isis Pharmaceuticals, 2292 Faraday Avenue, Carlsbad, California 92008

Received October 18, 2004

Abstract: We have identified a small interfering RNA (siRNA) motif, consisting entirely of 2′-*O*-methyl and 2′-fluoro nucleotides, that displays enhanced plasma stability and increased in vitro potency. At one site, this motif showed remarkable >500-fold improvement in potency over the unmodified siRNA. This marks the first report of such a potent fully modified motif, which may represent a useful design for therapeutic oligonucleotides.

The specific and reversible modulation of gene expression through the use of short synthetic oligonucleotides has proven useful in the study of gene function and as a therapeutic mechanism in man.[1] Recently, RNA interference (RNAi) has emerged as a novel mechanism that is activated in mammalian cells by small interfering RNAs (siRNAs), short RNA duplexes with strands of 21−23 nucleotides.[2,3] Once inside the cell, siRNAs associate with proteins to form an RNA-induced silencing complex (RISC).[4] A helicase activity associated with RISC separates the two strands of the duplex,[5] releasing the sense strand and permitting the binding of the antisense strand to its messenger RNA (mRNA) target. The resulting duplex is a substrate for a RISC-associated nuclease, recently identified as Ago2 (also known as eIF2C2 in man),[6] which cleaves the target transcript at a single site.[5,7]

Despite attempts to use siRNA in vivo,[8−14] the reduction of endogenous target mRNAs through the systemic delivery of siRNA has proven difficult. Although there have been conflicting reports on the nuclease stability of unmodified siRNA duplexes, there is evidence that many are degraded within minutes in mammalian serum.[9,15,16] It seems likely that siRNAs with increased nuclease stability will have a better chance at eliciting an in vivo response. Efforts to determine the optimal use of stabilizing chemistries have been the focus of several recent reports.[15,17−21] From these studies, the 2′-*O*-methyl (2′-OMe) and 2′-deoxy-2′-fluoro (2′-F) modifications have shown promise in stabilizing siRNA without disrupting the efficiency of mRNA target reduction. To further optimize the use of these and other chemistries in siRNA, we are conducting an extensive SAR analysis of chemically modified siRNA. One of the most promising designs from these studies is a fully modified duplex that consists of alternating 2′-OMe and 2′-F nucleotides. Surprisingly, duplexes with this substitution display increased in vitro potency and increased stability. Here, we report on this remarkably active motif and present our preliminary findings.

The duplexes used in our SAR study were designed to target one of two sites within the coding region of the human PTEN mRNA, both previously reported as valid target sites for siRNA.[22] Modified and unmodified duplexes were introduced into HeLa cells using a cationic lipid transfection reagent (lipofectin). In vitro activity was measured by performing RT-PCR on the PTEN mRNA and comparing to mRNA levels of untreated cells. All PTEN signals were normalized to total RNA, as measured with RiboGreen.[23]

Natural Dicer-generated siRNAs have 2-nucleotide 3′ overhangs on both ends of the short duplex.[2] In an effort to mimick this design, most synthetic siRNAs are designed with 3′ overhangs, typically with the sequence dTdT. Several recent reports have provided evidence that these overhangs bind to the PAZ domains found in numerous proteins, including the Ago2 component of RISC, perhaps functioning as a specificity determinant.[24−28] However, there have been other reports that blunt-ended RNA duplexes can function equally well and may be more stable to exonucleolytic degradation.[21] Given our goal of developing duplexes with optimal stability and activity, we explored the use of blunt-ended duplexes at both PTEN target sites (sites A and B). The activities of 19-base-pair duplexes having 3′-dTdT overhangs (**1** and **4**) were compared to those of otherwise identical blunt-ended duplexes (**2** and **5**) in a 10-point dose-response experiment (Figure 1). We found only a minimal impact on activity with the removal of the overhangs. To confirm the specificity of PTEN mRNA reduction, duplexes containing six mismatches (**3** and **6**) to the target site were included as negative controls in each experiment. Neither control affected PTEN mRNA or total RNA levels.

After validation of the use of blunt-ended constructs, the remaining SAR was performed without the use of 3′ overhangs. Among the duplex designs examined were several that belonged to a class of "alternating" motifs in which one type of modified nucleotide was placed in alternating positions with a ribonucleotide or a different modified nucleotide. In a recent publication, motifs of this type, using 2′-OMe and unmodified (2′-OH) nucleotides, were shown to have enhanced serum stability and single dose in vitro activities similar to those of the corresponding unmodified blunt-ended duplexes.[21] During the course of our studies, we examined siRNAs with the same 2′-OMe/2′-OH substitution. We found that duplexes with this motif had in vitro potencies similar to those of unmodified siRNAs (see Supporting Information). As part of our broader SAR studies, however, we also examined the effect of combining the 2′-OMe substitution with other chemistries, such as 2′-F, which has already been shown to be well-tolerated in siRNA.[15] This led to the identification of our most potent con-

* To whom correspondence should be addressed. Phone: 760-603-4697. Fax: 760-603-4654. E-mail: callerson@isisph.com.
† Department of Medicinal Chemistry.
‡ Department of Antisense Lead Identification.
§ Department of Research Chemistry.

10.1021/jm049167j CCC: $30.25
Published on Web 01/20/2005

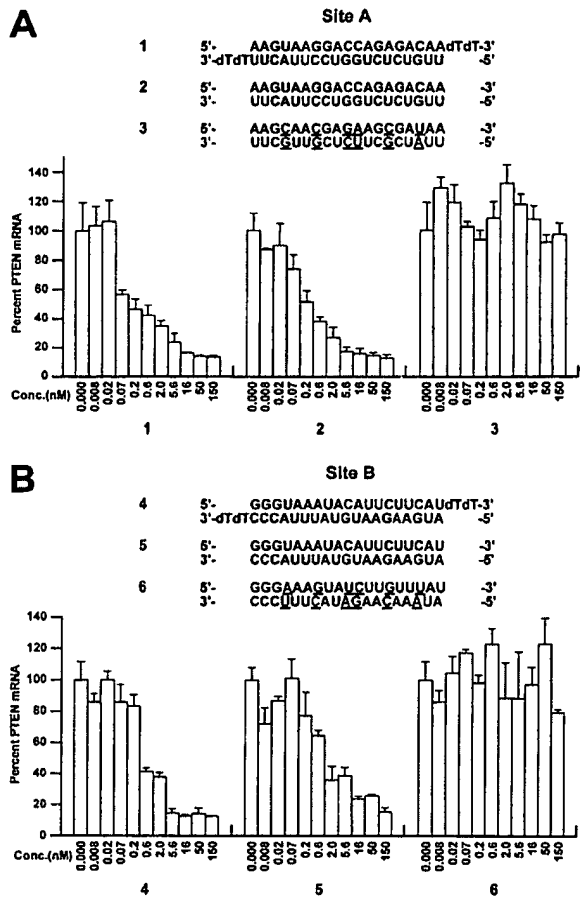

Figure 1. Reduction of endogenous PTEN mRNA in HeLa cells by siRNAs having 3′-dTdT overhangs or blunt ends. HeLa cells were transfected with siRNAs at the indicated concentrations in the presence of lipofectin and treated for 20 h followed by lysis and RT-PCR. Message levels are reported as percent of PTEN mRNA from untreated cells. The bottom strand of each duplex is complementary to the target mRNA (mismatches to the target site are indicated with an underline). (A) PTEN mRNA reduction by siRNAs targeted to site A. Cells were also treated with a duplex containing six mismatches to the target site as a negative control (**3**). (B) PTEN mRNA reduction by siRNAs targeted to site B. Cells were also treated with a duplex containing six mismatches to the target site as a negative control (**6**).

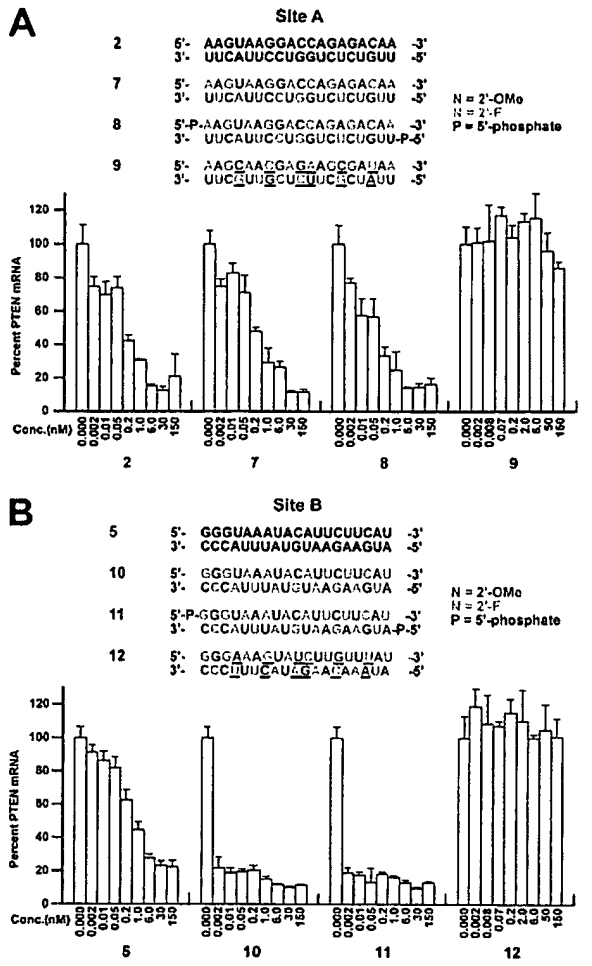

Figure 2. Reduction of endogenous PTEN mRNA in HeLa cells by unmodified or fully 2′-F/2′-OMe modified 19-base-pair oligonucleotide duplexes. HeLa cells were transfected with siRNAs at the indicated concentrations in the presence of lipofectin and treated for 20 h followed by lysis and RT-PCR. Message levels are reported as percent of PTEN mRNA from untreated cells. The bottom strand of each duplex is complementary to the target mRNA (mismatches to the target site are indicated with an underline). The 2′-F modification is indicated in green, the 2′-OMe modification is indicated in purple, while the presence of a 5′-phosphate is indicated by the letter "P". (A) PTEN mRNA reduction by duplexes targeted to site A. (B) PTEN mRNA reduction by duplexes targeted to site B.

struct design, in which both strands were substituted with alternating 2′-OMe and 2′-F nucleotides (Figure 2). From an eight-point dose-response analysis in HeLa cells, we were able to estimate IC_{50} values of each duplex (Table 1; see also Supporting Information).

At site A, the duplex with alternating 2′-F/2′-OMe chemistry (**7**, Figure 2) had biological activity that was roughly equivalent to that of the parent siRNA (**2**). At site B, however, the 2′-F/2′-OMe duplex (**10**) displayed dramatically improved potency. Even at the lowest concentration (2 pM), target reduction was greater than 75% relative to untreated control, minimally reflecting 500-fold improvement in potency over the unmodified siRNA (**5**). Throughout these studies, we were cognizant of the importance of the 5′-phosphates normally present on Dicer-generated siRNA duplexes. The 5′-phosphate on the antisense strand has been shown to be critical for efficient assembly and activation of RISC in mammalian systems.[29] However, it has been shown that

Table 1. Summary of in Vitro Activity, Plasma Stability, and Duplex Thermal Stability[a]

duplex	site	IC_{50} (nM)	plasma half-life (min)	T_m (°C)
2	A	0.26	~30	72.8
7	A	0.31	nd	93.9
8	A	0.068	>420	nd
5	B	0.81	nd	62.0
10	B	<0.002	nd	nd
11	B	<0.002	>420	82.0

[a] nd = not determined.

prephosphorylation is generally unnecessary because the siRNAs are phosphorylated by endogenous kinases. Anticipating that chemically modified duplexes might be less efficiently processed by these kinases,[30] we compared the activities of 2′-F/2′-OMe duplexes with preestablished 5′-phosphates (Figure 2, **8** and **11**). At site A, addition of a synthetic 5′-phosphate produced

modest improvement (5-fold) in potency (Table 1). Given the already potent activity of **10**, we were unable to resolve any beneficial effect of 5′-phosphorylation at site B. Similar effects from phosphorylation have been observed with this motif on other targets, where modestly active duplexes show improvement of in vitro potency upon addition of the 5′-phosphate, while the effect on extremely potent duplexes is difficult to resolve (data not shown). Furthermore, the 5′-phosphate on the antisense strand appears to be largely responsible for this improvement in potency, although the magnitude of the effect may depend on cell type (data not shown). We also prepared and tested modified duplexes that contained six mismatches to either of the target sites (**9** and **12**). Neither mismatch-containing duplex produced a significant reduction in PTEN mRNA or total RNA.

To examine the relative serum stabilities of these duplexes, we tested unmodified siRNA **2** and 2′-F/2′-OMe modified duplexes **8** and **11** for their ability to resist degradation in mouse plasma. Each of the duplexes was treated with 25% mouse plasma at 37 °C for up to 7 h. At various time points, aliquots were removed and examined for intact duplex by capillary gel electrophoresis.[31,32] From these measurements, we plotted percent intact duplex against time and assessed the relative stabilities of the three duplexes (Figure 3A, Table 1). From this straightforward analysis, the stability of the 2′-F/2′-OMe duplexes was striking. Even after 7 h, the duplexes were greater than 60% (**8**) or 70% (**11**) intact. While there was an initial loss of duplex in each case, this may correspond to rapid loss of imperfectly annealed strands. Regardless, the remaining duplex degrades at a rate that suggests a half-life of much greater than 7 h.

It has previously been shown that the use of 2′-F modifications can increase the thermal stability of oligonucleotide duplexes.[33] Because duplexes **7**, **8**, **10**, and **11** each contain a total of 19 2′-F nucleotides, we anticipated that these duplexes might have much greater thermal stabilities than their unmodified counterparts. To examine this possibility, we measured the thermal stabilities of two control duplexes (**2** and **5**) and two modified duplexes (**7** and **11**) (Figure 3B). In each case we see a roughly 20 °C increase in T_m with the fully modified duplexes. This corresponds to slightly more than 1 °C increase in T_m per 2′-F substitution. This increase in thermal stability is likely to explain in part the enhanced plasma stability of the modified duplexes and may improve the interaction between the antisense strand and the target mRNA.

It is surprising that duplexes with such high thermal stabilities can function so efficiently and potently relative to the unmodified siRNAs. Recent studies have suggested that RISC chooses which strand to retain on the basis of differences in thermodynamic stability at the 5′ ends of the strands, with the strand having the 5′ end of lower stability being more likely to load into RISC.[34,35] It is worth noting that one end of the site B duplex contains three consecutive G–C base pairs. Although the introduction of 2′-F nucleotides should raise the thermodynamic stability of both ends of the duplex, it may increase the already more-stable end above a critical threshold that the RISC-associated

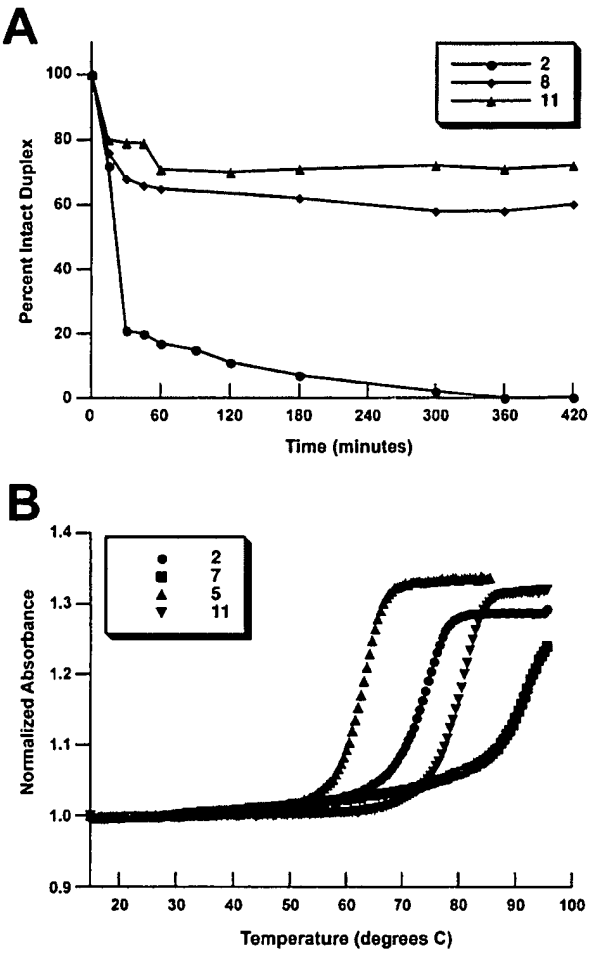

Figure 3. Comparison of the biophysical properties of unmodified blunt-ended siRNAs and 2′-F/2′-OMe modified duplexes. (A) Stability of duplexes in 25% (v/v) mouse plasma. Duplexes were treated with 25% mouse plasma at 37 °C for the indicated times, then examined by capillary gel electrophoresis to determine the amount of intact duplex (see Supporting Information for details). The plots shown are the result of two independent experiments. (B) Thermal denaturation profiles of both unmodified and modified duplexes in 100 mM NaCl, 10 mM sodium phosphate, pH 7.5, 0.1 mM EDTA, and 4 μM of each strand. Absorbance at 260 nm was measured as the temperature was raised from 15 to 85 °C or from 30 to 95 °C. Absorbances were normalized to facilitate graphical depiction. Melting temperatures (T_m) were calculated from first-derivative curves of at least two separate experiments and are summarized in Table 1.

helicase cannot overcome, shifting the bias for strand-loading more in favor of the antisense strand. We also observed that among the unmodified duplexes, the best activity comes from the duplex having the highest T_m, whereas the opposite is true for the 2′-F/2′-OMe motif. Although not definitive, these relationships may hint at the existence of an optimal thermal stability.

From these observations, the alternating 2′-F/2′-OMe motif appears to be an attractive design for creating functionally active and stable RNA duplexes. Clearly, these duplexes potently reduce levels of endogenous target mRNA, with the addition of a 5′-phosphate to the antisense strand further enhancing in vitro potency. The biophysical properties of this duplex motif, reflected in its enhanced serum and thermal stability, also favor its chances at surviving in serum, which will hopefully

translate to improved in vivo potency. The identification of this motif from our SAR analysis highlights the value of screening oligonucleotides containing multiple chemistries and may prove a useful strategy in related areas such as micro-RNA. Although promising, the utility and optimal design of this motif for in vivo applications and a biochemical explanation for the remarkable increase in potency remain to be determined and are the focus of ongoing studies. We anticipate that this and other chemically modified duplex motifs will ultimately prove useful in the design of clinically active nucleic acids.

Acknowledgment. The authors thank Bruce Ross, Mystie Nguyen, and Mingming Han for providing the 2′-*O*-methyl and 2′-deoxy-2′-fluoro nucleoside phosphoramidites, Hans Gaus, Sam Lee, and Jodee Steinberg for their assistance in oligonucleotide analysis, and Prasad Dande, Sue Freier, Bridget Lollo, and Brenda Baker for their thoughtful discussions about this project.

Supporting Information Available: Methods for the synthesis and purification of the oligonucleotides, mass spectral and capillary gel electrophoresis data of each compound, and details of the biological and biochemical assays. This material is available free of charge via the Internet at http://pubs.acs.org.

References

(1) Crooke, S. T. Molecular mechanisms of action of antisense drugs. *Biochim. Biophys. Acta* **1999**, *1489*, 31−44.
(2) Elbashir, S. M.; Harborth, J.; Lendeckel, W.; Yalcin, A.; Weber, K.; et al. Duplexes of 21-nucleotide RNAs mediate RNA interference in cultured mammalian cells. *Nature* **2001**, *411*, 494−498.
(3) Caplen, N. J.; Parrish, S.; Imani, F.; Fire, A.; Morgan, R. A. Specific inhibition of gene expression by small double-stranded RNAs in invertebrate and vertebrate systems. *Proc. Natl. Acad. Sci. U.S.A.* **2001**, *98*, 9742−9747.
(4) Hammond, S. M.; Bernstein, E.; Beach, D.; Hannon, G. J. An RNA-directed nuclease mediates post-transcriptional gene silencing in Drosophila cells. *Nature* **2000**, *404*, 293−296.
(5) Martinez, J.; Patkaniowska, A.; Urlaub, H.; Luhrmann, R.; Tuschl, T. Single-Stranded Antisense siRNAs Guide Target RNA Cleavage in RNAi. *Cell* **2002**, *110*, 563−574.
(6) Liu, J.; Carmell, M. A.; Rivas, F. V.; Marsden, C. G.; Thomson, J. M.; et al. Argonaute2 Is the Catalytic Engine of Mammalian RNAi. *Science (Washington, D.C.)* **2004**, *305*, 1437−1441.
(7) Haley, B.; Zamore, P. D. Kinetic analysis of the RNAi enzyme complex. *Nat. Struct. Mol. Biol.* **2004**, *11*, 599−606.
(8) Zhang, X.; Shan, P.; Jiang, D.; Noble, P. W.; Abraham, N. G.; et al. Small Interfering RNA Targeting Heme Oxygenase-1 Enhances Ischemia-Reperfusion-Induced Lung Apoptosis. *J. Biol. Chem.* **2004**, *279*, 10677−10684.
(9) Braasch, D. A.; Paroo, Z.; Constantinescu, A.; Ren, G.; Oz, O. K.; et al. Biodistribution of phosphodiester and phosphorothioate siRNA. *Bioorg. Med. Chem. Lett.* **2004**, *14*, 1139−1143.
(10) Song, E.; Lee, S. K.; Wang, J.; Ince, N.; Ouyang, N.; et al. RNA interference targeting Fas protects mice from fulminant hepatitis. *Nat. Med.* **2003**, *9*, 347−351.
(11) Zender, L.; Huetker, S.; Liedtke, C.; Tillmann, H. L.; Zender, S.; et al. Caspase 8 small interfering RNA prevents acute liver failure in mice. *Proc. Natl. Acad. Sci. U.S.A.* **2003**, *100*, 7797−7802.
(12) Sorensen, D. R.; Leirdal, M.; Sioud, M. Gene Silencing by Systemic Delivery of Synthetic siRNAs in Adult Mice. *J. Mol. Biol.* **2003**, *327*, 761−766.
(13) Layzer, J. M.; McCaffrey, A. P.; Tanner, A. K.; Huang, Z.; Kay, M. A.; et al. In vivo activity of nuclease-resistant siRNAs. *RNA* **2004**, *10*, 766−771.
(14) Soutschek, J.; Akinc, A.; Bramlage, B.; Charisse, K.; Constien, R.; et al. Therapeutic silencing of an endogenous gene by systemic administration of modified siRNAs. *Nature (London)* **2004**, *432*, 173−178.
(15) Chiu, Y. L.; Rana, T. M. siRNA function in RNAi: A chemical modification analysis. *RNA* **2003**, *9*, 1034−1048.
(16) Braasch, D. A.; Jensen, S.; Liu, Y.; Kaur, K.; Arar, K.; et al. RNA Interference in Mammalian Cells by Chemically-Modified RNA. *Biochemistry* **2003**, *42*, 7967−7975.
(17) Capodici, J.; Kariko, K.; Weissman, D. Inhibition of HIV-1 Infection by Small Interfering RNA-Mediated RNA Interference. *J. Immunol.* **2002**, *169*, 5196−5201.
(18) Harborth, J.; Elbashir, S. M.; Vandenburgh, K.; Manninga, H.; Scaringe, S. A.; et al. Sequence, Chemical, and Structural Variation of Small Interfering RNAs and Short Hairpin RNAs and the Effect on Mammalian Gene Silencing. *Antisense Nucleic Acid Drug Dev.* **2003**, *13*, 83−105.
(19) Amarzguioui, M.; Holen, T.; Babaie, E.; Prydz, H. Tolerance for mutations and chemical modifications in a siRNA. *Nucleic Acids Res.* **2003**, *31*, 589−595.
(20) Holen, T.; Amarzguioui, M.; Babaie, E.; Prydz, H. Similar behaviour of single-strand and double-strand siRNAs suggests they act through a common RNAi pathway. *Nucleic Acids Res.* **2003**, *31*, 2401−2407.
(21) Czauderna, F.; Fechtner, M.; Dames, S.; Aygun, H.; Klippel, A.; et al. Structural variations and stabilising modifications of synthetic siRNAs in mammalian cells. *Nucleic Acids Res.* **2003**, *31*, 2705−2716.
(22) Vickers, T. A.; Koo, S.; Bennett, C. F.; Crooke, S. T.; Dean, N. M.; et al. Efficient Reduction of Target RNAs by Small Interfering RNA and RNase H-Dependent Antisense Agents. *J. Biol. Chem.* **2003**, *278*, 7108−7118.
(23) Hashimoto, J. G.; Beadles-bohling, A. S.; Wiren, K. M. Comparison of RiboGreen and 18S rRNA quantitation for normalizing real-time RT-PCR expression analysis. *BioTechniques* **2004**, *36*, 54, 56, 58−60.
(24) Lingel, A.; Simon, B.; Izaurralde, E.; Sattler, M. Structure and nucleic-acid binding of the Drosophila Argonaute 2 PAZ domain. *Nature (London)* **2003**, *426*, 465−469.
(25) Song, J.-J.; Liu, J.; Tolia, N. H.; Schneiderman, J.; Smith, S. K.; et al. The crystal structure of the Argonaute2 PAZ domain reveals an RNA binding motif in RNAi effector complexes. *Nat. Struct. Biol.* **2003**, *10*, 1026−1032.
(26) Yan, K. S.; Yan, S.; Farooq, A.; Han, A.; Zeng, L.; et al. Structure and conserved RNA binding of the PAZ domain. *Nature (London)* **2003**, *426*, 469−474.
(27) Ma, J.-B.; Ye, K.; Patel, D. J. Structural basis for overhang-specific small interfering RNA recognition by the PAZ domain. *Nature (London)* **2004**, *429*, 318−322.
(28) Lingel, A.; Simon, B.; Izaurralde, E.; Sattler, M. Nucleic acid 3′-end recognition by the Argonaute2 PAZ domain. *Nat. Struct. Mol. Biol.* **2004**, *11*, 576−577.
(29) Schwarz, D. S.; Hutvágner, G.; Haley, B.; Zamore, P. D. Evidence That siRNAs Function as Guides, Not Primers, in the Drosophila and Human RNAi Pathways. *Mol. Cell* **2002**, *10*, 537−548.
(30) Nykanen, A.; Haley, B.; Zamore, P. D. ATP requirements and small interfering RNA structure in the RNA interference pathway. *Cell (Cambridge, Mass.)* **2001**, *107*, 309−321.
(31) Leeds, J. M.; Graham, M. J.; Truong, L.; Cummins, L. L. Quantitation of phosphorothioate oligonucleotides in human plasma. *Anal. Biochem.* **1996**, *35*, 36−43.
(32) Geary, R. S.; Matson, J.; Levin, A. A. A nonradioisotope biomedical assay for intact oligonucleotide and its chain-shortened metabolites used for determination of exposure and elimination half-life of antisense drugs in tissue. *Anal. Biochem.* **1999**, *274*, 241−248.
(33) Kawasaki, A. M.; Casper, M. D.; Freier, S. M.; Lesnik, E. A.; Zounes, M. C.; et al. Uniformly modified 2′-deoxy-2′-fluoro phosphorothioate oligonucleotides as nuclease-resistant antisense compounds with high affinity and specificity for RNA targets. *J. Med. Chem.* **1993**, *36*, 831−841.
(34) Schwarz, D. S.; Hutvagner, G.; Du, T.; Xu, Z.; Aronin, N.; et al. Asymmetry in the assembly of the RNAi enzyme complex. *Cell* **2003**, *115*, 199−208.
(35) Khvorova, A.; Reynolds, A.; Jayasena, S. D. Functional siRNAs and miRNAs exhibit strand bias. *Cell* **2003**, *115*, 209−216.

JM049167J

TAB 11

THE JOURNAL OF BIOLOGICAL CHEMISTRY
Vol. 270, No. 43, Issue of October 27, pp. 25702–25708, 1995
Printed in U.S.A.

Chemical Modification of Hammerhead Ribozymes

CATALYTIC ACTIVITY AND NUCLEASE RESISTANCE*

(Received for publication, June 5, 1995, and in revised form, August 9, 1995)

Leonid Beigelman, James A. McSwiggen, Kenneth G. Draper, Carolyn Gonzalez, Kristi Jensen, Alexander M. Karpeisky, Anil S. Modak, Jasenka Matulic-Adamic, Anthony B. DiRenzo, Peter Haeberli, David Sweedler, Danuta Tracz, Susan Grimm, Francine E. Wincott, Varykina G. Thackray, and Nassim Usman‡

From the Departments of Chemistry and Biochemistry, Cell Biology and Enzymology, Ribozyme Pharmaceuticals, Inc., Boulder, Colorado 80301

A systematic study of selectively modified, 36-mer hammerhead ribozymes has resulted in the identification of a generic, catalytically active and nuclease stable ribozyme motif containing 5 ribose residues, 29–30 2′-*O*-Me nucleotides, 1–2 other 2′-modified nucleotides at positions U4 and U7, and a 3′-3′-linked nucleotide "cap." Eight 2′-modified uridine residues were introduced at positions U4 and/or U7. From the resulting set of ribozymes, several have almost wild-type catalytic activity and significantly improved stability. Specifically, ribozymes containing 2′-NH_2 substitutions at U4 and U7, or 2′-*C*-allyl substitutions at U4, retain most of their catalytic activity when compared to the all-RNA parent. Their serum half-lives were 5–8 h in a variety of biological fluids, including human serum, while the all-RNA parent ribozyme exhibits a stability half-life of only ~0.1 min. The addition of a 3′-3′-linked nucleotide "cap" (inverted T) did not affect catalysis but increased the serum half-lives of these two ribozymes to >260 h at nanomolar concentrations. This represents an overall increase in stability/activity of 53,000–80,000-fold compared to the all-RNA parent ribozyme.

Trans-acting ribozymes exert their activity in a highly specific manner and are therefore not expected to be detrimental to non-targeted cell functions. Because of this specificity, the concept of exploiting ribozymes for cleaving a specific target mRNA transcript is now emerging as a therapeutic strategy in human disease and agriculture (Cech, 1992; Bratty *et al.*, 1993). For ribozymes to function as therapeutic agents, they may be introduced exogenously or produced endogenously in the target cells. In the former case, the chemically modified ribozyme must maintain its catalytic activity while also being stable to nucleases. A major advantage of chemically synthesized ribozymes is that site-specific modifications may be introduced at any position in the molecule. This approach provides flexibility in designing ribozymes that are catalytically active and stable to nucleases. In this manuscript we show that using this site-specific, chemical modification strategy, ribozymes can be designed that have wild-type catalytic activity and are not cleaved by nucleases.

A variety of selective and uniform structural modifications have been applied to oligonucleotides to enhance nuclease resistance (Uhlmann and Peyman, 1990; Beaucage and Iyer, 1993; Milligan *et al.*, 1993). Improvements in the chemical synthesis of RNA (Scaringe *et al.*, 1990; Wincott *et al.*, 1995) have led to the ability to similarly modify ribozymes containing the hammerhead ribozyme core motif (Usman and Cedergren, 1992; Yang *et al.*, 1992) (Fig. 1). Yang *et al.* (1992) demonstrated that 2′-*O*-Me modification of a ribozyme at all positions except G5, G8, A9, A15.1, and G15.2 (see numbering scheme in Fig. 1) led to a catalytically active molecule having a greatly decreased k_{cat} value *in vitro*, but a 1000-fold increase in nuclease resistance over that of an all-RNA ribozyme when tested in a yeast extract. In another study (Paolella *et al.*, 1992), a persubstituted 2′-*O*-allyl-containing ribozyme with ribose residues at positions U4, G5, A6, G8, G12, and A15.1 showed a 5-fold decrease in catalytic activity compared to the all-RNA ribozyme (based on k_{cat}/K_m), while the stability of this ribozyme in bovine serum was increased substantially (30% intact material after 2 h compared to a <1-min half-life for the all-RNA ribozyme). Shimayama *et al.* (1993) found it necessary to introduce 2 additional phosphorothioate linkages at positions C3, U4 and to replace U7 by A or G in a phosphorothioate-DNA/RNA chimera containing 21 phosphorothioate (P=S)[1] substitutions (13 P=S DNAs in Stem/Loop II plus 5 and 3 P=S DNAs in Stems I and III, respectively). These ribozymes showed a 100-fold increase in stability relative to the all-RNA ribozyme, but the catalytic activities of these chimeras were reduced 15-fold (U7 → A7) and 42-fold (U7 → G7) compared to the wild-type ribozyme. Substitution of all pyrimidine nucleotides in a hammerhead ribozyme by their 2′-amino or 2′-fluoro analogs resulted in a 25–50-fold decrease in activity and a 1200-fold increase in stability in rabbit serum compared to the unmodified ribozyme (Pieken *et al.*, 1991).

The above data suggest that a strategy of uniform modification cannot be directly applied to ribozymes, since it is necessary to preserve a reasonable level of catalytic activity and therefore to leave some residues, especially in the catalytic core, unmodified. We have constructed a generic, catalytically active, nuclease stable hammerhead ribozyme motif that contains only 5 ribose residues; the remaining residues consist of 2′-*O*-Me nucleotides with one or two other 2′-modified sugars at positions U4 and/or U7 (Figs. 1 and 2). Two of these ri-

* The costs of publication of this article were defrayed in part by the payment of page charges. This article must therefore be hereby marked "*advertisement*" in accordance with 18 U.S.C. Section 1734 solely to indicate this fact.

‡ To whom correspondence should be addressed: Ribozyme Pharmaceuticals, Inc., 2950 Wilderness Pl., Boulder, CO 80301. Tel.: 303-449-6500; Fax: 303-449-6995.

[1] The abbreviations used are: P=S, phosphorothioate; 2′-F, 2′-deoxy-2′-fluorouridine; 2′-NH_2, 2′-deoxy-2′-aminouridine; iT, 3′-3′-linked thymidine; Rz, ribozyme; t_A, time required to cleave 50% of a short matched substrate; t_S, time required to degrade 50% of the full-length ribozyme; k_{cat}^S, maximum ribozyme cleavage rate under single turnover (enzyme excess) conditions; K_M^S, Michaelis constant under single turnover (enzyme excess) conditions.

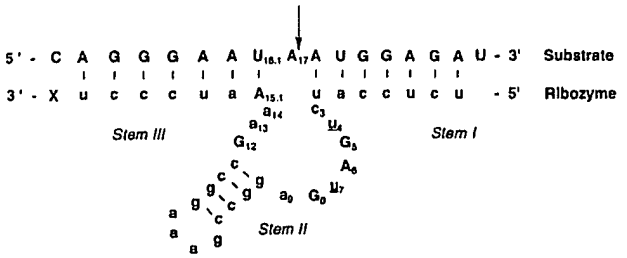

FIG. 1. **Sequences of ribozyme and substrate used in this study.** Conserved nucleotides within the central core are *numbered* according to Hertel *et al.* (1993). *Lowercase letters* represent sites that were substituted with 2'-*O*-methyl nucleotides in the final, nuclease resistant motif. *Underlined letters* at U4 and U7 indicate positions that were replaced by the eight 2'-substituted nucleotides shown in Fig. 2 (compounds **1–8**). *Uppercase letters* represent *ribo*nucleotides; five positions (G5, A6, G8, G12, and A15.1) within the nuclease-resistant ribozyme were kept as ribonucleotides to maintain catalytic activity. *X* represents the 3'-3'-linked (inverted) T residue (Fig. 2, compound 9) that was added to the 3'-end of Rzs **29** and **30**. *Arrow* indicates the site of substrate cleavage.

bozymes (containing 2'-NH_2 modifications at U4 and U7 or 2'-*C*-allyl modifications at U4) have almost wild-type catalytic activity and a 5–8 h half-life in human serum at nanomolar concentrations. The addition of a 3'-3'-linked thymidine nucleotide to these ribozymes maintains their catalytic activity and increases their half-lives in serum to >260 h.

EXPERIMENTAL PROCEDURES

Synthesis of Ribozymes—Automated RNA synthesis and deprotection was carried out on an Applied Biosystems model 394 DNA/RNA synthesizer using the method of Scaringe *et al.* (1990), modified according to Wincott *et al.* (1995). Syntheses were carried out at 2.5 μmol on a derivatized aminomethyl polystyrene solid support (Applied Biosystems). A 5-min coupling step was used for 2'-*O*-silyl protected RNA (Pharmacia Biotech Inc.) and modified phosphoramidites (Fig. 2).[2] A 2.5-min coupling step was used for 2'-*O*-Me RNA (Milligen/Biosearch). Average coupling yields, determined by colorimetric quantitation of trityl fractions, were 97.5–99%. Phosphorothioate linkages at the 3'- and 5'-ends of Rz **5** were introduced by a sulfurization step[3] with Beaucage's reagent (Iyer *et al.*, 1990). Ribozymes were gel-purified, eluted, ethanol-precipitated, rinsed twice with 70% ethanol, dried, and resuspended in TE buffer.

Nucleoside Composition—The nucleoside compositions of the ribozymes were confirmed by nuclease digestion of the ribozyme and analysis by reverse phase high performance liquid chromatography. The ribozymes were converted to nucleosides by incubation of 0.3 A_{260} units of ribozyme with 10 units of P1 nuclease (EC 3.1.30.1; Boehringer Mannheim) and 2 units of calf intestinal alkaline phosphatase (EC 3.1.3.1; Boehringer Mannheim) in 30 mM NaOAc, 1 mM $ZnSO_4$, at pH 5.2 (total volume = 100 μl) overnight at 50 °C. The digested material was injected directly onto a C18 column (Rainin, Dynamax, ODS 4 × 250 mm), and nucleosides were separated by an acetonitrile gradient buffered with 50 mM potassium phosphate, pH 7.0. The retention times were compared with monomer standards.

Radiolabeling of Ribozymes and Substrates—Ribozymes and substrates were 5'-end-labeled using T4 polynucleotide kinase and [γ-^{32}P]ATP. For internal labeling, ribozymes were synthesized in two halves with the junction 5' to the GAAA sequence in Loop II (Fig. 1). The 3'-half-ribozyme portion was 5'-end-labeled using T4 polynucleotide kinase and [γ-^{32}P]ATP, and was then ligated to the 5'-half-ribozyme portion using T4 RNA ligase. Labeled ribozymes were isolated from half-ribozymes and unincorporated label by gel electrophoresis.

Ribozyme Activity Assay—Ribozymes and 5'-^{32}P-end-labeled substrate were heated separately in reaction buffer (50 mM Tris-Cl, pH 7.5, 10 mM $MgCl_2$) to 95 °C for 2 min, quenched on ice, and equilibrated to the final reaction temperature (37 °C or as indicated) prior to starting the reactions. Reactions were carried out in enzyme excess, and were started by mixing ~1 nM substrate with the indicated amounts of ribozyme (5–200 nM, 40 nM for the initial screens) to a final volume of 50 μl. Aliquots of 5 μl were removed at 1, 5, 15, 30, 60, and 120 min, quenched in formamide loading buffer, and loaded onto 15% polyacrylamide, 8 M urea gels. The fraction of substrate and product present at each time point was determined by quantitation of scanned images from a Molecular Dynamics PhosphorImager. Ribozyme cleavage rates were calculated from plots of the fraction of substrate remaining *versus* time using a double exponential curve fit (Kaleidagraph, Synergy Software). The fast portion of the curve was generally 60–90% of the total reaction, so that observed cleavage rates (k_{obs}) and activity half-times (t_A = $\ln(2)/k_{obs}$) were taken from fits of the first exponential. Detailed kinetic analyses of Rzs **1**, **2**, **25**, and **26** were performed in the same way except that reactions were carried out at 25 °C and pH 6.5 to slow down the reactions and to enable more accurate determination of kinetic parameters. Plots of k_{obs} *versus* ribozyme concentration were fit to the Michaelis-Menten equation using a non-linear, least squares routine (Kaleidagraph, Synergy Software) to determine values for k_{cat}^S and K_M^S. Values for the combined parameter, k_{cat}^S/K_M^S, were confirmed by performing cleavage reactions at low ribozyme concentration (5–20 nM), then determining k_{cat}^S/K_M^S from the initial slope of the k_{obs} *versus* ribozyme concentration plot.

Ribozyme Stability Assay—Five hundred pmol of gel-purified 5'-end-labeled or internally labeled ribozymes were ethanol-precipitated and then resuspended in 20 μl of appropriate fluid (human serum, human plasma, human synovial fluid, or fetal calf serum) by vortexing for 20 s at room temperature. Samples were placed at 37 °C, and 2 μl aliquots were withdrawn after the times indicated in the figures (30 s to 72 h). Aliquots were quenched by the addition of 20 μl of 95% formamide, 0.5 × TBE (50 mM Tris, 50 mM borate, 1 mM EDTA) and were frozen prior to gel loading. Ribozymes were size-fractionated by electrophoresis in 20% acrylamide, 8 M urea gels. Gels were imaged on a Molecular Dynamics PhosphorImager, and the stability half-life (t_S) for each ribozyme was calculated from exponential fits of plots of the percentage of intact ribozyme *versus* the time of incubation.

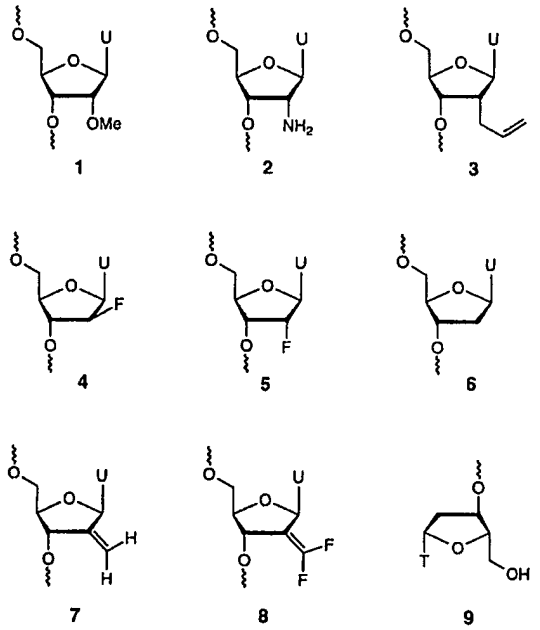

FIG. 2. **Structures of the 2'-modified nucleosides used in this study. 1**, 2'-*O*-Me-U; **2**, 2'-amino-U; **3**, 2'-*C*-allyl-U; **4**, 2'-arabinofluoro-U; **5**, 2'-fluoro-U; **6**, 2'-deoxy-U; **7**, 2'-methylene-U; **8**, 2'-difluoromethylene-U; **9**, 3'-3' inverted T.

RESULTS AND DISCUSSION

Modification and Testing Strategy—We focused our efforts on substitutions of the 2'-hydroxyl group since these modifications were considered least likely to perturb the overall structure of the hammerhead ribozyme and were more easily introduced than backbone modifications. Ribozymes were chemically synthesized and gel-purified, and the nucleotide

[2] Beigelman, L., Karpeisky, A., Matulic-Adamic, J., Haeberli, P., Sweedler, D., and Usman, N. (1995) *Nucleic Acids Res* **23**, in press.

[3] A. D. DiRenzo, K. Levy, P. Haeberli, S. Grimm, C. Shaffer, N. Usman, and F. Wincott, manuscript in preparation.

TABLE I
Cleavage Activity and Nuclease Resistance of Ribozymes 1–5

Rz	Modification[a]	Activity (t_A)[b]	Stability (t_S)[c]	Relative stability/activity β (Rz n) = $\frac{t_S/t_A(\text{Rz } n)}{t_S/t_A(\text{Rz } 1)}$
		min	*min*	
1	All RNA: UCUCCAU CUGAUGAGGCCGAAAGGCCGAA AAUCCCU	1	0.1	1
2	2′-*O*-Me arms: ucuccAU CUGAUGAGGCCGAAAGGCCGAA AAucccU	1	0.1	1
3	5+5 P=S arms: ucuccaU CUGAUGAGGCCGAAAGGCCGAA Aaucccu	3	0.1	0.3
4	2′-C-Allyl: ucuccAu cuGAuGAGGCCGAAAGGCCGAA AAucccT	13	120	92
5	2′-Fluoro-Pyr: ucuccAu cuGAuGAGGccGAAAGGccGAA AAucccT	30	15	5

[a] Uppercase sequences are ribonucleotides. Lowercase, underlined sequences contain the indicated modifications at the sugar or (in the case of Rz **3**) at the five phosphodiester linkages *between* the underlined sequences. In Rzs **4** and **5** the "t" at the 3′-end denotes deoxythymidine.
[b] Ribozyme activity expressed as cleavage half-time against the substrate shown in Fig. 1.
[c] Ribozyme stability expressed as half-life of ribozyme in human serum. Times <1 min are estimated and may be shorter.

content was verified by nucleoside composition analysis. The ribozymes were then assayed for *in vitro* cleavage activity, and for nuclease resistance in a range of biological fluids. Activity measurements were made in enzyme excess at concentrations (10 nM ribozyme, ~1 nM substrate) that approach saturating conditions for the all-RNA control ribozyme. Ribozyme activity is reported in Tables I and II as the activity half-time (t_A) at 40 nM ribozyme; a larger number represents a slower cleavage rate and is less desirable. The stability of ribozymes to nuclease digestion was assessed in fetal calf serum, human serum, human plasma, and human synovial fluid using 5′-^{32}P-end-labeled ribozymes. Ribozyme stability is reported in Tables I and II as the stability half-life in human serum (t_S); a larger number represents a slower degradation rate. To compare one ribozyme's activity and stability to another, we have defined a parameter, β, which is the ratio of the stability and activity half-times compared to a reference, Rz **1** (Table I). Thus, in Tables I and II,

$$\beta(\text{Rz } n) = \frac{t_S/t_A(\text{Rz } n)}{t_S/t_A(\text{Rz } 1)} \qquad \text{(Eq. 1)}$$

Larger β values represent an improvement in ribozyme activity and/or stability relative to Rz **1**.

5′- and 3′-Modified Ribozymes Are Catalytically Active but Not Stable in Biological Fluids—To establish a base line for ribozyme catalytic activity and stability in biological fluids, ribozymes were synthesized containing RNA only (Rz **1**, Table I), or RNA at all positions except in the substrate-binding arms (Stem I, positions 2.2–2.6, and Stem III, positions 15.3–15.7, Fig. 1). Table I shows that 2′-*O*-Me sugar, or phosphorothioate backbone modifications in the substrate-binding arms (Rz **2** and **3**, respectively) had minimal effects on catalytic activity. However, ribozyme stability in human serum also remained unchanged with these modifications, and all three ribozymes were rapidly degraded (Fig. 3). No full-length ribozymes were present after 30 s in any of the biological fluids tested; however, stable fragments were observed in ribozymes containing 2′-*O*-Me modifications (Fig. 3). Modification of the Stem I and III backbones with phosphorothioate substitutions did not increase the nuclease resistance of the ribozymes or result in the generation of stable ribozyme fragments (Fig. 3).

The profile of stable fragments generated with the 2′-*O*-Me modified ribozymes varied with the medium and, to a lesser degree, with the base sequence of ribozyme stems (data not shown). At the earliest times, modified ribozymes were digested to fragments between 6 and 10 nucleotides in length whose relative abundance varied somewhat between experiments. Over time, all of the fragments were cleaved at their 3′-termini to generate smaller fragments. The amount of 3′-exonuclease activity was greatest in fetal calf serum, less in human serum and plasma, and least in human synovial fluid. The sensitivity of the 2′-*O*-Me fragments to cleavage by the 3′-exonuclease activity varied between Rz **2** and other ribozymes having the same 2′-*O*-Me content but of different sequence (data not shown). Comparison of nucleoside composition suggests that these patterns of digestion cannot be attributed solely to the primary sequence of the ribozyme fragments.

TABLE II
Cleavage Activity and Nuclease Resistance of Ribozymes 6–30

Rz	2′-Modification[a] (U4/U7)	Activity (t_A)[b]	Stability (t_S)[c]	Relative stability/activity β (Rz n) = $\frac{t_S/t_A(\text{Rz } n)}{t_S/t_A(\text{Rz } 1)}$
		min	*min*	
6	OH/*O*-Me	1	0.1	1
7	*O*-Me/*O*-Me	4	260	650
8	$=CH_2$/*O*-Me	6.5	250	380
9	*O*-Me/$=CH_2$	8	320	400
10	$=CH_2$/$=CH_2$	8.5	250	300
11	$=CF_2$/*O*-Me	4.5	400	900
12	*O*-Me/$=CF_2$	5.5	250	220
13	$=CF_2$/$=CF_2$	>15	380	250
14	F/*O*-Me	3	300	1000
15	*O*-Me/F	8	300	375
16	F/F	3.5	300	850
17	H/*O*-Me	5.5	250	450
18	*O*-Me/H	>10	250	<250
19	H/H	4	280	700
20	araF/*O*-Me	5.5	500	900
21	*O*-Me/araF	4	350	875
22	araF/araF	>15	500	<330
23	NH_2/*O*-Me	10	500	500
24	*O*-Me/NH_2	5.5	500	900
25	NH_2/NH_2	2	300	**1500**
26	*C*-Allyl/*O*-Me	3	>500	**>1700**
27	*O*-Me/*C*-Allyl	3	300	1000
28	*C*-Allyl/*C*-Allyl	3	300	1000
29	*C*-Allyl/*O*-Me + iT	3	**16,000**	**53,000**
30	NH_2/NH_2 + iT	2	**16,000**	**80,000**

[a] Modifications follow the numbering scheme shown in Fig. 1.
[b] Ribozyme activity expressed as cleavage half-time against the substrate shown in Fig. 1.
[c] Ribozyme stability expressed as half-life of ribozyme in human serum. Times <1 min are estimated and may be shorter.

Uniform Modifications in the Ribozyme Core Reduce Catalytic Activity but Enhance Nuclease Resistance—Other researchers have reported increased nuclease resistance of hammerhead ribozymes through uniform substitution of ribopyrimidines with 2′-modified-pyrimidines. For example, Eckstein and co-workers have shown that uniform substitution of all pyrimidine nucleotides by 2′-F or 2′-NH_2 analogs greatly increased the stability of a hammerhead ribozyme, but also

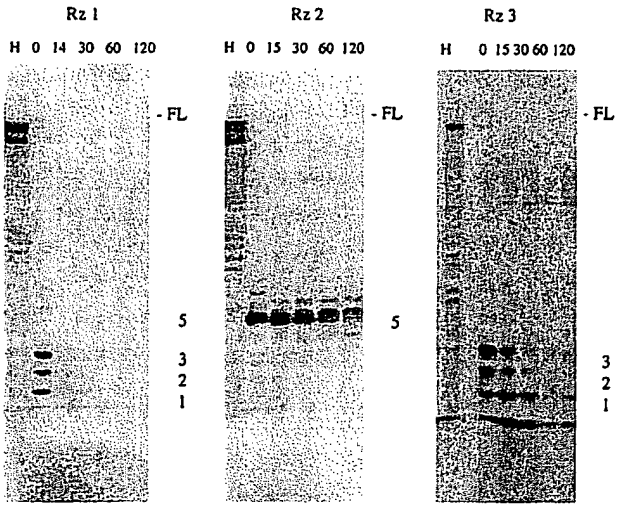

FIG. 3. **Nuclease resistance of minimally modified Rzs 1–3 in human serum.** ^{32}P-5′-End-labeled ribozymes were resuspended in fresh human serum and incubated for the indicated times at 37 °C. After quenching in stop buffer, ribozyme samples were size-fractionated on polyacrylamide gels as described under "Experimental Procedures." Ribozyme **1** is all RNA, Rz **2** contains 2′-*O*-Me arms, and Rz **3** contains P=S (phosphorothioate) arms (see Table I). Times of incubation (minutes) are shown above each panel. *H* = base hydrolyzed ribozyme size markers. *Numbers* to the *right* of each panel show the approximate size, in nucleotides, of the ribozyme fragments generated. *FL*, full-length ribozyme band position

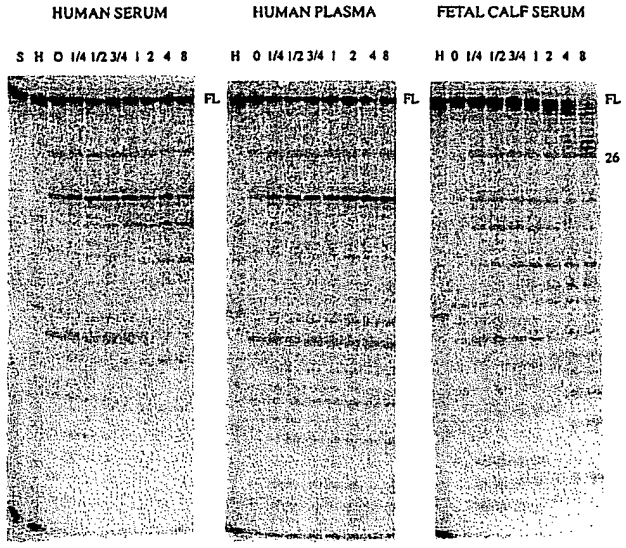

FIG. 4. **Comparative stability of 2′-*C*-allyl substituted, Rz 4, in human serum, human plasma, and fetal calf serum.** Time courses with ^{32}P-5′-end-labeled ribozyme were performed as in Fig. 3 and under "Experimental Procedures." Times of ribozyme incubation (hours) are shown above each panel. *H*, base hydrolyzed ribozyme size marker; *S*, ribozyme resuspended in saline; *FL*, full-length ribozyme band position. Approximate size (in nucleotides) of the major digestion products are shown in the panel margins.

reduced activity by 25–50-fold (Peiken *et al.*, 1991; Heidenreich *et al.*, 1994). We chose to test ribozymes containing uniform 2′-*C*-allyl and 2′-F pyrimidine substitutions. The choice of the 2′-*C*-allyl modification was based on the observation that 2′-*O*-allyl substitutions in hammerhead ribozymes improve stability but cannot be introduced at positions U4 and U7 without a significant detrimental effect on catalysis (Paolella *et al.*, 1992). The 2′-*C*-allyl group should be less bulky than the 2′-*O*-allyl group near the sites required for catalysis, but may still provide sterically and conformationally based nuclease protection.

The uniformly substituted 2′-*C*-allyl-pyrimidine ribozyme showed no activity in the cleavage assay (data not shown), which was likely due to the inability of Stem II to form (De Mesmaeker *et al.*, 1993). Thus, another ribozyme was synthesized that lacked the 2′-*C*-allyl-pyrimidine substitutions in Stem II (Rz **4**). Ribozyme **4**, showed a 13-fold reduction in cleavage activity relative to Rz **1** (t_A = 13 min), but also exhibited enhanced nuclease resistance in all sera (t_S = 120 min in human serum). A significant amount of full-length ribozyme was present after 4 h (Fig. 4 and Table I). Incubation of Rz **4** in serum resulted in the slow formation of stable oligonucleotide fragments of ~16 nucleotides in length (Fig. 4). This digestion pattern suggested that Stem-Loop II was a primary site of nuclease activity in these ribozymes. Our data and the observations of Eckstein and colleagues (indicating that pyrimidines are the primary sites of endonuclease cleavage in hammerhead ribozymes; Heidenreich *et al.* (1993)) suggested that modification of the pyrimidines in Stem-Loop II might afford even greater nuclease protection.

The 3′-exonuclease degradation of the *C*-allyl modified ribozyme was minimal over the time period. In contrast, the 2′-F-pyrimidine modified Rz **5** showed better protection against endonuclease attack, but gave less protection from 3′-exonuclease activity than the *C*-allyl modifications. The cleavage activity of Rz **5** was reduced 30-fold (t_A = 30 min) relative to Rz **1**. Since the 3′-exonuclease degradation of Rz **5** was much more pronounced than the Stem II endonuclease degradation of Rz **4**, the overall stability of Rz **5** was ~8-fold lower than Rz **4** (Table I).

It has been shown that 2′-*O*-Me modifications stabilize RNA-RNA duplexes (Inoue *et al.*, 1987) and do not have detrimental effects on the catalytic properties of hammerhead ribozymes when incorporated into the binding arms (Goodchild, 1992). We confirmed this latter observation by comparing the activity of Rz **1** with that of Rz **2**. The effect of 2′-*O*-Me substitutions in the catalytic core on catalysis is less predictable (Paolella *et al.*, 1992; Yang *et al.*, 1992) but may be beneficial for stability considering the nuclease resistance of the 2′-*O*-Me fragments generated from Rz **2** (see below).

Selective Ribozyme Modifications Maintain Catalytic Activity and Enhance Nuclease Resistance—We considered two models of essential hydroxyl groups for the hammerhead ribozyme catalytic core in the development of our consensus, nuclease-resistant motif. Yang *et al.* (1992) showed that hammerhead ribozymes containing 2′-*O*-Me nucleosides at all positions except (ribonucleotides) G5, G8, A9, A15.1, and G15.2 resulted in a ribozyme with significantly reduced activity, but with a 10^3-fold increase in nuclease resistance in yeast extracts. Paolella *et al.* (1992) placed 2′-*O*-allyl nucleosides at all positions except U4, G5, A6, G8, G12, and A15.1 and saw better activity (20% of wild type), while maintaining reasonable nuclease resistance (RNase A resistance increased by a factor of 10^2 and t_S in bovine serum increased to ~1 h). These results indicated that a modicum of ribonucleotide positions were required within the ribozyme core to maintain catalytic activity.

Based on the above data, we postulated a consensus motif (Fig. 1) that focused on positions U4 and U7 as pyrimidines within the core that might be 2′-modified without a drastic loss in catalytic activity. To test the importance of the U4 modification, Rz **6** was synthesized using a substitution pattern identical to the one reported by Paolella *et al.* (1992), except that 2′-*O*-Me was used instead of 2′-*O*-allyl at nonessential positions. The choice of 2′-*O*-Me substitutions was based on reports that this 2′-modification (i) confers stability to the hammerhead ribozyme (Yang *et al.*, 1992), (ii) is more stable to nucle-

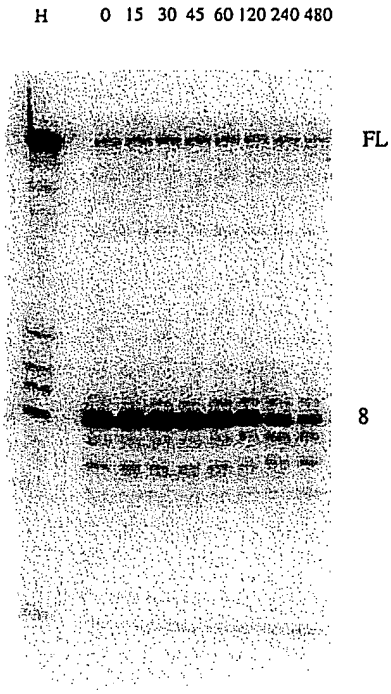

FIG. 5. **Stability of U7 2′-*O*-Me substituted Rz 6 in human serum.** Ribozyme **6** contains 2′-*O*-Me substitutions at all positions shown in lowercase in Fig. 1, with the exception of position U4, which retains the ribose sugar. Time courses with ^{32}P-5′-end-labeled ribozyme were performed as in Fig. 3 and under "Experimental Procedures." Times of ribozyme incubation (minutes) are shown above each panel. *H*, base hydrolyzed Rz **6** size marker; *FL*, full-length ribozyme band position. Approximate size (in nucleotides) of the major digestion products are shown in the panel margins.

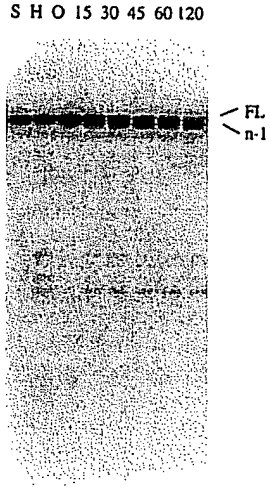

FIG. 6. **Stability of U4/U7 2′-*O*-Me substituted Rz 7 in human serum.** Rz **7** contains 2′-*O*-Me substitutions at all positions shown in lowercase in Fig 1, including positions U4 and U7. Time courses with ^{32}P-5′-end-labeled ribozyme were performed as in Fig. 3 and under "Experimental Procedures." Medium and times of ribozyme incubation (in minutes) are shown above each panel. *H*, base hydrolyzed Rz **5** size marker; *S*, ribozyme resuspended in saline; *FL*, full-length ribozyme band position; *n-1*, Rz **7** missing the 3′-terminal nucleotide.

ases than either 2′-F or 2′-NH_2 analogs (Kawasaki *et al.*, 1993), (iii) is naturally occurring, thereby reducing the possibility of toxicity *in vivo*, and (iv) is relatively easily synthesized and incorporated. The resulting catalytic activity of Rz **6** was the same as the all-RNA Rz **1** (t_A = 1 min). Unfortunately, Rz **6** showed no improvement in nuclease resistance. In human serum Rz **6** was rapidly cleaved to give smaller fragments that were ~8 nucleotides in length (Fig. 5). The generation of 8-mer cleavage fragments from the 5′-end of Rz **6** suggested that the U4 site (the only unmodified pyrimidine residue within Rz **6**) remained hypersensitive to nucleases. The different stability of Rz **6** compared to the reported 2′-*O*-allyl analog (Paolella *et al.*, 1992) could reflect a different accessibility of position U4 in a more sterically hindered 2′-*O*-allyl core compared to the less bulky 2′-*O*-Me core of Rz **6** and/or different nuclease compositions of bovine and human sera. The stability over time of the intact ribozyme fragment from Rz **6** suggested that the 2′-*O*-Me modification may be as good as the *C*-allyl modification at providing nuclease resistance. Thus, another 2′-*O*-Me substituted ribozyme was made and tested (Rz **7**) that contained the same substitutions as Rz **6** with an additional 2′-*O*-Me substitution at the U4 position. Ribozyme **7** showed a 4-fold reduction in catalytic activity (t_A = 4 min) but also gave a dramatic improvement in the nuclease resistance of the ribozyme (t_S = 260 min, Fig. 6), so that the overall stability/activity ratio, β, improved 650-fold for Rz **7** compared to the all-RNA Rz **1**.

To further elaborate on this model, the seven 2′-modified-uridine nucleotides shown in Fig. 2 were introduced into positions U4 and U7, (ribozymes **8–28**). These modifications were chosen for a variety of reasons. 2′-Fluoro- and 2′-NH_2-U modifications have been successfully applied by Eckstein's group (Heidenreich *et al.*, 1993) but have not been used in a highly 2′-*O*-methylated motif. The 2′-ara-F-U modification was introduced to probe the influence of configuration of the fluoro substituent on activity and stability. 2′-Deoxy-2′-methylene and difluoromethylene nucleotides were introduced under the assumption that imposing conformational restrictions on ribose sugar puckering of these monomers could provide increased nuclease resistance without reducing catalytic activity. Yamagata *et al.* (1992) showed by x-ray analyses that the C1′, C2′, and C3′ carbons in 2′-deoxy-2′-methylene pyrimidine nucleosides are nearly coplanar. Finally, 2′-dU was introduced to probe the effect of removing substituents from the 2′-position. In the case of single U4 or U7 substitutions, the other uridine site contained a 2′-*O*-Me uridine.

The cleavage activity (t_A), human serum half-lives (t_S), and overall stability/activity ratios (β) for Rzs **8–28** are shown in Table II. All modifications to U4 and/or U7 gave significant increases in nuclease resistance for these ribozymes, while varying levels of ribozyme activity were observed. The most dramatic increases in nuclease resistance were seen in Rzs **20**, **22–24**, and **26**, where stability times of greater than 500 min were observed (equivalent to >5000-fold stability increase relative to Rz **1**). Ribozyme **25** gave a less dramatic increase in stability (t_S = 300 min); however, its catalytic activity (t_A = 2 min) made it attractive for further investigation. All of the ribozymes containing U4/U7 modifications were active to some degree, and the majority had activity decreases of less than 5-fold relative to Rz **1**. The best overall ribozymes in terms of combined stability and activity were ribozymes **25** and **26** with β values of 1500–1700.

Certain trends that correlated with the type of 2′-modification and catalytic activity were noted. Modifications that distorted the normal ribose ring pucker resulted in ribozymes with reduced activity; examples included Rzs **8–10** (2′-methylene) and **11–13** (2′-difluoromethylene). Double modification of both U4 and U7 with these nucleotides had an even more pronounced negative effect (Rzs **10** and **13**). 2′-Fluoro substitutions at U4 and U7 were less detrimental to catalysis than the related 2′-arabino-F-substitutions (Rzs **14–16** *versus* Rz **20–**

TABLE III

Single turnover kinetic parameters of ribozymes 1, 2, 25, and 26

Kinetic parameters were determined from single turnover experiments at pH 6.5 and 25 °C.

Rz	k_{cat}^S	K_M^S	k_{cat}^S/K_M^S
	min^{-1}	nM	$\times 10^7\ M^{-1}\ min^{-1}$
1	0.4	13	3
2	0.95	25	4
25	1.2	20	6
26	0.14	56	0.3

22). An especially striking difference was observed for the F/F-modified Rz **16** when compared to araF/araF-modified Rz **22**. Our observations with the F/F-modified Rz **16** are consistent with an earlier proposal (Heidenreich *et al.*, 1993) for a hydrogen bonding network, which includes the 2'-hydroxyl of U4 and U7 and is relatively undisturbed by 2'-F substitutions due to their hydrogen acceptor properties. The greater reduction in activity observed for the araF/araF-modified Rz **22** could then be explained as a significant disruption of these hydrogen bonds due to the altered configuration at the 2'-position. However, this model would suggest that all modifications that remove or shift the position of the 2'-hydroxyl at U4 and U7 should significantly reduce ribozyme activity. In fact, only moderate (4-fold) reductions in activity are observed for H/H-modified Rz **19**, and for a recently tested ara/ara-modified ribozyme (data not shown).

The high activity of Rz **25** (U4/U7 = 2'-NH_2-U) is in agreement with the recently published observation that incorporation of 2'-NH_2-U into both the U4 and U7 positions rescues the activity of uniformly 2'-F-substituted ribozymes at pyrimidine sites (Heidenreich *et al.*, 1994). Interestingly, the combination of 2'-NH_2-U and 2'-*O*-Me substitution at positions U4 and U7 yielded Rz **24** (*O*-Me/NH_2) with moderate and Rz **23** (NH_2/*O*-Me) with low catalytic activity. Only the double modification (NH_2/NH_2) provided a highly active ribozyme. The intrinsic dual role of the amino group as a potential hydrogen bond donor and acceptor could be responsible for the observed effect if both 2'-NH_2 groups are the partners in a hydrogen bonding network. In contrast, the relatively high catalytic activity of the 2'-*C*-allyl modified Rzs **26–28** is not consistent with the hydrogen bonding network proposed by Heidenreich *et al.* (1993) since it is unclear how the 2'-*C*-allyl group could participate in the normal hydrogen bonding or Mg^{2+} coordination networks that create the active catalytic conformation.

Having identified two ribozymes with substantially increased stability (Rzs **25** and **26**), we wanted to confirm that the activity screens were correctly representing the activity of these ribozymes. Thus, more complete activity profiles were determined for Rzs **25** and **26** and were compared to the kinetic parameters of the control Rzs **1** and **2**. Table III shows that Rzs **1**, **2**, and **25** all have similar kinetic behavior. These ribozymes show little difference in the values of the specificity constant, k_{cat}^S/K_M^S, while the less certain estimates of k_{cat}^S and K_M^S vary by only 2-fold. In contrast to these three ribozymes, Rz **26** shows a ~10-fold reduction in k_{cat}^S/K_M^S, which is almost completely due to reductions in k_{cat}^S.

We have attempted to compare our findings with the interactions seen in two recently published and very similar crystal structures (Pley *et al.*, 1994, Scott *et al.*, 1995). However, it is difficult to compare our results to these crystal structures for two reasons. First, most of our substitutions are conservative 2'-*O*-Me sugar substitutions, which should cause a minimum of steric clash with neighboring groups and which can still act as H-bond acceptors, while the remaining, extensive substitutions have focused on the 2'-positions only at U4 and U7. Second, the crystal structures appear to represent a ground-state structure

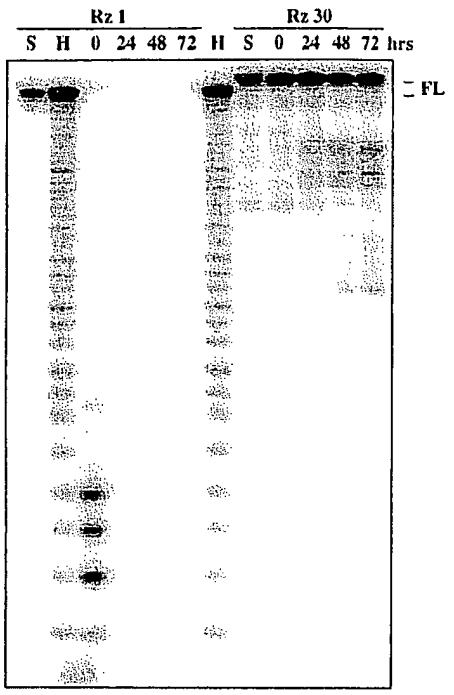

FIG. 7. **Stability of internally labeled Rz 30 in human serum.** Ribozyme **30** (U4/U7 2'-amino with 3'-3' inverted T) was labeled with ^{32}P at the phosphate 5'- to the GAAA sequence in the Stem II loop (Fig. 1) and incubated in human serum as in Fig. 3. For comparison, the all-RNA Rz **1** was 5'-labeled with ^{32}P and incubated under the same conditions. The addition of 3'-3' inverted T to Rz **30** and the absence of a 5'-phosphate makes this ribozyme migrate more slowly than Rz **1** on the acrylamide gel. Times of ribozyme incubation (in hours) are shown above each panel. *H*, base hydrolyzed Rz **1** size marker; *S*, ribozyme resuspended in saline; *FL*, full-length ribozyme band position. *Time 0 h* is actually the time required to add the ribozyme to serum, mix, and quench in stop buffer (~30 s).

that is fairly distant from the transition state. Nevertheless, McKay and colleagues described three positions (U4, G5, and G8) at which H-bond contacts are made with the 2'-hydroxyl. The H-bond contacts at G5 and G8 are in agreement with the observations that these hydroxyl groups cannot be substituted without substantial loss of activity. However, the data for position U4 would suggest that H-bond interactions with this 2'-hydroxyl are not essential for cleavage activity, since substitutions that abolish H-bonds (=CF_2 in Rz **11**, and *C*-allyl in Rz **26**) show the same moderate reductions in activity as do substitutions that maintain H-bonds (F in Rz **14**).

3'-Modifications Maintain Catalytic Activity and Extend Ribozyme Serum Half-life at Nanomolar Concentrations—Ribozymes **7–28** all showed dramatic improvements in nuclease resistance compared to the all-RNA Rz **1**, or even compared to the highly modified Rz **6**, which still contains a ribonucleotide at U4. However, all of these ribozymes still exhibit slow degradation at the 3'-end (*cf.* Fig. 6). Addition of a 3'-3'-linked, inverted T (iT) residue at the 3'-end of DNA oligonucleotides has been reported to inhibit the digestion of DNA by 3'-exonucleases (Ortigão *et al.*, 1992). We therefore added an iT to Rzs **25** and **26** to give Rzs **29** and **30**. The iT residue protected the 3'-terminus of the ribozymes for at least 48 h, when present at 25 nM in either human serum or fetal calf serum (data not shown). We viewed this as a conservative estimate of nuclease resistance due to a low level of phosphatase activity present in both sera.

To eliminate the effect of 5'-phosphatase activity on ribozyme stability measurements, the stability of Rz **30** was

evaluated using ribozymes that contained an internal ^{32}P label (see "Experimental Procedures"). Fig. 7 shows that >75% of internally labeled Rz **30** remained intact after a 72 h incubation in human serum (t_S = 16,000 min). In contrast, the all-RNA Rz **1** was degraded to small fragments within the 30 s that it took to add ribozyme to serum, mix, and quench the reaction (*time 0 h*, Fig. 1). During the incubation of Rz **30**, a small number of minor bands appeared that have mobilities consistent with digestion at the five remaining ribose sites within the ribozyme. Thus, even greater stabilization of the ribozymes is likely to require substitution of the 5 remaining ribose residues.

To verify that the 3'-exonuclease activity in serum was not significantly diminished during the 72 h assay, Rzs **1** and **2** were added to a sample of the serum after the 72 h incubation period. These nuclease-sensitive ribozymes were degraded immediately (data not shown).

The presence of the inverted T residue at the 3'-end of Rzs **29** and **30** has no effect on catalytic activity. Their activity half-times were identical to the equivalent Rzs **26** and **25**, respectively, which lack the inverted T (Table II). Thus, Rzs **29** and **30** show an overall 50,000–80,000-fold increase in the relative ribozyme stability/activity compared to the all-RNA ribozyme.

Incubation of Nuclease-resistant Ribozymes in Human Serum Does Not Alter Catalytic Activity—To assess the effect on catalytic activity of prolonged incubation of Rzs **29** and **30** in human serum, samples of the Rzs were removed from the serum after 72 h and assayed for activity. To inhibit nuclease digestion of the substrate in serum, yeast tRNA was added to each sample. No diminution in ribozyme catalytic activity was noted in this assay (data not shown).

Conclusions—We have systematically investigated the influence of certain 2'-modifications on hammerhead ribozymes, with the goal of conferring high cleavage activity and increased nuclease resistance in biological sera. We have identified a consensus motif of 2'-hydroxyl groups required to maintain catalytic activity in the context of a persubstituted 2'-*O*-Me hammerhead ribozyme. In this motif, the 5 purine ribonucleotides G5, A6, G8, G12, and A15.1 remain unmodified. Selective modifications, at positions U4 and U7 in the "5-ribose" hammerhead ribozyme, maintain catalytic activity while dramatically increasing the nuclease resistance of the ribozymes in biological sera. The best U4 and U7 modifications for stability and activity were U4/U7 2'-NH_2 and U4 2'-*C*-allyl/U7 2'-*O*-Me, which provided more than a 1500-fold increase in stability/activity ratios (β) over the unmodified all-RNA ribozyme. An additional increase in β values to 53,000–80,000 was achieved by introducing a 3'-3'-linked thymidine to the 3'-end of these ribozymes.

Acknowledgments—We thank Tom Cech, Daniel Herschlag, and Gerald Joyce for suggestions and critical reading of the manuscript.

REFERENCES

Beaucage, S. L. & Iyer, R. P. (1993) *Tetrahedron* **49**, 6123–6194
Bratty, J., Chartrand, P., Ferbeyre, F. & Cedergren, R. (1993) *Biochim. Biophys. Acta* **1216**, 345–359
Cameron, F. H. & Jennings, P. A. (1989) *Proc. Natl. Acad. Sci. U.S.A.* **86**, 9139–9143
Cech, T. (1992) *Curr. Opin. Struct. Biol.* **2**, 605–609
De Mesmaeker, A., Lebreton, J., Hoffmann, P. & Freier, S. M. (1993) *Synlett* 677–679
Goodchild, J. (1992) *Nucleic Acids Res.* **20**, 4607–4612
Heidenreich, O., Pieken, W. & Eckstein, F. (1993) *FASEB J.* **7**, 90–96
Heidenreich, O., Benseler, F., Fahrenholz, A. & Eckstein, F. (1994) *J. Biol. Chem.* **269**, 2131–2138
Hertel, K. J., Pardi, A., Uhlenbeck, O. C., Koizumi, M., Ohtsuka, E., Uesugi, S., Cedergren, R., Eckstein, F., Gerlach, W. L., Hodgson, R. & Symons, R. H. (1992) *Nucleic Acids Res.* **20**, 3252
Inoue, H., Hayase, Y., Imura, A., Iwai, S., Miura, K. & Ohtsuka, E. (1987) *Nucleic Acids Res.* **15**, 6131–6148
Iyer, R. P., Phillips, L. R., Egan, W., Regan, J. B. & Beaucage, S. L. (1990) *J. Org. Chem.* **55**, 4693–4701
Kawasaki, A. M., Casper, M. D., Freier, S. M., Lesnik, E. A., Zounes, M. C., Cummins, L. L., Gonzalez, C. & Cook, P. D. (1993) *J. Med. Chem.* **36**, 831–841
Milligan, J. F., Matteucci, M. D. & Martin, J. C. (1993) *J. Med. Chem.* **36**, 1923–1937
Ortigão, J. F. R., Rösch, H., Selter, H., Frölich, A., Lorenz, A., Montenarh, M. & Seliger, H. (1992) *Antisense Res. & Dev.* **2**, 129–146
Paolella, G., Sproat, B. S. & Lamond, A. I. (1992) *EMBO J.* **11**, 1913–1919
Pieken, W. A., Olsen, D. B., Benseler, F., Aurup, H. & Eckstein, F. (1991) *Science* **253**, 314–317
Pley, H. W., Flaherty, K. M. & McKay, D. B. (1994) *Nature* **372**, 68–74
Ruffner, D. E., Stormo, G. D. & Uhlenbeck, O. C. (1990) *Biochemistry* **29**, 10695–10702
Scaringe, S. A., Franklyn, C. & Usman, N. (1990) *Nucleic Acids Res.* **18**, 5433–5441
Scott, W. G., Finch, J. T. & Klug, A. (1995) *Cell* **81**, 991–1002
Shimayama, T., Nishikawa, F., Nishikawa, S. & Taira, K. (1993) *Nucleic Acids Res.* **21**, 2605–2611
Uhlmann, E. & Peyman, A. (1990) *Chem. Rev.* **90**, 543–584
Usman, N. & Cedergren, R. J. (1992) *Trends Biochem. Sci.* **17**, 334–339
Wincott, F. E., DiRenzo, A., Shaffer, C., Grimm, S., Tracz, D., Workman, C., Sweedler, D. & Usman, N. (1995) *Nucleic Acids Res.* **23**, 2677–2684
Yang, J.-H., Usman, N., Chartrand, P. & Cedergren, R. J. (1992) *Biochemistry* **31**, 5005–5009
Yamagata, Y., Tomota, K.-I., Marubayashi, N., Ueda, I., Sakata, S., Matsuda, A., Takenuki, K. & Ueda, T. S. (1992) *Nucleosides & Nucleotides* **11**, 835–853

TAB 12

THE JOURNAL OF BIOLOGICAL CHEMISTRY

Vol. 268, No. 19, Issue of July 5, pp. 14514-14522, 1993
Printed in U.S.A.

Evaluation of 2'-Modified Oligonucleotides Containing 2'-Deoxy Gaps as Antisense Inhibitors of Gene Expression*

(Received for publication, January 14, 1993, and in revised form, March 25, 1993)

Brett P. Monia‡§, Elena A. Lesnik¶, Carolyn Gonzalez¶, Walt F. Lima¶, Danny McGee‖, Charles J. Guinosso‖, Andrew M. Kawasaki‖, P. Dan Cook‖, and Susan M. Freier¶

From the ‡Department of Molecular Pharmacology, ¶Department of Molecular, Cellular, and Structural Biology, and the ‖Department of Medicinal Chemistry, ISIS Pharmaceuticals, Carlsbad, California 92008

We have used a previously described 17-mer phosphorothioate (Monia, B. P., Johnston, J. F., Ecker, D. J., Zounes, M. A., Lima, W. F., and Freier, S. M. (1992) *J. Biol. Chem.* 267, 19954–19962) for structure-function analysis of 2'-sugar modifications including 2'-*O*-methyl, 2'-*O*-propyl, 2'-*O*-pentyl, and 2'-fluoro. These modifications were analyzed for hybridization affinity to complementary RNA and for antisense activity against the Ha-*ras* oncogene in cells using a highly sensitive transactivation reporter gene system. Hybridization analysis demonstrated that all of the 2'-modified oligonucleotides hybridized with greater affinity to RNA than an unmodified 2'-deoxy oligonucleotide with the rank order of affinity being 2'-fluoro > 2'-*O*-methyl > 2'-*O*-propyl > 2'-*O*-pentyl > 2'-deoxy.Evaluation of antisense activities of uniformly 2'-modified oligonucleotides revealed that these compounds were completely ineffective in inhibiting Ha-*ras* gene expression. Activity was restored if the compound contained a stretch of at least five 2'-deoxy residues. This minimum deoxy length correlated perfectly with the minimum length required for efficient RNase H activation *in vitro* using partially purified mammalian RNase H enzyme. These chimeric 2'-modified/deoxy phosphorothioates displayed greater antisense potencies in inhibiting Ha-*ras* gene expression, compared with the unmodified uniform deoxy phosphorothioate. Furthermore, antisense potency correlated directly with affinity of a given 2' modification for it's complementary RNA. These results demonstrate the importance of target affinity in the action of antisense oligonucleotides and of RNase H as a mechanism by which these compounds exert their effects.

Sequence-specific inhibition of gene expression by antisense oligonucleotides has been successfully employed for a variety of viral and cellular targets (reviewed in Refs. 1–5). These compounds, which inhibit gene expression by acting on pre-mRNA and mRNA targets, can be broadly classified into two categories; those leading to a reduction in target RNA levels and those that do not. Inhibition of RNA function by antisense oligonucleotides without affecting RNA stability may occur through the disruption of important RNA-protein or RNA-RNA interactions that are essential for RNA function, such as those involved in protein translation and RNA processing. For example, translation arrest, without consequence to mRNA stability, has been demonstrated *in vitro* using compounds targeted to translation initiation sites (6–10). It has been proposed that oligonucleotide hybridization to the AUG start codon can block translation initiation by inhibiting ribosome assembly (7, 9). However, direct evidence supporting this mechanism of action for antisense oligonucleotides in mammalian cells remains limited (11, 12).

Many mechanisms have been proposed for oligonucleotide-mediated destabilization of target RNAs (reviewed in Ref. 5). The primary mechanism by which antisense oligonucleotides are believed to cause a reduction in target RNA levels is through the action of RNase H (4), an endonuclease that cleaves the RNA strand of RNA-DNA duplexes (13). This enzyme, thought to play a natural role in DNA replication, has been shown to be capable of cleaving the RNA component of oligonucleotide-RNA duplexes in cell free systems as well as in *Xenopus* oocytes (14–21). However, direct evidence supporting a role for RNase H as a mechanism for oligonucleotide-mediated inhibition of gene expression in mammalian cells remains extremely limited (12).

Susceptibility of unmodified phosphodiester oligonucleotides to nucleolytic degradation has made them unattractive molecules for oligonucleotide therapeutics (22). To alleviate this problem, chemical modifications have been introduced into oligonucleotides to increase their resistance to nucleolytic degradation (4, 23). In addition to nuclease resistance, chemical modifications may confer other pharmacologic advantages to oligonucleotides, such as enhanced target specificity and affinity, and cell penetration (5, 23–26). However, modifications that impart nuclease resistance often possess additional properties that limit their usefulness. For example, methylphosphonate modifications have been reported to influence oligonucleotide uptake efficiency by cells and confer nuclease stability (24, 27–30). However, these oligonucleotides exhibit weaker affinity for RNA targets, as compared with unmodified oligonucleotides, and are not substrates for RNase H (8, 31, 32). Similarly, 2'-*O*-methyl oligonucleotides, which exhibit enhanced target RNA affinity (23, 26, 33, 34) and nuclease stability,[1] as compared with unmodified oligonucleotides, also are not substrates for RNase H (35). Thus, although 2'-*O*-methyl and methylphosphonate oligonucleotides have certain desirable properties, the fact that they are not substrates for RNase H may limit their usefulness as antisense agents.

Attempts to take advantage of the beneficial properties of oligonucleotide modifications while maintaining the substrate

* The costs of publication of this article were defrayed in part by the payment of page charges. This article must therefore be hereby marked "*advertisement*" in accordance with 18 U.S.C. Section 1734 solely to indicate this fact.

The nucleotide sequence(s) reported in this paper has been submitted to the GenBank™/EMBL Data Bank with accession number(s) J00277 and M15077.

§ To whom correspondence should be addressed: ISIS Pharmaceuticals, 2280 Faraday Ave., Carlsbad, CA 92008. Tel.: 619-931-9200.

[1] B. P. Monia, unpublished experiments.

requirements for RNase H have led to the employment of chimeric oligonucleotide analogs (31, 32, 35–42). These analogs, which contain a region of modified nucleotides and an unmodified region that retains the ability to direct RNase H cleavage, have been examined primarily using backbone modifications, most commonly the methylphosphonates (32, 35–37, 39–42). In these studies, modified backbone linkages were introduced primarily to confer nuclease resistance to oligonucleotides. Although these backbone modifications reduce DNA-RNA duplex stability (26, 31, 32, 34), backbone-modified/phosphodiester chimeras have been shown to activate RNase H-dependent cleavage of target RNAs *in vitro* (31, 32, 36, 37).

Studies using methylphosphonate chimeric oligonucleotides have shown that the minimum phosphodiester length required to direct efficient RNase H cleavage of a target RNA using *Escherichia coli* RNase H is either three (36) or four (31) linkages. Similar studies have been reported using mammalian RNase H cleavage assays *in vitro* (37). In this case, a series of backbone modifications, including methylphosphonates, containing different phosphodiester lengths was examined for cleavage efficiency. This study demonstrated, among other things, that the minimum number of phosphodiester linkages required for efficient activation of mammalian RNase H *in vitro* by a backbone-modified chimeric oligonucleotide is five. More recently, it has been shown that methylphosphonate/phosphodiester chimeras display increased specificity and efficiency for target RNA cleavage using *E. coli* RNase H *in vitro* (25, 32). Backbone-modified chimeric oligonucleotides have also been reported to be effective antisense inhibitors in *Xenopus* oocytes and to inhibit proliferation of mammalian cells in culture (39, 41).

Chimeric oligonucleotides containing 2' sugar modifications mixed with RNase H-sensitive deoxy residues have not been as well characterized as the backbone-modified chimeras. Inoue *et al.* (35) employed 2'-*O*-methyl oligonucleotides containing unmodified deoxy gaps to direct cleavage *in vitro* by *E. coli* RNase H to specific sites within the complementary RNA strand. By using these RNA "restriction endonucleases," it was also demonstrated that these compounds required a minimum deoxy gap of four bases for efficient target RNA cleavage. However, oligonucleotides of this nature have not been examined for cleavage efficiency using mammalian RNase H nor have they been tested for antisense activity in cells. Furthermore, studies on the ability to direct RNase H cleavage and antisense activity of 2' sugar modifications other than 2'-*O*-methyl have been extremely limited (43, 44).

Here, we describe a systematic study in which chimeric oligonucleotides containing various 2' sugar modifications were characterized for hybridization affinity, ability to direct target RNA cleavage by mammalian RNase H, and for antisense activity in cultured cells. The antisense target for these studies was the Ha-*ras* oncogene containing a GGC → GTC point mutation at codon 12 (45). Our results indicate that antisense activity can be significantly enhanced through the use of high affinity 2' sugar modifications provided they are equipped with RNase H-sensitive deoxy gaps of the appropriate length. Furthermore, our findings demonstrate the importance of target affinity in the action of antisense oligonucleotides and of RNase H in the mechanism by which these compounds exert their effects.

MATERIALS AND METHODS

Cells and Reagents—The human epitheloid carcinoma cell line HeLa 229 was obtained from the American Type Tissue Collection (Bethesda, MD). HeLa cells were grown as previously described (46). DOTMA[2] (Lipofectin) solution (*N*-[1-((2,3-dioleyloxy-propyl]-*N,N,N*-triethylammonium chloride) was purchased from GIBCO-BRL in a 1:1 mixture with dioleoylphosphatidylethanolamine. Opti-MEM was purchased from GIBCO. Synthetic, crystalline luciferin and chemicals required for standard calcium phosphate plasmid transfections were purchased from Sigma.

Oligonucleotide Synthesis—2'-*O*-Alkyl and 2'-fluoro monomers were synthesized as previously described (44, 47). Synthesis of phosphorothioate (deoxy and 2' modified) and phosphodiester oligonucleotides and oligoribonucleotides were performed using an Applied Biosystems 380B automated DNA synthesizer as previously described (44, 46, 47). Purification of oligonucleotide products was also as previously described (44, 46, 47). Purified oligonucleotide products were greater than 90% full-length material as determined by polyacrylamide gel electrophoresis analysis.

Melting Curves—Absorbance *versus* temperature curves were measured at 260 nm using a Gilford 260 spectrophotometer interfaced to an IBM PC computer and a Gilford Response II spectrophotometer. The buffer contained 100 mM Na^+, 10 mM phosphate, and 0.1 mM EDTA, pH 7. Oligonucleotide concentration was 4 μM each strand, determined from the absorbance at 85 °C and extinction coefficients calculated according to Puglisi and Tinoco (48). T_m values, free energies of duplex formation, and association constants were obtained from fits of data to a two-state model with linear sloping base lines (49). Reported parameters are averages of at least three experiments.

Preparation of RNA Transcripts for Gel Shift Analysis—The plasmid pT24-C3, containing the c-Ha-*ras*-1-activated oncogene (codon 12, GGC→GTC) was obtained from the American Type Culture Collection (Bethesda, MD). Polymerase chain reaction technology was employed for the construction of a T7 transcription template that directs the synthesis of a 47-base segment of activated c-Ha-*ras* mRNA (50). This transcript contains sequences corresponding to nucleotides +18 to +64 (relative to the translation initiation site) of Ha-*ras* mRNA (45). 5' sequences of Ha-*ras* exon 1, corresponding to nucleotides +18 to +64, were polymerase chain reaction amplified as previously described (50). RNA transcripts were prepared, labeled, and purified as previously described (50). The transcripts were either 5'-end-labeled using *T4* polynucleotide kinase and [γ-^{32}P]ATP or 3'-end-labeled with *T4* RNA ligase and [α-^{32}P]ATP. The labeled products were gel purified on 12% polyacrylamide gel electrophoresis.

Gel Shift Assay—Hybridization reactions were prepared in 20 μl containing 100 mM sodium, 10 mM phosphate, 0.1 mM EDTA, 1000 counts/min of *T7*-generated RNA (approximately 10 pM), and antisense oligonucleotide ranging in concentration from 1 pM to 10 μM. Reactions were incubated 24 h at 37 °C. Following hybridization, 5 μl of loading buffer was added to the reactions and reaction products were resolved on 20% native polyacrylamide gels, prepared using 45 mM Tris-borate and 1 mM $MgCl_2$. Electrophoresis was carried out at 10 °C, and gels were quantitated and association constants calculated using a Molecular Dynamics PhosphorImager as described previously (50).

RNase H Analysis—RNase H assays were performed using a chemically synthesized 25 base oligoribonucleotide corresponding to bases +23 to +47 of activated (codon 12, G→U) Ha-*ras* mRNA (45, 46). The 5'-end-labeled RNA was used at a concentration of 20 nM and incubated with a 10-fold molar excess of antisense oligonucleotide in a reaction containing 20 mM Tris-Cl, pH 7.5, 100 mM KCl, 10 mM $MgCl_2$, 1 mM dithiothreitol, 10 μg of tRNA and 4 units of RNasin in a final volume of 10 μl. The reaction components were preannealed at 37 °C for 15 min then allowed to slow cool to room temperature. Complete annealing was assessed by polyacrylamide gel electrophoresis analysis using native gels. HeLa cell nuclear extracts were used as a source of mammalian RNase H (51). Reactions were initiated by addition of 2 μg of nuclear extract (5 μl), and reactions were allowed to proceed for 10 min at 37 °C. Reactions were stopped by addition of denaturing load buffer and reaction products were loaded on a 20% polyacrylamide gel containing 7 M urea. RNA cleavage products were resolved and visualized by electrophoresis followed by autoradiography. Quantitation of cleavage products was performed using a Molecular Dynamics PhosphorImager (50).

ras Transactivation Reporter Gene Constructs—The expression plasmid RA-17, containing a activated (codon 12, GGC→GTC) Ha-*ras* cDNA insert under control of the constitutive SV40 promoter, was a kind gift from Dr. Bruno Tocque (Rhone-Poulenc Sante, Vitry, France). The *ras*-responsive reporter gene pRDO53 (52) was a kind

[2] The abbreviations used are: DOTMA, *N*-[1-((2,3-dioleyloxypropyl]-*N,N,N*-triethylammonium chloride; kb, kilobase(s).

gift from Dr. Michael Ostrowski (Duke University, Durham, NC).

DNA Transfections and Luciferase Assay—HeLa cells were maintained as monolayers on 6-well plates in Dulbecco's modified Eagle's medium supplemented with 10% fetal bovine serum and 100 units/ml penicillin. Transient DNA transfections were performed by the calcium phosphate precipitation technique (53) with 12 μg of total DNA/plate (2 μg/well), including 5 μg of pRDO53 (*ras*-responsive reporter gene), and 5 μg of RA-17 (Ha-*ras* expression plasmid). Cells were treated with DNA precipitate for 4–5 h, glycerol shocked, and cells were harvested 36–48 h following glycerol treatment. Medium containing 10% fetal bovine serum was replaced with medium containing 0.5% fetal bovine serum 16 h before harvest (52). Luciferase expression in transient transfected HeLa cells was determined and normalized for transfection efficiency against total protein as previously described (46, 52).

Oligonucleotide Treatment of Cells—Approximately 12 h (overnight incubation) following plasmid transfection, cells were washed one time with phosphate-buffered saline prewarmed to 37 °C and Opti-MEM containing 5 μg/ml DOTMA was added to each plate (1.0 ml/well). Oligonucleotides were added from 50 μM stocks to each well and incubated 4 h at 37 °C. Following treatment, media was removed and replaced with Dulbecco's modified Eagle's medium containing 10% fetal bovine Serum, and the cells were incubated at 37 °C (54).

RESULTS

In a previous report, a series of oligodeoxynucleotide phosphorothioates ranging in length between 5 and 25 bases were tested for antisense activity and selectivity for the Ha-*ras* sequence containing a G → T transversion at codon 12 (46). In that study, we demonstrated that both antisense activity and mutant selectivity are critically dependent on oligonucleotide length and concentration. Furthermore, antisense activity was shown to correlate directly with relative affinity of an oligonucleotide for it's RNA target. The oligonucleotide which conferred the greatest mutant selectivity in that report was a 17-mer, the sequence of which is shown in Fig. 1.

Based on the sequence of the mutant selective 17-mer, a series of chimeric phosphorothioate 2′-*O*-methyl oligonucleotides were synthesized that contain between 1 and 9 centered 2′-deoxy residues. These centered deoxy residues form what we refer to as a "deoxy gap" in an otherwise uniform 2′-*O*-methyl molecule. Uniform phosphorothioate linkage was included in these oligonucleotides to ensure stability against serum and intracellular nucleases.[1] These oligonucleotides, along with a non-chimeric 2′-*O*-methyl 17-mer (full 2′-*O*-methyl) and a uniform deoxy 17-mer (full deoxy), are diagramed in Fig. 1. These compounds were characterized for hybridization efficiency, ability to direct RNase H cleavage *in vitro* using mammalian RNase H, and for antisense activity against Ha-*ras*.

The results from hybridization analysis of the 2′-*O*-methyl deoxy gap series against a 25-mer synthetic oligoribonucleotide complement are shown in Fig. 2. T_m values for a given oligonucleotide correlated directly with 2′-*O*-methyl content. As 2′-*O*-methyl modifications were replaced with 2′-deoxy nucleosides, T_m values were reduced at approximately 1.2 °C/substitution. All of the oligonucleotides containing 2′-*O*-methyl modifications displayed T_m values substantially higher than the full deoxy compound of the same sequence. These observations are in agreement with previous reports claiming 2′-*O*-methyl oligonucleotides bind RNA with higher affinity than full deoxy oligonucleotides (23, 26, 33, 34).

The experiments described above allow evaluation of base-pairing properties of oligonucleotides to a unstructured RNA complement. In cells, however, the target is not a simple complementary oligoribonucleotide but a complex cellular RNA that in all likelihood possesses significant secondary structure. Target structure has been shown to dramatically influence oligonucleotide binding (50, 55). This is presumably due to the thermodynamic costs of disrupting RNA secondary structure prior to antisense oligonucleotide binding. Since previous reports have claimed the existence of secondary

Deoxy Number	Sequence
17	C C A C A C C G A C G G C G C C
0	[C C A C A C C G A C G G C G C C]C
1	[C C A C A C C G]A [C G G C G C C]C
3	[C C A C A C C]G A C[G G C G C C]C
4	[C C A C A C C]G A C G[G C G C C]C
4	[C C A C A C] C G A C[G G C G C C]C
5	[C C A C A C] C G A C G[G C G C C]C
7	[C C A C A]C C G A C G G [C G C C]C
9	[C C A C]A C C G A C G G C[G C C]C

FIG. 1. **2′-*O*-Methyl chimeric, antisense oligonucleotide design.** Phosphorothiate oligonucleotides, targeted to mutant Ha-*ras* codon 12 sequences (GGC → GTC), were synthesized that contain between 1 and 9 centered deoxy residues in a otherwise uniformly modified 2′-*O*-methyl oligonucleotide. Sequences containing 2′-*O*-methyl modifications are *boxed*; *deoxy number* refers to the number of deoxy residues forming a centered "gap" within the oligonucleotide. Oligonucleotides are shown 5′ to 3′.

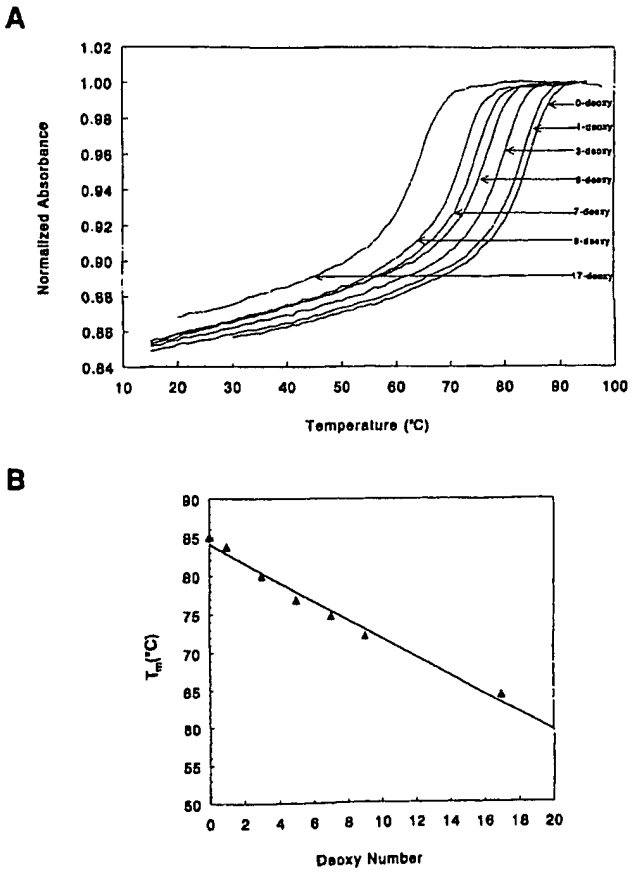

FIG. 2. **Hybridization of the phosphorothiate chimeric oligonucleotides described in Fig. 1 to a 25-mer fragment of RNA corresponding to residues +23 to +37 of mutant (codon 12, GGC → GTC) Ha-*ras* mRNA.** *A*, absorbance normalized at 95 °C *versus* temperature for a equimolar mixture of antisense oligonucleotide and RNA complement. *B*, T_m *versus* deoxy gap size for the chimeric oligonucleotides. Hybridization conditions are given in the text.

structures in Ha-*ras* mRNA in the codon 12 region (50, 56), we extended the hybridization experiments described above to include a larger Ha-*ras* target which has previously been shown to contain a stable stem loop structure in the codon 12 region (50).

Effects of 2'-*O*-methyl modifications on antisense hybridization to the structured Ha-*ras* target were determined by gel shift analysis (50). As shown in Fig. 3, the full deoxy 17-mer formed the least stable duplex whereas the full 2'-*O*-methyl 17-mer formed the most stable duplex. Furthermore, as 2'-*O*-methyl content was decreased, a concomitant reduction in binding affinity to the structured target was observed. Comparison of binding affinities of oligonucleotides to structured *versus* unstructured RNA demonstrated that absolute affinities differed considerably for the two targets (Table I). For example, the seven-gap oligonucleotide displayed a K_d of 8×10^{-16} M for the single stranded target and a K_d of 9×10^{-8} M for the hairpin target. Trends, however, were similar for both targets; increased 2'-*O*-methyl content caused increased duplex stability.

Ability to direct RNase H cleavage of a complementary RNA by 2'-*O*-methyl deoxy gap oligonucleotides was determined *in vitro* using HeLa nuclear extracts. These extracts contain both type 1 and type 2 RNase H (13).[1] Only some of the compounds within the 2'-*O*-methyl deoxy gap series (Fig. 1) were capable of directing efficient RNase H cleavage (Fig. 4*A*). No cleavage was observed with the fully modified 2'-*O*-methyl oligonucleotide or one containing a single deoxy residue. A deoxy length of three directed RNase H cleavage at very low efficiency. In contrast, the 2'-*O*-methyl oligonucleotide containing 5 deoxy residues directed RNase H cleavage at high efficiency, as did compounds containing 7 and 9 deoxy residues. Subsequent to these findings, two 2'-*O*-methyl oligonucleotides containing centered deoxy gaps of four were designed (Fig. 1) and tested for efficiency of RNase H activation relative to the other gapped compounds. Although the four deoxy gap compounds could activate cleavage slightly better than the three deoxy gap compound, their overall efficiency relative to oligonucleotides containing longer gaps was very poor.[1] These results indicate that the minimum

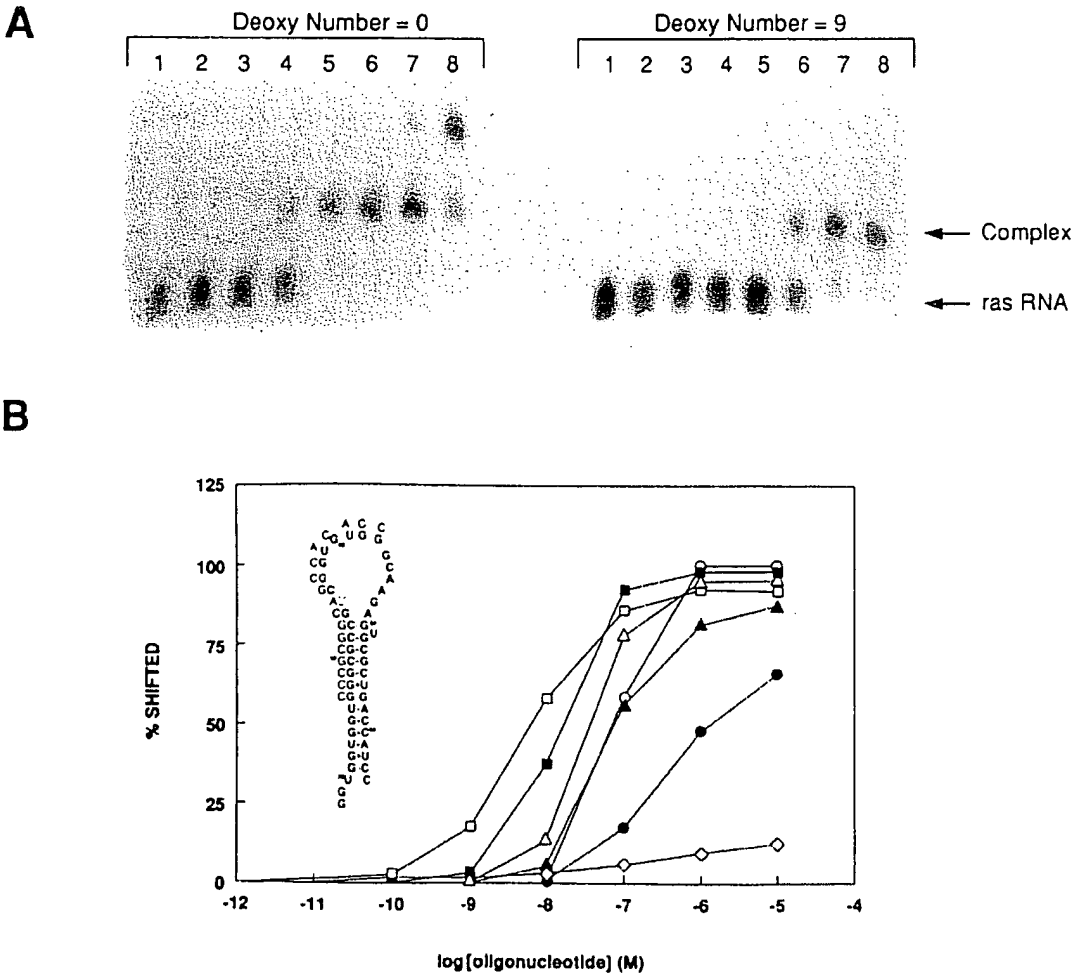

FIG. 3. **Antisense oligonucleotide binding to 47-mer Ha-*ras* hairpin RNA target.** *A*, gel shift analysis of end-labeled hairpin target with uniform 2'-*O*-methyl oligonucleotide (*Deoxy Number = 0*) compared to a 2'-*O*-methyl chimeric oligonucleotide containing a nine-base deoxy gap (*Deoxy Number = 9*), as a function of oligonucleotide concentration. *Lanes 1–8* refer to antisense oligonucleotide concentration; *1*, none; *2*, 10^{-11} M; *3*, 10^{-10} M; *4*, 10^{-9} M; *5*, 10^{-8} M; *6*, 10^{-7} M; *7*, 10^{-6} M; *8*, 10^{-5} M. Complex refers to RNA-oligonucleotide duplex. *B*, fraction of hairpin target shifted *versus* concentration of antisense oligonucleotide for the seven oligonucleotides described in Fig. 1. ◇, deoxy number = 17; ●, deoxy number = 9; ▲, deoxy number = 7; ○, deoxy number = 5; △, deoxy number = 3; ■, deoxy number = 1; □, deoxy number = 0 (full 2'-*O*-methyl). *Inset*, structure of 47-mer Ha-*ras* stem-loop shown with sequence of 17-mer antisense oligonucleotide used in these studies. See text for gel shift and quantitation procedures.

TABLE I

Correlation of oligonucleotide O-methyl content with binding affinity to structured versus unstructured RNA

K_d values were determined for 2′-*O*-methyl chimeric oligonucleotides binding to a 25-mer complementary Ha-*ras* RNA (unstructured) or a 47-mer complementary Ha-*ras* RNA (structured) containing a previously described stem-loop structure (50). No. of modifications refers to 2′-*O*-methyl substitutions (see Fig. 1). K_d values for binding of oligonucleotides to the unstructured target were determined from melting curves whereas K_d values for binding to the structured target were determined from gel shift assays. See text for methods.

No. of 2′ modifications	K_d	
	Unstructured	Structured
	M	
16	3×10^{-19}	8×10^{-9}
15	4×10^{-19}	2×10^{-8}
13	1×10^{-17}	5×10^{-8}
11	2×10^{-16}	9×10^{-8}
9	8×10^{-16}	9×10^{-8}
7	6×10^{-15}	2×10^{-6}
0	3×10^{-13}	$>1 \times 10^{-5}$

deoxy length required for efficient activation of mammalian RNase H by the 17-mer phosphorothioate is 5 residues.

Chimeric methylphosphonate oligonucleotides have recently been reported to activate RNase H cleavage more efficiently than unmodified compounds (32). To determine if this is also true for chimeric 2′-*O*-methyl oligonucleotides, these compounds were tested for ability to activate RNase H cleavage *in vitro* at lower enzyme concentrations. In contrast to chimeric methylphosphonate oligonucleotides, 2′-*O*-methyl deoxy gap chimeras were found to be less efficient activators of RNase H, as compared with a full deoxy oligonucleotide (Fig. 4*B*). Furthermore, RNase H cleavage efficiency improved as 2′-*O*-methyl content was reduced.

The results described above demonstrate that 1) affinity of an oligonucleotide for its target RNA can be increased substantially by incorporation of 2′-*O*-methyl modifications, with relative affinity being directly proportional to 2′-*O*-methyl content; and 2) mammalian RNase H activity has a minimum recognition requirement of 5 deoxy residues in a chimeric 2′-*O*-methyl/deoxy oligonucleotide. To test the role of target affinity in antisense-mediated inhibition and of RNase H in the mechanism by which these compounds exert their effects, 2′-*O*-methyl deoxy gap oligonucleotides were tested for antisense activity against the Ha-*ras* oncogene. Antisense activity against full-length Ha-*ras* mRNA was determined using a previously described transient, cotransfection, reporter gene system (52) in which Ha-*ras* gene expression was monitored with a *ras*-responsive enhancer element linked to the reporter gene luciferase (Fig. 5). Antisense experiments were performed initially at a single oligonucleotide concentration (100 nM). As shown in Fig. 6*A*, chimeric 2′-*O*-methyl oligonucleotides containing deoxy gaps of 1 or 3 residues, as well as the full 2′-*O*-methyl compound, showed no inhibitory effects on Ha-*ras* gene expression. However, compounds containing gaps of 5 or more residues showed marked inhibition of the Ha-*ras* target. In fact, these compounds displayed activities substantially greater than that of the full deoxy parent compound.

Dose-response experiments were performed using the four active compounds from Fig. 6*A*, along with the 2′-*O*-methyl chimeras containing 4 deoxy residues (Fig. 1). Oligonucleotide-mediated inhibition of Ha-*ras* expression was dose-dependent (Fig. 6*B*). Chimeric oligonucleotides containing deoxy gaps longer than four displayed inhibitory activities much greater than that of the full deoxy oligonucleotide. The most active compound was the seven deoxy chimera, which

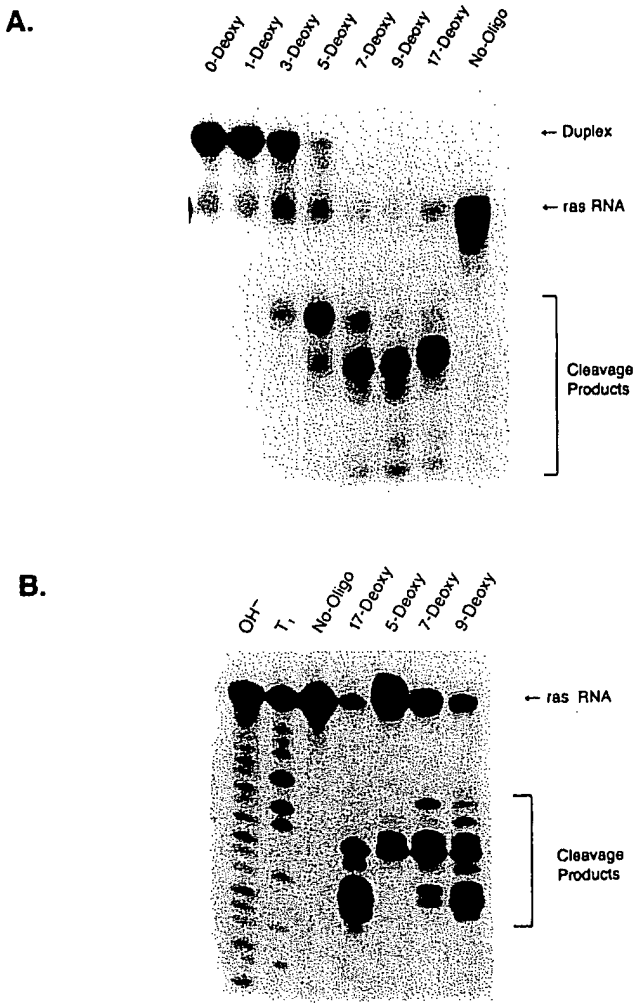

FIG. 4. **RNase H-dependent cleavage of complementary Ha-*ras* RNA by 2′-*O*-methyl chimeric phosphorothioate oligonucleotides.** A synthetic, end-labeled, 25-mer RNA containing mutant Ha-*ras* codon 12 sequences (+23 to +47) was preannealed with the appropriate oligonucleotide and treated with HeLa RNase H for 10 min at 37 °C. Following termination of reactions, cleavage products were resolved on a 20% acrylamide gel under denaturing conditions. *A*, 2 μg of HeLa extract added; *B*, 0.2 μg of HeLa extract added. Lane designations refer to the length of the centered deoxy gap in a 2′-*O*-methyl chimeric oligonucleotide (refer to Fig. 1). OH^- = base hydrolysis ladder of single-stranded Ha-*ras* RNA; T_1 refers to RNase T_1 digestion of single-stranded Ha-*ras* RNA.

displayed approximately seven times greater antisense activity than the full deoxy oligonucleotide. Chimeric compounds containing 4 deoxy residues showed activity only at the highest concentration employed.

The above results show that 2′-*O*-methyl oligonucleotides can be employed as effective, RNase H-dependent, antisense inhibitors provided a specific number of 2′-*O*-methyl modifications are replaced with deoxy residues. Furthermore, all of the 2′-*O*-methyl chimeric compounds that contained the appropriate number of deoxy residues for efficient RNase H activation were significantly more effective than the unmodified oligonucleotide in inhibiting Ha-*ras* gene expression. This latter observation is most likely explained by the increased target affinity conferred to oligonucleotides as a result of 2′-*O*-methyl modification. Since some reduction in 2′-*O*-methyl content was required for antisense activity, a direct correlation between target affinity and antisense activity was

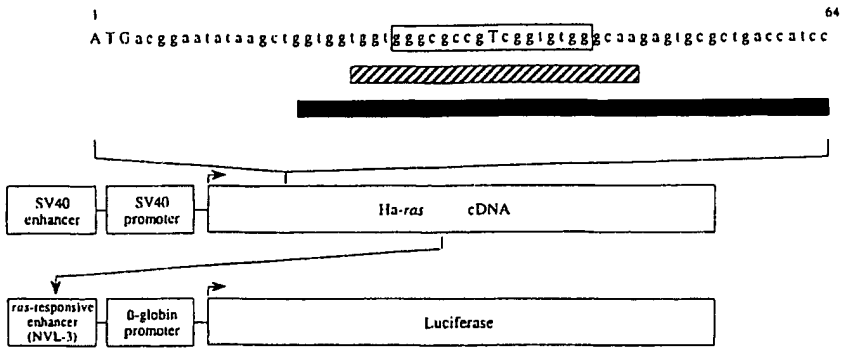

FIG. 5. **Ha-*ras* reporter gene assay.** Constitutive expression of full-length mutant (codon 12 GGC → GTC) Ha-*ras* cDNA sequences, driven by the SV40 promoter/enhancer element, was monitored in transiently, cotransfected, HeLa cells using the *NVL-3 ras*-responsive enhancer element linked to the reporter gene luciferase (52). DNA sequences +1 to +64 of Ha-*ras* cDNA are shown. *Boxed* sequences show target site of antisense oligonucleotides described in this study. *Hatched box* indicates 25-mer complementary RNA sequence used for T_m and RNase H analysis of oligonucleotides. *Solid box* indicates RNA 47 mer sequence that comprises a putative Ha-*ras* hairpin loop structure used for structured target binding analysis (Fig. 3). For actual RNA sequences, thymine was replaced with uracil. See text for transfection and assay procedures.

not observed for this series of compounds. However, a direct correlation between antisense activity and ability to activate RNase H *in vitro* was observed for this series. This correlation is shown in Fig. 7 where relative antisense activities of chimeric oligonucleotides and their abilities to activate RNase H cleavage *in vitro* were plotted as a function of deoxy length. This relationship demonstrates the importance of RNase H as a mechanism of action for antisense-mediated effects on gene expression.

If 2'-*O*-methyl deoxy gap oligonucleotides are more effective than full deoxy oligonucleotides as antisense inhibitors due to enhanced target affinity, it should be possible to shorten these compounds to a length where relative affinities and antisense activities between 2'-*O*-methyl chimeras and the full deoxy 17-mer are equal. To test this, 2'-*O*-methyl oligonucleotides containing deoxy gaps of 5 or 7 residues were shortened to lengths of 15, 13, and 11 bases, T_m values were determined and relative antisense activities were assessed. As expected, T_m values were reduced as oligonucleotide length was reduced (Fig. 8*A*). Furthermore, T_m correlated well with 2'-*O*-methyl content; five deoxy gap oligonucleotides always displayed higher T_m values than seven deoxy gap oligonucleotides of the same length. 2'-*O*-Methyl chimeras that displayed T_m values most similar to that of the 17-mer full deoxy compound (T_m = 64.2 °C, Fig. 2) ranged between 13 and 15 bases in length.

Fig. 8*B* shows the antisense activities of shortened 2'-*O*-methyl deoxy gap oligonucleotides compared to the full deoxy 17-mer compound. Antisense activities of 2'-*O*-methyl chimeras correlated well with oligonucleotide length. Longer oligonucleotides were always more effective than shorter ones. In addition, oligonucleotides containing 7 deoxy residues were always more active than those containing 5. This latter observation may reflect the optimal deoxy length required for efficient RNase H activation; 5 deoxy residues may be sufficient for cleavage but 7 may be optimal. Finally, relative antisense activities between the 17-mer full deoxy compound and the 2'-*O*-methyl 13- and 15-mer compounds were similar. This observation supports the conclusion that chimeric 2'-*O*-methyl oligonucleotides are more effective antisense inhibitors due to increased target affinity.

The above results demonstrate that 2'-*O*-methyl chimeric oligonucleotides can be employed as effective antisense inhibitors and that 2'-*O*-methyl modifications can provide important advantages over unmodified oligodeoxynucleotides. We have extended these structure-activity studies by examining the effects of other 2' sugar modifications on target affinity and antisense activity. For these studies, 2'-*O*-propyl, 2'-*O*-pentyl, and 2'-fluoro substituents were examined in our parent 17-mer phosphorothioate sequence. As with fully modified 2'-*O*-methyl compounds, these sugar modifications do not activate RNase H cleavage in uniformly modified oligonucleotides.[1] Therefore, chimeric oligonucleotide design is required for these modifications when being employed as antisense agents that act through RNase H-dependent mechanisms. These modifications were examined in the 17-mer oligonucleotide with a centered 7-base deoxy gap (Table II).

T_m values for each of the 2'-modified chimeras shown in Table II were determined against a 25-mer oligoribonucleotide complement. All of the 2' modifications caused an increase in oligonucleotide target affinity (T_m) relative to the parent uniform deoxy compound (Table II). However, the amount of affinity gained was clearly affected by the nature of the substituent. The 2'-fluoro-modified chimera displayed the highest T_m value of the 2'-modified series whereas the 2'-*O*-pentyl oligonucleotide displayed the lowest. Furthermore, an inverse relationship was observed between alkyl chain length at the 2' position and T_m. We have made similar observations concerning the relationship between 2'-*O*-alkyl chain length and T_m in a variety of oligonucleotide sequences.[3]

The 2'-modified oligonucleotides listed in Table II were tested for antisense activity against Ha-*ras* using the transactivation reporter gene assay. All of the 2'-modified chimeric compounds displayed significant antisense activity (Fig. 9). However, the nature of the modification clearly affected oligonucleotide activity. A relationship was observed between alkyl chain length at the 2' position and antisense activity; as chain length was increased, antisense activity decreased. The most active oligonucleotide in the series was the 2'-fluoro compound. As shown in Table II, a direct correlation was observed between oligonucleotide target affinity (T_m) and antisense activity. These results demonstrate further the importance of oligonucleotide target affinity in antisense-mediated effects on gene expression.

DISCUSSION

We have previously identified a 17-mer phosphorothioate antisense oligonucleotide targeted to the Ha-*ras* codon 12

[3] E. A. Lesnik, unpublished experiments.

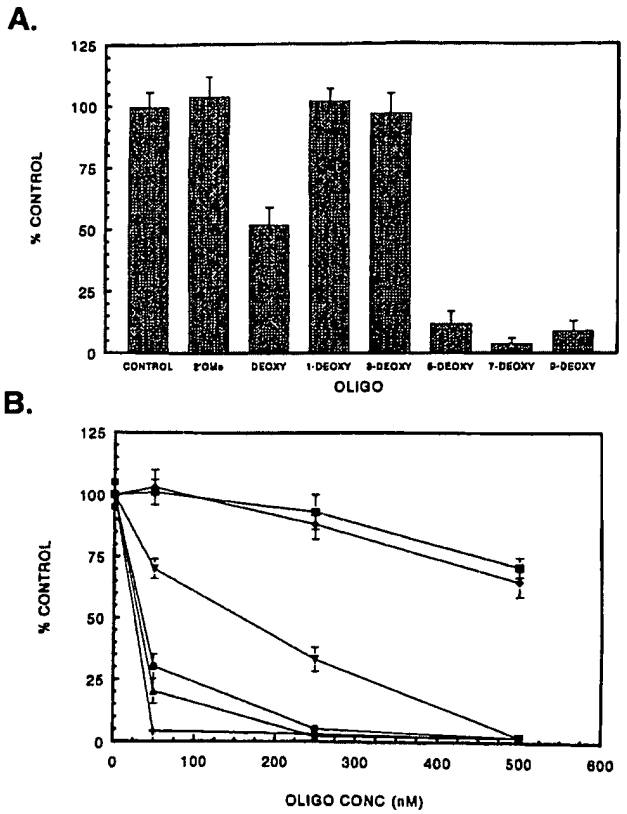

FIG. 6. **Antisense activity of phosphorothioate 2′-*O*-methyl chimeric oligonucleotides targeted to Ha-*ras* codon 12 RNA sequences.** HeLa cells transfected with a mutant Ha-*ras* expression plasmid and a *ras*-responsive luciferase reporter gene (see Fig. 5) were treated with oligonucleotides in the presence of DOTMA (5 μg/ml), and luciferase activity was determined 24–36 h later (see text). *A*, single dose activity (100 nM) of uniform 2′-*O*-methyl (*2′OMe*), uniform deoxy (*DEOXY*), or 2′-*O*-methyl oligonucleotides containing centered 1-, 3-, 5-, 7-, or 9-base deoxy gaps. Control represents treatment with randomized "control" phosphorothioate/deoxy oligonucleotide (GAT-CGA-GAT-CTG-ATC-CTT-AG). *B*, dose-response activity of uniform deoxy (▼) or 2′-*O*-methyl oligonucleotides containing centered 4- (■,♦), 5- (●), 7- (+), or 9-base (▲) deoxy gaps. Oligonucleotide sequences with modifications are shown in Fig. 1. Results are expressed as the mean of the % control activity ± S.D. ($n = 6$). % control represents *ras*-dependent expression of luciferase in transfected cells in the absence of oligonucleotide.

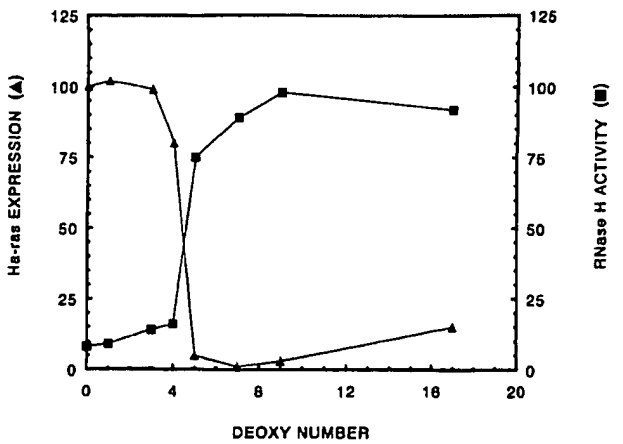

FIG. 7. **Correlation between antisense activity and ability to activate HeLa RNase H as a function of deoxy gap length using phosphorothioate 2′-*O*-methyl chimeric oligonucleotides.** Antisense activity against Ha-*ras* oncogene expression was determined as described in Fig. 6*B* at 500 nM oligonucleotide concentration. RNase H activity was assayed as described in Fig. 4*A*. All of the oligonucleotides tested in Fig. 4*A* were included in this analysis as well as a 2′-*O*-methyl oligonucleotide containing a 4-base deoxy gap (gel not shown). *DEOXY NUMBER* refers to the length of the centered deoxy region (see Fig. 1 for oligonucleotide description).

point mutation (GGC → GTC) which displayed both antisense activity and point mutation specificity (46). In this study, we have incorporated a series of 2′ modifications within this oligonucleotide and characterized their effects on hybridization stability, ability to activate RNase H, and antisense activity in cultured cells. 2′-*O*-Methyl modifications were found to greatly increase duplex stability, with 2′-*O*-methyl content correlating directly with target affinity. 2′-*O*-Propyl and 2′-*O*-pentyl modifications were also found to increase duplex stability, but relative target affinity decreased with increased alkyl chain length. Fluoro modifications at the 2′ sugar position conferred the greatest increase in duplex stability.

Correlation of duplex stability with substituent size has been observed previously for sequences containing 2′-substituted deoxyadenosines (26, 34, 47). The order of stability was 2′fluoro dA > 2′-*O*-methyl dA > 2′-*O*-ethyl dA > 2′-*O*-propyl dA = 2′-*O*-allyl dA > 2′-*O*-butyl dA > 2′-*O*-pentyl dA > 2′-*O*-benzyl dA > 2′-*O*-nonyl dA. This correlation may be related to the ability of 2′ substituents to act as hydrogen-bond acceptors. X-ray, NMR, and modeling studies suggest a spine of hydrogen-bonded water molecules in the minor groove contributes to the stability of a nucleic acid duplex (57, 58). Small, electronegative fluorine is a good hydrogen-bond acceptor and may stabilize this water spine. In contrast, large substituents may interfere with formation of this network of hydrogen bonds.

Uniform modification of the 17-mer phosphorothioate compound with 2′-*O*-methyl residues rendered the molecule unable to activate HeLa RNase H *in vitro*. We have made similar observations with uniformly modified 2′-*O*-propyl, 2′-*O*-pentyl, and 2′-fluoro oligonucleotides.[1] However, partially modified chimeric oligonucleotides containing deoxy gaps of 5 residues or longer could activate RNase H *in vitro*, although RNase H efficiency was significantly lower than the parent uniform deoxy oligonucleotide. This minimum deoxy recognition length was absolutely required for antisense activity in cultured cells, demonstrating the importance of RNase H as a mechanism of action for antisense compounds. This conclusion is further supported by our findings that treatment of Ha-*ras* transformed cells with 2′ sugar-modified chimeric phosphorothioates, as well as with uniform deoxy phosphorothioates, results in complete elimination of Ha-*ras* mRNA. Treatments with uniform 2′ sugar-modified compounds has no detectable effects on Ha-*ras* transcript levels.[1] We have also observed reduced Ha-*ras* protein (p21) levels in cells treated with uniform deoxy phosphorothioates and 2′ sugar-modified chimeric compounds whereas no detectable reduction in Ha-*ras* p21 levels is observed in cells treated with uniform 2′ sugar-modified phosphorothioates.[1] Furthermore, oligonucleotide-mediated reduction in Ha-*ras* p21 levels is associated with a reduction in proliferation rates of Ha-*ras* transformed cells in culture.[1]

Increased oligonucleotide target affinity attained by incorporation of 2′ sugar modifications correlated directly with increased antisense activity in cells, provided the modified oligonucleotides contained RNase H-sensitive deoxy gaps of the appropriate length. Furthermore, reduction in target affinity of 2′-*O*-methyl chimeras attained by shortening oligonucleotide length also correlated directly with reduced anti-

A.

Length	Tm (°C)	Sequence
17	77.2	CCACACCGACGGCGCCC
15	69.8	CACACCGACGGCGC
13	62.1	ACACCGACGGCG
11	47.3	CACCGACGGC
17	74.6	CCACACCGACGGCGCCC
15	66.2	CACACCGACGGCGC
13	58.0	ACACCGACGGCG
11	27.7	CACCGACGGC

B.

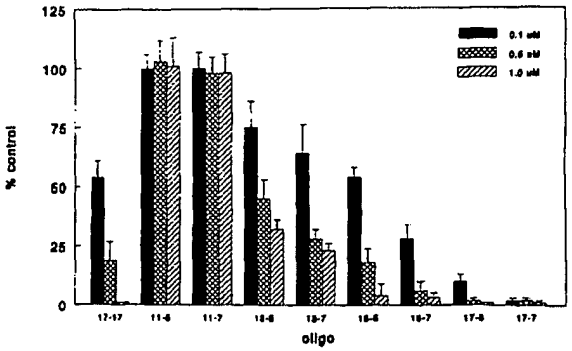

FIG. 8. **T_m analysis and dose response activity of shortened phosphorothioate 2'-*O*-methyl chimeric oligonucleotides containing 5- or 7-base deoxy gaps.** *A*, oligonucleotide design and T_m analysis. Hybridization was performed to a 25-mer synthetic fragment of RNA corresponding to residues +23 to +37 of mutant (codon 12, GGC → GTC) Ha-*ras* mRNA. Sequences containing 2'-*O*-methyl modifications are shown in *boxes*. Hybridization conditions are given in the text. *B*, antisense activities of a uniform deoxy phosphorothioate and shortened chimeric oligonucleotides against the Ha-*ras* oncogene using the reporter system described in Fig. 5. *Abscissa numbering* describes both the length of the oligonucleotide (*1st number*) followed by the length of the centered deoxy gap region (*e.g., 13–7* refers to a 13-mer chimera containing a 7-base deoxy gap). *17–17* refers to the parent uniform deoxy 17-mer compound (see Fig. 1). Results are expressed as the mean of the % control activity ± S.D. ($n = 6$). % control represents *ras*-dependent expression of luciferase in transfected cells in the absence of oligonucleotide.

TABLE II

Correlation of T_m with antisense activity 2'-modified 17-mer/7-base deoxy gap

T_m values for 2'-modified chimeric oligonucleotides were determined as described in text. IC_{50} values for inhibition of Ha-*ras* gene expression were extrapolated from data in Fig. 9. Sequences contained within box were modified at the 2' sugar position with indicated substituents.

CCACACCGACGGCGCCC

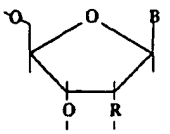

2' Modification (R)	Tm (°C)	IC50 (nM)
Deoxy	64.2	150
O-pentyl	68.5	150
O-propyl	70.4	70
O-methyl	74.7	20
Fluoro	76.9	10

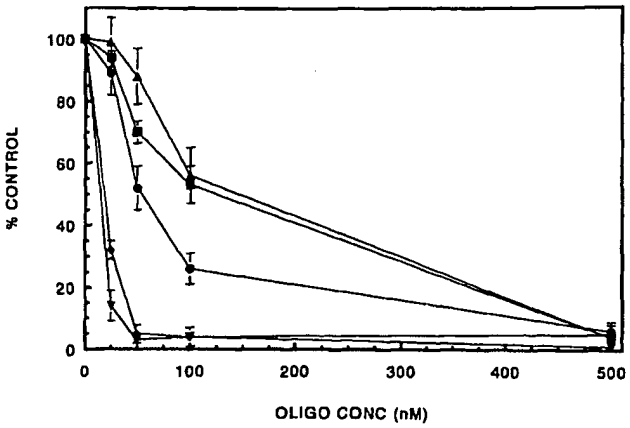

FIG. 9. **Dose-response antisense activities of phosphorothioate 2'-modified chimeric oligonucleotides containing seven-base deoxy gaps.** Antisense activities against the Ha-*ras* oncogene were determined as described in prior figures. Oligonucleotide sequences with modifications are shown in Table II. Sequences containing indicated 2' modifications are shown in *boxes*. ▲, uniform deoxy phosphorothioate; ■, 2'-*O*-pentyl chimera; ●, 2'-*O*-propyl chimera; ♦, 2'-*O*-methyl chimera; ▼, 2'-fluoro chimera. Refer to Table II for IC_{50} and T_m values for each oligonucleotide. Results are expressed as the mean of the % control activity ± S.D. ($n = 4$).

sense activity in cells. These observations, together with the finding that these compounds are actually poorer substrates for RNase H as compared with unmodified compounds, suggest that 2'-modified deoxy gap oligonucleotides are more effective antisense inhibitors due to enhanced target affinity conferred by modifications at the 2' sugar position.

Studies using methylphosphonate/phosphodiester chimeras have shown that the minimum number of unmodified backbone linkages required for efficient activation of mammalian RNase H *in vitro* is five (37). In other studies, *E. coli* RNase H has been shown to require a minimum of only three (36) or four (31) unmodified linkages for efficient activation. We report here similar observations with 2'-modified/deoxy chimeras. A minimum of 5 deoxy residues was required for efficient activation of HeLa RNase H when centered in the middle of the 17-mer phosphorothioate. We have also found that as few as 3 deoxy residues in this 17-mer is sufficient to activate *E. coli* RNase H.[1] It is unclear why *E. coli* RNase H differs from its mammalian homolog in the minimum DNA recognition length required for efficient activation. One possibility is that the nucleic acid binding domain of the *E. coli* protein is smaller than its mammalian counterpart. This possibility is suggested by the fact that *E. coli* RNase H is substantially smaller than eukaryotic RNase H enzymes (13).

Although 5 consecutive deoxy residues in the center of the 17-mer phosphorothioate is sufficient for maintaining efficient RNase H and antisense activity, it is important to note that the position of a 5-residue deoxy gap greatly influences the ability of the duplex to activate RNase H and elicit antisense effects. We have found that placement of a five-base gap at either the 5' or 3' side of the 17-mer renders the oligonucleotide a poor activator of mammalian RNase H *in vitro* and a poor inhibitor in cells. Furthermore, small shifts in the position of a centered five-base gap (*i.e.* one or two nucleotides in either direction) in the 17-mer also renders the

duplex a poor activator of the enzyme and a poor antisense inhibitor. In contrast, placement of a larger gap (*e.g.* 7 deoxy residues) at either the 5′ or 3′ side of the oligonucleotide, or to different sites within the middle of the molecule, has little to no effect on the chimeras' ability to activate RNase H and elicit antisense effects in cells.[1] Marked differences in RNase H cleavage efficiency *in vitro* with 2′-modified chimeric oligonucleotides containing identical deoxy gap sizes, but designed against other antisense targets, have also been observed.[1] As was observed for the Ha-*ras* target described here, differences in RNase H activity *in vitro* directed by these chimeric compounds correlated well with antisense activity in cells. These observations indicate that, in addition to gap length, other factors can strongly influence the efficiency of RNase H activity and should be considered when designing chimeric oligonucleotides. One possible explanation for the influence of gap position on differences in RNase H efficiency is that RNase H enzymes possess some nucleotide sequence preferences within the target duplex for binding and/or catalysis and, when restricted to a small recognition site within a duplex, sequence composition can strongly influence RNase H efficiency. In fact, we have detected some nucleotide sequence preferences for RNA cleavage in a RNA-DNA duplex by mammalian RNase H enzymes *in vitro*.[1]

Although chemical modifications placed in the backbone, sugar, or base of a nucleotide offer many potential advantages for oligonucleotide pharmacology, their usefulness is often limited by their inability to activate RNase H. As we have shown here, this limitation can be overcome and the beneficial properties of a chemical modification be manifested through the use of chimeric oligonucleotides. In addition to increased potency conferred by high affinity 2′ sugar modifications, the ability to use short oligonucleotides containing high affinity modifications may have certain pharmacologic as well as practical advantages. Increased cell penetration by oligonucleotides containing lipophilic 2′ sugar modifications is an additional potential advantage of these compounds. Furthermore, chimeric oligonucleotides may offer advantages beyond those conferred by a particular chemical modification. For example, methylphosphonate chimeras have been reported to increase antisense specificity by reducing nonspecific RNase H cleavage of partially complementary RNA-oligonucleotide duplexes *in vitro* (25). In addition, chimeras may be useful for directing site-specific cleavage of RNAs (35) and for discriminating between cleavage of perfectly complementary RNAs and those containing mismatches within the RNase H activating domain of an oligonucleotide (46). Further studies to explore these potential advantages for chimeric oligonucleotides are in progress.

Acknowledgments—We thank Drs. Stanley T. Crooke, David J. Ecker, Richard H. Griffey, and Claude Helene for helpful discussions during the course of these studies. We also thank Mary Ann Zounes for oligonucleotide synthesis.

REFERENCES

1. Toulme, J. J., and Helene, C. (1988) *Gene (Amst.)* **72,** 51–58
2. Stein, C. A., and Cohen, J. S. (1988) *Cancer Res.* **48,** 2659–2668
3. Dolnick, B. J. (1990) *Biochem. Pharmacol.* **40,** 671–675
4. Neckers, L., Whitesell, L., Rosolen, A., and Geselowitz, D. A. (1992) *Crit. Rev. Oncol.* **3,** 175–231
5. Crooke, S. (1992) *Annu. Rev. Pharmacol. Toxicol.* **32,** 329–376
6. Blake, K. R., Murakami, A., and Miller, P. S. (1985) *Biochemistry* **24,** 6132–6136
7. Shakin, S. H., and Liebhaber, S. A. (1986) *J. Biol. Chem.* **261,** 16018–16025
8. Maher, L. J., III, and Dolnick, B. J. (1988) *Nucleic Acids Res.* **16,** 3341–3347
9. Markus-Sekura, C. J. (1988) *Anal. Biochem.* **172,** 289–295
10. Cazenave, C., Stein, C. A., Loreau, N., Thuong, N. T., Neckers, L. M., Subasinghe, C., Helene, C., Cohen, J. S., and Toulme, J. J. (1989) *Nucleic Acids Res.* **17,** 4255–4261
11. Sburlati, A. R., Manrow, R. E., and Berger, S. L. (1991) *Proc. Natl. Acad. Sci. U. S. A.* **88,** 253–257
12. Chiang, M.-Y., Chan, H., Zounes, M. A., Freier, S. M., Lima, W. F., and Bennett, C. F. (1991) *J. Biol. Chem.* **266,** 18162–18171
13. Crouch, R. J., and Dirksen, M.-L. (1982) in *Nucleases* (Linn, S. M., and Robberts, R. J., eds) pp. 211–241, Cold Spring Harbor Laboratory, Cold Spring Harbor, NY
14. Doris-Keller, H. (1979) *Nucleic Acids Res.* **7,** 179–187
15. Haeuptle, M.-T., Frank, R., and Dobberstein, B. (1986) *Nucleic Acids Res.* **14,** 1427–1432
16. Minshull, J., and Hunt, T. (1986) *Nucleic Acids Res.* **14,** 6433–6442
17. Sankar, S., Cheah, K.-C., and Porter, A. G. (1989) *Eur. J. Biochem.* **184,** 34–39
18. Dash, P., Lotan, I., Knapp, M., Kandel, E. R., and Goelet, P. (1987) *Proc. Natl. Acad. Sci. U. S. A.* **84,** 7896–7900
19. Walter, R. Y., and Walder, J. A. (1988) *Proc. Natl. Acad. Sci. U. S. A.* **85,** 5011–5015
20. Shuttleworth, J., and Colman, A. (1988) *EMBO J.* **7,** 4327–4334
21. Woolf, T. M., Melton, D. A., and Jennings, C. G. B. (1992) *Proc. Natl. Acad. Sci. U. S. A.* **89,** 7305–7309
22. Wickstrom, E. (1986) *J. Biochem. Biophys. Methods* **13,** 97–102
23. Cook, P. D. (1993) in *Antisense Research and Applications* (Crooke, S. T., and Lebleu, B., eds) CRC Press, Inc., Boca Raton, FL, in press
24. Agrawal, S., Sarin, P. S., Zamecnik, M., and Zamecnik, P. C. (1992) in *Gene Regulation: Biology of Antisense RNA and DNA* (Erickson, R. P., and Izant, J. G., eds) pp. 273–283, Raven Press, Ltd., New York
25. Giles, R. V., and Tidd, D. M. (1992) *Nucleic Acids Res.* **20,** 763–770
26. Freier, S. M. (1993) in *Antisense Research and Applications* (Crooke, S. T., and Lebleu, B., eds) CRC Press, Inc., Boca Raton, FL, in press
27. Miller, P. S., McParkland, K. B., Jayaraman, K., and Ts'o, P. O. P. (1982) *Biochemistry* **20,** 1874–1880
28. Agrawal, S., and Goodchild, J. (1987) *Tetrahedron Lett.* **28,** 3539–3542
29. Shoji, Y., Akhtar, S., Periasamy, A., Herman, B., and Juliano, R. L. (1991) *Nucleic Acids Res.* **19,** 5543–5550
30. Akhtar, S., Basu, S., Wickstrom, E., and Juliano, R. L. (1991) *Nucleic Acids Res.* **19,** 5551–5559
31. Furdon, P. J., Dominski, Z., and Kole, R. (1989) *Nucleic Acids Res.* **17,** 9193–9204
32. Giles, R. V., and Tidd, D. M. (1992) *Anti-Cancer Drug Design* **7,** 37–48
33. Inoue, H., Hayase, Y., Imura, A., Iwai, S., Miura, K., and Ohtsuka, E. (1987) *Nucleic Acids Res.* **15,** 6131–6135
34. Sproat, B. S., and Lamond, A. I. (1993) in *Antisense Research and Applications* (Crooke, S. T., and Lebleu, B., eds) CRC Press, Inc., Boca Raton, FL, in press
35. Inoue, H., Hayase, Y., Iwai, S., and Ohtsuka, E. (1987) *FEBS Lett.* **215,** 327–330
36. Quartin, R. S., Brakel, C. L., and Wetmur, J. G. (1989) *Nucleic Acids Res.* **17,** 7253–7262
37. Agrawal, S., Mayrarrd, S. H., Zamecnik, P. C., and Pederson, T. (1990) *Proc. Natl. Acad. Sci. U. S. A.* **87,** 1401–1405
38. Hayase, Y., Inoue, H., and Ohtsuka, E. (1990) *Biochemistry* **29,** 8793–8797
39. Dagle, J. M., Walder, J. A., and Weeks, D. L. (1990) *Nucleic Acids Res.* **18,** 4751–4757
40. Baker, C., Holland, D., Edge, M., and Colman, A. (1990) *Nucleic Acids Res.* **18,** 3537–3543
41. Potts, J. D., Dagle, J. M., Walder, J. A., Weeks, D. L., and Runyan, R. B. (1991) *Proc. Natl. Acad. Sci. U. S. A.* **88,** 1516–1520
42. Dagle, J. M., Andracki, M. E., De Vine, R. J., and Walder, J. A. (1991) *Nucleic Acids Res.* **19,** 1805–1810
43. Schmidt, S., Niemann, A., Krynetskaya, F., Oretskaya, T. S., Metelev, V. G., Suchomleov, V. V., Shabarova, Z. A., and Cech, D. (1992) *Biochim. Biophys. Acta* **1130,** 41–46
44. Kawasaki, A. M., Casper, M. D., Freier, S. M., Lesnik, E. A., Zounes, M. C., Cummins, L. L., Gonzalez, C., and Cook, P. D. (1993) *J. Med. Chem.* **36,** 831–841
45. Reddy, E. P., Reynolds, R. K., Santos, E., and Barbacid, M. (1982) *Nature* **300,** 149–152
46. Monia, B. P., Johnston, J. F., Ecker, D. J., Zounes, M. A., Lima, W. F., and Freier, S. M. (1992) *J. Biol. Chem.* **267,** 19954–19962
47. Guinosso, C. J., Hoke, G. D., Freier, S. M., Martin, J. F., Ecker, D. J., Mirabelli, C. K., Crooke, S. T., and Cook, P. D. (1991) *Nucleosides & Nucleotides* **10,** 259–262
48. Puglisi, J. D., and Tinoco, I., Jr. (1989) *Methods Enzymol.* **180,** 304–325
49. Petersheim, M., and Turner, D. H. (1983) *Biochemistry* **22,** 256–263
50. Lima, W. F., Monia, B. P., Ecker, D. J., and Freier, S. M. (1992) *Biochemistry* **31,** 12055–12061
51. Dignam, J. D., Lebowitz, R. M., and Roeder, R. G. (1983) *Nucleic Acids Res.* **11,** 1475–1489
52. Owen, R. D., and Ostrowski, M. C. (1990) *Proc. Natl. Acad. Sci. U. S. A.* **87,** 3866–3870
53. Ausubel, F. M., Brent, R., Kingston, R. E., Moore, D. D., Seidman, J. G., Smith, J. A., and Struhl, K. (eds) (1987) *Current Protocols in Molecular Biology,* Greene Publishing Associates and Wiley-Interscience, New York
54. Bennett, C. F., Chiang, M.-Y., Chan, H., Shoemaker, J., and Mirabelli, C. (1992) *Mol. Pharmacol.* **41,** 1023–1033
55. Ecker, D. J., Vickers, T., Bruice, T. W., Freier, S. M., Jenison, R. D., Manoharan, M., and Zounes, M. *Science* **267,** 958–961
56. Daaka, Y., and Wickstrom, E. (1990) *Oncogene Res.* **5,** 267–275
57. Drew, H. R., and Dickerson, R. E. (1981) *J. Mol. Biol.* **151,** 535–556
58. Subramanian, P. S., Ravishanker, G., and Beveridge, D. L. (1988) *Proc. Natl. Acad. Sci. U. S. A.* **85,** 1836–1840